

# Asymptotic Safety in QFT

-

## from quantum gravity to graphene

### Dissertation

zur Erlangung des akademischen Grades  
*doctor rerum naturalium* (Dr. rer. nat.)

vorgelegt dem Rat der Physikalisch-Astronomischen Fakultät der  
Friedrich-Schiller-Universität Jena

von M. Sc. Benjamin Knorr  
geboren am 30.12.1990 in Rodewisch

## **Gutachter**

1. Prof. Dr. Andreas Wipf (Friedrich-Schiller-Universität Jena)
2. Dr. Astrid Eichhorn (Ruprecht-Karls-Universität Heidelberg)
3. Dr. Gian Paolo Vacca (Università di Bologna)

Datum der Disputation: 04.09.2017

# Abstract

In this work we investigate properties of scale invariant theories. This kind of theories describe a variety of phenomena, and two particular examples are discussed. On the one hand, more than 100 years after the discovery of General Relativity by Einstein, we still don't know how to unify gravity and quantum mechanics. One possibility is that on very small scales, gravity could be scale invariant, allowing for a finite ultraviolet completion. On the other hand, we will study the phase diagram of graphene and related materials. Scale invariant points in phase diagrams are related to second order phase transitions, and near these universal behaviour is found.

To investigate these systems, nonperturbative renormalisation group methods are used. In order to achieve trustworthy results, also technical progress, both analytical and numerical, had to be made. On the analytical side, the Mathematica package *xAct* is used to derive the equations underlying the scale invariance of the theories. To solve these numerically, pseudo-spectral methods are systematically introduced in the present context for the first time.

The results thus obtained support the ultraviolet completion of gravity by a scale invariant point. The dependence on gauge fixing and parametrisation is investigated, and found to be reasonably small. The 2-loop counterterm, being the hallmark of the perturbative nonrenormalisability of gravity, is shown to be irrelevant at the scale invariant point. Finally, the split-Ward identities are partially solved by resolving correlation functions.

Regarding graphene and similar materials, different levels of approximation show a very good convergence of results for critical exponents and anomalous dimensions at the phase transition studied. The combined power of both analytical and numerical methods excels particularly - without either, the calculations wouldn't be possible.

# Zusammenfassung

In dieser Arbeit werden skaleninvariante Theorien untersucht. Diese Art von Theorien beschreiben eine Vielzahl an Phänomenen, und im Weiteren werden zwei solche diskutiert. Einerseits haben wir, über 100 Jahre nach Einsteins Aufstellung der Allgemeinen Relativitätstheorie, noch keine Einsicht, wie die Gravitation mit der Quantenmechanik zu vereinbaren ist. Eine Möglichkeit besteht darin, dass Gravitation bei sehr kleinen Längen skaleninvariant ist, und so eine Ultraviolett-komplettierung ermöglichen würde. Andererseits werden wir das Phasendiagramm von Graphen und verwandten Materialien studieren. Skaleninvariante Punkte im Phasendiagramm beschreiben Phasenübergänge zweiter Ordnung, und sind mit universellem Verhalten verknüpft.

Zur Untersuchung dieser Systeme werden nichtperturbative Renormierungsgruppenmethoden angewandt. Um verlässliche Resultate zu erhalten, musste sowohl analytischer als auch numerischer Fortschritt erreicht werden. Auf der analytischen Seite wird das Mathematica-Paket *xAct* benutzt, um die der Skaleninvarianz zugrundeliegenden Gleichungen herzuleiten. Um diese Gleichungen numerisch zu lösen, werden pseudospektrale Methoden erstmals in diesem Kontext systematisch eingeführt.

Die so erreichten Resultate sprechen für die Ultraviolett-komplettierung der Gravitation durch einen skaleninvarianten Punkt. Eich- und Parametrisierungsvarianz fallen gering aus. Die 2-Schleifen-Divergenz, die die perturbative Nichtrenormierbarkeit der Gravitation anzeigt, ist am skaleninvarianten Punkt abwesend, und der entsprechende Operator irrelevant. Außerdem werden sogenannte split-Wardidentitäten partiell durch die Berechnung von Korrelationsfunktionen gelöst.

Bezüglich Graphen und verwandter Materialien zeigen unterschiedliche Näherungsstufen eine ausgezeichnete Konvergenz für die Werte von kritischen Exponenten sowie anomalen Dimensionen am untersuchten Phasenübergang. Die kombinierte Stärke von analytischen und numerischen Methoden zeigt sich hier besonders, so wären die Resultate nicht erreichbar gewesen, wenn auch nur eines von beiden gefehlt hätte.

# Contents

<b>1. Introduction</b>	<b>4</b>
<b>2. Flows in quantum field theory and condensed matter systems</b>	<b>11</b>
2.1. Functional renormalisation group . . . . .	11
2.2. Truncations, fixed points and asymptotic safety . . . . .	14
2.3. Gauge theories . . . . .	15
<b>3. Technical toolbox</b>	<b>18</b>
3.1. Tensor algebra . . . . .	18
3.2. Pseudo-spectral expansion . . . . .	20
3.3. Algorithmic details and implementation . . . . .	24
3.4. Example: Fixed point structure of the $O(N)$ model . . . . .	25
<b>4. Quantum gravity</b>	<b>28</b>
4.1. The gravitational two-loop counterterm in Asymptotic Safety . . . . .	28
4.1.1. Tensor monomial basis and perturbative analysis . . . . .	30
4.1.2. Nonperturbative analysis - truncation . . . . .	32
4.1.3. $\beta$ functions . . . . .	33
4.1.4. Fixed points and RG flow . . . . .	34
4.2. Gauge and parameterisation dependence . . . . .	37
4.2.1. Quantum gravity and parameterisations . . . . .	39
4.2.2. Parameterisation dependent RG flow . . . . .	44
4.2.3. Generalised parameterisation dependence . . . . .	47
4.3. Correlation functions . . . . .	59
4.3.1. Vertex expansion in quantum gravity . . . . .	59
4.3.2. Local quantum gravity . . . . .	60
4.3.3. Gauge dependence and curvature correlations . . . . .	68
4.4. Beyond the vertex expansion . . . . .	73
4.4.1. Cayley-Hamilton theorem . . . . .	73
4.4.2. Towards a local potential approximation in quantum gravity . . . . .	76
<b>5. Gross-Neveu-Yukawa models</b>	<b>80</b>
5.1. Dirac materials . . . . .	80

5.2. Gross-Neveu-Yukawa model with CDW order parameter . . . . .	82
5.2.1. Truncation . . . . .	83
5.2.2. Results . . . . .	85
5.3. $\mathcal{N} = 1$ Wess-Zumino model . . . . .	89
5.3.1. Supersymmetric flows . . . . .	90
5.3.2. Results . . . . .	91
<b>6. Conclusion</b>	<b>93</b>
<b>A. Code for the derivation of the flow equations for the <math>O(N)</math> model</b>	<b>I</b>
<b>B. Solving flows with pseudo-spectral methods</b>	<b>VII</b>
B.1. Flows of the $O(N)$ model . . . . .	VII
B.1.1. Flows for $d = 3$ and at large $N$ : A comparison . . . . .	VII
B.1.2. Flows for $d = 3$ and $N = 1, 4$ . . . . .	IX
B.1.3. Flow between two criticalities for $N = 1$ . . . . .	XI
B.2. Quantum mechanics with a bounded potential . . . . .	XII
B.2.1. Models . . . . .	XII
B.2.2. Exact results . . . . .	XIII
B.2.3. WKB approximation . . . . .	XIV
B.2.4. One-loop approximation . . . . .	XV
B.2.5. Flow of the effective potential . . . . .	XVI
B.2.6. Large $N$ approximation . . . . .	XIX
<b>C. Gauge and parameterisation dependent flow equations</b>	<b>XX</b>
<b>D. Basis for correlation functions</b>	<b>XXIII</b>
<b>E. General inverse and determinant of the metric</b>	<b>XXV</b>
<b>F. Inversion of tensors</b>	<b>XXIX</b>
<b>G. Functional truncations in pure <math>U(1)</math> gauge theory</b>	<b>XXXIII</b>
<b>H. Clifford algebra</b>	<b>XXXVII</b>
<b>I. Supersymmetric quantum mechanics</b>	<b>XXXVIII</b>
I.1. Flow equation in superspace . . . . .	XL
I.1.1. Supercovariant derivative expansion in NNLO . . . . .	XL
I.1.2. Supersymmetric regulator functional . . . . .	XLI
I.2. Effective potential and first excited energy . . . . .	XLII
I.2.1. On-shell effective potential . . . . .	XLII

I.2.2. Numerical results . . . . .	XLIII
I.3. Supersymmetry breaking . . . . .	XLVI
I.3.1. Problems with the expansion in powers of $F$ . . . . .	XLVI
I.3.2. Numerical results . . . . .	XLVIII

# 1. Introduction

Nature looks very different at different length scales. Already the Greeks postulated that matter consists of small components which they called  $\alpha\tau\omicron\mu\omicron\nu$  (atomon), literally the indivisible. It might be puzzling that everything that we experience in everyday life is indeed composed of discrete structures. On the other hand, if we look at our solar system, we humans play a negligible role in the dynamics of the celestial bodies. There is thus a natural hierarchy in the importance of degrees of freedom at a given length scale: only degrees of freedom with a typical scale similar to the natural scale of a given process contribute significantly to it. Small fluctuations cannot affect the motion too much and details are in that sense washed out. Likewise, fluctuations of much larger length scale are not influenced by the process, and can be seen as frozen. For most things in real life, we can just forget about the fact that the underlying structure of matter is atoms and molecules, and describe the motion of a thrown ball idealised as an extended classical object with spherical symmetry. Similarly, to calculate the motion of the Earth around the Sun, we can safely neglect the human degrees of freedom, and our solar system is in the same way irrelevant for the large scale structure of our Universe.

These simple examples make clear that an effective description of nature will involve different degrees of freedom at different length scales. There is also a natural direction from small scales to larger scales, from atoms to molecules, from molecules to brokkoli, from brokkoli to planets, and ultimately to the whole Universe<sup>1</sup>. The aim of this thesis is to study some aspects of the scale dependence of nature in seemingly completely distinct systems, which however share many structural features.

Not only do the effective degrees of freedom depend on the length scale considered, but also the interaction of these degrees of freedom are dependent on the length or energy scale<sup>2</sup>. As an example, imagine to throw a ball to somebody. Depending on how fast the ball is thrown, different interactions between ball and the hit person can happen. At 1m/s, the target person should be able to catch the ball, and might return it to you. The situation changes if the balls' velocity is increased to say 100m/s, which might end up in having to call an ambulance and being charged by a law suit. Even more extreme, if the ball is thrown relativistically, the quantum structure of the air can be probed. The energy might be so

---

<sup>1</sup>An impressive interactive animation of the scales in our Universe can be found at [1].

<sup>2</sup>We will interchangeably use length and energy scale in this work. Large length scales correspond to small energy scales and infrared, whereas small length scales correspond to high energies and the ultraviolet.



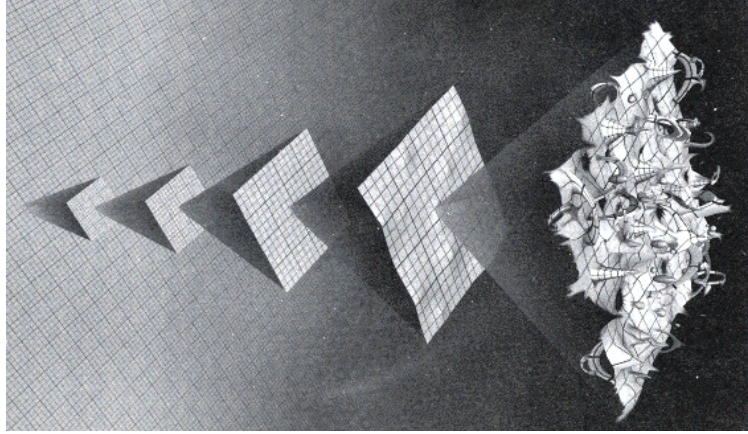


Fig. 1.1.: Artist's depiction of quantum spacetime. Image taken from [4].

high that the air is ionised and destroys everything in its neighbourhood, including you and the person you threw the ball to [2].

In a very similar fashion, elementary particles, which are loosely speaking to the best of our knowledge the microscopic degrees of freedom, interact differently with changing energy scale. This is encoded in so-called running couplings, and the dependence on energy is described by  $\beta$  functions. The best model that describes these interactions to an amazing accuracy is the Standard Model, a quantum field theory with symmetry group  $SU(3) \times SU(2) \times U(1)$ . These groups capture the strong, weak, and electromagnetic interaction. One particularly astonishing prediction of the Standard Model is the g-factor of the electron,

$$g = 2 \left( 1 + \frac{\alpha}{2\pi} + \dots \right) \approx 2.0023193043617(15), \quad (1.1)$$

where  $\alpha$  is the fine-structure constant. Classically, it is exactly 2, and corrections are due to QED (and to lesser extend QCD) vacuum effects. The agreement on the numerical value of the g-factor between theory and experiment is 12 decimal digits [3].

Our daily experience shows however that something is missing in the Standard Model, which is intimately tied to the names of Newton and Einstein - gravity. To date, there is no satisfactory theory of quantum gravity, even without matter. Many competing theories are on the market, including loop quantum gravity [5–14], string theory [15–20], causal dynamical triangulations [21–27], causal sets [28–34], asymptotic safety [35–47], group field theory [48–56] and several more [57, 58], however none of them solves all open problems. One of the fundamental questions here is what happens to spacetime itself at very small length, or very high energy scales, of the order of the Planck energy,

$$E_{\text{Pl}} = \sqrt{\frac{\hbar c^5}{G_N}} \approx 1.956 \times 10^9 J \approx 1.22 \times 10^{19} GeV. \quad (1.2)$$

This energy corresponds to the rest mass energy of a particle of Planck mass:  $21.7647\mu\text{g}$ ,

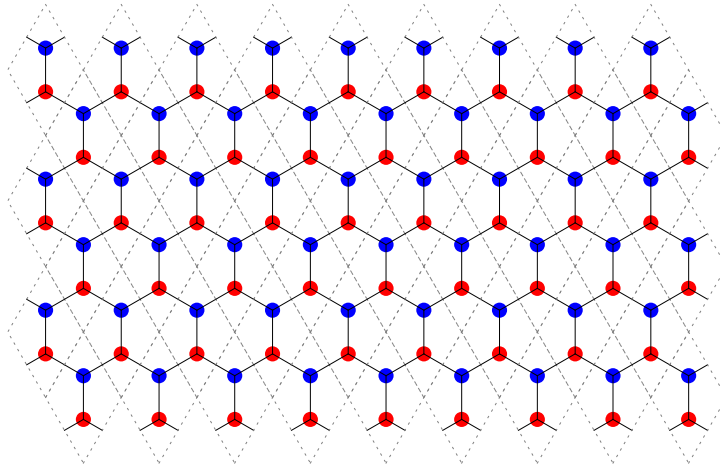


Fig. 1.2.: Honeycomb lattice structure of graphene. The diamond-shaped unit cell consists of two atoms, marked in red and blue for illustration.

which is approximately the US RDA for vitamin D for adults [59]. One could imagine that spacetime is fundamentally discrete, and the smooth geometry that we observe only emerges at larger length scales, similar to the smoothening of the discrete atom structure in everyday objects as tables or cats. Definitely quantum effects will play a role in the microscopic structure of spacetime. An artists depiction of this is shown in Figure 1.1, where one zooms into spacetime more and more, finally probing ripples of spacetime itself. Part of this thesis is concerned with a particular approach, asymptotic safety, to find a theory of quantum gravity.

The attentive reader might now raise the question whether we should care at all what spacetime does at these tiny length scales, as firstly we might never be able to measure it anyway, and secondly it might be not important for the infrared observations that we have access to. Technically, the property that aspects of macroscopic physics don't depend on microscopic details is called universality [60], and has been observed in many systems, *e.g.* the BKT phase transition in liquid-helium films [61, 62] and atomic gases [63–66], or a phase transition described by the Ising model [67] (originally proposed to describe ferromagnets) in binary mixtures [68–70] and potentially the chiral phase transition [71–74]. This is definitely a fair statement, although one should stress that fundamental research is important, even if the impact on real life is not immanent. If Einstein hadn't been funded to eventually develop General Relativity, we wouldn't have GPS which undoubtably has a major impact on the real world. Another argument lies in the intrinsic human thirst of knowledge, to understand the why and how of the Universe. General Relativity again is a prominent example, which predicted a lot of by now observed phenomena, from black holes to gravitational lensing [75–77], and more recently gravitational waves [78].

Let us for a moment apparently switch topics completely. In 2010, the Nobel Prize in physics was awarded to Andre Geim and Konstantin Novoselov “for groundbreaking exper-

---

iments regarding the two-dimensional material graphene” [79]. Graphene has very distinguished material properties, which are due to the hexagonal, or honeycomb lattice structure of its carbon atoms, indicated in Figure 1.2. To only name a few, graphene is very strong, yet still flexible, and has excellent thermal and electrical conducting properties. The relativistic symmetry of the low energy effective degrees of freedom in graphene induced many studies of effective field theories using Dirac fermions [80–114]. Similar materials have also been studied extensively [115–141].

Now, what in all worlds do graphene and quantum gravity have in common? The short answer is that several properties of these systems are (believed to be) governed by a so-called interacting fixed point. At fixed points, a given system is scale invariant, which means that it looks the same on every length scale. A real world example which comes close to being scale invariant is romanesco - the whirly structure of its parts repeats itself when zooming in on it. Fractals are another, more mathematical example which also exhibit approximate scale invariance, or self-similarity. A prominent example for this is the Mandelbrot set, see Figure 1.3.

Drawing from the properties of these fixed points, several very interesting questions might be answered. On the gravity side, the quest is to find an ultraviolet completion, or (together with the Standard Model) a “theory of everything”. In the authors eyes, this is one of the most important fundamental questions in physics. Regarding the material properties of graphene and related materials, one hope might be to make predictions on the properties of high  $T_c$  superconductors. Also, very soon silicon might have to be replaced as material for computer chips due to quantum tunneling becoming important in transistors at a size of a few nanometers. In 2008, graphene-based single-electron transistors were produced for the first time, and the relevant scale was estimated to be about 1nm [142]. The most recent silicon-based chips that are commercially available have a 14nm microarchitecture (Intel Skylake and AMD Zen).

The fact that the systems that we want to study are supposed to have an interacting, as contrasted to a noninteracting, fixed point puts several technical difficulties on us. Conventionally, *e.g.* when studying the Standard Model, perturbative expansions around the uncoupled theory can be employed to calculate the energy dependence of the couplings. Even though for most examples this expansion is only asymptotic<sup>3</sup>, reasonable results can be obtained by resummation techniques. This is in general impossible for a theory which is interacting strongly, and nonperturbative methods have to be used. Several methods are on the market which all have their advantages and disadvantages. By a lattice discretisation [143, 144], the theory can be probed directly in a nonperturbative manner, gauge invariance can be maintained explicitly, and one has easy access to observables like the Polyakov loop. On the other hand, fermions are notoriously difficult to implement, and even worse, in some

---

<sup>3</sup>This is a technical term referring to the property that the series doesn’t converge to the function that one wanted to represent.

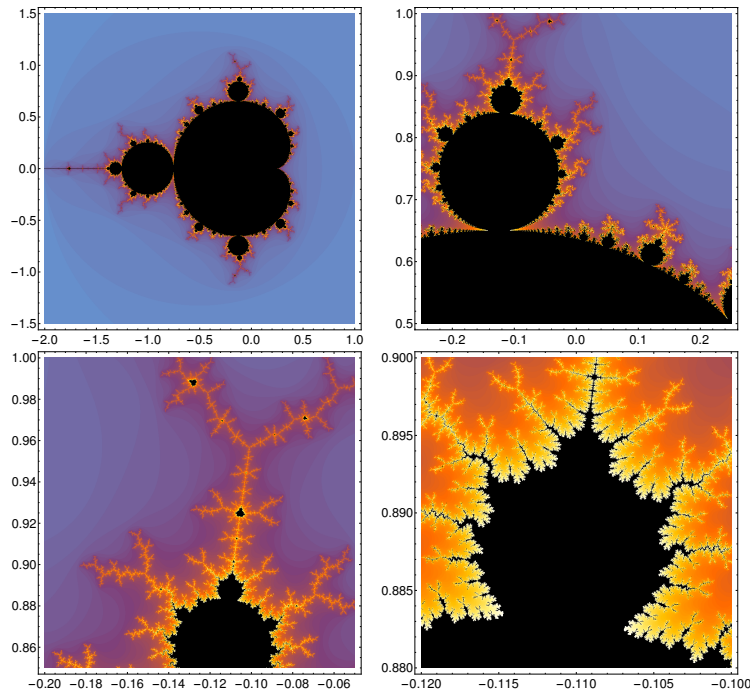


Fig. 1.3.: The Mandelbrot set, which is an example for approximate scale invariance.

parts of the parameter space, the so-called sign problem can arise, where the lattice approach practically breaks down. More recently, a very promising approach came up in the study of scale invariant theories, namely the conformal bootstrap method [145–149]. The idea here is to guess the relevant operators in the theory and then to solve consistency conditions arising from the operator product expansion of correlation functions. With this method, an incredible precision can be reached for observables like the critical exponent, which governs how the correlation length diverges near a phase transition. One downside is that only conformal theories can be studied yet, but sometimes one is interested in the full scale dependence of quantities, and neither can one study effective low energy theories which don't possess a suitable fixed point.

We will settle with another approach, the functional renormalisation group. It is based on the idea to find an interpolating function between the microscopic and the macroscopic description of the theory, and following Wilson [150], to "integrate out" degrees of freedom from high energies to low energies, in complete analogy to the physical intuition that we laid down in the beginning. One can derive an exact integro-differential equation which maps out this interpolation [151, 152]. The disadvantage here is that this equation is so complicated that presumably we will never be able to solve it exactly, except in very special cases. Therefore, approximations are necessary. Ideally, the approximated theory is still close to the original theory, and precise results can be obtained. For this one has to identify and describe the physical degrees of freedom which govern the dynamics of the system, and this can be a tough problem in general. Still, a lot of nice results have been obtained in

---

recent years, and thus also confidence in and understanding of the method has grown.

Let us now pose the concrete research questions that we want to address in this work. Regarding the quantisation of gravity, an often heard criticism of the asymptotic safety approach was that as soon as the two-loop counterterm is included in the approximation, the scenario will break down. The significance of this counterterm comes from perturbation theory, where it hallmarks the above mentioned difficulty to quantise gravity by standard means. We will show that this criticism can be refuted - the operator is irrelevant at the ultraviolet fixed point of asymptotic safety. Another point of potential danger is that the scale dependence of couplings is not directly observable, and thus generically depends on gauge fixing and the choice of parameterisation. We will study the influence of different gauge fixings and parameterisations on the ultraviolet completion. Finally, as a first step towards observables, we will calculate correlation functions in quantum gravity. There, we study correlators on both flat and curved backgrounds, and present a method to go beyond common vertex expansion schemes.

For graphene and related materials, we study a particular low energy effective model to describe aspects of the phase diagram. In particular, we study the phase transition between the semimetal and the charge-density-wave phase. We show, by studying different levels of approximation, that the so-called derivative expansion seems to show very good convergence, and we present precise estimates on critical quantities.

This thesis is structured as follows: in chapter 2, we repeat some basic notions of quantum field theory and the functional renormalisation group. Chapter 3 collects the analytical and numerical tools used in this work. We first sketch how the analytic equations used in this work are derived by means of computer algebra, a notebook of a minimal working example which is described there can be found in appendix A. Subsequently we introduce the numerical tools that we use to solve the aforementioned equations. Both conceptual and implementational details are presented. The chapter ends with an explicit example, namely the  $O(N)$  model at criticality. Further results obtained with these numerical tools, which don't fit into the main discussion of the thesis, are collected in appendix B.

Starting from chapter 4, we present the main results of the thesis, beginning with the quantisation of gravity. First, we discuss the two-loop counterterm and its (in-)significance in the Asymptotic Safety Scenario in section 4.1. Section 4.2 deals with gauge and parameterisation dependence in gravitational renormalisation group flows. Parts of the explicit results of this section are collected in appendix C. We continue with correlation functions in quantum gravity in section 4.3, with some information collected in appendix D. The final part of this chapter, section 4.4, tries to go beyond the vertex expansion to deal with correlation functions. Some related results are collected in the appendices E, F and G.

After the gravitational part, chapter 5 collects results on the condensed matter part of this thesis. We start with a short physical introduction to Dirac materials in section 5.1. Subsequently, we discuss results for the critical Gross-Neveu-Yukawa model in section 5.2,

and its supersymmetric version, the Wess-Zumino model, in section 5.3. Appendix H collects conventions on the Clifford algebra, whereas appendix I comprises further supersymmetric results. We close with a conclusion in chapter 6.

*The compilation of this thesis is solely due to the author. However many parts of the presented results are based on work with colleagues, and were published in several articles. The implementation of the pseudo-spectral code explained in chapter 3 was done in collaboration with Julia Borhardt, as were the results on flows in appendix B, [153, 154]. The results on the two-loop counterterm in quantum gravity in section 4.1 were obtained with Holger Gies, Stefan Lippoldt and Frank Saueressig [47]. The analysis of gauge and parameterisation dependence in section 4.2 was carried out together with Holger Gies and Stefan Lippoldt [155]. Results on correlation functions in quantum gravity in the first part of section 4.3 were obtained with Nicolai Christiansen, Jan Meibohm, Jan Pawłowski and Manuel Reichert [45], the second part presents unpublished results together with Stefan Lippoldt, as does appendix F. All supersymmetric results, including section 5.3 and appendix I, are due to collaboration with Marianne Heilmann, Tobias Hellwig, Marcus Ansorg and Andreas Wipf [156].*

## 2. Flows in quantum field theory and condensed matter systems

In this chapter we lay the foundations to understand the results presented subsequently. The typical starting point in quantum field theory (QFT) is the path integral. From there, using a scalar field as example, we derive an equivalent formulation by means of the effective average action. This object fulfills an exact functional integro-differential equation. We then elucidate the relation of this formulation with scale invariance as mentioned in the introduction. Further, the embedding of critical phenomena as well as the problems encountered with gauge theories are discussed.

### 2.1. Functional renormalisation group

A great deal of information about a QFT is stored in its correlation functions<sup>4</sup>. The prime example in introductory lectures is electron-electron scattering, which is described by a four-point function (two incoming, two outgoing electrons). To obtain this correlator, we have to average the product of four fields at different spacetime points over all allowed physical field configurations. Configurations are weighted with the microscopic, or classical action  $S$ , so that

$$\langle \phi(x_1) \dots \phi(x_4) \rangle := \mathfrak{N} \int \mathcal{D}\phi \phi(x_1) \dots \phi(x_4) e^{iS[\phi]}. \quad (2.1)$$

Here,  $\mathfrak{N}$  is a normalisation constant which is of no interest to us. For practical calculations, we often have to perform a Wick rotation, which effectively changes the weight to  $e^{-S_E[\phi]}$ , with the euclideanised action  $S_E$ . We will assume in the rest of this work that this is always possible in our cases. Another point to note is that the measure  $\mathcal{D}\phi$  will in general not exist, and has to be regularised. Again, for simplicity we assume that this has been taken care of, and we will not bother any longer with it, but indicate that the integral is regularised at an ultraviolet cutoff scale  $\Lambda$ .

An efficient way to access all correlation functions is the generating functional  $Z[J]$ , or

---

<sup>4</sup>The folklore is that *all* information is stored in them, but this is strictly speaking not true. This is immediately clear when one considers, *e.g.*, the geodesic distance of two spacetime events [157], which is commonly not introduced as an operator in the action.

the generating functional of connected correlators  $W[J]$ ,

$$Z[J] \equiv e^{W[J]} = \int_{\Lambda} \mathcal{D}\phi e^{-S_E[\phi] + J \cdot \phi}, \quad (2.2)$$

where we used de Witt's compressed notation for the source term  $J \cdot \phi = \int d^d x \sqrt{g} J(x) \phi(x)$ . Correlation functions are then obtained by  $n$ -fold functional differentiation w.r.t. the field and setting the source to zero afterwards.

Even more efficient in storing the correlation functions is the effective action  $\Gamma$ , which is the Legendre transform of  $W$ :

$$\Gamma[\phi] = \sup_J (J \cdot \phi - W[J]). \quad (2.3)$$

By construction, the effective action is convex. An easy calculation elucidates the meaning of the effective action. Taking the functional derivative w.r.t. the field, we obtain the quantum equation of motion,

$$\frac{\delta \Gamma[\phi]}{\delta \phi(x)} = J^{\text{sup}}(x), \quad (2.4)$$

which governs the dynamics of the expectation value of the field, including all quantum effects.

Shifting the argument in the definition of the generating functional, and using the definition of the effective action, we can derive a functional differential equation for the effective action:

$$e^{-\Gamma[\phi]} = \int_{\Lambda} \mathcal{D}\varphi e^{-S_E[\phi + \varphi] + \frac{\delta \Gamma[\phi]}{\delta \phi} \cdot \varphi}. \quad (2.5)$$

It is possible to solve this equation directly by some approximation scheme, *e.g.* a vertex expansion of  $\Gamma[\phi]$ , schematically

$$\Gamma[\phi] = \sum_{n=0}^{\infty} \frac{1}{n!} \Gamma^{(n)} \cdot \phi^n. \quad (2.6)$$

The expansion coefficients  $\Gamma^{(n)}$  are the one-particle irreducible proper vertices. If this ansatz is inserted into (2.5), an infinite tower of coupled equations arises, the so-called Dyson-Schwinger equations. They are of great use when the ultraviolet theory is fixed, as for example in standard gauge theories, see *e.g.* [158–163]. Since we are also interested in quantum gravity, where we don't know the microscopic action, we will follow a different route.

In the introduction, we mentioned Wilson's idea to successively integrate out modes. This idea can be implemented by the functional renormalisation group (FRG), which we will explain in the following. The key point is to introduce a so-called effective average action  $\Gamma_k$  which interpolates between the microscopic action  $S$  in the ultraviolet (UV) and the standard effective action  $\Gamma$  in the infrared (IR), where  $k$  is the interpolation parameter which ranges



from the UV cutoff  $\Lambda$  down to 0. To construct this interpolating functional, we introduce a regulator term  $\Delta S_k$ , such that

$$e^{W_k[J]} = \int_{\Lambda} \mathcal{D}\phi e^{-S_E[\phi] - \Delta S_k[\phi] + J \cdot \phi}. \quad (2.7)$$

The regulator term is quadratic in the field  $\phi$  and can be seen as a momentum dependent mass term,

$$\Delta S_k[\phi] = \frac{1}{2} \phi \cdot \mathfrak{R}_k \cdot \phi. \quad (2.8)$$

The kernel  $\mathfrak{R}_k$  needs to satisfy three properties to guarantee well-definedness and the correct limits in the IR and UV:

- it should regularise the IR by gapping modes with an effective mass  $\sim k$ ,

$$\lim_{q^2/k^2 \rightarrow 0} \mathfrak{R}_k(q^2) \sim k^2 > 0, \quad (2.9)$$

- it should vanish for  $k \rightarrow 0$ ,

$$\lim_{k^2/q^2 \rightarrow 0} \mathfrak{R}_k(q^2) = 0, \quad (2.10)$$

- and it has to diverge near the UV cutoff scale,

$$\lim_{k^2 \rightarrow \Lambda^2 \rightarrow \infty} \mathfrak{R}_k(q^2) \rightarrow \infty. \quad (2.11)$$

For convenience, let us introduce the RG “time”  $t$  by

$$t = \ln \frac{k}{\Lambda}. \quad (2.12)$$

With a simple calculation, one can derive a functional integro-differential equation for the parametric dependence of the effective average action, the so-called Wetterich equation [151, 152],

$$\partial_t \Gamma_k = \frac{1}{2} \text{STr} \left[ \left( \Gamma_k^{(2)} + \mathfrak{R}_k \right)^{-1} \cdot \partial_t \mathfrak{R}_k \right]. \quad (2.13)$$

The STr stands for the super-trace, which sums over discrete indices, gives fermionic contributions a negative sign, and acts as functional trace regarding differential operators. By construction, this equation is finite both in the IR (by the momentum dependent mass gap) and the UV (by the vanishing of the regulator for large arguments), and is thus well-defined. The right-hand side is called the flow of the effective action, and the  $t$ -derivative of a dimensionless coupling is exactly its  $\beta$  function.

Equation (2.13) has several remarkable properties. For once, it is an exact equation, and thus carries the full information of the path integral. Second, it is of one-loop form, nevertheless it is nonperturbative. Finally, it allows for systematic approximation schemes

(in this context often called truncations), which makes it practically usable. We shall not discuss the derivation and other properties of (2.13) further, rather referring the reader to standard literature [35, 151, 152, 164–170]. To reduce clutter of notation, in the rest of this work we will drop the subscript  $k$  on scale dependent quantities if there is no danger of confusion.

## 2.2. Truncations, fixed points and asymptotic safety

It is plausible that (2.13) is far to difficult to be solvable in the general case, thus we have to resort to approximations. The very existence of approximation schemes is a nontrivial statement. To see this, let us introduce the so-called theory space  $\mathcal{F}$ . Having fixed the field content of a given theory, we want the fields to behave appropriately, *i.e.* they need to be in some kind of Schwartz space  $\mathcal{S}^5$ . The theory space is then defined as the space of all functionals  $\Gamma : \mathcal{S} \rightarrow \mathbb{R}$  which are invariant under the symmetry group  $G$  of the theory,

$$\mathcal{F} = \{\Gamma : \mathcal{S} \rightarrow \mathbb{R} | \forall g \in G, g\Gamma = \Gamma\} . \quad (2.14)$$

In general,  $\mathcal{F}$  is a Banach space of infinite dimension, and it is not clear whether we can define a basis at all. To make any progress, we will assume that we can in fact define a basis in terms of invariant monomials,  $F_n$ . For a fixed index set  $I$ , we can thus expand

$$\Gamma = \sum_{n \in I} \lambda_n F_n . \quad (2.15)$$

The generalised couplings  $\lambda_n$  are then coordinates of  $\mathcal{F}$ . Both the couplings and invariant monomials can be interpreted in a general sense. In particular, the potential of a scalar field would be interpreted as a generalised coupling corresponding to the unit monomial, and the wave function renormalisation as the coordinate of the kinetic term monomial. The set of  $\beta$  functions of all considered couplings define a vector field on  $\mathcal{F}$ , and integral curves are RG trajectories. Geometrically, when we approximate a theory, we project this vector field on a subspace spanned by our chosen index set  $I$ . A good approximation preserves the important features of the full theory space.

The theory space is characterised by special points where all  $\beta$  functions of dimensionless couplings vanish. These points are called fixed points, and correspond to the scale invariant points mentioned in the introduction. To define dimensionless couplings, we use the RG scale  $k$ . If  $d_\lambda$  is the mass dimension of the coupling  $\lambda$ , then the dimensionless coupling  $\bar{\lambda}$  is defined as

$$\bar{\lambda} = k^{-d_\lambda} \lambda . \quad (2.16)$$

---

<sup>5</sup>In fact, in a more precise setting, one would have to deal with sections of bundles over a manifold. This makes the definition of a suitable Schwartz space even more difficult [171].

By construction, every theory space has at least one fixed point, namely where all dimensionless couplings vanish. This is the Gaussian fixed point. In this work, we are more interested in so-called non-Gaussian, or interacting fixed points, which are characterised by the fact that not all couplings vanish.

Not only the existence of fixed points is of interest, we also want to know about their stability, *i.e.* how do trajectories in their neighbourhood behave. For this, we linearise the flow around the fixed point. The (generalised) eigenvalues of the linearised flow determine the stability. If a given eigenvalue is positive, the corresponding eigenvector, which is a combination of monomials, is attracted towards the fixed point when the scale is lowered, *i.e.* in the IR, and likewise repulsed from it when the scale is increased, *i.e.* in the UV. These eigenvectors are called irrelevant. By contrast, if the eigenvalue is negative, the attraction is towards the fixed point in the UV and the repulsion away from the fixed point in the IR. We call the corresponding eigenvector relevant. Eigenvectors with vanishing eigenvalue are called marginal. Critical exponents are the negative of the eigenvalues.

The classification into relevant, irrelevant and marginal applies both to quantum gravity and condensed matter systems. In the first case, the idea is that the UV completion is achieved by an interacting fixed point which has only finitely many relevant directions. We want to end up exactly in the fixed point in the UV to arrive at a fundamental theory valid at all energy scales, and if the critical manifold of the fixed point is finite-dimensional, we only have to specify a finite number of couplings by experiment. The latter condition ensures predictivity. This scenario of a UV completion by such a fixed point is called asymptotic safety (AS) scenario of quantum gravity. In a more general setting, AS is a generalisation of asymptotic freedom. In the latter, it is the Gaussian fixed point which gives rise to the UV completion.

In a condensed matter context, we typically consider low energy effective theories, and study phase transitions. To see universal behaviour, we only need to be near the fixed point, and thus we also have to tune the relevant couplings to select a suitable trajectory. If there is only one relevant parameter, then the relevant critical exponent is related to the divergence of the correlation length at a second order phase transition. In this context, fixed points with only one relevant parameter are often called stable.

## 2.3. Gauge theories

Theories with gauge symmetries bring some obstacles to the calculation of the flow. In path integral language, we would integrate over physically equivalent configurations, and essentially get the volume of the gauge group at every spacetime point. This clearly diverges for any manifold or noncompact gauge group. From the perspective of the flow equation, the same divergence arises: the propagator enters the flow equation, and it has zero modes when gauge symmetries are present.

A further problem arises in quantum gravity. The very formulation of the FRG relies on the fact that we can distinguish high from low momentum modes. In a background invariant setting, such a statement doesn't make sense. A way around is the so-called background field method, which we shall explain in this section.

In the background field method, we split the quantum field  $g$  into an arbitrary background  $\bar{g}$  and a fluctuation  $h$ , which is not restricted to be small in any sense. The nature of this splitting is in general a question of taste, physical predictions cannot depend on it<sup>6</sup>. In approximations, there will be a residual dependence, and we will investigate this issue later.

With this splitting, manifest background gauge/diffeomorphism invariance can be implemented, and we can actually formulate gauge fixing terms and a regulator which respect this background symmetry [35]. At the end of the calculation, *i.e.* after all modes have been integrated out ( $k = 0$ ), we can set the fluctuation to zero and end up with the full effective action.

The above reasoning would apply if the action, gauge fixing and regulator would indeed respect the splitting in background and fluctuation. It is however obvious that the gauge fixing and the regulator break the split symmetry by construction. Still, the effective action at  $k = 0$  depends on only one field. For that reason, we actually have to deal with an effective action which now depends on two fields individually. The information on the breaking of the split symmetry is encoded in the split-Ward, or Nielsen identities. Schematically, it relates the derivative of the effective action w.r.t. to the background metric to that w.r.t. the fluctuation field,

$$\frac{\delta\Gamma}{\delta h} \sim \frac{\delta\Gamma}{\delta\bar{g}} + \mathcal{R} + \mathcal{G}, \quad (2.17)$$

where  $\mathcal{R}$  and  $\mathcal{G}$  are contributions that arise from the fact that the regulator and the gauge fixing depend on the background and the fluctuation individually.

There are basically two approaches to deal with this issue. The first possibility is to try and solve both the flow equation and the Nielsen identities simultaneously, see *e.g.* [35, 39, 40, 165, 172–184]. This bears both conceptual and technical difficulties, that is why we focus on another approach. Instead of solving the Nielsen identities at every scale, we see it as a kind of boundary condition in the IR, and we will solve the flow for the two-field system. In the context of gravity, this has been established by so-called bimetric flows [39, 44, 173, 185, 186], which consider the two metrics, and fluctuation flows [41, 43, 45, 187–189], which consider the background metric and the fluctuation as fields. Both approaches are closely related, but the exact mapping is nontrivial.

Let us stress that the Nielsen identities have to be taken seriously. As a worst case scenario for what can go wrong, we refer to [190] where the authors show that by improper treatment, the (universal!) 1-loop  $\beta$  function for QCD can be changed. On the other hand, it is fair to notice that calculations in quantum gravity are complex, and it only became possible in the

---

<sup>6</sup>This statement is true if the change in the measure is taken into account.

recent past to actually go beyond the background approximation, which basically neglects the difference of background and full metric. Some of the results that we will discuss later use the background field approximation, and some go beyond it.

## 3. Technical toolbox

This chapter is devoted to the technical tools used to derive and solve the flow equations. In the first section, as a concrete example, we discuss the derivation of  $\beta$  functions of the  $O(N)$  model with the help of the Mathematica package *xAct* [191–196]. Its intended use is mainly calculations in gravity, but it can be easily extended to treat any kind of field content. Afterwards, we present how to numerically solve the equations encountered in the search for fixed points. This is done by pseudo-spectral methods, which are exceptionally well suited for smooth problems due to their high accuracy and low computational cost. We first focus on the basics and main properties of pseudo-spectral expansions, then sketch the actual implementation of these methods. To illustrate their usage, we finally solve the fixed point equations for the  $O(N)$  model at NLO in the derivative expansion derived in the beginning of this chapter. For an extensive discussion of pseudo-spectral methods, see [197–200].

### 3.1. Tensor algebra

We will assume that the reader is familiar with the basics of *xAct*, which can be found in the documentation of the package available on the web page [191]. To illustrate the use of *xAct* in the derivation of flow equations, we shall study the concrete problem of deriving the flow equation for the  $O(N)$  model in next-to-leading order (NLO) in the derivative expansion. For this, the following ansatz for the effective average action as a functional of the  $O(N)$ -symmetric vector  $\phi^a$  is used:

$$\Gamma = \int d^3x \left( \frac{1}{2} Z_\phi(\rho) (\partial_\mu \phi_a) (\partial^\mu \phi^a) + \frac{1}{2} Y_\phi(\rho) (\partial_\mu \rho) (\partial^\mu \rho) + V(\rho) \right). \quad (3.1)$$

The index  $a$  runs from 1 to  $N$ , and we introduced  $\rho = \phi_a \phi^a / 2$ . The regulator is chosen as

$$\Delta S = \int d^3x \left( \frac{1}{2} \phi_a \mathfrak{R}_\phi \left( \frac{p^2}{k^2} \right) \phi^a \right), \quad (3.2)$$

and the aim is to derive the  $\beta$  functions of  $V$ ,  $Z_\phi$  and  $Y_\phi$ . We take special care of all index structure, since this is also necessary in the code. In particular, the same index cannot stand on the same height in a given expression.

A notebook containing the derivation of these flow equations is included in the supplemen-

tal material of [201], and we reproduce the full code in appendix A. We will explain some details here. After reading the necessary packages, constants for the number  $N$  of the symmetry and the dimension are defined. Then, the flat spacetime together with its metric are defined. Another flat manifold with metric is needed for the  $O(N)$  symmetry of the fields. The vector field  $\phi^a$  is then a tensor with a single  $O(N)$  index. Several definitions follow to give the calculation some ease. This includes momentum vectors and constant symbols for lengths of momentum vectors as well as scalar functions  $V$ ,  $Z$  and  $Y$ , the regulator and shortcuts for the transverse and longitudinal propagator. We finally implement a modified version of a variational derivative, VD, which acts in momentum space. Its arguments are the vector field w.r.t. which the derivative is taken, its momentum vector and its index. The section Truncation sets up the truncation and the regulator.

With these preparations, one can actually start the calculation. The first task is to calculate the propagator, which is the inverse of the regularised two-point function. The latter is calculated with the above mentioned variational derivative VD. We can parameterise the propagator by a longitudinal and a transverse part, and then use the SolveConstants function to find the coefficients. The final ingredient for the flow equations are the three- and four-point vertex, which are defined in the same section.

Now, all ingredients are together, and the calculation of the flow equations is just a trace of matrix products, taking care of the correct momentum/index structure and prefactors. The flow equations can directly be read off of the calculated traces.

This completes the derivation of the flow equations for the  $O(N)$  model, and we will show how to solve them in the next chapter by pseudo-spectral methods. Before we do so, let us mention how we can treat fermions.

For fermionic fields, it is enough to use a vector bundle. Spinors are vectors on this bundle, whereas their adjoints are covectors. No metric exists in general on this bundle, but everything we need is a delta anyway, which is defined automatically. With this vector bundle, gamma matrices and their products can be defined straightforwardly. For example,  $\gamma_\mu$  in the code is a tensor with one spacetime and two vector bundle indices. The Clifford algebra can be implemented without specifying an explicit representation.

The sole difficulty in treating fermions is their anticommutativity. This is solved by a construction which the author called “ordered fermion product” (OFP). An OFP carries a list of ordered fermions, and an indicator which is needed to resolve products of OFPs. All fermionic fields by construction can only appear inside such an OFP. With this, one can easily define the functional derivative of an OFP w.r.t. a fermion, where care must be taken whether the derivative acts from the left or from the right.

## 3.2. Pseudo-spectral expansion

To simplify the discussion, in the following we will consider a single function depending on a single variable. The methods extend rather straightforwardly to the general case by using a tensor product. To be precise, let  $f : [a, b] \rightarrow \mathbb{R}$  be a smooth function on a fixed interval  $[a, b]$ <sup>7</sup>. Without loss of generality, we will restrict ourselves to  $[-1, 1]$ . The aim is to solve the differential equation

$$\mathcal{L}[f](x) = 0, \quad (3.3)$$

where  $\mathcal{L}$  is a nonlinear differential operator. To solve this equation, the idea is to expand  $f$  into a series of orthogonal polynomials. In particular, we will choose Chebyshev polynomials of the first kind, such that

$$f(x) = \sum_{n=0}^{\infty} f_n T_n(x). \quad (3.4)$$

The  $T_n$  are defined by the relation

$$T_n(\cos(x)) = \cos(nx), \quad n \in \mathbb{N}_0, \quad (3.5)$$

solve the differential equation

$$(1 - x^2) T_n''(x) - x T_n'(x) + n^2 T_n(x) = 0, \quad (3.6)$$

and are orthogonal w.r.t. the measure  $\mu(x) = 1/\sqrt{(1 - x^2)}$ ,

$$\int_{-1}^1 \mu(x) T_n(x) T_m(x) dx = \frac{\pi}{1 + \delta_{n0}} \delta_{nm}. \quad (3.7)$$

The equation (3.4) is exact as long as  $f$  is in a suitable function space, which we will always assume in the following. The key observation is that if  $f$  is sufficiently “nice”, *i.e.* typically smooth, then the expansion converges very quickly, and only a small number of coefficients of the infinite sum have to be retained to represent it accurately. This will be discussed in more detail below.

To solve (3.3), we insert (3.4) with a finite number of terms,  $n \leq N$ , and evaluate it at a given set of points. At these so-called collocation points, we enforce the differential equation strictly, thus obtaining a nonlinear system of equations for the coefficients  $f_n$ . This then can be solved with standard methods as a Newton-Raphson iteration. Alternatively, one can use a Galerkin method, which employs the orthogonality to project onto the first  $N$  polynomials. Under suitable assumptions [197], both methods agree up to machine precision. Also notice that there is a one-to-one map between the coefficients  $f_n$  and the values of the function  $f$  at the collocation points, and both can be used in the actual implementation.

---

<sup>7</sup>Infinite intervals can be treated by a compactification.



Fig. 3.1.: Collocation points of the Gauß grid for  $N = 40$ .

By the theorem of conserved difficulty, there is of course a price to pay for the high accuracy and efficiency in the expansion in orthogonal polynomials. Since the basis functions are nonvanishing almost everywhere, the discretised differential matrices are dense. This is in contrast to, *e.g.*, the finite difference method, where only a number of neighbouring points is considered to calculate any derivative. To nevertheless obtain decent convergence and speed, the domain can be decomposed, and the function is then expanded on every subdomain. The resulting systems are only coupled via continuity, and thus give rise to much sparser matrices. This hybrid of spectral methods and finite elements is often called spectral elements method.

Let us come back to the series (3.4) and discuss the specific choice of Chebyshev polynomials. An equally valid choice would be to use Legendre Polynomials, which are defined on the same interval and share the main convergence properties. Still, it was shown [202, 203] that Chebyshev polynomials converge slightly better in the generic case. The latter are intimately related to Fourier series, which explains their exceptional convergence. Yet, no periodicity condition has to be imposed on the function  $f$ .

If  $f$  is defined on an infinite interval, it might be tempting to use Laguerre or Hermite polynomials instead of Chebyshev polynomials together with a compactification. It is however easy to see that this is in general not a good idea for the following reason. The asymptotic behaviour of the function  $f$  is fixed, but the asymptotic behaviour of a finite sum of Laguerre or Hermite polynomials changes when altering the number of terms retained. Increasing the order of a Laguerre or Hermite series thus doesn't necessarily lead to a better representation of the interpolated function.

The convergence of the collocation method crucially depends on the choice of collocation points. It turns out that there is actually one class of point sets which is useful in practice, and the different grid choices essentially differ in the treatment of the boundary of the interval. The Lobatto grid includes both boundaries,

$$x_n = -\cos\left(\frac{n\pi}{N}\right), \quad (3.8)$$

the Gauß grid contains neither,

$$x_n = -\cos\left(\frac{\left(n + \frac{1}{2}\right)\pi}{N + 1}\right), \quad (3.9)$$

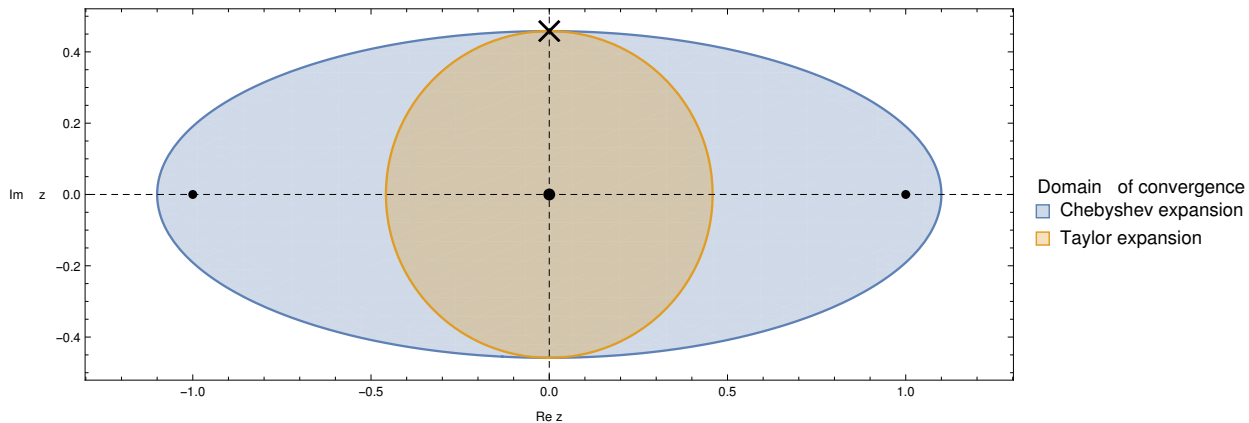


Fig. 3.2.: Comparison of the domains of convergence of a Taylor expansion (orange) and a Chebyshev expansion (blue) if the interpolated function has a pole at  $\mathbf{i}/2$ . The Taylor expansion converges in a disk with radius  $1/2$ , whereas the Chebyshev expansion converges in an ellipse with foci  $\pm 1$  and semi-minor axis  $1/2$ , which is a superset of the disk.

and the left (right) Radau grid contains only the left (right) boundary,

$$x_n = \cos\left(\frac{(N-n)\pi}{N + \frac{1}{2}}\right), \quad \text{or} \quad (3.10)$$

$$x_n = -\cos\left(\frac{n\pi}{N + \frac{1}{2}}\right). \quad (3.11)$$

As an example, the Gauß grid for  $N = 40$  is shown in Figure 3.1. The Runge phenomenon, known from interpolation on an equidistant grid, is avoided due to the nonequidistant distribution with asymptotic density of points  $1/\sqrt{(1-x^2)}$  [204]. This underlines that the choice of collocation points is the key for accuracy.

Let us now discuss some mathematical properties of Chebyshev expansions, focussing on convergence. Darboux's principle tells us that rate and domain of convergence of any given expansion is dictated by the singularity structure of the function  $f$ , including poles, logarithms, branch cuts, discontinuities and fractional powers. In Figure 3.2, we compare the domains of convergence of a Taylor expansion (orange) and a Chebyshev expansion (blue) of a function which is assumed to have a pole at  $x = \mathbf{i}/2$ , depicted by the cross. The Taylor expansion converges in a disk with radius  $1/2$ , but the domain of convergence of the Chebyshev expansion is an ellipse with foci  $\pm 1$  and semi-minor axis  $1/2$ , strictly including the disk of the Taylor expansion. In particular, the whole real interval  $[-1, 1]$  is inside the domain of convergence of the Chebyshev expansion. This is always the case as long as there is no singularity (in the above sense) contained in this interval.

After this rather intuitive treatment of convergence, let us introduce some basic notions. The algebraic index is the largest  $q \in \mathbb{R}_+$  such that

$$\lim_{n \rightarrow \infty} |f_n| n^q < \infty. \quad (3.12)$$

For finite  $q$ , we say that the series (3.4) converges algebraically, and the coefficients decrease in absolute value as a power law,  $f_n \sim \mathcal{O}(n^{-q})$ . If (3.12) is true for all real  $q$ , the coefficients decrease faster than any power law, and the series is said to converge exponentially. With this, we can define the rate of exponential convergence by

$$\lim_{n \rightarrow \infty} \frac{|\ln(|f_n|)|}{n} = \begin{cases} \infty, & \text{supergeometric,} \\ 0 < c < \infty, & \text{geometric,} \\ 0, & \text{subgeometric.} \end{cases} \quad (3.13)$$

Note that the rate of convergence is an asymptotic quantity. In practical applications, the effective rate of convergence might differ from the asymptotic one, if the actual rate of convergence only sets in at a precision lower than what is resolved.

Finally, let us discuss the quality of the approximated series. Three different types of errors arise. The most obvious one is the truncation error, which originates from the fact that only finitely many coefficients of the series are taken into account. The so-called interpolation error comes from the collocation method, namely that we insist that the interpolant and the function agree on a finite set of points. Finally, the most subtle error comes from the fact that a truncated series differs from the exact expansion up to the same order due to discretisation effects. Since in practice, we do not know the exact solution, we have to estimate these errors. It is often assumed that all three errors have the same order of magnitude, and we will do so too. The truncation error can practically be estimated by the rate of convergence and the size of the last retained coefficient, noting that all Chebyshev polynomials are bounded by unity. For geometric exponential convergence,

$$\left| f(x) - \sum_{n=0}^N f_n T_n \right| \leq \sum_{n=N+1}^{\infty} |f_n| \leq \kappa \sum_{n=N+1}^{\infty} e^{-cn} = \frac{\kappa e^{-cN}}{e^c - 1} \sim |f_N|, \quad (3.14)$$

while for algebraic convergence,

$$\begin{aligned} \left| f(x) - \sum_{n=0}^N f_n T_n \right| &\leq \sum_{n=N+1}^{\infty} |f_n| \leq \kappa \sum_{n=N+1}^{\infty} n^{-q} = \kappa \zeta(q, N+1) \\ &= \left( \frac{N}{q-1} - \frac{1}{2} + \mathcal{O}(N^{-2}) \right) \kappa N^{-q} \sim N |f_N|. \end{aligned} \quad (3.15)$$

Here  $\kappa$  is a positive real constant which depends on the function  $f$ , and  $\zeta(a, b)$  is the Hurwitz zeta function. In practice, one can fit the last few retained coefficients to estimate  $c$  and  $q$ , respectively.

### 3.3. Algorithmic details and implementation

Now we will discuss some details of the actual use of pseudo-spectral methods, and show why not only theoretically, but also practically they offer many advantages. To evaluate a sum of Chebyshev polynomials, the Clenshaw algorithm [205] is used, which is a generalisation of Horner's method, and can be applied to any class of functions which is defined by a three-term recurrence. For Chebyshev polynomials, one computes the values  $b_n$  with

$$\begin{aligned} b_{N+2} &= b_{N+1} = 0, \\ b_n &= f_n + 2xb_{n+1} - b_{n+2}. \end{aligned} \tag{3.16}$$

The value of the function  $f$  at  $x$  is then given by

$$f(x) = f_0 + xb_1 - b_2. \tag{3.17}$$

Due to the recursive nature of the Clenshaw algorithm, it is both fast and stable. A similar algorithm exists to calculate the coefficients  $f'_n$  of the Chebyshev expansion of the derivative of  $f$ . Clearly,  $f'$  is a polynomial of order  $N - 1$ , and the coefficients are

$$\begin{aligned} f'_{N-1} &= 2Nf_N, \\ f'_{N-2} &= 2(N-1)f_{N-1}, \\ f'_n &= 2(n+1)f_{n+1} + f'_{n+2}, \\ f'_0 &= f_1 + \frac{1}{2}f'_2. \end{aligned} \tag{3.18}$$

It is also possible to invert this algorithm to get an expansion of the primitive function. With these preparations, (3.3) can indeed be transformed to a system of nonlinear equations for the coefficients  $f_n$ . This system is then solved by a stabilised Newton-Raphson iteration. The Jacobian that arises there can be made almost block-diagonal if multiple domains are used. To calculate the Jacobian, automatic differentiation is employed, which delivers derivatives w.r.t. coefficients numerically to machine precision. For an introduction to automatic differentiation see [206–208]. To achieve high performance, a curiously recurring template pattern is employed.

Numerical results on differential equations that are presented in this work are based on C++ code written jointly with Julia Borchardt, using the libraries BOOST [209], Eigen [210] and Blitz [211]. Fixed point equations were discussed in [153], whereas flows were studied in [154]. Several other works have used (parts of) the code [156, 201, 212, 213].

### 3.4. Example: Fixed point structure of the $O(N)$ model

To illustrate the use of pseudo-spectral methods in the present context, we will now discuss the  $O(N)$  model in 3 dimensions for  $N = 1, 3$  at NLO in the derivative expansion. For  $N = 1$ , we end up with the well-known Wilson-Fisher fixed point [214]. It is probably the best studied model in the FRG [153, 215–224], and describes the critical behaviour of interacting spins. The case  $N = 3$  describes many properties of magnetic materials, *e.g.* the Curie transition in isotropic ferromagnets, and antiferromagnets at the Néel transition point [225]. The results for  $N = 1$  have been published in [201].

Both models are described by the following ansatz for the effective average action:

$$\Gamma = \int d^3x \left( \frac{1}{2} Z_\phi(\rho) (\partial_\mu \phi_a) (\partial^\mu \phi^a) + \frac{1}{2} Y_\phi(\rho) (\partial_\mu \rho) (\partial^\mu \rho) + V(\rho) \right). \quad (3.19)$$

The index  $a$  of the  $O(N)$ -symmetric vector field  $\phi^a$  runs from 1 to  $N$ , and we introduced  $\rho = \phi_a \phi^a / 2$ . For  $N = 1$ , the two kinetic terms are linearly dependent, and we will set  $Y = 0$  in this case. The regulator is chosen as

$$\Delta S = \int d^3x \left( \frac{1}{2} \phi_a \mathfrak{R}_\phi \left( \frac{p^2}{k^2} \right) \phi^a \right), \quad (3.20)$$

and we choose the Litim regulator for definiteness [226]. To discuss critical behaviour, dimensionless or renormalised quantities have to be introduced. At the present order of approximation, there is an ambiguity in how to define the renormalised quantities, namely in the choice of where we normalise the wave function renormalisation  $Z_\phi$ . In the following, we will fix  $Z_\phi(0) = 1$ , a broader discussion of this issue together with regulator variations can be found in [201] for the Ising model. The anomalous dimension is thus defined as

$$\eta = -\partial_t \ln Z_\phi(0). \quad (3.21)$$

The flow equations were derived with *xAct* as described in the previous chapter. As a side remark, since the potential itself doesn't appear on the right-hand side of the flow equation, only its derivatives, we will solve the flow equation for the derivative of  $V$ .

We will start with the Ising model. In Figure 3.3, the solution to the fixed point equations is shown. For the first critical exponent and the anomalous dimension, we find

$$\begin{aligned} \theta_1 &= 1.597, \\ \eta &= 0.049. \end{aligned} \quad (3.22)$$

This can be compared to results obtained by other methods, *e.g.* Monte Carlo (MC) [227]

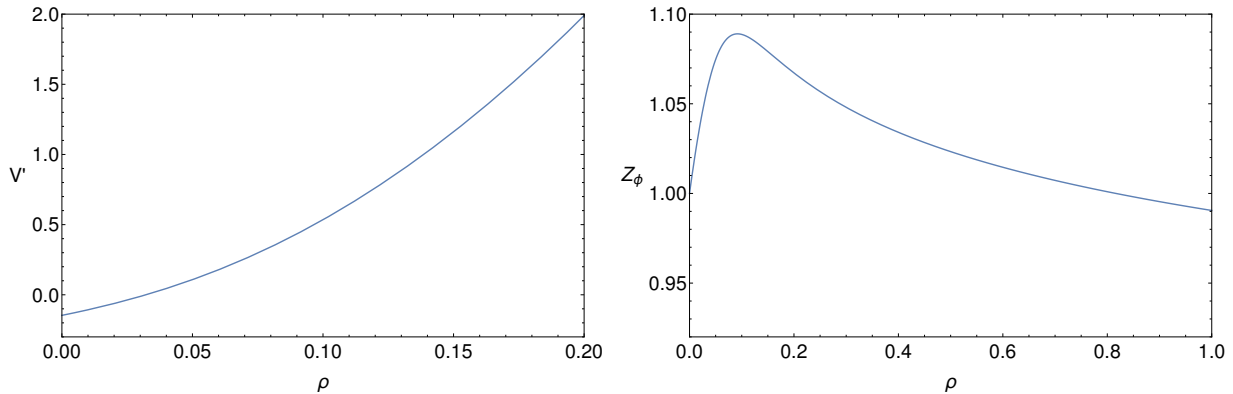


Fig. 3.3.: The solution to the fixed point equations of the Ising model.

and conformal bootstrap (CBS) [149]:

$$\begin{aligned}
 \theta_1^{\text{MC}} &= 1.58725(25), \\
 \eta^{\text{MC}} &= 0.03627(10), \\
 \theta_1^{\text{CBS}} &= 1.587375(10), \\
 \eta^{\text{CBS}} &= 0.0362978(20).
 \end{aligned}
 \tag{3.23}$$

The first critical exponent agrees rather well with the (computationally much more expensive) results from MC and CBS, the anomalous dimension needs further improvement. These results can be optimised by varying the regulator [201], reducing this discrepancy. Even better results can be obtained by the so-called BMW-approximation [221, 228], which retains both field and momentum dependence, but is again computationally much more expensive.

In a similar fashion, we can now discuss the  $O(3)$  model. Again, we show the solution to the fixed point equations in Figure 3.4, this time comprising three functions. The first critical exponent and the anomalous dimension are

$$\begin{aligned}
 \theta_1 &= 1.430, \\
 \eta &= 0.052.
 \end{aligned}
 \tag{3.24}$$

Again, we compare to recent MC [229] and CBS [230] results:

$$\begin{aligned}
 \theta_1^{\text{MC}} &= 1.4053(20), \\
 \eta^{\text{MC}} &= 0.0378(3), \\
 \theta_1^{\text{CBS}} &= 1.4043(55), \\
 \eta^{\text{CBS}} &= 0.03856(124).
 \end{aligned}
 \tag{3.25}$$

The same comments as in the Ising case apply here - the critical exponent is reasonably close for the rather small costs, and significant improvement is expected once momentum

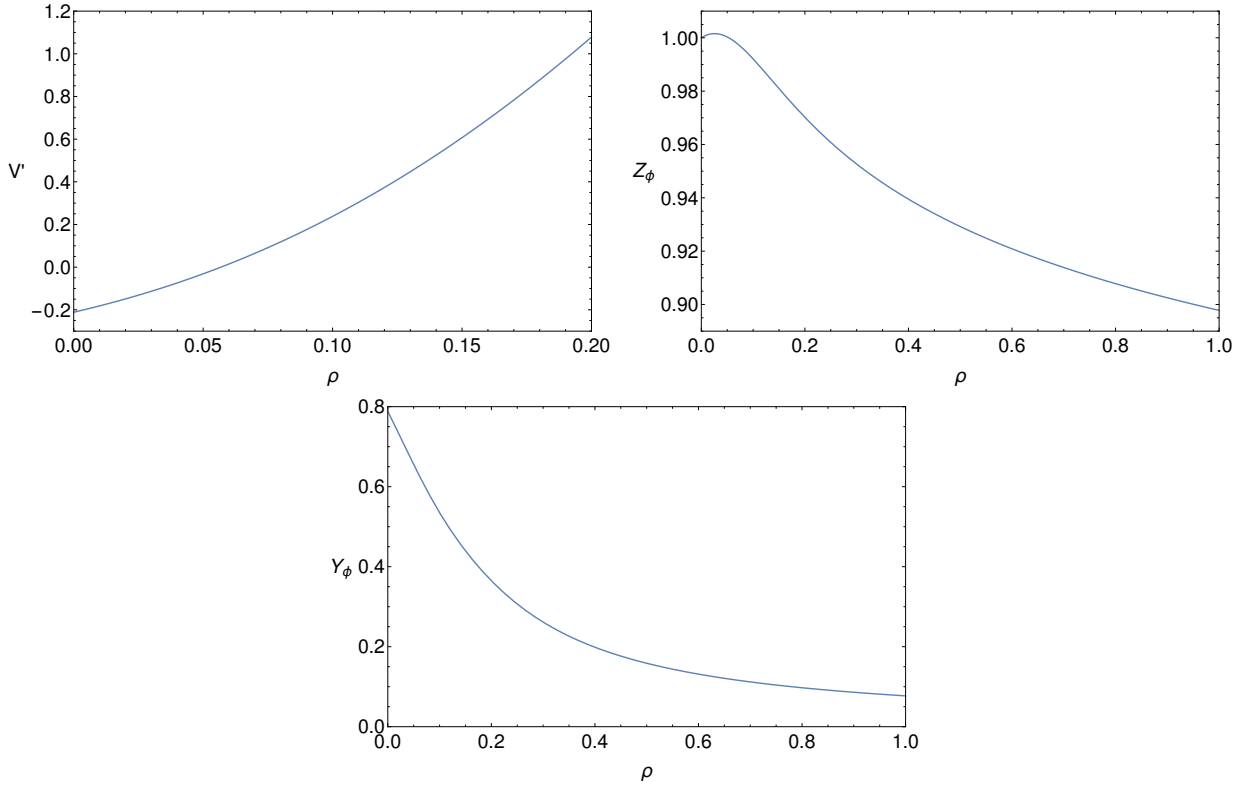


Fig. 3.4.: The solution to the fixed point equations of the Heisenberg, or  $O(3)$  model.

dependence is included.

We should stress that to obtain these results numerically, the code ran only a few seconds on an Intel i7-4770S@3.1GHz. This is to be contrasted to the immense computational cost of MC and CBS calculations.

## 4. Quantum gravity

After the technical part, we will now turn our attention to the first physical application, the quantisation of gravity. This chapter discusses four different aspects of the Asymptotic Safety (AS) approach to quantum gravity. In the first part, we present the most impressive result of the whole thesis: we show that the 2-loop counterterm, which hallmarks the breakdown of perturbation theory in gravity, is an irrelevant operator at the interacting fixed point of AS. Second, we study the gauge and parameterisation dependence of background flows, which also checks what potentially can happen in more extended truncations. Afterwards, we switch to genuine bimetric calculations. There, we discuss results on gravitational correlation functions obtained by a vertex expansion in the fluctuation field, and introduce a new notion of locality. We will consider couplings up to linear order in the background curvature. Some aspects of the gauge dependence of correlation functions is discussed. Finally, we open a new door to possible truncations by showing how to overcome the limitations of vertex expansions in quantum gravity, allowing for the resolution of arbitrarily high correlation functions.

The first part was published in [47], the second in [155], the third in [45] and includes yet unpublished results obtained with Stefan Lippoldt; the final part is still work in progress.

In this section we work exclusively with Euclidean signature, assuming that a Wick rotation can be done back to Lorentzian signature. A potential way to overcome this is the use of an ADM decomposition [231–237].

### 4.1. The gravitational two-loop counterterm in Asymptotic Safety

General relativity, based on the Einstein-Hilbert action, provides a highly successful classical description of gravitational phenomena from sub-millimeter to cosmic scales. A central puzzle for the construction of a consistent quantum theory of gravity is its perturbative nonrenormalisability. This is manifested by the fact that an expansion in terms of Newton's constant about flat spacetime gives rise to a divergence at two-loop order. This spoils meaningful predictions for  $S$ -matrix elements, unless a Goroff-Sagnotti counterterm of the form [238–240]

$$\Gamma_{\text{div}}^{\text{GS}} = \frac{1}{\epsilon} \frac{209}{2880} \frac{32\pi G}{(16\pi^2)^2} \int d^4x \sqrt{g} C_{\mu\nu}{}^{\kappa\lambda} C_{\kappa\lambda}{}^{\rho\sigma} C_{\rho\sigma}{}^{\mu\nu} \quad (4.1)$$



with the Weyl tensor  $C_{\mu\nu\rho\sigma}$ , is added to the bare action in order to cancel the divergence (in dimensional regularisation). In combination with power counting arguments, this is taken as a signal that an infinite number of counterterms is needed to render the full perturbative expansion meaningful. Since renormalisation theory relates each counterterm to a free parameter to be fixed from experimental data, the appearance of the Goroff-Sagnotti term suggests that the perturbative quantisation of the Einstein-Hilbert action requires fixing infinitely many parameters. This observation is often interpreted as evidence that conventional quantisation of gravity is doomed to fail.

The presence of the counterterm (4.1) triggered the investigation of a variety of alternative routes towards quantising gravity, *e.g.* by modifying the quantisation rules, changing the fundamental degrees of freedom, or abandoning local quantum field theory altogether as a fundamental framework for quantum gravity [241–243]. Ultimately, any consistent quantum gravity theory allowing for a classical limit containing Einstein’s theory of gravity, as well as its semi-classical extension as a low energy effective theory for quantised gravitons, has to clarify the fate of the divergencies related to the Goroff-Sagnotti term.

This requirement is more than a technical necessity, as renormalisability - beyond being a strategy of handling divergencies - is a statement about the separability of low energy observables from physics at highest energy scales. For instance, quantum gravity scenarios that start from discretised building blocks of spacetime and a fundamental length scale may render all divergencies finite. Still,  $S$ -matrix elements would generically receive large contributions from potentially large higher order operators, requiring to fix a substantial, if not infinite, set of physical parameters.

At first sight, a natural solution appears to be that the divergencies cancel, *e.g.* because of a new symmetry at a more fundamental level. While certainly possible, the problem of separation of low energy physics from highest energy scales may come in again through the backdoor, as this symmetry has to be broken (or restored) at low energy potentially requiring a fine-tuned separation of scales and a large number of parameters.

An indiscriminate association of (4.1) with quantum field theory approaches to quantum gravity ignores the fact that the Wilsonian viewpoint of renormalisation already offers a solution to this puzzle: higher dimensional operators decouple from the low energy physics proportional to an inverse power of a high scale  $\Lambda$ , provided such operators do not acquire large anomalous dimensions. For instance, the  $C^3$  operator in (4.1) would be expected to decouple  $\sim 1/\Lambda^2$  if the anomalous dimension was small. If so, the  $1/\epsilon$ -pole may merely indicate a subleading log-correction as sensed by dimensional regularisation. This may sound like a circular argument, as such conclusions can only be drawn in perturbation theory after the theory has been renormalised. Nevertheless, the Wilsonian viewpoint is known to hold also in systems with a similar breakdown of perturbative quantisation, where a well-controllable UV limit is facilitated by the existence of an interacting RG fixed point [244–246].

In this section, we provide novel evidence that the Goroff-Sagnotti term is indeed an irrelevant operator from the Wilsonian viewpoint. Our results demonstrate that the challenge posed by the perturbative two-loop analysis is solved by a renormalisation flow that decouples the high scale physics from (semi-)classical Einsteinian low energy gravity in much the same way as in conventional quantum field theories. For this, we determine the decoupling of the Goroff-Sagnotti term towards the IR quantitatively.

The new ingredient compared to the perturbative analysis is the investigation of the RG flow beyond the perturbative Gaussian fixed point (GFP). In fact, our results confirm the existence of an interacting non-Gaussian fixed point (NGFP) that controls the high energy limit of gravity, as required for the AS scenario [35, 245–250]. By now, the existence of a suitable NGFP has been established within many approximations [38, 41–45, 186, 251–264]. In particular, it has been shown in the case of gravity coupled to scalar matter that the AS mechanism remains intact once the one-loop counterterm is included [256, 257]. Paralleling this observation, we establish that the Goroff-Sagnotti term supplements only a subdominant quantitative correction to the high energy behaviour of pure gravity: the  $C^3$  operator approaches an interacting fixed point in the UV and becomes irrelevant towards the IR at an even enhanced rate compared to canonical scaling.

This demonstrates that the AS scenario for quantum gravity can solve this long-standing puzzle in a constructive and quantifiable manner, disclosing the two-loop divergence of (4.1) as a mere perturbative artifact.

#### 4.1.1. Tensor monomial basis and perturbative analysis

We start by a short outline of how quantum gravity based on the perturbative quantisation of the Einstein-Hilbert action,

$$\Gamma^{\text{EH}} = \frac{1}{16\pi G_N} \int d^4x \sqrt{g} (-R + 2\Lambda), \quad (4.2)$$

fails. Here,  $G_N$  is the Newton's constant,  $\Lambda$  the cosmological constant and  $R$  the Ricci scalar. Before we consider perturbation theory, we introduce a basis for curvature terms. It turns out to be useful to employ a completely tracefree basis, which is equivalent to using the irreducible components of the respective tensors. The basis in four dimensions up to order three, ordered w.r.t. the power of curvature tensors, is given by

- order 0:  $\mathbb{1}$ ,
- order 1:  $R$ ,
- order 2:  $R^2$ ,  $S_{\mu\nu}S^{\mu\nu}$  and  $C_{\mu\nu\rho\sigma}C^{\mu\nu\rho\sigma}$ ,
- order 3:  $R\Delta R$ ,  $S_{\mu\nu}\Delta S^{\mu\nu}$ ,  $R^3$ ,  $RS_{\mu\nu}S^{\mu\nu}$ ,  $S_{\mu}^{\nu}S_{\nu}^{\rho}S_{\rho}^{\mu}$ ,  $S_{\mu\rho}S_{\nu\sigma}C^{\mu\nu\rho\sigma}$ ,  $RC_{\mu\nu\rho\sigma}C^{\mu\nu\rho\sigma}$  and  $C_{\mu\nu}^{\kappa\lambda}C_{\kappa\lambda}^{\rho\sigma}C_{\rho\sigma}^{\mu\nu}$ .

In this,  $S_{\mu\nu}$  is the tracefree part of the Ricci tensor, and  $\Delta = -D^2$  is the Laplacian of the covariant derivative  $D$ . In higher dimensions, two further invariants exist,  $S_{\mu\nu}C^{\mu\alpha\beta\gamma}C^{\nu}_{\alpha\beta\gamma}$  and  $C^{\alpha}_{\mu}{}^{\beta}_{\nu}C^{\mu}_{\rho}{}^{\nu}_{\sigma}C^{\rho}_{\alpha}{}^{\sigma}_{\beta}$ . In four dimensions, the first vanishes because of the identity

$$C^{\alpha\mu\nu\rho}C^{\beta}_{\nu\mu\rho} = \frac{1}{2}C^{\alpha\mu\nu\rho}C^{\beta}_{\mu\nu\rho}, \quad (4.3)$$

which follows from the first Bianchi identity. The second is proportional to the other  $C^3$  invariant in four dimensions, which can be derived from antisymmetrisation over 6 indices. All other possible invariants that can be formed can be mapped onto this basis. In particular, with the help of the second Bianchi identity, one can show that

$$\begin{aligned} C_{\mu\nu\rho\sigma}\Delta C^{\mu\nu\rho\sigma} = & -\frac{(d-2)(d-3)}{d(d-1)}R\Delta R + 4\frac{d-3}{d-2}S_{\mu\nu}\Delta S^{\mu\nu} + 4\frac{d-3}{(d-1)(d-2)}RS_{\mu\nu}S^{\mu\nu} + 4\frac{d(d-3)}{(d-2)^2}S^{\nu}_{\mu}S^{\rho}_{\nu}S^{\mu}_{\rho} \\ & - 4\frac{d-3}{d-2}S_{\mu\rho}S_{\nu\sigma}C^{\mu\nu\rho\sigma} - \frac{2}{d}RC_{\mu\nu\rho\sigma}C^{\mu\nu\rho\sigma} - 2S_{\mu\nu}C^{\mu\alpha\beta\gamma}C^{\nu}_{\alpha\beta\gamma} \\ & + C^{\kappa\lambda}_{\mu\nu}C^{\rho\sigma}_{\kappa\lambda}C^{\mu\nu}_{\rho\sigma} + 4C^{\alpha}_{\mu}{}^{\beta}_{\nu}C^{\mu}_{\rho}{}^{\nu}_{\sigma}C^{\rho}_{\alpha}{}^{\sigma}_{\beta} + D_{\sigma}D_{\kappa}\left(-4C^{\sigma}_{\mu}{}^{\kappa}_{\nu}S^{\mu\nu}\right. \\ & \left.- 8\frac{d-3}{d-2}S^{\sigma}_{\mu}S^{\mu\kappa} + 4\frac{d-3}{d-2}g^{\sigma\kappa}S_{\mu\nu}S^{\mu\nu} + 2\frac{(3d-4)(d-3)}{d(d-1)}RS^{\sigma\kappa} - 2\frac{(d-3)(d-2)}{d^2}g^{\sigma\kappa}R^2\right). \end{aligned} \quad (4.4)$$

This equation shows that a covariantly constant Weyl tensor influences the Goroff-Sagnotti term, and one must be careful in choosing a suitable background.

Let us now discuss the perturbative argument. By power counting at the one-loop order, all operators quadratic in curvature will be generated [265]. This is to say, the one-loop divergence has the form

$$\Gamma_{\text{div}}^{1l} \sim \frac{1}{\epsilon} \int d^4x \sqrt{g} \left( a_1 R^2 + a_2 S_{\mu\nu} S^{\mu\nu} + a_3 C_{\mu\nu\rho\sigma} C^{\mu\nu\rho\sigma} \right), \quad (4.5)$$

with coefficients  $a_i$  that have to be determined. At the end of the day, only on-shell divergences have to be renormalised. The on-shell condition, *i.e.* Einstein's field equations, in the tracefree basis read

$$R = 4\Lambda \quad \text{and} \quad S_{\mu\nu} = 0. \quad (4.6)$$

Thus, if we restrict to the case of a vanishing cosmological constant (which is reasonably close to observation), the first two terms in (4.5) are off-shell divergences. Finally, in four dimensions, the Euler characteristic

$$\chi_E = \frac{1}{32\pi} \int d^4x \sqrt{g} \left( \frac{1}{6}R^2 - 2S_{\mu\nu}S^{\mu\nu} + C_{\mu\nu\rho\sigma}C^{\mu\nu\rho\sigma} \right) \quad (4.7)$$

is a topological invariant, which removes the final divergence. Thus gravity based on an Einstein-Hilbert action is one-loop finite.

At two loops, the same on-shell argument can be used, and all but one of the basis elements of third order in curvature vanishes. The only potential divergence can come with

the monomial  $C_{\mu\nu}{}^{\kappa\lambda}C_{\kappa\lambda}{}^{\rho\sigma}C_{\rho\sigma}{}^{\mu\nu}$ . It turns out that no cancellation mechanism is present, and the expected divergence indeed arises. This was shown first by Goroff and Sagnotti [238, 239], and later confirmed by van de Ven [240], the resulting divergence being (4.1).

### 4.1.2. Nonperturbative analysis - truncation

We study the gravitational RG flow projected onto the Einstein-Hilbert action supplemented by the two-loop counterterm (4.1). Our ansatz for the gravitational part of the effective average action, closely following [240], reads

$$\Gamma = \Gamma^{\text{EH}} + \Gamma^{\text{GS}}. \quad (4.8)$$

Here

$$\Gamma^{\text{GS}} = \bar{\sigma} \int d^4x \sqrt{g} C_{\alpha\beta}{}^{\mu\nu} C_{\mu\nu}{}^{\rho\sigma} C_{\rho\sigma}{}^{\alpha\beta} \quad (4.9)$$

is the two-loop counterterm found by Goroff and Sagnotti with a scale dependent coupling  $\bar{\sigma}$ . The gravitational part of the effective average action is supplemented by a standard gauge fixing procedure and we adhere to the harmonic gauge used in [35]. Gauge fixing and dependence of results on gauge choices will be discussed in the next section in more detail to allow for a clean presentation of the results of this section. The perturbative result (4.1) suggests that  $\bar{\sigma}$  diverges at least as  $\ln k$  for  $k \rightarrow \infty$  even in the flat space on-shell limit  $\Lambda \rightarrow 0$  and after the Newton coupling has been renormalised.

The RG flow of the couplings is found by substituting the ansatz (4.8) into the flow equation and computing the coefficients multiplying the curvature terms appearing in (4.2) and (4.9). The evaluation of the trace utilises the technology of the universal RG machine [266] together with off-diagonal heat kernel methods [267–272].

Two crucial features make this formidable computation feasible: firstly, we use the Ricci scalar, tracefree Ricci tensor, and Weyl tensor to construct a basis for the interaction monomials containing a fixed number of covariant derivatives. The essential building block of the RG flow is the second functional derivative  $\Gamma^{(2)}$  of the action. The corresponding term  $\Gamma^{\text{GS}^{(2)}}$  arising from (4.9) results in a sum of terms containing at least one power of the Weyl tensor. Since  $C$  is tracefree by construction, all its contractions with the metric vanish, such that no term  $\sim \sqrt{g}R$  or  $\sim \sqrt{g}$  is generated. This entails that there is no feedback of the Goroff-Sagnotti term on the RG flow of Newton's constant and the cosmological constant. We conclude already at this point that the AS properties observed in the Einstein-Hilbert sector are stable upon the inclusion of the Goroff-Sagnotti term. Secondly, the contribution of the Goroff-Sagnotti term to the two-point correlator is of the form  $\bar{\sigma} (C + \text{higher powers of the curvature})$ . This structure implies that the  $\beta$  function encoding the flow of  $\bar{\sigma}$  is a cubic in  $\bar{\sigma}$  with coefficients depending on Newton's constant and the cosmological constant. As a cubic has at least one real zero, also the Goroff-Sagnotti coupling

must have a fixed point and hence the associated dimensionless coupling does not necessarily diverge for  $k \rightarrow \infty$ . The remaining crucial question is whether the  $C^3$  term is a relevant (as suggested by perturbation theory) or an irrelevant operator. In case of irrelevance, the Goroff-Sagnotti term does neither require the fixing of an additional physical parameter nor induces a proliferation of counterterms.

In order to determine the coefficients of this cubic it suffices to isolate the term  $\sim C^3$  from the flow equation. As the curvature terms are orthogonal, any term containing a Ricci scalar or tracefree Ricci tensor will not contribute to  $C^3$  and it is sufficient to keep track of powers of the Weyl tensor and its covariant derivatives. Formally, this can be achieved with a background metric  $\bar{g}_{\mu\nu}$  of a Ricci-flat  $K3$ -surface; our results are, however, independent of such a convenient background choice. The vertices entering the computation have been constructed with the Mathematica package *xAct* [191–196]. Employing the simplifications of a  $K3$ -background, the Goroff-Sagnotti vertex contains 900 terms whereas the Einstein-Hilbert vertex has only a single term. The computation was done with *xAct* within one month of CPU time on a core with 2.8 GHz. Most of the CPU time is used for the two vertex diagram due to the enormous number of terms generated by the product rule for covariant derivatives. This makes the present computation quite formidable.

### 4.1.3. $\beta$ functions

The RG flow resulting from the ansatz (4.8) is conveniently written in terms of dimensionless couplings  $g_i \equiv \{\lambda, g, \sigma\}$ ,

$$\lambda \equiv \Lambda k^{-2}, \quad g \equiv G k^2, \quad \sigma \equiv \bar{\sigma} k^2, \quad (4.10)$$

and expressed in terms of the  $\beta$  functions

$$\partial_t g_i \equiv \beta_{g_i}(\lambda, g, \sigma). \quad (4.11)$$

The  $\beta$  functions for the dimensionless Newton's constant and cosmological constant have been known since the beginning of the AS program [35]. In four spacetime dimensions and for the Litim regulator [226] they read

$$\begin{aligned} \beta_g &= (2 + \eta_N) g, \\ \beta_\lambda &= (\eta_N - 2) \lambda + \frac{g}{2\pi} \left( \frac{5}{1-2\lambda} - 4 - \frac{5}{6} \eta_N \frac{1}{1-2\lambda} \right). \end{aligned} \quad (4.12)$$

Here  $\eta_N$  denotes the anomalous dimension of Newton's constant,

$$\eta_N = \frac{g B_1}{1 - g B_2}, \quad (4.13)$$

with

$$\begin{aligned} B_1 &= \frac{1}{3\pi} \left( \frac{5}{1-2\lambda} - \frac{9}{(1-2\lambda)^2} - 5 \right), \\ B_2 &= -\frac{1}{6\pi} \left( \frac{5}{2(1-2\lambda)} - \frac{3}{(1-2\lambda)^2} \right). \end{aligned} \quad (4.14)$$

The ansatz (4.8) complements this system by a  $\beta$  function for  $\sigma$ ,

$$\beta_\sigma = c_0 + (2 + c_1)\sigma + c_2\sigma^2 + c_3\sigma^3, \quad (4.15)$$

where the coefficients  $c_i(g, \lambda)$  are given by

$$\begin{aligned} c_0 &= \frac{1}{64\pi^2(1-2\lambda)} \left( \frac{2-\eta_N}{2(1-2\lambda)} + \frac{6-\eta_N}{(1-2\lambda)^3} - \frac{5\eta_N}{378} \right), \\ c_1 &= \frac{3g}{16\pi(1-2\lambda)^2} \left( 5(6 - \eta_N) + \frac{23(8-\eta_N)}{8(1-2\lambda)} - \frac{7(10-\eta_N)}{10(1-2\lambda)^2} \right), \\ c_2 &= \frac{g^2}{2(1-2\lambda)^3} \left( \frac{233(12-\eta_N)}{10} - \frac{9(14-\eta_N)}{7(1-2\lambda)} \right), \\ c_3 &= \frac{6\pi g^3(18-\eta_N)}{(1-2\lambda)^4}. \end{aligned} \quad (4.16)$$

We emphasise that the highest order coefficient  $c_3$  is positive for any admissible  $\lambda$ , positive Newton coupling  $g > 0$ , and  $\eta_N < 18$ . Positive  $c_3$  gives rise to at least one real fixed point where the coupling  $\sigma$  is irrelevant. We have verified that  $c_3$  is gauge independent, and that its positivity is independent of the metric parameterisation [155, 273–278], which we will study in another context in the next section. The  $\beta$  function (4.15) is computed *for the first time* and constitutes one of the main result of this thesis.

The gauge independence of  $c_3$  can readily be understood. For this, note that the coefficient  $c_3$  comes from contributions where the two variations in the calculation of  $\Gamma^{(2)}$  each act on one Weyl tensor, such that only a single Weyl tensor remains. One then needs three such insertions to get the coefficient cubic in  $\sigma$ , which is exactly  $c_3$ . Thus, we only have to look at the first variation of the Weyl tensor, where we can neglect the background curvature:

$$\delta C_{\mu\nu}{}^{\rho\sigma} = 2D^{[\rho}D_{[\nu}h^{\text{T}}{}_{\mu]}{}^{\sigma]} + D^2\delta_{[\nu}^{[\sigma}h^{\text{T}}{}_{\mu]}{}^{\rho]} + \mathcal{O}(R). \quad (4.17)$$

We can see that the first variation of the Weyl tensor only includes the transverse traceless mode of the fluctuation,  $h^{\text{T}}$ , which is the physical tensorial mode to linear order, and thus independent of gauge choices.

#### 4.1.4. Fixed points and RG flow

The Wilsonian viewpoint links renormalisability to fixed points  $g_{i,*}$  of the underlying RG flow where the  $\beta$  functions vanish. Linearising the  $\beta$  functions at a fixed point, local properties of the flow are encoded in the critical exponents. Relevant directions, corresponding to free parameters of the theory to be fixed by experiment, are associated with positive critical

exponents.

Already the first calculations [35, 36, 279] revealed that the system (4.12) exhibits a GFP and an NGFP,

$$\begin{aligned} \text{GFP}^{\text{EH}} : \quad & \lambda_* = 0, \quad g_* = 0 \\ \text{NGFP}^{\text{EH}} : \quad & \lambda_* = 0.193, \quad g_* = 0.707. \end{aligned} \tag{4.18}$$

The GFP corresponds to a free theory and is a saddle point: trajectories with a positive Newton coupling do not end at the GFP at high energies, reflecting the perturbative non-renormalisability of the Einstein-Hilbert action in the Wilsonian framework. The NGFP exhibits a complex pair of critical exponents

$$\theta_{1,2} = 1.475 \pm 3.043 \mathbf{i}. \tag{4.19}$$

Thus the NGFP is UV attractive for both Newton's constant and the cosmological constant making it suitable for AS.

The  $\beta$  function (4.15) clarifies the fate of the fixed point structure (4.18) once the counterterm (4.9) is taken into account. Substituting  $\lambda_* = g_* = 0$  into the  $\beta$  function for  $\sigma$  shows that the  $\text{GFP}^{\text{EH}}$  is mapped to

$$\text{GFP}^{\text{GS}} : \quad \lambda_* = 0, \quad g_* = 0, \quad \sigma_* = -\frac{7}{128\pi^2}. \tag{4.20}$$

The stability coefficients of this fixed point coincide with the classical mass dimension of the coupling constants; the GFP remains a saddle point.

Focusing on the NGFP, it is illuminating to first study the Einstein-Hilbert induced approximation of the  $\beta$  function, where only the terms originating from (4.2) contribute to the running of  $\sigma$ . Since the contribution of the counterterm to the  $\beta$  function (4.15) is captured by the coefficients  $c_1, c_2$ , and  $c_3$  this approximation corresponds to setting  $c_1 = c_2 = c_3 = 0$ . In this limit the flow has a unique fixed point solution,

$$\text{sGFP}^{\text{GS}} : \quad \lambda_* = 0.193, \quad g_* = 0.707, \quad \sigma_* = -0.049, \tag{4.21}$$

with critical exponent  $\theta_3 = -2$ . This is the analogue of the Gaussian fixed point for  $\sigma$  shifted by the finite interactions of  $g$  and  $\lambda$  at the NGFP (4.18). The stability coefficient indicates that the new direction is irrelevant in agreement with power counting arguments.

Taking into account the full nonlinear contributions from the  $C^3$  term, the cubic (4.15) again has exactly one real root

$$\text{NGFP}^{\text{GS}} : \quad \lambda_* = 0.193, \quad g_* = 0.707, \quad \sigma_* = -0.305, \tag{4.22}$$

extending the NGFP known from the Einstein-Hilbert projection. The new critical exponent  $\theta_3 = -79.39$  is again negative, so that the new direction exhibits an even enhanced irrele-

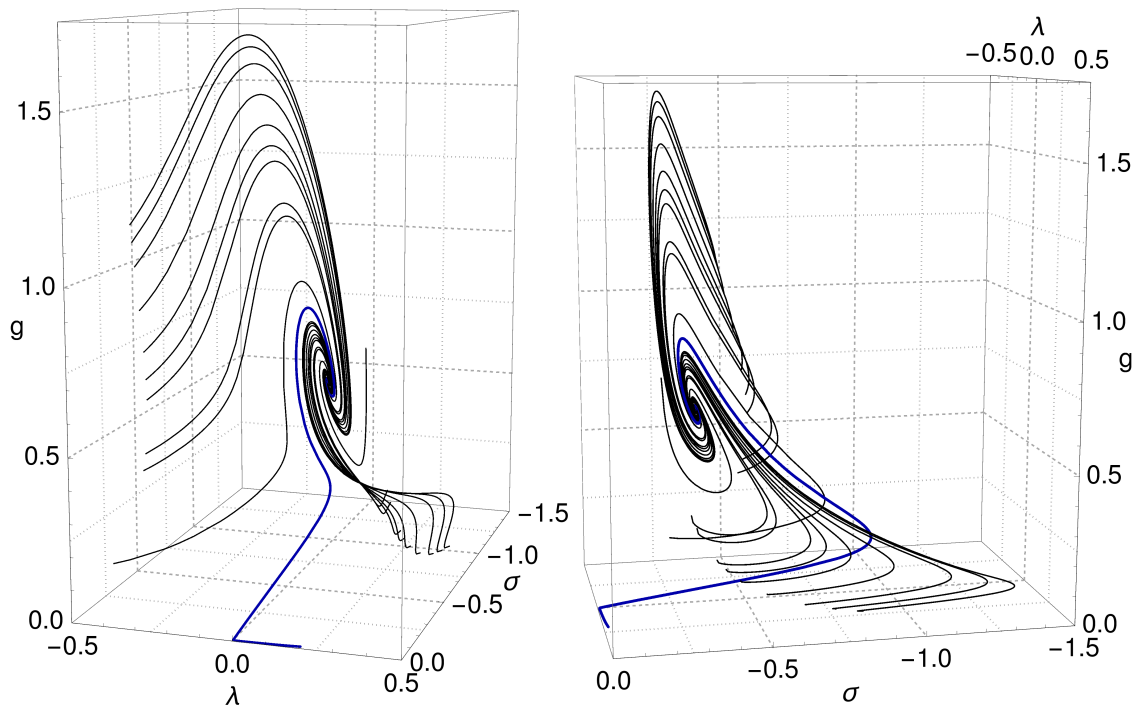


Fig. 4.1.: Phase diagram in  $(g, \lambda, \sigma)$  space from two perspectives depicting trajectories emanating from the NGFP. The thick blue line marks a trajectory with a long semi-classical regime near the GFP.

vance. In fact, the positivity of  $c_3$  ensures that  $\sigma$  always has a fixed point for which  $C^3$  is an irrelevant perturbation.

Figure 4.1 shows the phase diagram in the theory space spanned by  $(g, \lambda, \sigma)$ . The flow is governed by the interplay of the GFP (4.20) and the NGFP (4.22). The left panel depicts a  $(g, \lambda)$  perspective illustrating that the inclusion of the Goroff-Sagnotti term leaves AS as observed with the Einstein-Hilbert ansatz [35, 279] and the  $R^2$ -extension [258] fully intact. The thick blue line exemplifies a trajectory which crosses over from the NGFP at high energies to the GFP at low energies. In the vicinity of the GFP the trajectory develops a long semi-classical regime where the couplings scale classically. The right panel presents a  $(g, \sigma)$  perspective; following the semi-classical trajectory towards higher energies, we observe that the Goroff-Sagnotti coupling is first enhanced but then also attracted by the NGFP in the deep UV. The dimensionful Goroff-Sagnotti coupling  $\bar{\sigma} \rightarrow \sigma_*/k^2$  hence vanishes asymptotically for  $k \rightarrow \infty$ .

While the present ansatz (4.8) and calculation scheme give a unique answer (4.22) for the fixed point, the number of real roots of the cubic  $\beta$  function (4.15) depends sensitively on the fixed point values for  $g$  and  $\lambda$ . The inclusion of higher order operators thus has the potential to yield three fixed points. This does, however, not change our conclusion about



the irrelevance of the Goroff-Sagnotti term, as two of these fixed points have properties equivalent to those discussed above. As an example, let us consider the case where we neglect the cosmological constant, setting  $\lambda = 0$  at all scales. Then, the NGFP for Newton's constant has three extensions to the  $g, \sigma$ -plane. The one corresponding to (4.22) is located at  $g_* = 12\pi/23 \simeq 1.639$ ,  $\sigma_* = -0.226$  and has critical exponents  $\theta_1 = 23/11 \simeq 2.09$  and  $\theta_3 = -77.38$ . A second fixed point with the same  $g_*$  and  $\theta_1$  corresponds to the shifted Gaussian fixed point for the Goroff-Sagnotti coupling with  $\sigma_* = -0.0023$  and critical exponent  $\theta_3 = -6.06$ . This confirms the existence of the NGFP also in the zero-cosmological constant case analysed by Goroff and Sagnotti.

## 4.2. Gauge and parameterisation dependence

Physical observables are independent of their computational derivation. Still, many practical computations are based on convenient choices for intermediate auxiliary tools such as coordinate systems, gauges, etc. Appropriate parameterisations of the details of a system simply decrease the computational effort. Beyond pure efficiency aspects, such suitable parameterisations can also be conceptually advantageous or even offer physical insight. This is similar to coordinate choices in classical mechanics where polar coordinates with respect to the ecliptic plane in celestial mechanics support a better understanding in comparison with, say, Cartesian coordinates with a  $z$ -axis pointing towards Betelgeuse.

Appropriate parameterisations become particularly significant in quantum calculations. While on-shell quantities such as  $S$ -matrix elements are invariant observables [280–282], off-shell quantities generically feature parameterisation dependencies, including gauge, field parameterisation and regularisation scheme dependencies [283–285]. Further ordering schemes such as perturbative expansions may defer such dependencies to higher orders (such as scheme dependence in mass independent schemes), but these are merely special and not always useful limits. Approximation schemes that can also deal with nonperturbative regimes may even introduce further artificial parameterisation dependencies which have to be carefully removed (*e.g.* discretisation artefacts in lattice regularisations).

In an ideal situation, this parameterisation dependence of a nonperturbative approximation could be quantified and proven to be smaller than the error of the truncated solution. However, as soon as a result is parameterisation dependent, it is likely that some pathological parameterisation can be constructed that modifies the result in an arbitrary fashion. This suggests to look for general criteria of *good parameterisations* that minimise the artificial dependence in approximation schemes which adequately capture the physical mechanisms.

*A priori* criteria suggest the construction of parameterisations that support the identification of physically relevant degrees of freedom, such as the use of Coulomb-Weyl gauge in quantum optics, or the use of pole mass regularisation schemes in heavy-quark physics. Further *a priori* criteria include symmetry preserving properties (covariant gauges, nonlinear

field parameterisations) or strict implementations of a parameterisation condition such as the Landau gauge limit  $\alpha \rightarrow 0$ . A major advantage of the latter is that some redundant degrees of freedom decouple fully from the dynamical equations in such a limit.

Good parameterisations may also be identified *a posteriori* by allowing for a family of parameterisations and identifying stationary points in the parameter space. This realises the principle of minimum sensitivity [286, 287] (originally advocated for regularisation scheme dependencies), suggesting those points as candidate parameters for minimising the influence of parameterisation dependencies.

In this section, we investigate a two-parameter family of covariant gauges, a family of field parameterisations and the role of momentum dependent field rescalings in quantum gravity in this spirit. The family of gauges includes a (nonharmonic) generalisation of the harmonic gauge (de Donder gauge), the latter being particularly useful for the analysis of gravitational waves which presumably are the asymptotic states of quantum gravity. The a priori criteria suggest to implement this gauge in the Landau gauge limit to decouple a redundant part of the Hilbert space. In fact, in this limit we find a subtlety in the form of a degeneracy in the subspace of scalar field components which is special to gravity.

We also investigate a one-parameter family of field parameterisations that includes the most widely used linear split [288] as well as the exponential split [289–293] studied more recently in the context of AS [273–275, 278] – both of which find support by discriminative a priori arguments. We also take a brief look at the most general ultralocal four-parameter family of parameterisations to quadratic order, corroborating the results of the one-parameter family. In addition, we study the influence of momentum dependent field rescalings which are commonly used in gravity in connection with the York decomposition. In the context of the FRG, these parameterisation dependencies can mix nontrivially with the regularisation of the spectrum of fluctuations. Therefore, the analysis of parameterisation dependencies also explores implicitly the stability of the system in the UV.

Interestingly, we observe a nontrivial interplay between all these parameterisation dependencies. Still, several stationary points can be observed in the results for the RG flow where the system develops a remarkable insensitivity to the details of the parameterisation choices. In particular, for the stable parameterisations, we observe the existence of a UV stable non-Gaussian fixed point which provides further quantitative evidence for the existence of an asymptotically safe metric quantum gravity [245, 246]. In the stationary regime of the parameterisation based on the exponential split, the resulting RG flow exhibits several remarkable properties: (1) a possible dependence on the residual gauge parameter drops out implying an enhanced degree of gauge invariance, (2) the RG flow becomes particularly simple, such that the phase diagram in the plane of Newton’s and cosmological constant can be computed analytically, (3) no singularities arise in the flow, such that a large class of RG trajectories (including those with a classical regime) can be extended to arbitrarily high and low scales, (4) the UV critical exponents are real and close to their canonical counterparts,

and (5) indications are found that the AS scenario may not extend straightforwardly to dimensions much higher than  $d = 4$ .

### 4.2.1. Quantum gravity and parameterisations

The technical goal of quantum gravity is to construct a functional integral over suitable integration variables which in the long range limit can be described by a diffeomorphism invariant effective field theory of metric variables approaching a classical regime for a wide range of macroscopic scales. The fact that the first part of this statement is rather un-specific is reflected by the large number of legitimate quantisation proposals [5, 57, 294]. Independently of the precise choice of integration variables, a renormalisation group approach appears useful in order to facilitate a scale dependent description of the system and a matching to the long range classical limit which is given at least to a good approximation by an (effective) action of Einstein-Hilbert type, see (4.2).

We confine ourselves again to a quantum gravity field theory assuming that the metric itself is already a suitable integration variable. A first step towards a diffeomorphism invariant functional integral then proceeds via the Faddeev-Popov method involving a gauge choice for intermediate steps of the calculation. In this section, we use the background field gauge with the gauge fixing quantity,

$$F_\mu = \left( \delta_\mu^\beta \bar{D}^\alpha - \frac{1 + \beta}{d} \bar{g}^{\alpha\beta} \bar{D}_\mu \right) g_{\alpha\beta}, \quad (4.23)$$

which should vanish if the gauge condition is exactly matched. Here,  $g_{\alpha\beta}$  is the full (fluctuating) metric, whereas  $\bar{g}_{\alpha\beta}$  denotes a fiducial background metric which remains unspecified, but assists to keep track of diffeomorphism invariance within the background field method. Gauge fixing is implemented in the functional integral by means of the gauge fixing action

$$\Gamma_{\text{gf}} = \frac{1}{32\pi G_N \alpha} \int d^d x \sqrt{\bar{g}} \bar{g}^{\mu\nu} F_\mu F_\nu. \quad (4.24)$$

More precisely, this gauge choice defines a two-parameter  $(\alpha, \beta)$  family of covariant gauges. For instance, the choice  $\beta = 1$  corresponds to the harmonic/de Donder gauge which together with  $\alpha = 1$  (Feynman gauge) yields a variety of technical simplifications, being used in standard effective field theory calculations [295–297] as well as in functional RG studies [35, 250] of quantum gravity. More conceptually, the Landau gauge limit  $\alpha \rightarrow 0$  appears favourable, as it implements the gauge condition in a strict fashion and is a fixed point under RG evolution [298, 299]. We will return to this statement in the next section on correlation functions.

In the Euclidean formulation considered here, the parameter  $\alpha$  is bound to be nonnegative to ensure the positivity of the gauge fixing part of the action (this restriction may not be

necessary for a Lorentzian formulation). The parameter  $\beta$  can be chosen arbitrarily except for the singular value  $\beta_{\text{sing}} = d - 1$ . To elucidate this singularity, let us take a closer look at the induced Faddeev-Popov ghost term:

$$\Gamma_{\text{gh}} = - \int d^d x \sqrt{\bar{g}} \bar{C}_\mu \mathcal{M}^\mu{}_\nu C^\nu, \quad \mathcal{M}^\mu{}_\nu = \frac{\delta F^\mu}{\delta v^\nu}, \quad (4.25)$$

where  $v^\nu$  characterises the vector field along which we study the Lie derivative generating the coordinate transformations,

$$\frac{\delta g_{\alpha\beta}}{\delta v^\nu} = \frac{\delta}{\delta v^\nu} \mathcal{L}_v g_{\alpha\beta} = 2 \frac{\delta}{\delta v^\nu} D_{(\alpha} v_{\beta)}. \quad (4.26)$$

The corresponding variation of the gauge fixing condition yields

$$\delta F^\mu = 2 \left( \bar{g}^{\mu\alpha} \bar{D}^\beta - \frac{(1+\beta)}{d} \bar{g}^{\alpha\beta} \bar{D}^\mu \right) D_{(\alpha} \delta v_{\beta)}. \quad (4.27)$$

Let us decompose the vector  $\delta v_\beta$  into a transversal part  $\delta v_\beta^{\text{T}}$  and a longitudinal part  $D_\beta \delta\chi$ . For the following argument, it suffices to study the limit of the quantum metric approaching the background metric  $g_{\mu\nu} \rightarrow \bar{g}_{\alpha\beta}$ , which diagrammatically corresponds to studying the inverse ghost propagator ignoring higher vertices,

$$\delta F^\mu = (\delta_\nu^\mu \bar{D}^2 + \bar{R}_\nu^\mu) \delta v^{\text{T}\nu} + \frac{1}{2} \left( (d-1-\beta) \bar{D}^\mu \bar{D}_\nu + 4 \bar{R}_\nu^\mu \right) \bar{D}^\nu \delta\chi + \mathcal{O}(g - \bar{g}). \quad (4.28)$$

In this form it is obvious that the longitudinal direction  $\bar{D}^\nu \delta\chi$  is not affected by the gauge fixing for  $\beta = d - 1$  to zeroth order in the curvature. In other words, the gauge fixing is not complete for this singular case  $\beta_{\text{sing}} = d - 1$ . This singularity is correspondingly reflected by the ghost propagator. The Faddeev-Popov operator in (4.25) reads

$$\mathcal{M}^\mu{}_\nu = 2 \bar{g}^{\mu\beta} \bar{D}^\alpha D_{(\alpha} g_{\beta)\nu} - 2 \frac{1+\beta}{d} \bar{g}^{\alpha\beta} \bar{D}^\mu D_{\alpha} g_{\beta\nu}. \quad (4.29)$$

Decomposing the ghost fields  $\bar{C}_\mu, C^\nu$  also into transversal  $\bar{C}_\mu^{\text{T}}, C^{\text{T}\nu}$  and longitudinal parts  $\bar{D}^\mu \bar{\eta}, \bar{D}^\nu \eta$  we find for the ghost Lagrangian

$$\bar{C}_\mu \mathcal{M}^\mu{}_\nu C^\nu = \bar{C}_\mu^{\text{T}} \left( \delta_\nu^\mu \bar{D}^2 + \bar{R}_\nu^\mu \right) C^{\text{T}\nu} - \bar{\eta} \left( \frac{d-1-\beta}{2} \bar{D}^4 + \bar{R}^{\mu\nu} \bar{D}_\mu \bar{D}_\nu \right) \eta + \mathcal{O}(g - \bar{g}), \quad (4.30)$$

where we have performed partial integrations in order to arrive at a convenient form and dropped covariant derivatives of the curvature. This form of the inverse propagator of the ghosts makes it obvious that a divergence of the form  $\frac{1}{d-1-\beta}$  arises in the longitudinal parts. This divergence at  $\beta_{\text{sing}} = d - 1$  related to an incomplete gauge fixing will be visible in all our results below. In fact,  $\beta$  should be restricted to values smaller than the singular value - for larger values, the scalar ghost propagates with the wrong sign of the kinetic term.

Let us now turn to the metric modes. As a technical tool, we parameterise the fully dynamical metric  $g_{\mu\nu}$  in terms of a fiducial background metric  $\bar{g}_{\mu\nu}$  and fluctuations  $h_{\mu\nu}$  about the background. Background independence is obtained by keeping  $\bar{g}_{\mu\nu}$  arbitrary and requiring that physical quantities such as scattering amplitudes are independent of  $\bar{g}_{\mu\nu}$ . Still, these requirements do not completely fix the parameterisation of the dynamical field  $g = g[\bar{g}; h]$ . Several parameterisations have been used in concrete calculations. The most commonly used parameterisation is the *linear split* [288]

$$g_{\mu\nu} = \bar{g}_{\mu\nu} + h_{\mu\nu}. \quad (4.31)$$

By contrast, the *exponential split* [289–293]

$$g_{\mu\nu} = \bar{g}_{\mu\rho} (e^h)^\rho{}_\nu, \quad (4.32)$$

is a parameterisation that has been discussed more recently to a greater extent [273–275, 278]. In both cases,  $h$  is considered to be a symmetric matrix field (with indices raised and lowered by the background metric). If a path integral of quantum gravity is now defined by some suitable measure  $\mathcal{D}h$ , it is natural to expect that the space of dynamical metrics  $g$  is sampled differently by the two parameterisations, implying different predictions at least for off-shell quantities – unless the variable change from (4.31) to (4.32) is taken care of by suitable (ultralocal) Jacobians. While a parameterisation (and gauge condition) independent construction of the path integral has been formulated in a geometric setting [288, 300–303], its usability is hampered by the problem of constructing the full decomposition of  $h$  in terms of fluctuations between physically inequivalent configurations and fluctuations along the gauge orbit. Geometric functional RG flows have been conceptually developed in [172], with first results for AS obtained in [40], and recently to a leading order linear-geometric approximation in [304]. The relation between the geometric approach and the exponential parameterisation was discussed in [274].

Here, we take a more pragmatic viewpoint, and consider the different parameterisations of (4.31) and (4.32) as two different approximations of an ideal parameterisation. Since the functional RG actually requires the explicit form of  $g[\bar{g}; h]$  only to second order in  $h$  in the single metric approximation that we shall employ in this section, we mainly consider a one-parameter class of parameterisations of the type

$$g_{\mu\nu} = \bar{g}_{\mu\nu} + h_{\mu\nu} + \frac{\tau}{2} h_{\mu\rho} h_\nu^\rho + \mathcal{O}(h^3). \quad (4.33)$$

For  $\tau = 0$ , we obtain the linear split, whereas  $\tau = 1$  is *exactly* related to the exponential split within our truncation. Incidentally, it is straightforward to write down the most general,

ultralocal parameterisation to second order that does not introduce a scale,

$$\begin{aligned}
 g_{\mu\nu} &= \bar{g}_{\mu\nu} + h_{\mu\nu} \\
 &+ \frac{1}{2} \left( \tau h_{\mu\rho} h_{\nu}^{\rho} + \tau_2 \mathbf{h} h_{\mu\nu} + \tau_3 \bar{g}_{\mu\nu} h_{\rho\sigma} h^{\rho\sigma} + \tau_4 \bar{g}_{\mu\nu} \mathbf{h}^2 \right) \\
 &+ \mathcal{O}(h^3).
 \end{aligned} \tag{4.34}$$

Here,  $\mathbf{h} = h_{\mu}^{\mu}$  is the trace of the fluctuation. As mentioned above, third and higher order terms will not contribute to our present study anyway. Instead of exploring the full parameter dependence, we will highlight some interesting results in this more general framework below.

The key ingredient for a quantum computation is the propagator of the dynamical field. In our setting, its inverse is given by the second functional derivative (Hessian) of the action (4.2) including the gauge fixing (4.24) with respect to the fluctuating field  $h$ ,

$$\begin{aligned}
 16\pi G_N \Gamma_{hh}^{(2)\kappa\nu}{}_{\alpha\beta} \Big|_{h=0, C=0} &= \frac{1}{16\alpha} \left( 8\alpha \delta_{\alpha\beta}^{\kappa\nu} - [8\alpha - (1 + \beta)^2] \bar{g}^{\kappa\nu} \bar{g}_{\alpha\beta} \right) (-\bar{D}^2) - \frac{1 - \alpha}{\alpha} \delta_{(\alpha}^{\kappa} \bar{D}^{\nu)} \bar{D}_{\beta)} \\
 &+ \frac{1 + \beta - 2\alpha}{4\alpha} \left( \bar{g}^{\kappa\nu} \bar{D}_{(\alpha} \bar{D}_{\beta)} + \bar{g}_{\alpha\beta} \bar{D}^{(\kappa} \bar{D}^{\nu)} \right) \\
 &+ \bar{R} \left( \frac{4 - 3\tau}{12} \delta_{\alpha\beta}^{\kappa\nu} - \frac{1}{3} \bar{g}^{\kappa\nu} \bar{g}_{\alpha\beta} \right) - \lambda \left( (1 - \tau) \delta_{\alpha\beta}^{\kappa\nu} - \frac{1}{2} \bar{g}^{\kappa\nu} \bar{g}_{\alpha\beta} \right) \\
 &- (1 - \tau) \bar{S}_{(\alpha}^{(\kappa} \delta_{\beta)}^{\nu)} + \frac{1}{2} (\bar{S}^{\kappa\nu} \bar{g}_{\alpha\beta} + \bar{S}_{\alpha\beta} \bar{g}^{\kappa\nu}) - \bar{C}^{\kappa}{}_{(\alpha}{}^{\nu}{}_{\beta)}.
 \end{aligned} \tag{4.35}$$

The symbol  $\delta_{\alpha\beta}^{\kappa\nu}$  denotes the symmetrised product of kronecker deltas,  $\delta_{\alpha\beta}^{\kappa\nu} = \frac{1}{2} (\delta_{\alpha}^{\kappa} \delta_{\beta}^{\nu} + \delta_{\beta}^{\kappa} \delta_{\alpha}^{\nu})$ . Here and in the following, we specialise to  $d = 4$ , except if stated otherwise. A standard choice for the gauge parameters is harmonic de Donder gauge with  $\alpha = 1 = \beta$  for which some parts simplify considerably. Simplifications also arise for the exponential split  $\tau = 1$ ; in particular, a dependence on the cosmological constant  $\lambda$  remains only in the trace mode  $\sim \bar{g}^{\kappa\nu} \bar{g}_{\alpha\beta}$ . As discussed in the last section, terms proportional to  $S$  and  $C$  can be dropped since they don't contribute to the  $\beta$  functions for Newton's constant and the cosmological constant.

A standard tool for dealing with the tensor structure of the propagator is the York decomposition of the fluctuations  $h_{\mu\nu}$  into transverse traceless tensor modes, a transverse vector mode and two scalar modes,

$$h_{\mu\nu} = h_{\mu\nu}^T + 2\bar{D}_{(\mu} \xi_{\nu)}^T + \left( 2\bar{D}_{(\mu} \bar{D}_{\nu)} - \frac{1}{2} \bar{g}_{\mu\nu} \bar{D}^2 \right) \sigma + \frac{1}{4} \bar{g}_{\mu\nu} \mathbf{h}, \tag{4.36}$$

$$\bar{D}^{\mu} h_{\mu\nu}^T = 0, \quad \bar{g}^{\mu\nu} h_{\mu\nu}^T = 0, \quad \bar{D}^{\mu} \xi_{\mu}^T = 0. \tag{4.37}$$

It is convenient to split  $\Gamma^{(2)}$  into a pure kinetic part  $\mathcal{P}$  which has a nontrivial flat space limit, and a curvature dependent remainder  $\mathcal{F} = \mathcal{O}(\bar{R})$ . This facilitates an expansion of the propagator  $(\Gamma^{(2)})^{-1} = (\mathcal{P} + \mathcal{F})^{-1} = \sum_{n=0}^{\infty} (-\mathcal{P}^{-1} \mathcal{F})^n \mathcal{P}^{-1}$ .

Let us first concentrate on the kinetic part  $\mathcal{P}$ :

$$\mathcal{P}_{h^T}{}^{\mu\nu}{}_{\alpha\beta} = \frac{1}{32\pi G_N} \delta_{\alpha\beta}^{\mu\nu} (\Delta - 2(1 - \tau)\lambda), \quad (4.38)$$

$$\mathcal{P}_{\xi^T}{}^\mu{}_\alpha = \frac{1}{16\pi G_N \alpha} \delta_\alpha^\mu \Delta (\Delta - 2\alpha(1 - \tau)\lambda), \quad (4.39)$$

$$\mathcal{P}_{(\sigma\mathbf{h})} = \frac{1}{16\pi G_N} \begin{pmatrix} 3 \frac{(3-\alpha)\Delta - 4\alpha(1-\tau)\lambda}{4\alpha} \Delta^2 & \frac{3}{8\alpha} (\beta - \alpha) \Delta^2 \\ \frac{3}{8\alpha} (\beta - \alpha) \Delta^2 & \frac{(\beta^2 - 3\alpha)\Delta + 4\alpha(1+\tau)\lambda}{16\alpha} \end{pmatrix}, \quad (4.40)$$

where  $\Delta = -\bar{D}^2$ . In this form it is straightforward to calculate the propagator  $(\mathcal{P})^{-1}$ . In particular, the transverse traceless mode  $h^T$  does not exhibit any dependence on the gauge parameters. As discussed above, a priori criteria suggest the Landau gauge limit  $\alpha \rightarrow 0$  as a preferred choice for the gauge fixing, as it strictly implements the gauge fixing condition. Whereas the choice of  $\alpha$  and  $\beta$ , in principle, are independent, a subtle interplay can arise with certain regularisation strategies as will be highlighted in the following.

By taking the limit  $\alpha \rightarrow 0$  while keeping  $\beta$  finite, we make the gauge fixing explicit. In particular, we find for the gauge dependent modes

$$\mathcal{P}_{\xi^T}{}^{-1\mu}{}_\alpha \rightarrow \alpha \frac{16\pi G_N}{\Delta^2} \delta_\alpha^\mu, \quad (4.41)$$

$$\mathcal{P}_{(\sigma\mathbf{h})}^{-1} \rightarrow \frac{-\frac{16\pi G_N}{3} \Delta^{-2}}{\frac{(3-\beta)^2}{4} \Delta - (3 - \beta^2 + (3 + \beta^2)\tau)\lambda} \begin{pmatrix} \beta^2 & -6\beta\Delta \\ -6\beta\Delta & 36\Delta^2 \end{pmatrix}. \quad (4.42)$$

The transverse mode  $\xi_\mu^T$  decouples linearly with  $\alpha \rightarrow 0$  and hence is pure gauge in the present setting. Whereas finite parts seem to remain in the  $(\sigma\mathbf{h})$  subspace, we observe that the matrix  $\mathcal{P}_{(\sigma\mathbf{h})}^{-1}$  in (4.42) becomes degenerate in this limit (*i.e.*, the determinant of the matrix in (4.42) is zero). Effectively, only one scalar mode remains in the propagator. The nature of this scalar mode is a function of the second gauge parameter: taking the limit  $\beta \rightarrow -\infty$ , the remaining scalar mode can be identified with  $\sigma$ , while the limit  $\beta \rightarrow 0$  leaves us with a pure  $\mathbf{h}$  mode.

Whereas the transverse modes in (4.41) decouple smoothly in the limit  $\alpha \rightarrow 0$ , the decoupling of the scalar mode in (4.42) is somewhat hidden in the degeneracy of the scalar sector with the corresponding eigenmode depending on  $\beta$ . This can lead to a subtle interplay with regularisation techniques for loop diagrams as can be seen on rather general grounds by the following argument. Structurally, the propagator in the  $(\sigma\mathbf{h})$  sector has the following form in the limit  $\alpha \rightarrow 0$  and for small but finite  $\beta$ , cf. (4.42)

$$\left(\mathcal{P}_{(\sigma\mathbf{h})}\right)^{-1} \rightarrow \begin{pmatrix} \mathcal{O}(\beta^2) & \mathcal{O}(\beta) \\ \mathcal{O}(\beta) & \mathcal{O}(1) \end{pmatrix}. \quad (4.43)$$

Regularisations of traces over loops built from this propagator are typically adjusted to the

spectrum of the involved operators. Let us formally write this as

$$\mathrm{Tr} \left[ \mathcal{L}_{\mathfrak{R}} \mathcal{P}^{-1}(\dots) \right], \quad (4.44)$$

where  $\mathcal{L}_{\mathfrak{R}}$  denotes a regularising operator and the ellipsis stands for further vertices and propagators. Now, it is often useful to regularise all fluctuation operators at the same scale, *e.g.*, the spectrum of all  $\Delta$ 's should be cut off at one and the same scale  $k^2$ . Therefore, the regularising operator  $\mathcal{L}_{\mathfrak{R}}$  inherits its tensor structure from the Hessian  $\Gamma^{(2)}$  of (4.35). In the  $(\sigma\mathbf{h})$  sector, the regularising operator can hence acquire the same dependence on the gauge parameters as in (4.40),

$$\mathcal{L}_{\mathfrak{R},(\sigma\mathbf{h})} \rightarrow \frac{1}{\alpha} \begin{pmatrix} \mathcal{O}(1) & \mathcal{O}(\beta) \\ \mathcal{O}(\beta) & \mathcal{O}(\beta^2) \end{pmatrix}, \quad (4.45)$$

for  $\alpha \rightarrow 0$  and small  $\beta$ . The complete scalar contribution to traces of the type (4.44) would then be of the parametric form

$$\mathrm{Tr} \left[ \mathcal{L}_{\mathfrak{R}} \mathcal{P}^{-1}(\dots) \right]_{(\sigma\mathbf{h})} \rightarrow \frac{1}{\alpha} \mathcal{O}(\beta^2). \quad (4.46)$$

For finite  $\beta$ , such regularised traces can thus be afflicted with divergencies in the Landau gauge limit  $\alpha \rightarrow 0$ . If this happens, we still have the option to choose suitable values of  $\beta$ . In fact, (4.46) suggests that still a whole one-parameter family of gauges exists in the Landau gauge limit, if we set  $\beta = \gamma \cdot \sqrt{\alpha}$ , with arbitrary real but finite gauge parameter  $\gamma$  distinguishing different gauges.

We emphasise that this is a rather qualitative analysis. Since the limit of products is not necessarily equal to the product of limits, the trace over the matrix structure of the above operator products can still eliminate this  $1/\alpha$  divergence, such that any finite value of  $\beta$  remains admissible.

In the following we observe that the appearance of the  $1/\alpha$  divergence depends on the explicit choice of the regularisation procedure, as expected. Still, as this discussion shows, even if this divergence occurs, it can perfectly well be dealt with by choosing  $\beta = \gamma\sqrt{\alpha}$  and still retaining a whole one-parameter family of gauges in the Landau gauge limit.

### 4.2.2. Parameterisation dependent RG flow

Whereas exact solutions of the flow equation so far have only been found for simple models, approximate nonperturbative flows can be constructed with the help of systematic expansion schemes. In the case of gravity, a useful scheme is given by expanding  $\Gamma$  in powers of curvature invariants. The technical difficulties then lie in the construction of the inverse of the regularised Hessian  $(\Gamma^{(2)} + \mathfrak{R})^{-1}$ , corresponding to the regularised propagator, and performing the corresponding traces.



A conceptual difficulty lies in the fact that  $\Gamma[g, \bar{g}]$  should be computed on a subspace of action functionals that satisfy the constraints imposed by diffeomorphism invariance and background independence. In general, this requires to work with  $g$  and  $\bar{g}$  independently during large parts of the computation [173–175, 185]. Such bimetric approaches can, for instance, be organised in the form of a vertex expansion on a flat space as will be discussed in the next section, or via a level expansion as developed in [44], see [186, 187, 264] for further bimetric results. For the present study of parameterisation dependencies, we confine ourselves to a single metric approximation, defined by identifying  $g$  with  $\bar{g}$  on both sides of the flow equation, after the Hessian has been analytically determined. In this section, we therefore from now on do no longer have to distinguish between the background field and the fluctuation field as far as the presentation is concerned, and hence drop the bar notation for simplicity.

Spanning the action in terms of the Einstein-Hilbert truncation and neglecting the flow of the gauge fixing and ghost sector [260–262], we use the *universal RG machine* [266, 271, 272] as our computational strategy. The key idea is to subdivide the Hessian  $\Gamma^{(2)}$  into a kinetic part and curvature parts with a subsequent expansion in the curvature. This is complicated by terms containing uncontracted covariant derivatives in  $\Gamma^{(2)}$  which could invalidate the counting scheme. Within the present truncation, this problem is solved with the aid of the York decomposition (4.36). This helps both to set up the curvature expansion as well as to invert the kinetic terms in the corresponding subspaces of transverse traceless (TT), transverse vector (T) and scalar modes. From a technical point of view, we again use the package *xAct* to handle the extensive tensor calculus.

Schematically, the flow equation for the Einstein-Hilbert truncation can then be written as

$$\partial_t \Gamma = \int d^4x \sqrt{-g} \left( \mathcal{S}^{\text{TT}} + \mathcal{S}^{\text{T}} + \mathcal{S}^{\sigma h} + \mathcal{S}^{\text{gh}} + \mathcal{S}^{\text{Jac}} \right), \quad (4.47)$$

where the first three terms denote the contributions from the graviton fluctuations as parameterised by the York decomposition (4.36). The fourth term  $\mathcal{S}^{\text{gh}}$  arises from the Faddeev-Popov ghost fluctuations, cf. (4.30). The last term  $\mathcal{S}^{\text{Jac}}$  comes from the use of transverse decompositions of the metric (4.36) and the ghost fields (4.30). The corresponding functional integral measure over the new degrees of freedom involves Jacobians which – upon analogous regularisation – contribute to the flow of the effective average action.

At this point, we actually have a choice that serves as another source of parameterisation dependencies studied in this section: one option is to formulate the regularised path integral in terms of the decomposed fields as introduced above. In that case, the Jacobians are nontrivial and their contribution  $\mathcal{S}^{\text{Jac}}$  is listed in the appendix C, (C.21). Alternatively, we can reintroduce canonically normalised fields by means of a nonlocal field redefinition [37,

305],

$$\begin{aligned}
& \sqrt{\Delta - \text{Ric}} \xi^\mu \rightarrow \xi^\mu, \\
& \sqrt{\Delta^2 + \frac{4}{3} D_\mu R^{\mu\nu} D_\nu} \sigma \rightarrow \sigma, \\
& \sqrt{\Delta} \eta \rightarrow \eta,
\end{aligned} \tag{4.48}$$

and analogously for the longitudinal antighost field  $\bar{\eta}$ . (Here, we have used  $(\text{Ric } \xi)^\mu = R^{\mu\nu} \xi_\nu$ .) This field redefinition goes along with another set of Jacobians contributing to the measure of the rescaled fields. As shown in [37], the Jacobians for the original York decomposition and the Jacobians from the field redefinition (4.48) cancel at least to the order in background curvature we consider here. Therefore, if we set up the flow in terms of the redefined fields (4.48), the last term in (4.47) vanishes,  $\mathcal{S}_{\text{fr}}^{\text{Jac}} = 0$ .

For an exact solution of the flow, it would not matter whether or not a field redefinition of the type (4.48) is performed. Corresponding changes in the full propagators would be compensated for by the (dis-)appearance of the Jacobians. For the present case of a truncated nonperturbative flow, a dependence on the precise choice will, however, remain, which is another example for a parameterisation dependence. This dependence also arises from the details of the regularisation. The universal RG machine suggests to construct a regulator  $\mathfrak{R}$  such that the Laplacians  $\Delta$  appearing in the kinetic parts are replaced by the rule

$$\Delta \rightarrow \Delta + \mathfrak{R}(\Delta). \tag{4.49}$$

Since the field redefinition (4.48) is nonlocal, it also affects the kinetic terms and thus takes influence on the precise manner of how modes are regularised via (4.49). In other words, the dependence of our final results on using or not using the field redefinition (4.48) is an indirect probe of the regularisation scheme dependence and thus of the generalised parameterisation dependence we are most interested in here.

Here, we focus on the RG flow of the effective average action parameterised by the operators of the Einstein-Hilbert truncation. For this, we introduce the dimensionless versions of the gravitational coupling and the cosmological constant, analogously to the previous section, and determine the corresponding RG  $\beta$  functions for  $g$  and  $\lambda$ , by computing the  $\mathcal{S}$  terms on the right hand side of the flow (4.47) to linear order in the background curvature. Many higher order computations have been performed by now [38, 42, 248, 251–259, 306], essentially confirming and establishing the simple picture visible in the Einstein-Hilbert truncation.

Whereas the fixed point values  $g_*$  and  $\lambda_*$  are RG scheme dependent, the critical exponents  $\theta_i$  are universal and thus should be parameterisation independent in an exact calculation. Also, the product  $g_* \lambda_*$  has been argued to be physically observable in principle and thus should be universal [37]. Testing the parameterisation dependence of the critical exponents  $\theta_i$  and  $g_* \lambda_*$  therefore provides us with a quantitative criterion for the reliability of approxi-

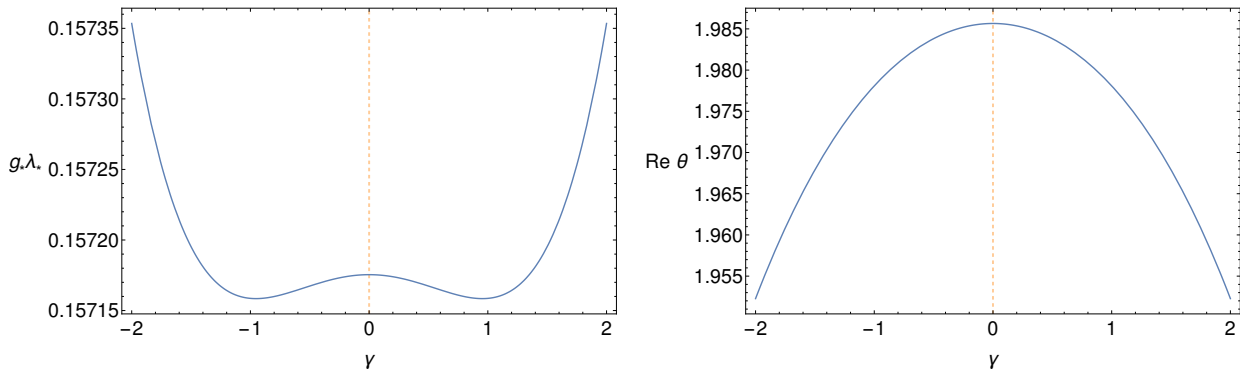


Fig. 4.2.: Linear split without field redefinition: residual dependence of our estimates for the universal quantities on the gauge parameter  $\gamma$  in the limit  $\alpha \rightarrow 0$ . We find a common stationary point at  $\gamma = 0$  and a remarkably small variation of the results on the level of 0.1% for  $g_* \lambda_*$  and 1.6% for  $\text{Re } \theta$  in the range  $\gamma \in [-2, 2]$ .

mative results.

### 4.2.3. Generalised parameterisation dependence

With these prerequisites, we now explore the parameterisation dependencies of the following scenarios: we consider the linear (4.31) and the exponential (4.32) split, both with and without field redefinition (4.48), and study the corresponding dependencies on the gauge parameters, focusing on a strict implementation of the gauge fixing condition  $\alpha \rightarrow 0$  (Landau gauge). As suggested by the principle of minimum sensitivity, we look for stationary points as a function of the remaining parameter(s) where universal results become most insensitive to these generalised parameterisations. For the following quantitative studies, we exclusively use the piecewise linear regulator [226, 307],  $\mathfrak{R}(x) = (k^2 - x)\theta(k^2 - x)$ , for reasons of simplicity. Studies of regulator scheme dependencies which can also quantify parameterisation dependencies have first been performed, *e.g.*, in [37, 248].

#### Linear split without field redefinition

Let us start with the case of the linear split (4.31) without field redefinition (4.48). Here, the degeneracy in the sector of scalar modes interferes with the regularisation scheme, as illustrated in (4.46). Hence, in the Landau gauge limit  $\alpha \rightarrow 0$ , we choose  $\beta = \gamma \sqrt{\alpha}$ , which removes any artificial divergence, but keeps  $\gamma$  as a real parameter that allows for a quantification of remaining parameterisation/gauge dependence. We indeed find a non-Gaussian fixed point  $g_*, \lambda_*$  for a wide range of values of  $\gamma$ . The critical exponents form a complex conjugate pair. The estimates for the universal quantities  $g_* \lambda_*$  and the real part of the  $\theta$ 's (being the measure for the RG relevance of perturbations about the fixed point) are depicted in Figure 4.2.

We observe a common point of minimum sensitivity at  $\gamma = 0$ . In a rather wide range of

parameterisation	$g_*$	$\lambda_*$	$g_*\lambda_*$	$\theta$
nfr $\tau = \alpha = \gamma = 0$	0.879	0.179	0.157	$1.986 \pm 3.064i$
nfr $\tau = 0, \alpha = \beta = 1$	0.718	0.165	0.119	$1.802 \pm 2.352i$
fr $\tau = \alpha = 0, \beta = 1$	0.893	0.164	0.147	$2.034 \pm 2.691i$
fr $\tau = 0, \alpha = \beta = 1$	0.701	0.172	0.120	$1.689 \pm 2.486i$
fr $\tau = \alpha = 0, \beta = -\infty$	0.983	0.151	0.148	$2.245 \pm 2.794i$
fr $\tau = 1, \beta = -\infty$	3.120	0.331	1.033	4, 2.148
fr $\tau = 1.22, \alpha = 0, \beta = -\infty$	3.873	0.389	1.508	3.957, 1.898

Tab. 4.1.: Non-Gaußian fixed point properties for several parameterisations, characterised by the gauge parameters  $\alpha, \beta$  or  $\gamma$ , as well as by the choice of the parameterisation split parameter  $\tau$  with  $\tau = 0$  corresponding to the linear split (4.31) and  $\tau = 1$ , being the exponential split (4.32). Whether or not a field redefinition (4.48) is performed is labeled by “fr” or “nfr”, respectively.

gauge parameter values  $\gamma \in [-2, 2]$ , our estimates for  $g_*\lambda_*$  and  $\text{Re}\theta$  vary only very mildly on the level of 0.1% and 1.6%. Given the limitations of the present simple approximation, this is a surprising degree of gauge independence lending further support to the AS scenario. The extremising values at  $\gamma = 0$  are near the results of [253, 254, 266] where the same gauge choice ( $\alpha = \beta = 0$ ) was used. The main difference can be traced back to the fact that our inclusion of the (dimensionful) Newton’s constant in the gauge fixing term (4.24) renders the gauge parameter  $\alpha$  dimensionless as is conventional. If we ignored the resulting dimensional scaling, our extremising result would be exactly that of [266] and in close agreement with [253, 254] with slight differences arising from the regularisation scheme. It is also instructive to compare with [308], where the on-shell contributions to the flow have been singled out yielding a gauge independent fixed point value for the cosmological constant of  $\lambda_* = 0.261$ . Though the calculation also employs the linear split without field redefinition, the on-shell projection requires special choices for the field decomposition, the ghost sector, and the regularisation scheme. The quantitative differences to our results which includes also off-shell contributions can be taken as a measure for the influence of all these sectors. We summarise a selection of our quantitative results in Table 4.1.

### Exponential split without field redefinition

As a somewhat contrary example, let us now study the case of the exponential split (4.32) also without field redefinition (4.48). Again, we find a non-Gaußian fixed point. The corresponding estimates for the universal quantities at this fixed point in the Landau gauge limit  $\alpha = 0$  are displayed in Figure 4.3. At first glance, the results seem similar to the previous ones with a stationary point at  $\gamma = 0$ . However, the product  $g_*\lambda_*$  shows a larger variation on the order of 5% and the critical exponent even varies by a factor of more than 40 in the range  $\gamma \in [-2, 2]$ . We interpret the strong dependence on the gauge parameter  $\gamma$  as a clear signature that these estimates based on the exponential split without field redefinition

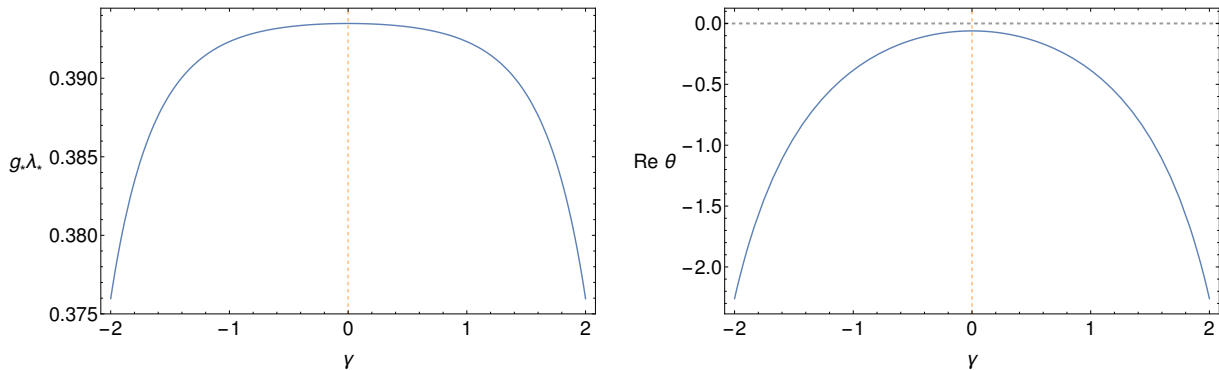


Fig. 4.3.: Exponential split without field redefinition: residual dependence of our estimates for the universal quantities on the gauge parameter  $\gamma$  in the limit  $\alpha \rightarrow 0$ . A common stationary point is again present at  $\gamma = 0$ , but the estimates for the universal quantities exhibit a substantial variation in the range  $\gamma \in [-2, 2]$ :  $g_* \lambda_*$  varies by  $\sim 5\%$  and  $\text{Re}\theta$  even by more than a factor of 40. The latter is a clear signal for the insufficiency of the parameterisation.

should not be trusted.

In fact, the real part of the critical exponents,  $\text{Re}\theta$ , have even changed sign compared to the previous case implying that the non-Gaussian fixed point has turned UV repulsive. Similar observations have been made in [273] for the harmonic Feynman-type gauge  $\alpha = 1 = \beta$  and an additional strong dependence on the regulator profile function  $\mathfrak{R}(x)$  has been found. We have verified that our results agree with those of [273] for the corresponding gauge choice. In summary, this parameterisation serves as an example that nonperturbative estimates can depend strongly on the details of the parameterisation (even for seemingly reasonable parameterisations) and the results can be misleading. The good news is that a study of the parameterisation dependence can – and in this case does – reveal the insufficiency of the parameterisation through its strong dependence on a gauge parameter.

### Linear split with field redefinition

For the remainder, we consider parameterisations of the fluctuation field which include field redefinitions (4.48). The canonical normalisation achieved by these field redefinitions has not merely aesthetic reasons. An important aspect is that the nonlocal field redefinition helps to regularise the modes in a more symmetric fashion: the kinetic parts of the propagators then become linear in the Laplacian which are all equivalently treated by the regulator (4.49). A practical consequence is that the interplay of the degeneracy in the scalar sector no longer interferes with the regularisation, *i.e.*, the gauge parameter  $\beta$  can now be chosen independently of  $\alpha$ . Concentrating again on the Landau gauge limit  $\alpha \rightarrow 0$ , we observe for generic split parameter  $\tau$  that  $\beta = 0$  no longer is an extremal point.

Our estimates for the universal quantities for the case of the linear split (4.31) with field redefinition (4.48) and  $\alpha \rightarrow 0$  are plotted in Figure 4.4. In order to stay away from the singularity at  $\beta = 3$ , cf. (4.30), we consider values for  $\beta < 3$  down to  $\beta \rightarrow -\infty$ . The

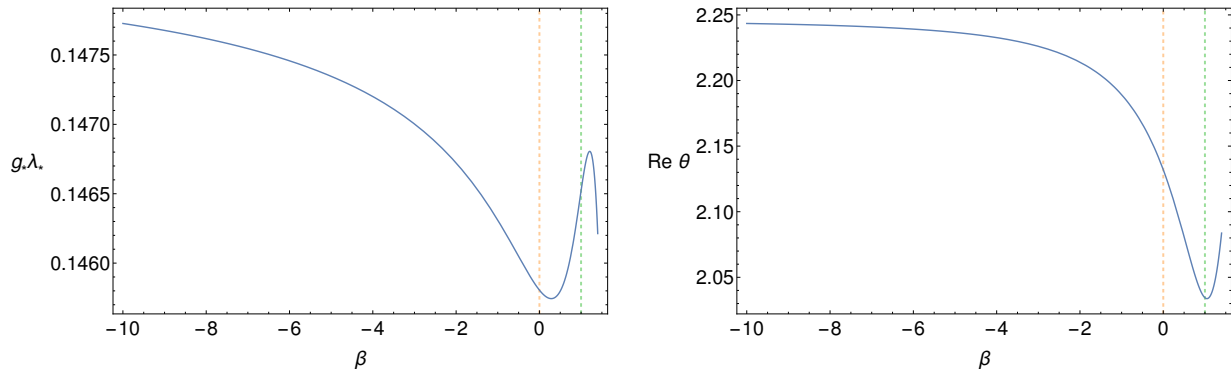


Fig. 4.4.: Linear split with field redefinition: residual dependence of our estimates for the universal quantities on the gauge parameter  $\beta$  in the limit  $\alpha \rightarrow 0$ . A common stationary point is approached for  $\beta \rightarrow -\infty$ . Near the harmonic gauge  $\beta = 1$  (green dashed vertical line), both quantities have an extremum. For the whole range of  $\beta$  values, the estimates for the universal quantities exhibit rather small variations of 1% for  $g_* \lambda_*$  and 10% for the more sensitive critical exponent  $\text{Re } \theta$ .

longitudinal ghost mode decouples in the limit  $\beta \rightarrow -\infty$ .

A non-Gaussian fixed point exists, and a common extremum of  $g_* \lambda_*$  and  $\text{Re } \theta$  occurs for  $\beta \rightarrow -\infty$ . Near  $\beta = 1$  marking the harmonic gauge condition, both quantities are also close to an extremum (which does not occur at exactly the same  $\beta$  value for both quantities). All fixed point quantities for this case are listed in Table 4.1 (“fr  $\tau = \alpha = 0$ ,  $\beta = 1$ ”). These values agree with the results of [40]. They are remarkably close, *e.g.*, to those for the linear split without field redefinition. The situation is similar for the other extremum  $\beta \rightarrow -\infty$  (“fr  $\tau = \alpha = 0$ ,  $\beta = -\infty$ ” in Table 4.1). For the whole infinite  $\beta$  range studied for this parameterisation,  $g_* \lambda_*$  varies on the level of 1%. The more sensitive critical exponent  $\text{Re } \theta$  varies by 10% which is still surprisingly small given the simplicity of the approximation. Let us emphasise again that varying  $\beta$  from infinity to zero corresponds to a complete exchange of the scalar modes from  $\sigma$  (longitudinal vector component) to  $\mathbf{h}$  (conformal mode) and hence to a rather different parameterisation of the fluctuating degrees of freedom.

### Exponential split with field redefinition

Finally, we consider the exponential split (4.31),  $\tau = 1$ , with field redefinition (4.48). Having performed the latter has a strong influence on the stability of the estimates of the universal quantities at the non-Gaussian fixed point, as is visible in Figure 4.5. Contrary to the linear split, we do not find a common extremum near small values of  $\beta$ : neither  $\beta = 0$  nor the harmonic gauge  $\beta = 1$  seem special, but, *e.g.*, the product  $g_* \lambda_*$  undergoes a rapid variation in this regime.

Rather, a common extremal point is found in the limit  $\beta \rightarrow -\infty$ . In fact,  $g_* \lambda_*$  becomes insensitive to the precise value of  $\beta$  for  $\beta \lesssim -2$  (with a local maximum near  $\beta \simeq -3$ , and an asymptotic value of  $g_* \lambda_* \simeq 1.033$  for  $\beta \rightarrow -\infty$ ). This estimate for  $g_* \lambda_*$  is significantly

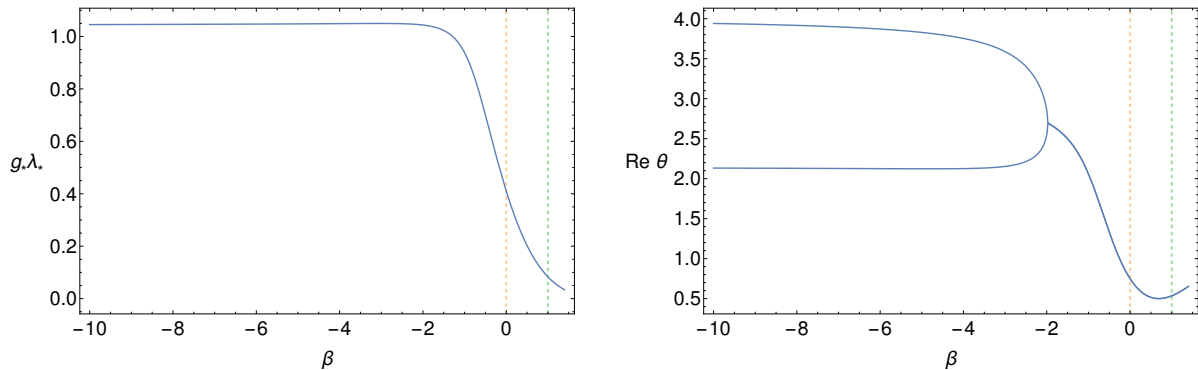


Fig. 4.5.: Exponential split with field redefinition: residual dependence of our estimates for the universal quantities on the gauge parameter  $\beta$  in the limit  $\alpha \rightarrow 0$ . A common stationary point is approached for  $\beta \rightarrow -\infty$ , whereas no common minimum sensitivity point is found near the harmonic gauge  $\beta = 1$  or  $\beta = 0$  (dashed vertical lines). Below  $\beta \lesssim -2$ , the critical exponents become real with the non-Gaussian fixed point remaining UV attractive. For  $\beta \rightarrow -\infty$ , the results become independent of the gauge parameter  $\alpha$ .

larger than for the other parameterisations. The deviation may thus be interpreted as the possible level of accuracy that can be achieved in the simple Einstein-Hilbert truncation.

As an interesting feature, the critical exponents become real for  $\beta \lesssim -2$ , and approach the asymptotic values  $\theta = \{4, 2.148\}$  for  $\beta \rightarrow -\infty$ . The leading exponent  $\theta = 4$  reflects the power counting dimension of the cosmological term. This is a straightforward consequence of the fact that the  $\lambda$  dependence in this parameterisation  $\tau = 1$ ,  $\beta \rightarrow -\infty$  disappears from the propagators of the contributing modes. The leading nontrivial exponent  $\theta = 2.148$  hence is associated with the scaling of the Newton’s constant near the fixed point, which is remarkably close to minus the power counting dimension of the Newton coupling. The latter is a standard result for non-Gaussian fixed points which are described by a quadratic fixed point equation [101, 309]. The small difference to the value  $\theta = 2$  arises from the RG improvement introduced by the anomalous dimension in the threshold functions (“ $\eta$ -terms” as discussed in the appendix C). Neglecting these terms, the estimate of the leading critical exponents in dimension  $d$  is  $d$  and  $d-2$ , as first discussed in [275]. Also our other quantitative results for the fixed point properties are in agreement with those of [275] within the same approximation.

The significance of the results within this parameterisation is further underlined by the observation that the results in the limit  $\beta \rightarrow -\infty$  become completely independent of the gauge parameter  $\alpha$ . In other words, the choice of the transverse traceless mode and the  $\sigma$  mode ( $\beta \rightarrow -\infty$ ) as a parameterisation of the physical fluctuations removes any further gauge dependence.

The present parameterisation has also some relation to [276, 277], where in addition to the exponential split the parameterisation was further refined to remove the gauge parameter dependence completely on the semi-classical level. More specifically, the parameterisation of

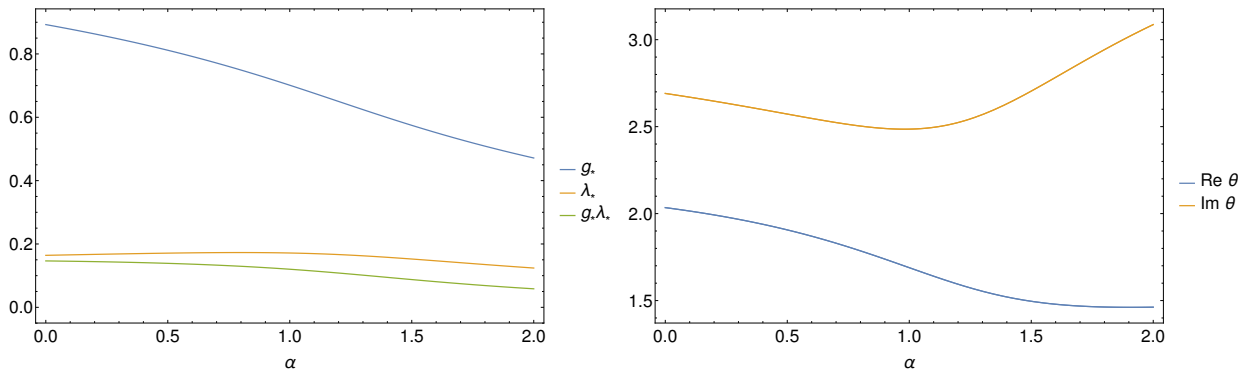


Fig. 4.6.: Linear split with field redefinition: dependence of estimates for the fixed point values (left panel) and the critical exponents (right panel) on the gauge parameter  $\alpha$  and harmonic gauge condition  $\beta = 1$ . No qualitative and only minor quantitative differences are found for the Feynman gauge  $\alpha = 1$  in comparison to the Landau gauge  $\alpha = 0$ .

the fluctuations was chosen so that only fluctuations contribute that also have an on-shell meaning. In essence, this removes any contribution from the scalar modes to the UV running. At the semi-classical level [277], the nontrivial critical exponent is 2 as in [275] and increases upon inclusion of RG improvement as in the present work. The increase determined in [276] is larger than in the present parameterisation and yields  $\theta \simeq 3$  which is remarkably close to results from simulations based on Regge calculus [310, 311].

The present parameterisation with  $\beta \rightarrow -\infty$  is also loosely related to unimodular gravity, as the conformal mode is effectively removed from the fluctuation spectrum. Still, differences to unimodular gravity remain in the gauge fixing and ghost sector as unimodular gravity is only invariant under transversal diffeomorphisms. It is nevertheless interesting to observe that corresponding FRG calculations yield critical exponents of comparable size [312, 313].

In fact, the present parameterisation allows for a closed form solution of the RG flow as will be presented below.

### Landau vs. Feynman gauge

Many of the pioneering computations in quantum gravity have been and still are performed within the harmonic gauge  $\beta = 1$  and with  $\alpha = 1$  corresponding to Feynman gauge. This is because this choice leads to a number of technical simplifications such as the direct diagonalisation of the scalar modes as is visible from the off-diagonal terms in (4.40). Concentrating on the linear split with field redefinition, we study the  $\alpha$  dependence for the harmonic gauge  $\beta = 1$  in the vicinity of the Landau and Feynman gauges. For early results on the  $\alpha$  dependence, see [314].

Our results for the non-Gaussian fixed point values are shown in the left panel of Figure 4.6. In essence, the fixed point values show only a mild variation during the transition from the Landau gauge  $\alpha = 0$  to the Feynman gauge  $\alpha = 1$ . In particular, the decrease of  $g_*$  is slightly



compensated for by a mild increase of  $\lambda_*$ . Effectively, the observed variation is only on a level which is quantitatively similar to other parameterisation dependencies, cf. Table 4.1.

A similar conclusion holds for the more sensitive critical exponents. Real and imaginary parts of the complex pair are shown in the right panel of Figure 4.6. Starting from larger values of  $\alpha$ , it is interesting to observe that the imaginary part  $\text{Im } \theta$  decreases with decreasing  $\alpha$ . This may be taken as an indication for a tendency towards purely real exponents; however, at about  $\alpha = 1$  this tendency is inverted and the exponents remain a complex pair in between Feynman gauge and Landau gauge within the present estimate.

In summary, we observe no substantial difference between the results in Feynman gauge  $\alpha = 1$  and those of Landau gauge  $\alpha = 0$  in any of the quantities of interest for the linear split and with field redefinition. Our results show an even milder dependence on the gauge parameter in comparison to the study of [37], where the regulator was chosen such as to explicitly lift the degeneracy in the sector of scalar modes in the limit  $\alpha \rightarrow 0$ . The present parameterisation hence shows a remarkable degree of robustness against deformations away from the a priori preferable Landau gauge. Hence, we conclude that the use of Feynman gauge is a legitimate option to reduce the complexity of computations.

### Generalised parameterisations

Having focused so far mainly on the gauge parameter dependencies for fixed values of the split parameter  $\tau$ , we now explore the one-parameter family of parameterisations for general  $\tau$ . For this, we use the Landau gauge  $\alpha = 0$  and take the limit  $\beta \rightarrow -\infty$ , where the fixed point estimates of all parameterisations used so far showed a large degree of stability. Figure 4.7 exhibits the results for the non-Gaussian fixed point values (left panel) and the corresponding critical exponents (right panel).

A comparison of the results for  $\tau = 0$  and  $\tau = 1$  reveals the differences already discussed above: an increase of the fixed point values and the occurrence of real critical exponents for the exponential split  $\tau = 1$ . From the perspective of the principle of minimum sensitivity, it is interesting to observe that the fixed point values develop extrema near  $\tau \simeq 1.22$ . The product  $g_*\lambda_*$  is maximal for  $\tau = 1 + \frac{\sqrt{3}}{24} \left(\frac{278}{\pi}\right)^{1/4}$ . Also for this parameterisation, the critical exponents of the fixed point are real and still close to the values for the exponential split, cf. Table 4.1. For even larger values of  $\tau$ , the critical exponents form complex pairs again.

To summarise, in the full three-parameter space defined by  $\tau$ ,  $\beta$  and  $\alpha \geq 0$ , we find a local extremum, *i.e.*, a point of minimum sensitivity, at  $\alpha = 0$ ,  $\beta \rightarrow -\infty$  and  $\tau$  near the exponential split value  $\tau = 1$ . From this a posteriori perspective, our results suggest that the exponential split (with field redefinition) in the limit where the scalar sector is represented by the  $\sigma$  mode may be viewed as a “best estimate” for the UV behaviour of quantum Einstein gravity. Of course, due to the limitations imposed by the simplicity of our truncation, this conclusion should be taken with reservations. The resulting RG flow for  $\tau = 1$  is in fact remarkably simple and will be discussed next.

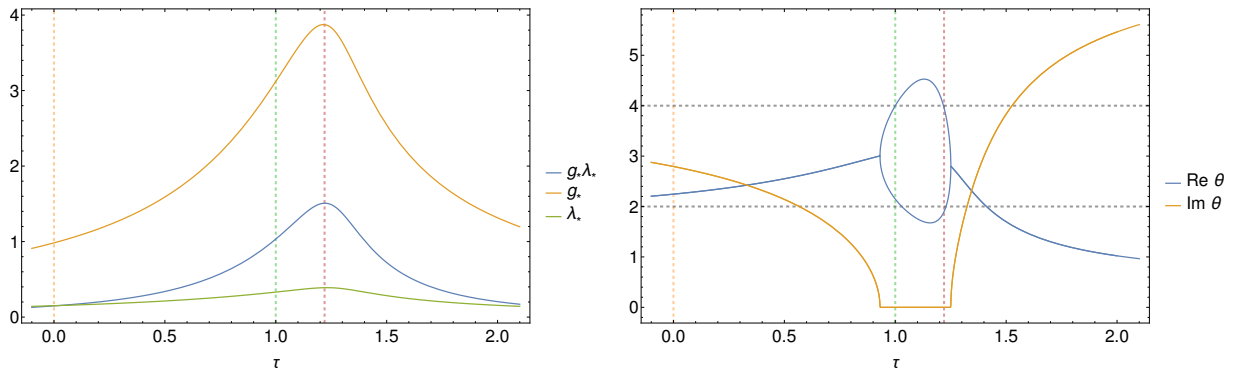


Fig. 4.7.: Parameterisation dependence of fixed point values (left panel) and critical exponents (right panel) as a function of the split parameter  $\tau$  for the Landau gauge  $\alpha = 0$  and  $\beta \rightarrow -\infty$ . The fixed point values exhibit extrema near  $\tau \simeq 1.22$ , for the product of fixed point values, this occurs at  $\tau = 1 + \frac{\sqrt{3}}{24} \left(\frac{278}{\pi}\right)^{1/4}$  (red dashed vertical line). In this regime, the critical exponents are real and close to their values for the exponential split  $\tau = 1$  (green dashed vertical line).

### Analytical solution for the phase diagram

Let us now analyse more explicitly the results for the RG flow for the exponential split with field redefinition in the limit  $\beta \rightarrow -\infty$ . Several simplifications arise in this case. The exponential split removes any dependence of the transverse traceless and vector components of the propagator on the cosmological constant. The remaining dependence on  $\lambda$  in the conformal mode is finally removed by the limit  $\beta \rightarrow -\infty$ . As a consequence, the cosmological constant does not couple into the flows of the Newton coupling nor into any other higher order coupling. Still, the cosmological constant is driven by graviton fluctuations. As emphasised above in subsection 4.2.3, any remaining gauge dependence on the gauge parameter  $\alpha$  drops out of the flow equations. For the RG flow of Newton coupling and cosmological constant, we find the simple set of equations:

$$\partial_t g \equiv \beta_g = 2g - \frac{135g^2}{72\pi - 5g}, \quad (4.50)$$

$$\partial_t \lambda \equiv \beta_\lambda = \left(-2 - \frac{135g}{72\pi - 5g}\right) \lambda - g \left(\frac{43}{4\pi} - \frac{810}{72\pi - 5g}\right). \quad (4.51)$$

In addition to the Gaussian fixed point, these flow equations support a fixed point at

$$g_* = \frac{144\pi}{145}, \quad \lambda_* = \frac{48}{145}, \quad g_* \lambda_* = \frac{6912\pi}{21025}, \quad (4.52)$$

cf. Table 4.1. Also the critical exponents can be determined analytically,

$$\theta_0 = 4, \quad \theta_1 = \frac{58}{27}. \quad (4.53)$$

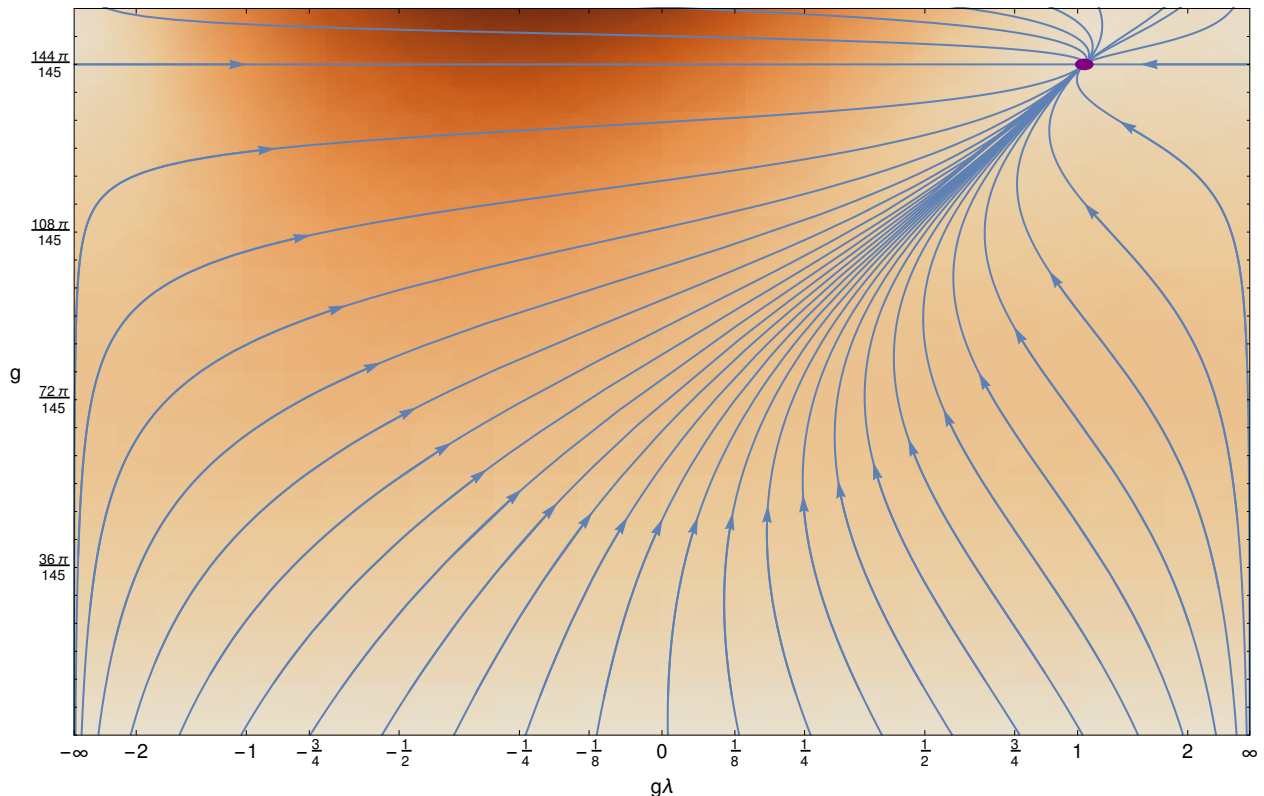


Fig. 4.8.: Global phase diagram in the  $(g, g\lambda)$  plane for the exponential split with field redefinition and  $\beta \rightarrow -\infty$ . Arrows point from IR to UV indicating the approach to the UV fixed point at  $g_* = 144\pi/145$  and  $\lambda_* = 48/145$ . The color indicates a measure for the flow velocity,  $(\partial_t g)^2 + (\partial_t(g\lambda/\sqrt{1+g^2\lambda^2}))^2$ .

The fact that the largest critical exponent corresponds to the power counting canonical dimension of the cosmological term is a straightforward consequence of the structure of the flow equations within this parameterisation: as we have  $\partial_t g = (2 + \eta(g))g$  and  $\partial_t \lambda = (-2 + \eta(g))\lambda + \mathcal{O}(g)$ , the existence of a non-Gaussian fixed point requires  $\eta(g_*) = -2$ . As the stability matrix is triangular, the eigenvalue associated with the cosmological term must be  $-4$  and thus  $\theta_0 = 4$ . Rather generically, other parameterisations lead to a dependence of  $\eta$  also on  $\lambda$  and thus to a more involved stability matrix.

In the physically relevant domain of positive gravitational coupling  $g > 0$ , the fixed point  $g_*$  separates a “weak” coupling phase with  $g < g_*$  from a “strong” coupling phase  $g > g_*$ . Only the former allows for trajectories that can be interconnected with a classical regime where the dimensionless  $g$  and  $\lambda$  scale classically, *i.e.*,  $\partial_t g \simeq 2g$  and  $\partial_t \lambda \simeq -2\lambda$  such that their dimensionful counterparts approach their observed values. Trajectories in the strong coupling phase run to larger values of  $g$  and terminate in a singularity of  $\beta_g$  at  $g_{\text{sing}} = 72\pi/5$  indicating the breakdown of the truncation.

All trajectories in the weak coupling phase with  $g < g_*$  run towards the Gaussian fixed point for  $g$  and thus, also the flow of  $\lambda$  in the infrared is dominated by the Gaussian fixed

point. This implies that all trajectories emanating from the non-Gaussian fixed point with  $g \leq g_*$  can be continued to arbitrarily low scales, *i.e.*, are infrared complete. They can thus be labeled by their deep infrared value of  $g\lambda$  approaching a constant, which may be identified with the product of Newton coupling and cosmological constant as observed at present. A plot of the resulting RG flow in the plane  $(g, g\lambda)$  is shown in Figure 4.8. It represents a global phase diagram of quantum gravity as obtained in the present truncation/parameterisation. We emphasise that no singularities appear towards the IR contrary to conventional single metric calculations based on the linear split.

The flows (4.50) and (4.51) can be integrated analytically. Converting back to dimensionful couplings, the flow of the running Newton coupling  $G(k)$  satisfies the implicit equation

$$G_N = \frac{G(k)}{\left(1 - \frac{145}{144\pi} k^2 G(k)\right)^{\frac{27}{29}}}, \quad (4.54)$$

where  $G_N$  is the Newton coupling measured in the deep infrared  $k \rightarrow 0$ . Expanding the solution at low scales about the Newton coupling yields

$$G(k) \simeq G_N \left(1 - \frac{15}{16\pi} k^2 G_N + \mathcal{O}\left((k^2 G_N)^2\right)\right) \quad (4.55)$$

exhibiting the antiscreening property of gravity.

The flow of the dimensionful running cosmological constant  $\Lambda(k)$  can be given explicitly in terms of that of the running Newton coupling,

$$\begin{aligned} \Lambda(k) = & \frac{162k^2}{25} - \frac{43G(k)k^4}{16\pi} + \ell k^2 \left(144\pi - 145G(k)k^2\right)^{\frac{25}{29}} \\ & - \frac{144\pi}{3625G(k)} \left(87 + 25\ell \left(144\pi - 145G(k)k^2\right)^{\frac{25}{29}}\right). \end{aligned} \quad (4.56)$$

Here,  $\ell = -\frac{29}{86400} (2^{-13} 3^{-21} \pi^{-54})^{\frac{1}{29}} (125\Lambda G_N + 432\pi)$ , and  $\Lambda$  is the value of the classical cosmological constant in the deep infrared  $k \rightarrow 0$ . The low scale expansion about  $k = 0$  yields

$$\Lambda(k) \simeq \Lambda \left(1 - \frac{15}{16\pi} k^2 G_N + \mathcal{O}\left(\frac{k^4}{\Lambda^2} \Lambda G_N, (k^2 G_N)^2\right)\right). \quad (4.57)$$

Thus,  $\Lambda(k)/G(k) = \Lambda/G_N + \mathcal{O}(k^4)$ , implying a comparatively slow running of the ratio towards the UV. This explicit solution of the RG flow might be useful for an analysis of ‘‘RG improved’’ cosmologies along the lines of [315–322].

### Generalised ultralocal parameterisations

For the most general, ultralocal parameterisation (4.34), it turns out that the flow equation in our truncation does only depend on the linear combinations  $T_1 := \tau/4 + \tau_3$  and  $T_2 := \tau_2/4 + \tau_4$ , leaving only two independent split parameters. Instead of exploring the full high dimensional

parameter space, we try to identify relevant points as inspired by our preceding results. For instance for the choice  $T_1 = 1/4$  and  $T_2 = -1/8$ , any dependence on  $\alpha$  drops out, indicating an enhanced insensitivity to the gauge choice. The resulting flow equations are

$$\partial_t g = 2g + \frac{135(\beta - 3)g^2}{(5\beta - 3)g - 72(\beta - 3)\pi}, \quad (4.58)$$

$$\partial_t \lambda = -2\lambda + \frac{g((-669 + 215\beta)g + 36(\beta - 3)\pi(4 - 15\lambda))}{4\pi((3 - 5\beta)g + 72(\beta - 3)\pi)}. \quad (4.59)$$

In the limit  $\beta \rightarrow -\infty$ , these are identical to the exponential split in the same limit. The non-Gaussian fixed point occurs at

$$g_* = \frac{144\pi(\beta - 3)}{145\beta - 411}, \quad \lambda_* = \frac{48(\beta - 3)}{145\beta - 411}, \quad g_*\lambda_* = 6912\pi \left( \frac{\beta - 3}{145\beta - 411} \right)^2. \quad (4.60)$$

Apart from the pathological choice  $\beta_{\text{sing}} = 3$  (incomplete gauge fixing) where this fixed point merges with the Gaussian fixed point, no further extremal point is observed except for the limit  $\beta \rightarrow -\infty$ . The critical exponents are

$$\theta_0 = 4, \quad \theta_1 = \frac{58}{27} + \frac{16}{45(\beta - 3)}. \quad (4.61)$$

Also the exponents become minimally sensitive to the choice of  $\beta$  for  $\beta \rightarrow -\infty$ .

As an oddity, we mention the particular case  $\beta = 3/5$ , where the flow equations acquire a pure one-loop form. In this case, the second critical exponent is exactly 2 as it must, since the slope of a parabolic  $\beta$  function at the interacting fixed point is minus the slope at the Gaussian fixed point [309].

More importantly, the interdependence of gauge and parameterisation choices is also visible in the following fact: we observe that the choice of the gauge parameter  $\beta \rightarrow -\infty$  removes any dependence of our flow on the parameter  $T_2$ , independent of the value of  $\alpha$ . In other words, this limit brings us back exactly to the case which we discussed above in subsection 4.2.3, such that the seemingly much larger class of parameterisations (4.34) collapses to a one-parameter family.

### Arbitrary dimensions

Finally, we discuss the stability of the UV fixed point scenario and its parameterisation dependence in arbitrary dimensions, focusing on  $d > 2$  (for a discussion of  $d = 2$  in the present context, see [273, 275, 277]). In fact, there are some indications in the literature that the parameterisation dependence is pronounced in higher dimensions. Whereas standard calculations based on the linear split generically find a UV fixed point in any dimension  $d > 2$  and gauge fixing parameter  $\alpha$ , see *e.g.* [323, 324], a recent refined choice of the parameterisation to remove gauge parameter dependence on the semi-classical level arrives

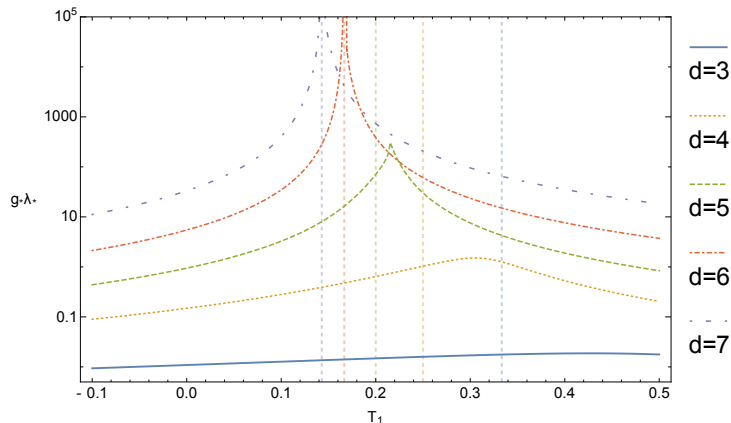


Fig. 4.9.: Parameterisation dependence of fixed point value for  $g_*\lambda_*$  as a function of the split parameter  $T_1$  in the Landau gauge  $\alpha = 0$  and  $\beta \rightarrow -\infty$  for different dimensions  $d = 3, 4, 5, 6, 7$  (from bottom to top). Vertical lines mark the value of the parameter  $T_1 = 1/d$  preferred by independence of the gauge parameter  $\alpha$ . For  $d \geq d_{\text{cr}} \simeq 5.731$ , the fixed point product  $g_*\lambda_*$  develops a singularity at  $T_1 = 1/d$ .

at a different result [276, 277]: the UV fixed point can be removed from the physical region if the number of physical gravity degrees of freedom becomes too large. As the latter increases with the dimensionality, there is a critical value  $d_{\text{cr}}$  above which asymptotically safe gravity does not exist. The resulting scenario is in line with the picture of paramagnetic dominance [263, 325], which is also at work for the QED and QCD  $\beta$  functions: the dominant sign of the  $\beta$  function coefficient arises from the paramagnetic terms in the Hessian which can be reversed if too many diamagnetically coupled degrees of freedom contribute.

Our results extend straightforwardly to arbitrary dimensions. Starting, for instance, with the most general parameterisation (4.34) in  $d$  dimensions, the flows of  $g$  and  $\lambda$  depend only on the linear combinations  $T_1 = \tau/d + \tau_3$  and  $T_2 = \tau_2/d + \tau_4$ . Comparable results as in  $d = 4$  dimensions apply: in the limit of  $\beta \rightarrow -\infty$ , also  $T_2$  drops out such that a one-parameter family remains. In turn, a complete independence of the gauge parameter  $\alpha$  can be realised with the parameterisation specified by  $T_1 = 1/d$  and  $T_2 = -1/(2d)$ .

We illustrate the stability properties of the AS scenario in arbitrary dimensions by choosing the Landau gauge limit  $\alpha \rightarrow 0$  as well as  $\beta \rightarrow -\infty$ , keeping  $T_1$  as a free parameter. Then, we know a priori that  $T_1 = 1/d$  would be a preferred choice from the view point of gauge invariance; it would also correspond to the exponential parameterisation  $\tau = 1$ ,  $\tau_3 = 0$ . Figure 4.9 displays the fixed point values for  $g_*\lambda_*$  as a function of  $T_1$  for various dimensions  $d = 3, \dots, 7$ . While  $d = 3$  exhibits a rather small parameterisation dependence,  $d = 4$  reproduces the earlier results of Figure 4.7 (left panel) now as a function of  $T_1$  with an extremum not far above  $T_1 = 1/4$ . By contrast,  $g_*\lambda_*$  develops a kink for  $d = 5$  that turns into a singularity for  $d = 6$  and larger. For increasing  $d$ , the kink approaches the preferred parameterisation  $T_1 = 1/d$  (vertical dashed lines in Figure 4.9). The singularity in  $g_*\lambda_*$  occurs for a critical dimension  $d_{\text{cr}} \simeq 5.731$ .

This observation suggests the following interpretation: whereas we can identify a UV fixed point for any dimension as long as we choose  $T_1$  sufficiently far away from  $T_1 = 1/d$ , we find a stable fixed point scenario only for  $d = 3$  and  $d = 4$  integer dimensions. Already for  $d = 5$ , the fixed point product  $g_*\lambda_*$  can change by two orders of magnitude by varying the parameterisation, which is at least a signature for the insufficiency of the truncation. For  $d \geq d_{\text{cr}} \simeq 5.731$ ,  $g_*\lambda_*$  can become unboundedly large as a function of the parameterisation, signaling the instability of the fixed point.

If these features persist also beyond our truncation, they suggest that the AS scenario may not exist far beyond the spacetime dimension  $d = 4$ . Whereas this does not offer a dynamical explanation of our spacetime dimension, it may serve to rule out the mutual coexistence of extra dimensions and asymptotically safe quantum gravity.

### 4.3. Correlation functions

In the remaining two sections of the quantum gravity part of this thesis, we go beyond the background field approximation used in the previous sections, and consider an effective action which depends on both the background metric and the fluctuation field. As discussed earlier, this is an important step towards a solution to the Nielsen identities, which encode that the effective action actually is a functional of only one metric. We will start by introducing the setting, then discuss correlation functions in flat and curved spacetime, and in the next section introduce a method to treat correlation functions of arbitrarily high order. Parts of this section are based on [45], as well as yet unpublished work with Stefan Lippoldt (correlation functions in curved spacetime and gauge dependence).

#### 4.3.1. Vertex expansion in quantum gravity

Lots of information on a quantum field theory is stored in its correlation functions. The most important information is stored in the propagator, which also drives the flow equation. In fact, in the presence of a background field, we have to be more precise here. The second variation that appears in the flow equation is a variation w.r.t. the fluctuation field. This immediately suggests that a good approximation scheme should resolve the fluctuation propagator as good as possible. By taking two fluctuation derivatives of the flow equation, one sees that the flow of the two-point function in turn is driven also by the three- and four-point function. Clearly, the flow of the  $n$ -point function involves correlators of order up to  $n + 2$ , indicating the infinite hierarchy of the flow equation. A natural expansion scheme is the vertex expansion, schematically<sup>8</sup>

$$\Gamma[\bar{g}, h] = \sum_n \frac{1}{n!} \Gamma^{(n)}[\bar{g}, 0] \cdot h^n. \quad (4.62)$$

<sup>8</sup>In this general discussion, we suppress the ghost fields.

For technical reasons, we will first study such an approximation on a flat background,  $\bar{g} = \delta$ , later also treating couplings to background curvature.

If we wouldn't break the Nielsen identities by the introduction of the regulator and the gauge fixing, derivatives w.r.t.  $\bar{g}$  and  $h$  would coincide. Since we cannot do so, these derivatives will not agree, and different couplings have to be introduced. Again, it is useful to introduce a basis to classify invariants. In appendix D, we introduce a basis for correlation functions with up to three fluctuation fields, two derivatives and one background curvature. On a flat background, it is also straightforward (up to numerical complexity) to treat the full momentum dependence of correlation functions [43].

The sheer size of the basis of the correlation functions shows that in practice it will be difficult to resolve all correlation functions up to a certain order. In a first treatment, severe approximations will be made in order to render computations feasible. We build on the parameterisation for vertex functions introduced in [43, 326]. In particular, we parameterise the correlation functions as<sup>9</sup>

$$\Gamma^{(n)}(\mathbf{p}) = \left( \prod_{i=1}^n \sqrt{Z(p_i^2)} \right) G_n^{\frac{n}{2}-1}(\mathbf{p}) \mathcal{T}^{(n)}(\mathbf{p}, \Lambda_n), \quad (4.63)$$

where  $\mathcal{T}^{(n)}$  is the classical tensor structure of the vertex obtained by the  $n$ -th functional derivative of ( $G_N$  times) the Einstein-Hilbert action, and the cosmological constant replaced by a uniform fluctuation coupling  $\Lambda_n$ , which represents the constant part of the vertex. Further,  $Z(p_i^2)$  is the momentum dependent wave function renormalisation, and the couplings  $G_n$  parameterise the interaction vertices between gravitons. We stress that the first genuine dynamical coupling is  $G_3$ . In the following we will approximate all fluctuation couplings  $G_n$  by a single, momentum independent  $G_3$ . An extension to resolve  $G_3$  and  $G_4$  has recently been put forward in [188]. It turns out that the general momentum dependence induced by the flow equation is well modelled by this ansatz.

As stressed earlier, an important issue in quantum gravity is the background independence of physical observables. We emphasise that in the present framework, based on an effective action  $\Gamma[\bar{g}, h]$ , we have the paradoxical situation that the background independence of observables necessitates the background dependence of the vertex functions  $\Gamma^{(n)}$  of the dynamical fields. Importantly, an ansatz  $\Gamma[\bar{g}, h] = \Gamma[\bar{g} + h]$  violates background independence and dynamical diffeomorphism invariance, see *e.g.* [40, 165, 172].

### 4.3.2. Local quantum gravity

In this section we present the first calculation of the genuine dynamical gravitational coupling  $G_3$ . Here we build on the general setup for flows of fully momentum dependent vertex functions in quantum gravity developed in [41, 43]. This expansion naturally resolves the

<sup>9</sup>With this choice, the fluctuation field  $h$  has mass dimension 1 in  $d = 4$ .



physically important difference between the graviton wave function renormalisation and the gravitational couplings. The existence of the UV and IR fixed points is confirmed in this enhanced approximation, thus providing further evidence for the AS scenario. Interestingly, the ultraviolet fixed point exhibits one irrelevant direction, along with two relevant ones, in accordance with the hypothesis of a finite dimensional critical hypersurface. For related results in  $f(R)$  gravity see *e.g.* [327, 328].

A well-defined Wilsonian block spinning requires locality of the flow in momentum space. Here we show that the flows of the graviton two- and three-point functions are local in momentum space. This nontrivial property is linked to diffeomorphism invariance.

### Locality

The FRG is based on the idea of a successive integration of momentum shells, or, more generally, spectral shells of spectral values of the given kinetic operator. Hence, it relies on the distinction of small and large momentum or spectral modes. A functional RG step implements the physics of momentum/spectral modes at a given scale  $k$  and is inherently related to local interactions.

Locality in momentum space implies in particular that the flows of vertices at a given momentum scale  $k$  decay relative to the vertex itself if all momentum transfers (momentum channels)  $t_i$  are taken to infinity. For example, for the four-point vertex we have  $t_1, t_2, t_3$  being the well-known  $s, t, u$ -channels, with *e.g.*  $s = (p_1 + p_2)^2$ . Hence, locality reads schematically

$$\lim_{t_i/k^2 \rightarrow \infty} \frac{|\partial_t \Gamma^{(n)}(\mathbf{p})|}{|\Gamma^{(n)}(\mathbf{p})|} = 0, \quad \text{with } \mathbf{p} = (p_1, \dots, p_n), \quad (4.64)$$

where a projection on one of the tensor structures of the vertex is implied. For the limit (4.64) each diagram in the flow of a given vertex has an infinite momentum transfer. Thus, the diagrams are only sensitive to fluctuations far above the cutoff scale.

It is easily proven that (4.64) applies to standard renormalisable quantum field theories in four dimensions including non-Abelian gauge theories that involve momentum dependent couplings. In these theories, the locality property follows from power counting arguments. However, for perturbatively nonrenormalisable theories in four dimensions power counting suggests nonlocal flows and (4.64) must be a consequence of nontrivial cancellations. In gravity this has been shown for the graviton propagator [41, 43]. It is also reflected in the symmetry relation between graviton diagrams contributing to the Yang-Mills propagator [329]. Moreover, it is easily verified that a  $\phi^4$ -theory with a momentum dependent coupling such as  $\phi^2 \partial^2 \phi^2$  does not satisfy the locality condition (4.64), as no cancellation between tensor structures is possible. We conjecture that momentum locality in quantum gravity is linked to diffeomorphism invariance.

Note that (4.64) does not hold, even for quantum field theories which are perturbatively renormalisable in four dimensions, if some of the channels  $t_i/k^2$  stay finite: the flow always

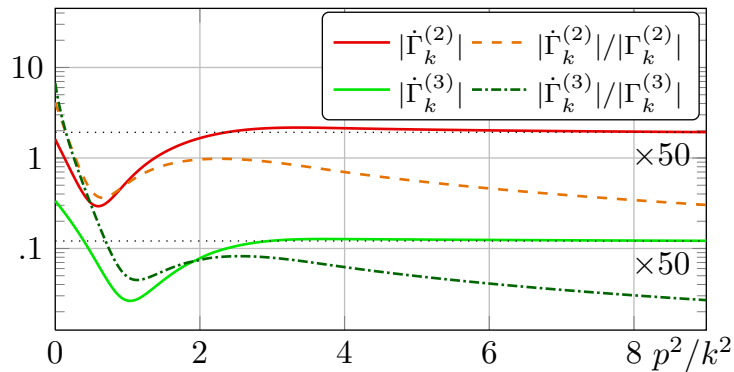


Fig. 4.10.: Logarithmic plot of the flows  $|\partial_t \Gamma^{(2)}|$  and  $|\partial_t \Gamma^{(3)}|$  (solid red and light green curves) and the corresponding ratios  $|\partial_t \Gamma^{(2)}|/|\Gamma^{(2)}|$  and  $|\partial_t \Gamma^{(3)}|/|\Gamma^{(3)}|$  (dashed orange and dash-dotted dark green curves) as functions of  $p^2/k^2$ . The norm refers to the tensor projection discussed below (4.65). All quantities are evaluated at  $(g, \mu_h, \lambda_3) = (1, 0.1, -0.7)$ . The flows are multiplied with 50 for convenience. The ratios decay with  $1/p^2$  for large  $p$  since the associated flows quickly approach constant values, satisfying (4.64).

involves diagrams with a finite momentum transfer. However, those diagrams correspond to IR processes such as Bremsstrahlung, which is why they do not reflect the UV behaviour of the theory. In summary the above discussion suggests that the relation (4.64) is a necessary requirement for local quantum field theories.

In the following, we show that (4.64) also applies to the graviton three-point function. Together with the momentum locality of the two-point function shown in [41, 43] this provides strong indications for the momentum locality of RG gravity. Figure 4.10 depicts the momentum dependence of the flows for the graviton two- and three-point functions,  $|\partial_t \Gamma^{(2)}|$  and  $|\partial_t \Gamma^{(3)}|$ , respectively as well as the corresponding ratios according to (4.64). Since  $|\partial_t \Gamma^{(2)}|$  and  $|\partial_t \Gamma^{(3)}|$  quickly approach constants, the ratios decay with  $1/p^2$  for large momenta.

### Flows of Correlation Functions

The flow of the three-point function is obtained by three field derivatives of the flow equation for the effective action. It is depicted in Figure 4.11. We employ a de Donder type linear gauge condition in the Landau gauge limit of vanishing gauge parameter ( $\alpha = 0, \beta = 1$ ).

The right hand side of the vertex flows usually includes all types of tensor structures admitted by symmetry irrespective of the ansatz for the vertices. For the flow equations for the couplings  $\Lambda_n$  and  $G_n$  we have to project the tensorial vertex flow appropriately: we focus on the transverse traceless parts of the flow, and reduce all external graviton legs to its spin-2 parts by using transverse traceless projectors  $\Pi_T$ . The flow of  $\Lambda_n$  is extracted from the momentum independent part of the  $n$ -th vertex flow at  $\mathbf{p} = 0$ . Consequently, we decompose  $\mathcal{T}^{(n)}(\mathbf{p}, \Lambda_n)$  into its momentum independent part  $\mathcal{T}^{(n)}(0, 1)$  and the part  $\mathcal{T}^{(n)}(\mathbf{p}, 0)$ , which is

Fig. 4.11.: Diagrammatic representation of the flow of the three-graviton vertex. Double and dashed lines represent graviton and ghost propagators, respectively, filled circles denote dressed vertices. Crossed circles are regulator insertions. All diagrams are symmetrised with respect to the interchange of external momenta  $\mathbf{p}$ .

at least quadratic in  $\mathbf{p}$ , according to

$$\mathcal{T}^{(n)}(\mathbf{p}; \Lambda_n) = \Lambda_n \mathcal{T}^{(n)}(0; 1) + \mathcal{T}^{(n)}(\mathbf{p}; 0). \quad (4.65)$$

The full tensor flow with transverse traceless external legs is then contracted with  $\mathcal{T}^{(n)}(0; 1)$  or  $\mathcal{T}^{(n)}(\mathbf{p}; 0)$  in order to yield scalar expressions that are related to the flow of  $\Lambda_n$  or  $G_n$ , respectively. In particular, we denote the contraction of the right-hand side with  $\mathcal{T}^{(n)}(0, 1)$  and  $\mathcal{T}^{(n)}(\mathbf{p}, 0)/\mathbf{p}^2$  by  $\text{Flow}_{\Lambda}^{(n)}$  and  $\text{Flow}_G^{(n)}$ , respectively. The factor of  $1/\mathbf{p}^2$  in the definition of the flow for the gravitational coupling accounts for the fact that the corresponding tensor projector is proportional to  $p^2$ . For convenience, the definition of  $\text{Flow}^{(n)}$  also includes the factor  $\prod_i Z_h^{-1/2}(p_i)$ . For the graviton three-point function these objects take the generic form

$$\text{Flow}_{\Lambda/G}^{(3)} = \int \frac{d^4 q}{(2\pi)^4} \left( \partial_t \mathfrak{R}(q^2) - \eta_{\phi_i}(q^2) \mathfrak{R}(q^2) \right) F_{\phi_i, \Lambda/G}(\mathbf{p}, q, G_n, \Lambda_n), \quad (4.66)$$

where  $n \in \{3, 4, 5\}$  and a sum over species of fields  $\phi_i$  is understood, which includes gravitons and the corresponding ghost fields. The contributions encoded in  $F_{\phi_i}$  originate from the diagrams displayed in Figure 4.11. Note that (4.66) is only a function of the anomalous dimension

$$\eta_{\phi_i}(p^2) := -\partial_t \ln Z_{\phi_i}(p^2), \quad (4.67)$$

since all wave function renormalisations  $Z_{\phi_i}$  drop out. The expressions for the flow of the three-point function still depend on the external momenta  $\mathbf{p} = (p_1, p_2, p_3)$ , where  $p_3$  can be eliminated using momentum conservation. Therefore, the kinematic degrees of freedom can be parameterised by the absolute values of the remaining two momenta  $|p_1|$ ,  $|p_2|$  and the angle  $\vartheta_{12}$  between them. For the proof of locality we work with the most general momentum configuration. For the flows  $\text{Flow}_{\Lambda/G}^{(3)}$  the maximally symmetric momentum configuration is used,

$$p := |p_1| = |p_2| \quad \vartheta_{12} = 2\pi/3. \quad (4.68)$$

In summary, we have specified a projection procedure for the spacetime indices and a kine-

matic configuration for the graviton field momenta. It remains to relate  $\text{Flow}_G^{(3)}$  and  $\text{Flow}_\Lambda^{(3)}$  to the flow of the couplings  $G_3$  and  $\Lambda_3$ , respectively. The flow of  $G_3$  is most conveniently isolated by evaluating the projected flow at two momentum scales  $p = k$  and  $p = 0$  and subtracting the results. For the dimensionless coupling  $g_3 = k^2 G_3$  we obtain

$$\partial_t g_3 = (2 + 3\eta_h(k^2))g_3 - \frac{24}{19}(\eta_h(k^2) - \eta_h(0))\lambda_3 g_3 + 2\mathcal{N}_g \sqrt{g_3} k \left( \text{Flow}_G^{(3)}(k^2) - \text{Flow}_G^{(3)}(0) \right), \quad (4.69)$$

with a normalisation factor  $\mathcal{N}_g^{-1} := \mathcal{T}^{(3)}(k; 0) \circ \Pi_T^3 \circ \mathcal{T}^{(3)}(k; 0)$ , where  $\circ$  denotes the pairwise contraction of indices. Another possibility is the evaluation with a  $p^2$ -derivative at  $p = 0$ . This procedure is less accurate in approximating the momentum dependence of the flow. On the other hand, it allows for an analytic flow equation for the couplings  $G_3$ . The difference between these momentum projections is discussed below. The flow of the dimensionless coupling  $\lambda_3 = \Lambda_3/k^2$  is obtained by evaluating the flow at  $p = 0$ , which leads to

$$\partial_t \lambda_3 = \left( \frac{3}{2}\eta_h(0) - 1 - \frac{\partial_t g_3}{2g_3} \right) \lambda_3 + \frac{\mathcal{N}_\lambda}{\sqrt{g_3}} \text{Flow}_\Lambda^{(3)}(0), \quad (4.70)$$

with  $\mathcal{N}_\lambda^{-1} := \mathcal{T}^{(3)}(0; 1) \circ \Pi_T^3 \circ \mathcal{T}^{(3)}(0; 1)$ . The setup is complemented by flow equations for the graviton gap parameter  $\mu = -2\Lambda_2/k^2$ , the fully momentum dependent anomalous dimensions  $\eta_{\phi_i}(p^2)$  and the coupling of the one-point function  $\lambda_1/\sqrt{g_1} = \Lambda_1 G_1^{-1/2}/k^3$ . The flows for the couplings  $\mu$  and  $\lambda_1/\sqrt{g_1}$  are extracted from the graviton two- and one-point functions at vanishing external momenta, respectively. The anomalous dimensions  $\eta_{\phi_i}(p^2)$  are solutions to Fredholm integral equations, extracted from the two-point functions, see [43].

The projection procedure just described can also be formulated on the level of monomials. For the flow of the constant part of the three-graviton vertex,  $\lambda_3$ , the invariant is

$$h_\mu{}^\nu h_\nu{}^\rho h_\rho{}^\mu, \quad (4.71)$$

whereas the flow of  $g_3$  is taken from the linear combination

$$\frac{6}{19} h_\mu{}^\rho h_\rho{}^\nu \bar{\Delta} h_\nu{}^\mu - \frac{1}{19} h_{\mu\nu} h_{\rho\sigma} \bar{D}^\mu \bar{D}^\nu h^{\rho\sigma} + \frac{14}{19} h^{\mu\nu} h^{\rho\sigma} \bar{D}_{(\mu} \bar{D}_{\rho)} h_{\nu\sigma}. \quad (4.72)$$

### Proof of Locality

In order to prove (4.64) for the three-point function, an arbitrary kinematic configuration is used and parameterised by  $|p_1|$ ,  $|p_2|$  and the angle  $\vartheta_{12}$ . The large momentum limit is then characterised by  $|p_1| = |p_2| = p \rightarrow \infty$ . Simple power counting of the momentum structure of the flow leads to the naïve expectation that  $\lim_{p/k \rightarrow \infty} \text{Flow}_G^{(3)} \sim p^2$ . In this case the ratio in (4.64) would tend to a constant. However, an analytic asymptotic expansion around  $p = \infty$  shows that the  $p^2$ -contribution vanishes identically in the large momentum limit by nontrivial

cancellations between all diagrams in Figure 4.11. As a consequence,  $\lim_{p/k \rightarrow \infty} \text{Flow}_G^{(3)}$  tends to a constant and the ratio in (4.64) vanishes. This is valid for all values of the angle  $\vartheta_{12}$ , *i.e.* for all kinematic configurations. For an explicit example see Figure 4.10 for the symmetric momentum configuration. The figure further displays that (4.64) is also satisfied by the graviton two-point function, see also [41, 43]. We conclude that locality is always satisfied by the flows of two- and three-point functions. We emphasise again that it is indispensable that all external momenta are taken to infinity. Indeed, for configurations with mixed UV-IR limit equation (4.64) does not hold.

### UV Fixed Point

Fixed points are defined by vanishing flows of all dimensionless dynamical couplings, that is  $g_3$ ,  $\lambda_3$  and  $\mu$  in the present setup. Most importantly, we find a UV fixed point with one irrelevant direction that is approximately directed along the  $\lambda_3$ -axis.

The following results are obtained with the regulator  $\mathfrak{R}(x) = \Gamma^{(2)}|_{\mu=0}(x)r(x)$  where  $xr(x) = (1-x)\theta(1-x)$  [226, 307]. Moreover, we identify  $\lambda_3 \equiv \lambda_4 \equiv \lambda_5$  in order to close the flow equations, and use the notation  $g := g_3$ . The UV fixed point described below is obtained with the finite difference procedure, leading to the flow equations (4.69) and (4.70), as well as the one for  $\mu$  already presented in [43]. The anomalous dimensions are evaluated with their full momentum dependence. The fixed point values read

$$(g_*, \mu_*, \lambda_{3*}) = (0.66, -0.59, 0.11), \quad (4.73)$$

with the critical exponents  $\theta_1$ ,  $\theta_2$  and  $\theta_3$  given by<sup>10</sup>

$$(\theta_{1/2}, \theta_3) = (1.4 \pm 4.1 \mathbf{i}, -14). \quad (4.74)$$

As already mentioned above, the UV fixed point (4.73) has the interesting property that it is not fully UV attractive: it exhibits two relevant and one irrelevant direction. In (4.74), this is reflected by two critical exponents with positive real parts,  $\theta_1$  and  $\theta_2$ , and one with negative real part,  $\theta_3$ . The irrelevant direction of the UV fixed point (4.73) is approximately directed along the  $\lambda_3$  axis. The critical exponents corresponding to the UV relevant directions of the fixed points are complex, which accounts for a spiral behaviour of RG trajectories in the vicinity of the UV fixed point. Note that  $\theta_3$  in (4.74) is one order of magnitude larger than  $\theta_1$  and  $\theta_2$ . This kind of instability of critical exponents was also found in [328] within  $f(R)$  gravity. There, a convergence of the critical exponents to smaller values was observed after the inclusion of higher order operators, *i.e.* higher powers  $R^n$ . Indeed,  $\theta_3$  becomes smaller if the dynamical couplings  $g_4$  and  $\lambda_4$  are included [188].

Finally, we have checked numerically that the momentum dependencies of our ansatz for

<sup>10</sup>Note that in the published version [45], the conventions for the critical exponents is exactly opposite.

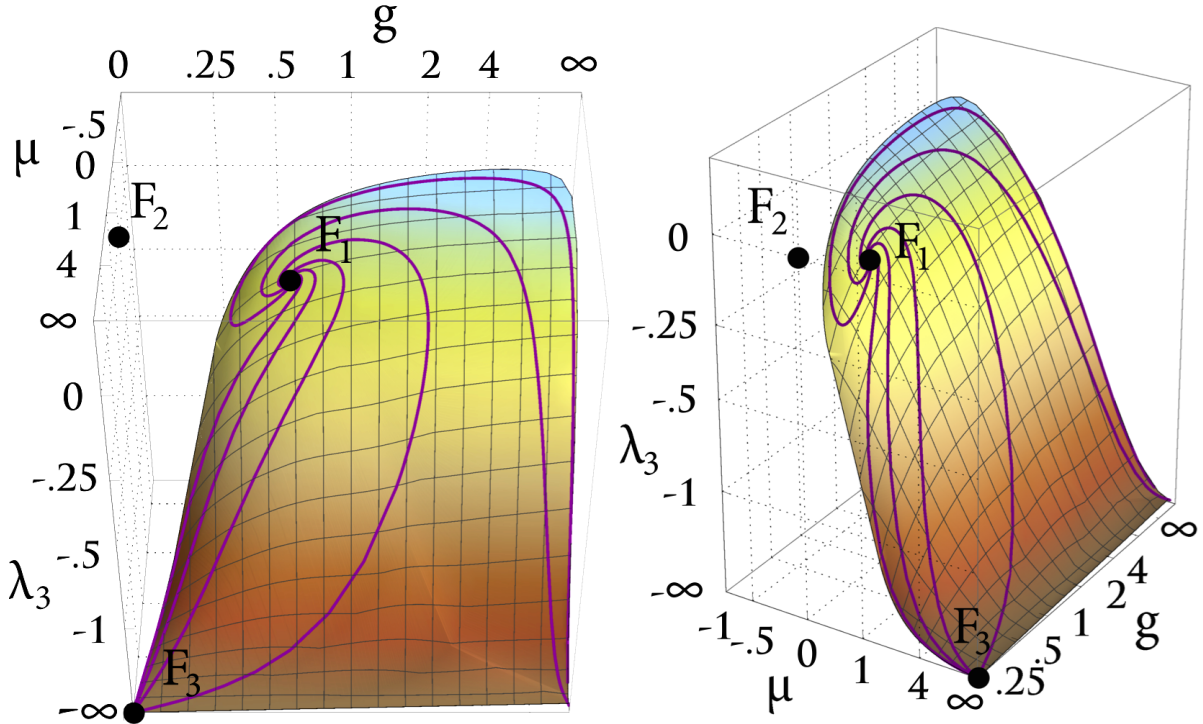


Fig. 4.12.: Phase diagram for the couplings  $g$ ,  $\lambda_3$  and  $\mu$  in two different views. The phase diagram was calculated using the analytic equations (4.75)-(4.78). The system exhibits a non-trivial UV fixed point,  $F_1$ , with two attractive and one repulsive direction. The Gaussian fixed point and a nontrivial IR fixed point are denoted as  $F_2$  and  $F_3$ , respectively. The set of trajectories that approach  $F_1$  constitute a two-dimensional UV critical hypersurface represented in gradient colours.

the vertex dressing and that of  $\text{Flow}^{(2)}$  and  $\text{Flow}_G^{(3)}$  are in very good agreement. Therefore, a momentum independent  $G_3$  is a valid approximation over the whole momentum range. In particular, the full momentum dependence of the anomalous dimensions was found to model very accurately the higher order  $p$  dependence of  $\text{Flow}_G^{(3)}$ .

### Global Phase Diagram and Analytic Flow Equations

The flow equation (4.69) does not have a closed analytic form. However, for a more accessible presentation, analytic flow equations are favourable. An analytic expression for  $\partial_t g$  is obtained by taking a derivative of  $\text{Flow}_G^{(3)}$  with respect to  $p^2$  at  $p = 0$ . We stress that this method is considerably less accurate in modelling the momentum dependence of the flow. Nonetheless, the resulting analytic flow equation for  $g$  shares the main features with (4.69). This even holds for graviton and ghost anomalous dimensions set to zero,  $\eta_h = \eta_c = 0$ . Table 4.2 displays the properties of the nontrivial fixed point as obtained from the different methods.

The analytic flow equations for the presented vertex flow of gravity with vanishing anoma-

	Finite difference		Derivative	
	$\eta(p^2)$	$\eta \equiv 0$	$\eta(p^2)$	$\eta \equiv 0$
$g_*$	0.66	0.96	0.58	0.57
$\mu_*$	-0.59	-0.35	-0.44	-0.16
$\lambda_{3*}$	0.11	-0.024	0.028	-0.16
$(\lambda_1/\sqrt{g_1})_*$	0.39	0.19	0.22	0.11
$\theta_i$	$1.4 \pm 4.1\mathbf{i}$	$2.1 \pm 2.4\mathbf{i}$	$1.6 \pm 5.5\mathbf{i}$	$1.5 \pm 1.8\mathbf{i}$
	-14	-5.8	-6.5	-1.6
	2.2	3	2.5	3

Tab. 4.2.: Properties of the UV fixed point for different momentum parameterisations, namely using a finite difference of the flow and a derivative at  $p = 0$ . The values acquired with the latter correspond to the analytic equations given in (4.75)-(4.78). Note that  $\lambda_1/\sqrt{g_1}$  is a nondynamical background coupling originating from the graviton one-point function.

lous dimensions are given by

$$\partial_t g = 2g + \frac{8g^2}{19\pi} \left( \frac{584\lambda_3^3 - 910\lambda_3^2 + 445\lambda_3 - \frac{299}{4}}{15(\mu+1)^5} - \frac{47}{8(\mu+1)^2} - \frac{5}{8} + \frac{864\lambda_3^3 + 133\lambda_3^2 - 112\lambda_3 + \frac{49}{4}}{6(\mu+1)^4} - \frac{60\lambda_3^2 - 58\lambda_3 - 15}{6(\mu+1)^3} \right), \quad (4.75)$$

$$\partial_t \lambda_3 = - \left( 1 + \frac{\partial_t g}{2g} \right) \lambda_3 + \frac{g}{\pi} \left( \frac{2\lambda_3^3 - 4\lambda_3^2 + 3\lambda_3 - \frac{11}{20}}{(\mu+1)^4} - 4 \frac{4\lambda_3^2 - \lambda_3}{(\mu+1)^3} + \frac{1 - 3\lambda_3}{(\mu+1)^2} + \frac{6}{5} \right), \quad (4.76)$$

$$\partial_t \mu = -2\mu + \frac{2g}{\pi} \left( \frac{16\lambda_3^2 - 8\lambda_3 + \frac{7}{4}}{3(\mu+1)^3} + \frac{2\lambda_3 - 1}{(\mu+1)^2} - 1 \right), \quad (4.77)$$

$$\partial_t \left( \frac{\lambda_1}{\sqrt{g_1}} \right) = -3 \frac{\lambda_1}{\sqrt{g_1}} + \frac{\sqrt{g}}{2\pi} \left( \frac{1}{(\mu+1)^2} + \frac{4}{3} \right). \quad (4.78)$$

Figure 4.12 shows the phase diagram for the couplings  $(g, \mu, \lambda_3)$  as calculated from (4.75)-(4.78). The purple lines are trajectories along the flow that terminate at the nontrivial UV fixed point  $F_1$ . The set of all trajectories constitutes the two-dimensional critical hypersurface represented in gradient colours. In the IR, the trajectories flow towards  $F_3 = (0, \infty, -\infty)$  or, alternatively, towards  $(\infty, \infty, -\infty)$ . The IR fixed point  $F_3$  was also observed in [43]. In the vicinity of  $F_3$  all couplings scale classically since for  $\mu \rightarrow \infty$  the loop contributions to the flow tend to zero. Neither the trivial Gaussian fixed point  $F_2$ , nor the third, nontrivial IR fixed point, which was first found in [43] and is located at  $(0, -1, \infty)$ , are reached by any UV finite trajectory in the present setup. For the latter, this is expected to change if the vertices are expanded about a curved background [330]. A detailed IR analysis is beyond the scope of this work.

### 4.3.3. Gauge dependence and curvature correlations

As a first step beyond the previous calculations, we now want to resolve correlation functions on a curved background, though still in a curvature expansion. For this, we resolve the following aspects of the graviton propagator: both gap parameters, corresponding to the tensor mode and the scalar mode, the full gauge dependence, and the full dependence on background curvature to linear order in a curvature expansion. We also study the three-graviton vertex in exactly the same approximation as in the previous section, however without anomalous dimensions. This section is based on yet unpublished work with Stefan Lippoldt.

As it turns out, it is useful to change the tensor structure of the regulator. Specifically, any regulator has to include at least the following terms:

$$\Delta S \sim \int d^4x \sqrt{\bar{g}} \left( h_{\mu\nu} \left[ \mathfrak{R}_1(\bar{\Delta}) \Pi_{\text{TL}}^{\mu\nu\rho\sigma} + \mathfrak{R}_2(\bar{\Delta}) \Pi_{\text{Tr}}^{\mu\nu\rho\sigma} \right] h_{\rho\sigma} \right). \quad (4.79)$$

Here,  $\Pi_{\text{TL}}$  ( $\Pi_{\text{Tr}}$ ) is the projector onto the traceless (trace) part. In fact, a regulator with these two structures is already enough to regularise everything. In the following, it will be crucial that we choose a regulator which doesn't depend on the gauge parameter  $\alpha$ . Our particular choice is

$$\Delta S \sim \int d^4x \sqrt{\bar{g}} \left( h_{\mu\nu} \mathfrak{R}(\bar{\Delta}) \left[ \Pi_{\text{TL}}^{\mu\nu\rho\sigma} - \frac{3 + \beta(\beta - 2)}{2} \Pi_{\text{Tr}}^{\mu\nu\rho\sigma} \right] h_{\rho\sigma} \right), \quad (4.80)$$

where prefactors are chosen such that in the Landau gauge limit,  $\bar{\Delta} \rightarrow \bar{\Delta} + \mathfrak{R}(\bar{\Delta})$ .

Since we want to resolve curved correlation functions, we have to specify the tensor monomials and couplings that we want to study. We amend the classical Einstein-Hilbert action by

$$\begin{aligned} \Gamma^{\text{curv}} = \frac{1}{32\pi} \int d^4x \sqrt{\bar{g}} h_{\mu\nu} & \left[ \mathcal{R}_C \bar{C}^{\mu\rho\nu\sigma} + \mathcal{R}_{\text{TLSTL}} \Pi_{\text{TL}}^{\mu\nu\tau\omega} \bar{S}_{\omega\lambda} \Pi_{\text{TL}\tau}^{\lambda\rho\sigma} + \mathcal{R}_{\text{RTL}} \bar{R} \Pi_{\text{TL}}^{\mu\nu\rho\sigma} \right. \\ & \left. + \mathcal{R}_{\text{STr}} \left( \bar{S}^{\mu\nu} \bar{g}^{\rho\sigma} + \bar{g}^{\mu\nu} \bar{S}^{\rho\sigma} \right) + \mathcal{R}_{\text{RTr}} \bar{R} \Pi_{\text{Tr}}^{\mu\nu\rho\sigma} \right] h_{\rho\sigma}, \end{aligned} \quad (4.81)$$

We also resolve the two gaps, which we specify in the following way. We start by the second variation of the Einstein-Hilbert action, then decompose the fluctuation  $h$  into traceless and trace part, and label the corresponding prefactors as  $\lambda_{\text{TL}}$  and  $\lambda_{\text{Tr}}$ , respectively. We finally introduce another gap,  $\tilde{\lambda}$ , by the relation

$$\tilde{\lambda} = \frac{-2\beta^2 \lambda_{\text{TL}} + 6\lambda_{\text{Tr}}}{(\beta - 3)^2}. \quad (4.82)$$

With this, in the Landau gauge limit, all propagators have the form  $\bar{\Delta} + \mathfrak{R}(\bar{\Delta}) - 2\lambda$ , either with  $\lambda_{\text{TL}}$  or with  $\tilde{\lambda}$ . These two gaps are thus gauge independent, and might reduce potential



gauge dependencies when coupling identifications are used<sup>11</sup>.

### Landau gauge limit

We will now show that the limit  $\alpha \rightarrow 0$  is indeed a fixed point of the flow, and that any choice of  $\beta$  in this limit is also a fixed point. For this, observe that the graviton propagator and all vertices on flat background are finite in the limit  $\alpha \rightarrow 0$ . To advance in the proof, we have to specify a projection onto the flow of  $\alpha$ . This is most naturally done with a York decomposition after the flow has been calculated. The flow of  $\alpha$  is then read off from the kinetic term of the transverse vector,  $\xi^{\text{T}\mu} \bar{\Delta}^2 \xi_\mu^{\text{T}}$ . On the other hand, the flow of  $\beta$  can then be uniquely obtained from the correlator  $\bar{\sigma} \bar{\Delta}^2 \bar{\sigma}$ , where  $\bar{\sigma}$  is the linear combination of the scalar modes which is pure gauge to linear order [308],

$$\bar{\sigma} = \sigma + \frac{\beta}{(d-1-\beta)\bar{\Delta} - \bar{R}} (\mathbf{h} + \bar{\Delta}\sigma). \quad (4.83)$$

Schematically, the flow equation for  $\alpha$  thus reads

$$\partial_t \frac{1}{\alpha} = -\frac{\partial_t \alpha}{\alpha^2} \sim \text{Flow}_{\xi^{\text{T}\mu} \bar{\Delta}^2 \xi_\mu^{\text{T}}}^{(2)}, \quad (4.84)$$

where the right-hand side is finite in the limit  $\alpha \rightarrow 0$ , since the propagator, vertices and the regulator insertion are all finite in this limit. The direct consequence is that in this limit, the flow of  $\alpha$  vanishes. Since the flow is quadratic in  $\alpha$ ,  $\alpha$  is a marginal parameter. Furthermore, for the flow of  $\beta$ , one obtains

$$\partial_t \frac{\beta}{\alpha} = \frac{1}{\alpha} \left( \partial_t \beta - \beta \frac{\partial_t \alpha}{\alpha} \right) \sim \text{Flow}_{\bar{\sigma} \bar{\Delta}^2 \bar{\sigma}}^{(2)}. \quad (4.85)$$

Since again the right-hand side is finite in the limit  $\alpha \rightarrow 0$ , we obtain that  $\partial_t \beta$  vanishes in this limit, showing that any choice of gauge fixing in the Landau gauge limit is a fixed point. Clearly also  $\beta$  is an exactly marginal parameter in this limit. This discussion underlines that the limit  $\alpha \rightarrow 0$  is indeed a physical limit which disentangles gauge and physical degrees of freedom also during the flow.

### Fixed point structure I - flat background

It is clear that the curvature couplings don't feed into the flow equations of the "flat" couplings  $g_3$ ,  $\lambda_{\text{TL}}$ ,  $\tilde{\lambda}$  and  $\lambda_3$ . We thus first study the system of these four couplings, and later the fixed point structure of the curvature couplings on the solution of this system.

To make contact with the previous section, we first choose  $\beta = 1$ , and investigate how the fixed point structure changes upon the inclusion of the second gap. It turns out that now,

<sup>11</sup>In the following discussion, we refrain from the redefinition  $\mu = -2\lambda$ .

we find two viable fixed points, both with two relevant and two irrelevant directions. The first fixed point, which might be related to the one found with a single gap, has coordinates

$$g_* = 0.196, \quad \lambda_{3*} = -0.008, \quad \lambda_{\text{TL}*} = 0.197, \quad \tilde{\lambda}_* = 0.399, \quad (4.86)$$

with critical exponents

$$\theta_{1,2} = 1.650 \pm 3.698i, \quad \theta_3 = -5.433, \quad \theta_4 = -28.59. \quad (4.87)$$

The second fixed point is situated at

$$g_* = 0.928, \quad \lambda_{3*} = 0.337, \quad \lambda_{\text{TL}*} = 0.201, \quad \tilde{\lambda}_* = 0.344, \quad (4.88)$$

and has purely real critical exponents,

$$\theta_1 = 21.42, \quad \theta_2 = 3.325, \quad \theta_3 = -7.486, \quad \theta_4 = -17.21. \quad (4.89)$$

By contrast, for  $\beta = 0$ , only one fixed point with positive  $g_3$  and two relevant directions is found,

$$g_* = 0.168, \quad \lambda_{3*} = 0.037, \quad \lambda_{\text{TL}*} = 0.250, \quad \tilde{\lambda}_* = 0.419, \quad (4.90)$$

with critical exponents

$$\theta_{1,2} = 0.933 \pm 5.169i, \quad \theta_3 = -3.318, \quad \theta_4 = -29.92. \quad (4.91)$$

There is a second fixed point in the physical regime with only one relevant direction at

$$g_* = 0.033, \quad \lambda_{3*} = -0.714, \quad \lambda_{\text{TL}*} = 0.077, \quad \tilde{\lambda}_* = 0.453. \quad (4.92)$$

Its critical exponents are

$$\theta_1 = 1.686, \quad \theta_{2,3} = -1.255 \pm 1.407i, \quad \theta_4 = -56.65. \quad (4.93)$$

We tend to view this fixed point as an artifact of the approximation since it is quite near to the singularity at  $\tilde{\lambda} = 1/2$ , which is vastly off-shell and might not be captured well by a background curvature expansion.

For  $\beta = -1$  (termed the physical gauge in [331]), the situation gets strange: both fixed points of the choice  $\beta = 0$  survive, however the fixed point with formerly 2 irrelevant directions now has only irrelevant directions, *i.e.* the flow is attracted towards the fixed point in the IR. In its form this fixed point is not suitable anymore for a UV completion in the sense

of AS. Its coordinates are at

$$g_* = 0.083, \quad \lambda_{3*} = -0.003, \quad \lambda_{\text{TL}*} = 0.272, \quad \tilde{\lambda}_* = 0.448. \quad (4.94)$$

The critical exponents are

$$\theta_{1,2} = -0.018 \pm 7.359\mathbf{i}, \quad \theta_3 = -4.474, \quad \theta_4 = -52.09, \quad (4.95)$$

thus this fixed point is very near to being a suitable fixed point. At present it is not clear how this strong dependence on the gauge choice comes about, and future investigations will have to settle this issue. It might well be that either more momentum dependence or higher order correlation functions need to be resolved to change the critical exponents for it to be a viable UV fixed point. Also, completely opposite to the background flows studied above, but following the trend just observed, in the limit  $\beta \rightarrow -\infty$ , no fixed point with positive  $g_3$  is found at all.

### Fixed point structure II - curvature couplings

As an exploratory study, we now again fix  $\beta = 1$  and study the curvature couplings at the first fixed point, (4.86). To uniquely project on the tensor structures, we employ the basis as introduced in appendix D. To make things explicit, we write down the flow equations for all couplings with this gauge choice<sup>12</sup>:

$$\begin{aligned} \partial_t \mathcal{R}_C &= \frac{g(\lambda_3(93-72\mathcal{R}_C)+36\lambda_3^2-17)}{162\pi\tilde{\epsilon}^2} + \frac{g(48\lambda_3^2-8\lambda_3-3)(\mathcal{R}_C-1)}{81\pi\tilde{\epsilon}^3} - \frac{8g\lambda_3}{9\pi\tilde{\epsilon}} \\ &\quad \epsilon_{\text{TL}} \\ &+ \frac{g(312\lambda_3^2-304\lambda_3+75)(\mathcal{R}_C-1)}{324\pi\tilde{\epsilon}} - \frac{2g(\lambda_3(33-63\mathcal{R}_C)+609\lambda_3^2+19)}{81\pi} \\ &\quad \epsilon_{\text{TL}}^3 \\ &+ \frac{g(\lambda_3(72\mathcal{R}_C-75)+36\lambda_3^2-10)}{162\pi\tilde{\epsilon}} + \frac{g((-120\lambda_3^2+272\lambda_3-87)\mathcal{R}_C-152\lambda_3+57)}{648\pi\tilde{\epsilon}^2} + \frac{g(25-52\lambda_3)}{18\pi} \\ &\quad \epsilon_{\text{TL}}^2 \\ &- \frac{g(4\lambda_3+1)^2}{216\pi\tilde{\epsilon}^4} + \frac{4g(\lambda_3-2)}{9\pi\tilde{\epsilon}^2} + \frac{g(60\lambda_3^2+72\lambda_3+11)}{162\pi\tilde{\epsilon}^3} \\ &+ \frac{g(7(264\lambda_3^2-80\lambda_3-3)\mathcal{R}_C-1648\lambda_3^2+240\lambda_3+86)}{216\pi\epsilon_{\text{TL}}^4} + \frac{2g}{3\pi}, \quad (4.96) \\ \partial_t \mathcal{R}_{\text{TLSTL}} &= \frac{5g(-28\lambda_3^2+\lambda_3(-36\mathcal{R}_{\text{STr}}+3\mathcal{R}_{\text{TLSTL}}+4)+1)}{54\pi\tilde{\epsilon}^2} - \frac{10g((12\lambda_3^2+4\lambda_3-3)\mathcal{R}_{\text{STr}}+(1-3\lambda_3)\lambda_3\mathcal{R}_{\text{TLSTL}})}{81\pi\tilde{\epsilon}^3} + \frac{10g\lambda_3}{9\pi\tilde{\epsilon}} \\ &\quad \epsilon_{\text{TL}} \\ &+ \frac{5g(3(64\lambda_3^2-40\lambda_3+7)\mathcal{R}_{\text{TLSTL}}-4(384\lambda_3^2-232\lambda_3+39)\mathcal{R}_{\text{STr}})}{324\pi\tilde{\epsilon}} + \frac{5g(252\lambda_3^2+\lambda_3(132-216\mathcal{R}_{\text{TLSTL}})+25)}{243\pi} \\ &\quad \epsilon_{\text{TL}}^3 \end{aligned}$$

<sup>12</sup>Note that with the chosen ansatz for the vertex expansion, (4.63), the fluctuation field  $h$  is dimensionful, and thus the curvature couplings are dimensionless. We also already identified all higher order couplings with the couplings of level 3.

$$\begin{aligned}
 & + \frac{5g(52\lambda_3^2 + \lambda_3(-36\mathcal{R}_{\text{STr}} + 3\mathcal{R}_{\text{TLSTL}} - 88) + 27)}{54\pi\tilde{\epsilon}} - \frac{5g(13\lambda_3 + 2)}{9\pi} \\
 & + \frac{\epsilon_{\text{TL}}^2}{648\pi\tilde{\epsilon}^2\epsilon_{\text{TL}}^2} \left( \frac{5g(4(3(1-2\lambda_3)^2 + (-408\lambda_3^2 + 224\lambda_3 - 33)\mathcal{R}_{\text{STr}}) + (216\lambda_3^2 - 128\lambda_3 + 21)\mathcal{R}_{\text{TLSTL}})}{486\pi\tilde{\epsilon}^3} \right. \\
 & + \frac{g(288\lambda_3^2 + 6\lambda_3(324\mathcal{R}_{\text{STr}} + 27\mathcal{R}_{\text{TLSTL}} - 8) - 35)}{648\pi\tilde{\epsilon}^4} \\
 & + \epsilon_{\text{TL}} \left( \frac{g(48\lambda_3^2 + 12\lambda_3 + 1)}{162\pi\tilde{\epsilon}^4} - \frac{2g\lambda_3}{3\pi\tilde{\epsilon}^3} \right) + \frac{g(\lambda_3 + 1)}{9\pi\tilde{\epsilon}^2} \\
 & - \frac{5g(3(40\lambda_3^2 - 64\lambda_3 + 13) + (204\lambda_3^2 - 16\lambda_3 - 33)\mathcal{R}_{\text{TLSTL}})}{324\pi\epsilon_{\text{TL}}^4} - \frac{5g}{3\pi}, \tag{4.97}
 \end{aligned}$$

$$\begin{aligned}
 \partial_t \mathcal{R}_{\text{RTL}} = & \frac{5g(24\lambda_3^2 - 16\lambda_3 + 3)(3\mathcal{R}_{\text{RTL}} + 9\mathcal{R}_{\text{RTr}} + 1)}{486\pi\tilde{\epsilon}^3} - \frac{5g(33\lambda_3 - 10)}{486\pi\tilde{\epsilon}^2} \\
 & + \frac{\epsilon_{\text{TL}}}{972\pi\tilde{\epsilon}^2} \left( \frac{5g(36\lambda_3^2 - 28\lambda_3 + (72\lambda_3^2 - 48\lambda_3 + 9)\mathcal{R}_{\text{RTL}} - 9(24\lambda_3^2 - 16\lambda_3 + 3)\mathcal{R}_{\text{RTr}} + 6)}{486\pi\tilde{\epsilon}} - \frac{5g(108\lambda_3^2 - 93\lambda_3 + 26)}{216\pi} \right) \\
 & - \frac{g(66\lambda_3^2 + 42\lambda_3 + 27(4\lambda_3 + 3)\mathcal{R}_{\text{RTL}} + 81(4\lambda_3 + 3)\mathcal{R}_{\text{RTr}} + 38)}{243\pi\tilde{\epsilon}^3} \\
 & + \frac{g(112\lambda_3^2 + 40\lambda_3 + 3(96\lambda_3^2 + 32\lambda_3 + 3)\mathcal{R}_{\text{RTL}} + 9(96\lambda_3^2 + 32\lambda_3 + 3)\mathcal{R}_{\text{RTr}} + 4)}{648\pi\tilde{\epsilon}^4} \\
 & + \frac{5g(24\lambda_3^2 - 16\lambda_3 + 3)(3\mathcal{R}_{\text{RTL}} + 1)}{243\pi\tilde{\epsilon}} - \frac{5g(208\lambda_3^2 + 348\lambda_3 + 72(8\lambda_3 - 3)\mathcal{R}_{\text{RTL}} - 149)}{324\pi} \\
 & + \epsilon_{\text{TL}} \left( \frac{g(48\lambda_3^2 + 12\lambda_3 + 1)}{324\pi\tilde{\epsilon}^4} - \frac{g(16\lambda_3 + 9)}{108\pi\tilde{\epsilon}^3} \right) + \frac{109g}{216\pi\tilde{\epsilon}^2} \\
 & - \frac{5g(1576\lambda_3^2 - 896\lambda_3 + 6(768\lambda_3^2 - 416\lambda_3 + 87)\mathcal{R}_{\text{RTL}} + 187)}{648\pi\epsilon_{\text{TL}}^4} - \frac{19g}{36\pi}, \tag{4.98}
 \end{aligned}$$

$$\begin{aligned}
 \partial_t \mathcal{R}_{\text{STr}} = & \frac{5g(3\lambda_3 - 2)(-12\mathcal{R}_{\text{STr}} + \mathcal{R}_{\text{TLSTL}} + 2)}{324\pi\tilde{\epsilon}^2} - \frac{5g(8\lambda_3 - 3)(\mathcal{R}_{\text{TLSTL}} - 12\mathcal{R}_{\text{STr}})}{648\pi\tilde{\epsilon}^3} - \frac{5g(\lambda_3 - 1)}{27\pi\tilde{\epsilon}} \\
 & + \frac{\epsilon_{\text{TL}}}{324\pi\tilde{\epsilon}} \left( \frac{5g(3\lambda_3 - 2)(-12\mathcal{R}_{\text{STr}} + \mathcal{R}_{\text{TLSTL}} + 2)}{648\pi\tilde{\epsilon}} - \frac{5g(8\lambda_3 - 3)(\mathcal{R}_{\text{TLSTL}} - 12\mathcal{R}_{\text{STr}})}{648\pi\tilde{\epsilon}^2} - \frac{5g(52\lambda_3 - 9)}{216\pi} \right) \\
 & + \frac{\epsilon_{\text{TL}}^2}{648\pi\tilde{\epsilon}} \left( \frac{5g(8\lambda_3 - 3)(\mathcal{R}_{\text{TLSTL}} - 12\mathcal{R}_{\text{STr}})}{324\pi} - \frac{5g(-78\lambda_3 + (48\lambda_3 - 26)\mathcal{R}_{\text{TLSTL}} + 9)}{432\pi\tilde{\epsilon}^4} \right) + \frac{g(16\lambda_3 + 3)(12\mathcal{R}_{\text{STr}} + \mathcal{R}_{\text{TLSTL}})}{432\pi\tilde{\epsilon}^4} \\
 & - \frac{g(18\lambda_3 + 12(3\lambda_3 + 1)\mathcal{R}_{\text{STr}} + 3\lambda_3\mathcal{R}_{\text{TLSTL}} + \mathcal{R}_{\text{TLSTL}} - 5)}{162\pi\tilde{\epsilon}^3} - \frac{g}{12\pi} \\
 & + \epsilon_{\text{TL}} \left( \frac{6g\lambda_3 + g}{108\pi\tilde{\epsilon}^4} - \frac{4g\lambda_3 + g}{108\pi\tilde{\epsilon}^3} \right) + \frac{g(20\lambda_3 - 11)}{216\pi\tilde{\epsilon}^2} + \frac{5g(128\lambda_3 - 39)\mathcal{R}_{\text{TLSTL}}}{432\pi\epsilon_{\text{TL}}^4}, \tag{4.99}
 \end{aligned}$$

$$\begin{aligned}
 \partial_t \mathcal{R}_{\text{RTr}} = & - \frac{g(\mathcal{R}_{\text{RTL}} + 3\mathcal{R}_{\text{RTr}} + 1)}{3\pi\tilde{\epsilon}^3} + \frac{g(3\mathcal{R}_{\text{RTL}} + 9\mathcal{R}_{\text{RTr}} + 1)}{8\pi\tilde{\epsilon}^4} + \epsilon_{\text{TL}} \left( \frac{g}{12\pi\tilde{\epsilon}^4} - \frac{g}{12\pi\tilde{\epsilon}^3} \right) \\
 & + \frac{5g}{24\pi\tilde{\epsilon}^2} + \frac{5g(8\mathcal{R}_{\text{RTL}} + 5)}{12\pi\epsilon_{\text{TL}}^3} - \frac{5g(3\mathcal{R}_{\text{RTL}} + 1)}{4\pi\epsilon_{\text{TL}}^4} - \frac{5g}{8\pi\epsilon_{\text{TL}}^2} - \frac{11g}{36\pi}. \tag{4.100}
 \end{aligned}$$

As a shorthand, we introduced  $\epsilon_{\text{TL}} = 1 - 2\lambda_{\text{TL}}$  and  $\tilde{\epsilon} = 1 - 2\tilde{\lambda}$ . Due to the orthogonality of the curvature tensors, the term with a Weyl tensor can only contribute to its own flow equation, likewise the terms with a tracefree Ricci tensor mix, as is the case with the terms with a Ricci scalar. The fixed point values of the curvature couplings read

$$\mathcal{R}_{\text{C}^*} = 0.164, \quad \mathcal{R}_{\text{TLSTL}^*} = 1.131, \quad \mathcal{R}_{\text{RTL}^*} = 0.453, \quad \mathcal{R}_{\text{STr}^*} = 0.476, \quad \mathcal{R}_{\text{RT}^*} = -0.252. \quad (4.101)$$

The critical exponents group, which is again due to the curvature tensor basis,

$$\theta_{\text{C}} = 1.386, \quad \theta_{\text{S1}} = 1.235, \quad \theta_{\text{S2}} = -1.441, \quad \theta_{\text{R1}} = 0.607, \quad \theta_{\text{R2}} = -31.49. \quad (4.102)$$

The relevant critical exponent  $\theta_{\text{S1}}$  mostly points into the direction of  $\mathcal{R}_{\text{STr}}$ , whereas the relevant critical exponent  $\theta_{\text{R1}}$  is strongly aligned with the coupling  $\mathcal{R}_{\text{RTL}}$ . The relatively small fixed point values indicate that the classical tensor structure seems to be a good approximation to the quantum tensor structure at the fixed point. Moreover, not all curvature couplings are relevant, lending further support to a finite-dimensional critical hypersurface.

Let us stress that we calculated the flow equations for the curvature-fluctuation correlations, (4.96)-(4.100), *for the first time*. They represent an important step towards correlation functions in an arbitrarily curved spacetime.

## 4.4. Beyond the vertex expansion

The results of the preceding section show that in bimetric truncations the situation is not yet under quantitative, and maybe even not under qualitative control. A natural question that arises is whether this is inherent in the vertex expansion, and if so, how one can go beyond it, and towards some kind of local potential approximation in quantum gravity. To lay the foundations for this step is the aim of this last section.

### 4.4.1. Cayley-Hamilton theorem

We first have to make sense of the statement that we want some kind of local potential approximation, *i.e.* a function which depends on the fluctuation field  $h_{\mu\nu}$ . Functions depend on scalar quantities, and in our context, these scalar quantities are the invariants of  $h_{\mu\nu}$  under coordinate transformations, *i.e.* under the action of the group  $GL(d)$ . This follows from the observation that we want indexfree objects, and in our Euclidean setup, this boils down to exactly  $GL(d)$  invariance. In the following, it is useful to work with the matrix  $\mathfrak{h} = \bar{g}^{-1}h$ , which is a rank  $(1, 1)$  tensor, such that powers of  $\mathfrak{h}$  are automatically covariant. It is furthermore convenient to introduce the trace and traceless part of  $\mathfrak{h}$ ,

$$\mathfrak{h} = \mathfrak{h}^{\text{TL}} + \frac{1}{d} \mathbf{h} \mathbb{1}_d, \quad (4.103)$$

where  $d$  is the dimension of spacetime and  $\mathbb{1}_d$  is the Kronecker delta. In the following, we will focus on scalar invariants of  $\mathfrak{h}$  without including derivatives, the generalisation is however straightforward. Clearly, since  $\mathfrak{h}$  is a usual matrix, the scalar invariants are just the  $d$  eigenvalues. Since the eigenvalues are difficult to handle in a functional QFT language, we have to find a different way to represent the invariants. This is possible via the Cayley-Hamilton theorem (CHT). Loosely speaking it states that substituting the matrix itself for the eigenvalue in the characteristic polynomial gives the zero matrix. This immediately gives a basis of monomials, namely the first  $d$  powers of the matrix, and an algorithm to expand any power of the matrix higher than  $d$  into this basis. Invariants are then the traces of these monomials and the determinant.

To be more concrete, in the following we specify again to  $d = 4$ . Since we are working in a traceless decomposition, the first invariant is always the trace itself. Our choice for the four invariants is

$$\begin{aligned}\mathfrak{h}_1 &= \mathfrak{h}, \\ \mathfrak{h}_2 &= \text{tr} \left[ \left( \mathfrak{h}^{\text{TL}} \right)^2 \right], \\ \mathfrak{h}_3 &= \text{tr} \left[ \left( \mathfrak{h}^{\text{TL}} \right)^3 \right], \\ \mathfrak{h}_4 &= \det \mathfrak{h}^{\text{TL}}.\end{aligned}\tag{4.104}$$

The CHT for  $\mathfrak{h}^{\text{TL}}$  then reads<sup>13</sup>

$$\left( \mathfrak{h}^{\text{TL}} \right)^4 - \frac{1}{2} \mathfrak{h}_2 \left( \mathfrak{h}^{\text{TL}} \right)^2 - \frac{1}{3} \mathfrak{h}_3 \mathfrak{h}^{\text{TL}} + \mathfrak{h}_4 \mathbb{1}_4 = 0.\tag{4.105}$$

The choice (4.104) is mainly due to the fact that it admits for a suitable truncation scheme. Invariants can be truncated from higher label to smaller label. On the other hand, since  $\mathfrak{h}^{\text{TL}}$  is a real symmetric matrix, if  $\mathfrak{h}_2 = 0$ , then also  $\mathfrak{h}_3 = \mathfrak{h}_4 = 0$ . A physical example for the usefulness of this truncation scheme are fluctuations in the form of gravitational waves,

$$\mathfrak{h}^{\text{TL}} = \begin{pmatrix} 0 & 0 & 0 & 0 \\ 0 & h_+ & h_\times & 0 \\ 0 & h_\times & -h_+ & 0 \\ 0 & 0 & 0 & 0 \end{pmatrix},\tag{4.106}$$

which gives

$$\begin{aligned}\mathfrak{h}_2 &= 2 \left( h_+^2 + h_\times^2 \right), \\ \mathfrak{h}_3 &= 0, \\ \mathfrak{h}_4 &= 0.\end{aligned}\tag{4.107}$$

---

<sup>13</sup>For the general matrix  $\mathfrak{h}$ , the theorem reads  $\mathfrak{h}^4 - (\text{tr } \mathfrak{h}) \mathfrak{h}^3 + \frac{1}{2} \left( (\text{tr } \mathfrak{h})^2 - \text{tr} (\mathfrak{h}^2) \right) \mathfrak{h}^2 - \frac{1}{6} \left( (\text{tr } \mathfrak{h})^3 - 3 \text{tr} (\mathfrak{h}^2) \text{tr } \mathfrak{h} + 2 \text{tr} (\mathfrak{h}^3) \right) \mathfrak{h} + \det (\mathfrak{h}) \mathbb{1}_4 = 0$ .

Here,  $h_+$  and  $h_\times$  are the two polarisation states of the gravitational wave in transverse traceless gauge. Clearly there are also more general constraints on allowed values of the invariants (4.104), which we shall however not discuss here.

Let us show a first application of this general setting. With the insights of the CHT, the most general parameterisation of the full metric in terms of a background metric and a fluctuation, without derivative terms, can be written down as

$$g = \bar{g} \left( \mathcal{A}_0 \mathbb{1}_4 + \mathcal{A}_1 \mathfrak{h}^{\text{TL}} + \mathcal{A}_2 [\mathfrak{h}^{\text{TL}}]^2 + \mathcal{A}_3 [\mathfrak{h}^{\text{TL}}]^3 \right), \quad (4.108)$$

where the  $\mathcal{A}_i$  are functions of the four invariants (4.104). The inverse metric  $g^{-1}$  has a similar exact representation,

$$g^{-1} = \left( \mathcal{B}_0 \mathbb{1}_4 + \mathcal{B}_1 \mathfrak{h}^{\text{TL}} + \mathcal{B}_2 [\mathfrak{h}^{\text{TL}}]^2 + \mathcal{B}_3 [\mathfrak{h}^{\text{TL}}]^3 \right) \bar{g}^{-1}. \quad (4.109)$$

The functions  $\mathcal{B}_i$  can be expressed explicitly in terms of the  $\mathcal{A}_i$ , and the general form is given in the appendix E. For the special case of the linear split, where

$$\mathcal{A}_0^{\text{lin}} = 1 + \frac{1}{4}\mathfrak{h}, \quad \mathcal{A}_1^{\text{lin}} = 1, \quad \mathcal{A}_2^{\text{lin}} = \mathcal{A}_3^{\text{lin}} = 0, \quad (4.110)$$

we find

$$\begin{aligned} \mathcal{B}_0^{\text{lin}} &= \frac{(\mathcal{A}_0^{\text{lin}})^3 - \frac{1}{2}\mathcal{A}_0^{\text{lin}}\mathfrak{h}_2 + \frac{1}{3}\mathfrak{h}_3}{(\mathcal{A}_0^{\text{lin}})^4 - \frac{1}{2}(\mathcal{A}_0^{\text{lin}})^2\mathfrak{h}_2 + \frac{1}{3}\mathcal{A}_0^{\text{lin}}\mathfrak{h}_3 + \mathfrak{h}_4}, \\ \mathcal{B}_1^{\text{lin}} &= -\frac{(\mathcal{A}_0^{\text{lin}})^2 - \frac{1}{2}\mathfrak{h}_2}{(\mathcal{A}_0^{\text{lin}})^4 - \frac{1}{2}(\mathcal{A}_0^{\text{lin}})^2\mathfrak{h}_2 + \frac{1}{3}\mathcal{A}_0^{\text{lin}}\mathfrak{h}_3 + \mathfrak{h}_4}, \\ \mathcal{B}_2^{\text{lin}} &= \frac{\mathcal{A}_0^{\text{lin}}}{(\mathcal{A}_0^{\text{lin}})^4 - \frac{1}{2}(\mathcal{A}_0^{\text{lin}})^2\mathfrak{h}_2 + \frac{1}{3}\mathcal{A}_0^{\text{lin}}\mathfrak{h}_3 + \mathfrak{h}_4}, \\ \mathcal{B}_3^{\text{lin}} &= -\frac{1}{(\mathcal{A}_0^{\text{lin}})^4 - \frac{1}{2}(\mathcal{A}_0^{\text{lin}})^2\mathfrak{h}_2 + \frac{1}{3}\mathcal{A}_0^{\text{lin}}\mathfrak{h}_3 + \mathfrak{h}_4}. \end{aligned} \quad (4.111)$$

This can be proven by multiplying (4.108) from the left with (4.109) and demanding that the product is the identity, repeatedly using the CHT. Similarly, we can calculate the determinant of  $g$ , the full expression is again deferred to the appendix E. For the linear split, we obtain the surprisingly simple expression

$$\det g = \left[ (\mathcal{A}_0^{\text{lin}})^4 - \frac{1}{2}(\mathcal{A}_0^{\text{lin}})^2\mathfrak{h}_2 + \frac{1}{3}\mathcal{A}_0^{\text{lin}}\mathfrak{h}_3 + \mathfrak{h}_4 \right] \det \bar{g}. \quad (4.112)$$

From this, we obtain the constraint

$$(\mathcal{A}_0^{\text{lin}})^4 - \frac{1}{2}(\mathcal{A}_0^{\text{lin}})^2\mathfrak{h}_2 + \frac{1}{3}\mathcal{A}_0^{\text{lin}}\mathfrak{h}_3 + \mathfrak{h}_4 > 0 \quad (4.113)$$

to ensure invertibility of the full metric. Let us again stress that there are *no approximations* in the preceding expressions, they directly follow from the linear parameterisation of the

metric and the CHT.

The tools developed here can be applied in a more general context, *e.g.* to study the general dependence on the background tracefree Ricci tensor, or the field strength tensor in gauge theories. As an illustration, we treat a pure  $U(1)$  gauge theory with a functional truncation in appendix G. It was recently argued that quantum gravity effects might cure the triviality problem of the  $U(1)$  sector of the Standard model [332]. Clearly, an investigation with functional truncations of the  $U(1)$  field strength needs to be carried out to substantiate or refute this argument.

#### 4.4.2. Towards a local potential approximation in quantum gravity

Having discussed the technical details, we can introduce the approximation scheme that we want to propose in order to go beyond the vertex expansion. The first step is the analogue of the local potential approximation in scalar field theories, *i.e.* we want to resolve the momentum independent parts of all correlation functions. This can be done by the ansatz

$$\Gamma^{\text{LPA}} = \frac{1}{16\pi G_N} \int d^4x \sqrt{g} (-R + 2\mathcal{V}) . \quad (4.114)$$

In this equation, the “fluctuation potential”  $\mathcal{V}$  is the generalisation of the cosmological constant, and depends on the invariants (4.104). In a first step, the Newton’s constant might be treated parametrically in all equations.

At this point, one should mention that if we would also resolve the full field dependence of all derivative terms, then a parameterisation of the full metric enters at no point in the calculation, so one might worry how to get back to the single metric effective action. The key observation is that the parameterisation (and with it the resolution of the Nielsen identities) is hidden in the choice of the initial condition of the flow. In this sense, the present approach is manifestly parameterisation independent.

One important comment on the viability of the truncation is necessary. Since we don’t give the fluctuation field  $h$  a mass dimension in this approach, it is expected that we strictly need to include an anomalous dimension. This comes from the following observation. The flow equation for the dimensionless fluctuation potential  $\bar{v}$  reads schematically

$$\partial_t \bar{v} = -4\bar{v} + \sum_{i=1}^4 \eta_{\mathfrak{h}_i} \mathfrak{h}_i \partial_{\mathfrak{h}_i} \bar{v} + \text{flow}_{\bar{v}} , \quad (4.115)$$

where the  $\eta_{\mathfrak{h}_i}$  are the anomalous dimensions of the  $\mathfrak{h}_i$ . The term with anomalous dimension, together with the first dimensional term, dictate the large field behaviour of  $\bar{v}$ . More explicitly, in the limit of  $\mathfrak{h}_i \rightarrow \infty$ , while keeping the other invariants finite,

$$\bar{v} \sim \mathfrak{h}_i^{4/\eta_{\mathfrak{h}_i}} . \quad (4.116)$$



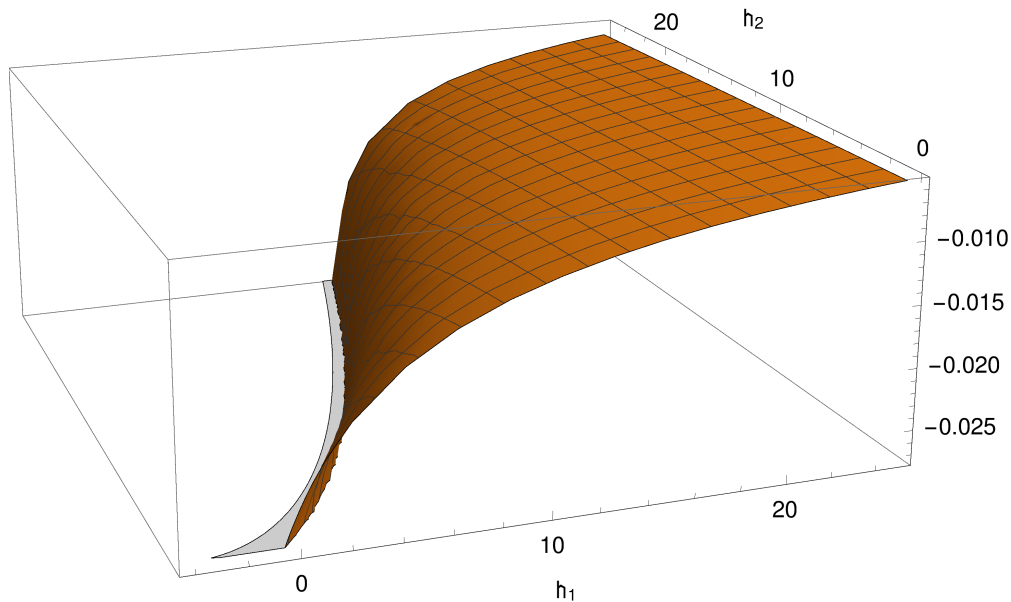


Fig. 4.13.: Ghost contribution to the fluctuation potential, if the graviton fluctuation is restricted to a combination of trace and gravitational wave. The fluctuations must fulfill  $\left(1 + \frac{1}{4}h_1\right)^2 - \frac{1}{2}h_2 > 0$  for an invertible metric.

Neglecting the anomalous dimension thus seems to be a qualitatively bad approximation. This is in some analogy to scalar theories at their lower critical dimension, where the scalar field also becomes dimensionless. The crucial difference is that in quantum gravity,  $h$  is dimensionless in any dimension<sup>14</sup>, and thus one should always include an anomalous dimension if one wants to resolve the field dependence qualitatively correctly.

It is rather ambitious to derive and solve the flow equation for  $\mathcal{V}$  with all four invariants. Still, as mentioned in the last section, seemingly reasonable truncation schemes exist, and current work is devoted to the derivation of truncated flow equations for the fluctuation potential. As a proof of concept, we shall derive the full ghost contribution to the flow of the fluctuation potential.

For a clean presentation, we stick to the gauge choice  $\beta = 1$ . It turns out that with a rather straightforward extension of the regulator, the contribution to the flow of  $\mathcal{V}$  is independent of  $\beta$ . The ghost action can be written as

$$\begin{aligned} \Gamma_{\text{gh}} &= \int d^4x \sqrt{\bar{g}} \bar{c}_\mu \bar{g}^{\mu\nu} \mathcal{F}_\nu^{\alpha\beta} \mathcal{L}_c g_{\alpha\beta} \\ &= - \int d^4x \sqrt{\bar{g}} \bar{c}_\mu [\bar{g}^{\mu\nu} g_{\nu\rho}] \bar{\Delta} c^\rho + \mathcal{O}(\bar{R}, \bar{D}h). \end{aligned} \quad (4.117)$$

Here,  $\mathcal{F}_\mu^{\alpha\beta} = \delta_\mu^\beta \bar{D}^\alpha - \frac{1}{2} \bar{g}^{\alpha\beta} \bar{D}_\mu$  is the gauge fixing operator and  $\mathcal{L}_c$  is the Lie derivative along

<sup>14</sup>In contrast to the previous sections, here we don't parameterise the vertices with factors of dimensionful couplings.

the vector  $c$ . The regulator is chosen as

$$\Delta S_{\text{gh}} = - \int d^4x \sqrt{\bar{g}} \bar{c}_\mu \mathfrak{R}(\bar{\Delta}) c^\mu. \quad (4.118)$$

For the calculation around flat background, we can switch to momentum space. The propagator is easily obtained for the general case by noting that we look for the inverse of

$$\Gamma_{\text{gh}}^{(2)} + \Delta S_{\text{gh}}^{(2)} = -p^2 \left( \bar{g}^{-1} g + \frac{\mathfrak{R}(p^2)}{p^2} \mathbb{1} \right) \equiv -p^2 \bar{g}^{-1} \tilde{g}, \quad (4.119)$$

where  $\tilde{g}$  is defined by the full metric  $g$  with the coefficient  $\mathcal{A}_0$  being shifted by  $\mathfrak{R}(p^2)/p^2$ . The propagator can thus be compactly written as

$$G_{\text{gh}} = -\frac{1}{p^2} \tilde{g}^{-1} \bar{g}, \quad (4.120)$$

where  $\tilde{g}^{-1}$  is given by the inverse of the full metric, expressed in terms of the (partly shifted) coefficients of the metric itself. We can now easily evaluate the trace,

$$\begin{aligned} -\text{tr}[G_{\text{gh}} \partial_t \mathfrak{R}] &= - \int d^4x \sqrt{\bar{g}} \frac{1}{8\pi^2} \int_0^\infty dp p^3 \left( \frac{1}{p^2} \tilde{g}^{\mu\nu} \bar{g}_{\mu\nu} \right) \partial_t \mathfrak{R}(p^2) \\ &= - \int d^4x \sqrt{\bar{g}} \frac{1}{8\pi^2} \int_0^\infty dp p \left( \partial_t \mathfrak{R}(p^2) \right) (4\mathcal{B}_0 + \mathfrak{h}_2 \mathcal{B}_2 + \mathfrak{h}_3 \mathcal{B}_3) \Big|_{\mathcal{A}_0 \rightarrow \mathcal{A}_0 + \mathfrak{R}(p^2)/p^2}, \end{aligned} \quad (4.121)$$

where the  $\mathcal{B}_i$  are the coefficients of the inverse metric, expressed in terms of the coefficients  $\mathcal{A}_i$  of the metric, as given in (4.111) for the linear parameterisation.

To illustrate this result, let us consider the special case of the Litim regulator [226, 307], the linear parameterisation and set  $\mathfrak{h}_3$  and  $\mathfrak{h}_4$  to zero. The integral can be calculated analytically, but nothing can be learned from its explicit form. We show the function in Figure 4.13. If one restricts the fluctuation to either pure trace or pure gravitational wave, the flow is

$$-\text{tr}[G_{\text{gh}} \partial_t \mathfrak{R}] = -2 \int d^4x \sqrt{\bar{g}} \frac{\mathfrak{h}_1 - 4 \ln \mathcal{A}_0}{\mathfrak{h}_1^2 \pi^2}, \quad (4.122)$$

or

$$-\text{tr}[G_{\text{gh}} \partial_t \mathfrak{R}] = - \int d^4x \sqrt{\bar{g}} \frac{\mathfrak{h}_2 - 2 \ln \left( 1 - \frac{1}{2} \mathfrak{h}_2 \right)}{8\pi^2 \mathfrak{h}_2}, \quad (4.123)$$

respectively. These functions are shown in Figure 4.14.

As a final remark in this section, we note that the Ricci scalar in the Einstein-Hilbert term can be rewritten into a form most suitable in the present context, namely in a sum of squares of Christoffel symbols. Since for the flow of  $\mathcal{V}$  we only need the second variation of the action, this form of the Ricci scalar makes this second variation particularly simple: as we project the flow equation onto constant  $h$  and flat background  $\bar{g} = \delta$ , and since the Christoffel symbols are linear in derivatives, the only contribution to the second variation

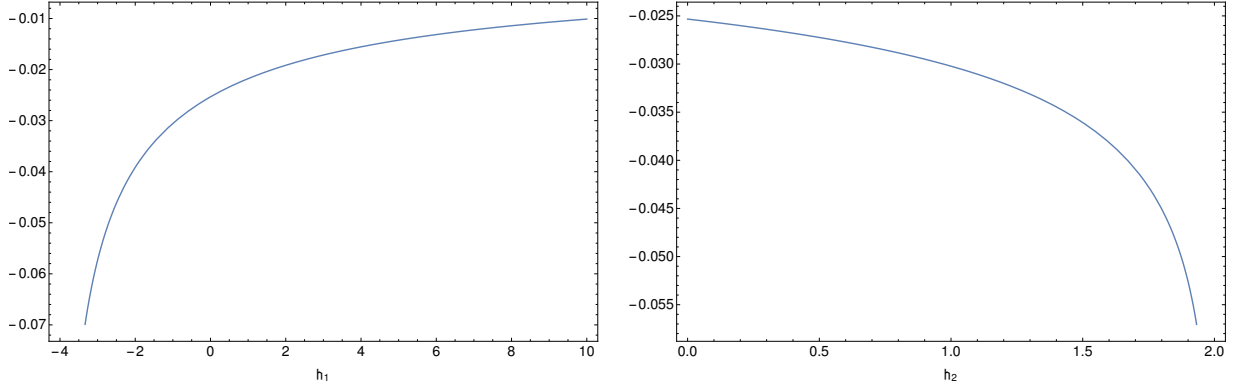


Fig. 4.14.: Ghost contribution to the fluctuation potential, if one only allows for trace fluctuations (left panel) or gravitational waves (right panel). The trace fluctuation must satisfy  $h_1 > -4$  in order for the background metric to be invertible. For purely gravitational wave gravitons, we have  $0 \leq h_2 < 2$ .

comes from the combination where each Christoffel symbol is varied once.

To show this, first note that the Ricci scalar can be expressed as

$$R = g^{\alpha\beta} \left[ \Gamma^\gamma_{\gamma\delta} \Gamma^\delta_{\alpha\beta} - \Gamma^\gamma_{\alpha\delta} \Gamma^\delta_{\gamma\beta} - \partial_\alpha \Gamma^\gamma_{\gamma\beta} + \partial_\gamma \Gamma^\gamma_{\alpha\beta} \right], \quad (4.124)$$

where  $\Gamma$  is the Christoffel symbol of the metric  $g$ , and  $\partial$  denotes the standard partial derivative. Using basic identities from differential geometry, partial integration and dropping boundary terms, we can rewrite

$$\begin{aligned} & \int d^d x \sqrt{g} g^{\alpha\beta} \left[ -\partial_\alpha \Gamma^\gamma_{\alpha\beta} + \partial_\gamma \Gamma^\gamma_{\alpha\beta} \right] \\ &= \int d^d x \left[ \Gamma^\gamma_{\gamma\beta} \partial_\alpha (\sqrt{g} g^{\alpha\beta}) - \Gamma^\gamma_{\alpha\beta} \partial_\gamma (\sqrt{g} g^{\alpha\beta}) \right] \\ &= \int d^d x \left[ \Gamma^\gamma_{\gamma\beta} (-\sqrt{g} g^{\mu\nu} \Gamma^\beta_{\mu\nu}) - \Gamma^\gamma_{\alpha\beta} \sqrt{g} (\Gamma^\delta_{\gamma\delta} g^{\alpha\beta} - (\Gamma^\alpha_{\gamma\delta} g^{\delta\beta} + \Gamma^\beta_{\gamma\delta} g^{\alpha\delta})) \right] \\ &= \int d^d x \sqrt{g} g^{\alpha\beta} \left[ -2\Gamma^\gamma_{\gamma\delta} \Gamma^\delta_{\alpha\beta} + 2\Gamma^\gamma_{\alpha\delta} \Gamma^\delta_{\gamma\beta} \right], \end{aligned} \quad (4.125)$$

and thus

$$\int d^d x \sqrt{g} R = \int d^d x \sqrt{g} g^{\alpha\beta} \left[ -\Gamma^\gamma_{\gamma\delta} \Gamma^\delta_{\alpha\beta} + \Gamma^\gamma_{\alpha\delta} \Gamma^\delta_{\gamma\beta} \right]. \quad (4.126)$$

Notably, the same result can be obtained if one treats the Christoffel symbols as (1,2)-tensors and rewrites the partial derivatives as covariant derivatives plus the corresponding Christoffel symbols, finally dropping the terms with covariant (in this case total) derivatives.

## 5. Gross-Neveu-Yukawa models

Having presented the results on the quantisation of gravity, we will now switch to graphene and related materials. We start by discussing some theoretical foundations of the study of graphene, and then present our approximations and results for a particular subsystem. Finally, we study the supersymmetric version of this model. In this chapter, we restrict exclusively to  $d = 3$ .

### 5.1. Dirac materials

To describe graphene and other Dirac materials, we effectively need to take into account the interactions of Dirac electrons which loosely speaking reside on the lattice sites. By tuning different interactions, *e.g.* on-site or nearest-neighbour interactions, different phases can be observed. Graphene is believed to be in the semimetallic (SM) phase [98, 333–337]. If on-site repulsion is increased, a phase transition to a spin-density-wave (SDW) phase is observed, whereas for stronger nearest-neighbour repulsion, the transition is towards a charge-density-wave (CDW) phase [82, 87, 92, 338]. More exotic states are possible, as topological quantum spin hall states [88–90, 97] or Kekulé states [93–96]. An interesting question is what happens at the critical point where these three phases meet. Possible scenarios include a further mixed phase (2nd order tetracritical point), a first order phase transition only between SDW and CDW (2nd order bicritical point with 1st order transition between the ordered phases), or also first order transitions between the SM phase and the other two phases (1st order triple point). This is depicted in Figure 5.1.

In the simplest approximation, these materials are described by a single-particle Hamiltonian for spin  $s$  electrons on the honeycomb lattice at half filling, together with on-site and nearest-neighbour interactions [114]. If only the Fourier modes near the points  $K$  and  $K'$  are considered, we end up with a low energy effective theory of free relativistic electrons on the honeycomb lattice, which can be described by a Dirac theory [85]. To describe the two phase transitions to CDW and SDW, we follow [114] and introduce two bosonic order parameters,

$$\begin{aligned}\chi &= \bar{\psi}\psi, \\ \phi^a &= \bar{\psi}(\sigma^a \otimes \mathbb{1}_4)\psi.\end{aligned}\tag{5.1}$$

Here,  $\psi$  is a Dirac spinor with two flavours in a four-dimensional reducible representation,  $\sigma^a$

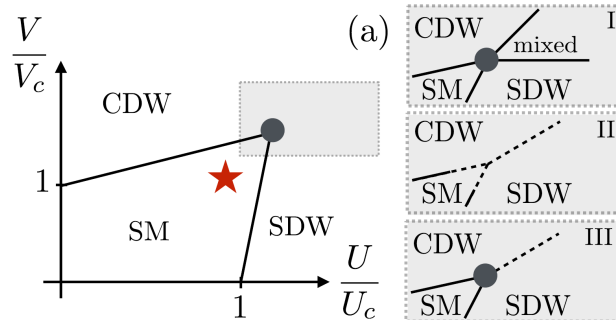


Fig. 5.1.: Structural phase diagram of graphene-like materials with on-site interaction  $U$  and nearest-neighbour interaction  $V$ . The start indicates the position of graphene. For the critical point in the shaded region, three possibilities come to mind: 2nd order tetracritical point (I), 1st order triple point (II) and 2nd order bicritical point with 1st order lines between the two ordered phases (III). Image taken from [114].

is the Pauli matrix, and  $\chi(\phi^a)$  is the CDW (SDW) order parameter field. The corresponding microscopic action reads

$$S = \int d^3x \left[ \bar{\psi} (\mathbb{1}_2 \otimes \gamma_\mu) \partial^\mu \psi + \bar{\psi} \{ (g_\chi \chi \mathbb{1}_2 + g_\phi \phi_a \sigma^a) \otimes \mathbb{1}_4 \} \psi + \frac{1}{2} (\partial_\mu \chi) (\partial^\mu \chi) + \frac{1}{2} (\partial_\mu \phi_a) (\partial^\mu \phi^a) + V(\rho_\chi, \rho_\phi) \right], \quad (5.2)$$

where  $\rho_X = X^2/2$ . Our conventions on the Clifford algebra are collected in appendix H. This model is a combination of two Gross-Neveu-Yukawa models with  $O(1)$  and  $O(3)$  symmetry, respectively. This kind of model plays an important role in many contexts. It can be regarded as a toy model for an asymptotically safe theory [339], which underlines the dual role of a given interacting fixed point in that it can describe either IR or UV. In four dimensions, the Higgs-top sector of the Standard Model [212, 340] is described by such a theory, and it serves as an effective low energy description of QCD [341–352] (quark-meson model). It is related to the standard Gross-Neveu model [353] by a Hubbard-Stratonovich transformation.

In the following, we will study one of the subsystems of (5.2), namely the one with CDW order parameter, in NLO in the derivative expansion. This will include all terms with at most two derivatives and two fermions. The SDW subsystem is much more complicated due to the additional index structure, and will be left for future research. The fixed point structure of the coupled system can be inferred in part from the subsystems. Clearly, an interesting possibility is a fully coupled fixed point, which was found in [114], but played no role for graphene. It remains to be seen if the same conclusions can be drawn in more extended approximations.

In some parts of the literature, the Gross-Neveu model with CDW (SDW) order parameter is called chiral Ising (Heisenberg) model, in analogy to the pure bosonic models [354].

Before coming to results, let us discuss the symmetries of the model [92, 355]. There is a

discrete  $\mathbb{Z}_2$  reflection symmetry,

$$\psi \rightarrow (\mathbb{1}_{N_f} \otimes \gamma_2)\psi, \bar{\psi} \rightarrow -\bar{\psi}(\mathbb{1}_{N_f} \otimes \gamma_2), \chi \rightarrow -\chi, \phi^a \rightarrow -\phi^a, \quad (5.3)$$

if at the same time the spatial momentum is reflected across the 1st axis. This corresponds to the sublattice exchange symmetry. There is a further  $SU(2)$  spin rotation symmetry,

$$\psi \rightarrow e^{i\theta n_a \sigma^a \otimes \mathbb{1}_4} \psi, \bar{\psi} \rightarrow \bar{\psi} e^{-i\theta n_a \sigma^a \otimes \mathbb{1}_4}, \chi \rightarrow \chi, \phi^a \rightarrow R^a_b \phi^b, \quad (5.4)$$

with the  $O(3)$  rotation matrix  $R^a_b = \delta^a_b - 2\theta \epsilon^a_{bc} n^c$ , where  $n^a$  is the rotation axis and  $\theta$  the rotation angle. Clearly, there is the  $U(1)$  charge conservation

$$\psi \rightarrow e^{i\theta} \psi, \bar{\psi} \rightarrow \bar{\psi} e^{-i\theta}. \quad (5.5)$$

On the honeycomb lattice, translational invariance corresponds to a chiral  $U(1)$  [91],

$$\psi \rightarrow e^{i\theta \mathbb{1}_2 \otimes \bar{\gamma}} \psi, \bar{\psi} \rightarrow \bar{\psi} e^{-i\theta \mathbb{1}_2 \otimes \bar{\gamma}}, \quad (5.6)$$

where  $\bar{\gamma} = \gamma_0 \gamma_1 \gamma_2$ . This symmetry is also related to the fact that the charge in every Dirac cone sector at the Dirac points is conserved individually. Thus, the phases of the modes near these points can be rotated independently. Furthermore, for the CDW order parameter, also the spin can be rotated independently, giving rise to a further  $SU(2)$ ,

$$\psi \rightarrow e^{i\theta n_a \sigma^a \otimes \bar{\gamma}} \psi, \bar{\psi} \rightarrow \bar{\psi} e^{-i\theta n_a \sigma^a \otimes \bar{\gamma}}. \quad (5.7)$$

This is however not a symmetry in the SDW sector.

## 5.2. Gross-Neveu-Yukawa model with CDW order parameter

The renormalisation group will generically generate all operators compatible with the symmetries, even if their coupling at some scale vanishes. This means that even if we start with the microscopic action (5.2), further operators will be generated during the RG flow. In the following, we will study a truncation of the theory space to all operators consistent with the symmetry which include at most two derivatives and bifermionic terms. In the first part, we spell out the explicit form of this truncation, whereas in the second part, we discuss the solution of the flow equations and compare to literature values. The results of this section are published in [201].

### 5.2.1. Truncation

Let us now build up the ansatz for the effective action for general flavour numbers  $N_f$ . The purely bosonic part of our ansatz for the action reads

$$\Gamma^{\text{bos}} = \int d^3x \left( \frac{1}{2} Z_\chi(\rho) (\partial_\mu \chi)^2 - V(\rho) \right), \quad (5.8)$$

where the potential  $V$  and the bosonic wave function renormalisation  $Z_\chi$  depend on the field  $\chi$  via  $\rho = \chi^2/2$ . To this, we add a kinetic term for the fermions with fermionic wave function renormalisation  $Z_\psi$ , and a Yukawa interaction  $g_\chi$ ,

$$\Gamma^{\text{ferm}} = \int d^3x \left( \frac{1}{2} Z_\psi(\rho) \left( \bar{\psi} (\mathbb{1}_{N_f} \otimes \not{\partial}) \psi - (\partial^\mu \bar{\psi}) (\mathbb{1}_{N_f} \otimes \gamma_\mu) \psi \right) + g_\chi(\rho) \chi \bar{\psi} \psi \right), \quad (5.9)$$

and further interaction terms,

$$\begin{aligned} \Gamma^{\text{int}} = \int d^3x & \left[ \mathbf{i} J_\psi(\rho) (\partial^\mu \rho) \bar{\psi} (\mathbb{1}_{N_f} \otimes \gamma_\mu) \psi + X_1(\rho) \chi (\partial_\mu \bar{\psi}) (\partial^\mu \psi) \right. \\ & + \frac{\mathbf{i}}{2} X_2(\rho) (\partial^\mu \chi) \left( \bar{\psi} \partial_\mu \psi - (\partial_\mu \bar{\psi}) \psi \right) + X_3(\rho) (\partial^2 \chi) \bar{\psi} \psi \\ & + \frac{1}{2} X_4(\rho) (\partial^\mu \chi) \left( \bar{\psi} (\mathbb{1}_{N_f} \otimes \Sigma_{\mu\nu}) \partial^\nu \psi - (\partial^\nu \bar{\psi}) (\mathbb{1}_{N_f} \otimes \Sigma_{\mu\nu}) \psi \right) \\ & \left. + \frac{1}{2} (X_5(\rho) + 2X_3'(\rho)) (\partial_\mu \chi)^2 \chi \bar{\psi} \psi \right]. \end{aligned} \quad (5.10)$$

Here,  $[\gamma_\mu, \gamma_\nu] = 2\Sigma_{\mu\nu}$ . All functions are considered to depend on the renormalisation group scale  $k$ , and the prefactors are chosen in such a way that all functions are real. The specific linear combination in front of the last term is for pure convenience. Notice that in this section only, we consider the action before Wick rotation. This is to ensure that our ansatz respects unitarity, which is easier to check for a Minkowskian action (for a Euclidean action, one has to impose reflection positivity [356]). Only after all algebraic manipulations have been executed, we perform the Wick rotation to Euclidean space to be able to perform the integration over the loop momentum.

In this ansatz, we neglect terms which contain  $\bar{\psi} \bar{\gamma} \psi$ . Such operators correspond to a different order parameter, and break time reversal symmetry [87, 114]. Further, one could form contractions of derivatives,  $\gamma_\mu$  and  $\Sigma_{\mu\nu}$  with the fully antisymmetric symbol  $\epsilon_{\mu\nu\rho}$ . The negligence of both can be justified a posteriori: the explicit calculation shows that no such operator is generated by the above ansatz, at least to NLO.

The combination of (5.8), (5.9) and (5.10) significantly extends previous work, which only resolved the field dependence of the potential [92, 100, 114, 153, 169, 339, 357], or the potential and the standard Yukawa interaction [350, 358], while retaining field independent wave function renormalisations, *i.e.* anomalous dimensions.

Critical phenomena of physical systems are described by fixed points, which are characterised by the vanishing of all flows of the dimensionless quantities. For this, renormalised

quantities are introduced. The renormalised fields read

$$\begin{aligned}
 \hat{\chi} &= Z_\chi(0)^{1/2} k^{-1/2} \chi, \\
 \hat{\psi} &= Z_\psi(0)^{1/2} k^{-1} \psi, \\
 \hat{\bar{\psi}} &= Z_\psi(0)^{1/2} k^{-1} \bar{\psi}.
 \end{aligned}
 \tag{5.11}$$

The renormalised potential and wave function renormalisations are defined as

$$\begin{aligned}
 \hat{V}(\hat{\rho}) &= k^{-3} V(\rho), \\
 \hat{Z}_\chi(\hat{\rho}) &= Z_\chi(0)^{-1} Z_\chi(\rho), \\
 \hat{Z}_\psi(\hat{\rho}) &= Z_\psi(0)^{-1} Z_\psi(\rho),
 \end{aligned}
 \tag{5.12}$$

and the renormalised interaction terms are

$$\begin{aligned}
 \hat{g}_\chi(\hat{\rho}) &= Z_\chi(0)^{-1/2} Z_\psi(0)^{-1} k^{-1/2} g_\chi(\rho), \\
 \hat{J}_\psi(\hat{\rho}) &= Z_\chi(0)^{-1} Z_\psi(0)^{-1} k J_\psi(\rho), \\
 \hat{X}_{1-4}(\hat{\rho}) &= Z_\chi(0)^{-1} Z_\psi(0)^{-1} k^{3/2} X_{1-4}(\rho), \\
 \hat{X}_5(\hat{\rho}) &= Z_\chi(0)^{-3/2} Z_\psi(0)^{-1} k^{5/2} X_5(\rho).
 \end{aligned}
 \tag{5.13}$$

The anomalous dimensions are given by

$$\begin{aligned}
 \eta_\chi &= -\partial_t \ln Z_\chi(0), \\
 \eta_\psi &= -\partial_t \ln Z_\psi(0).
 \end{aligned}
 \tag{5.14}$$

We chose to normalise the renormalised wave function renormalisations to 1 at vanishing field. This is natural for the flavour numbers that we discuss, since in that regime, the fixed point lies in the symmetric regime. For other systems, it might be more convenient to fix these functions at the vacuum expectation value, see [201] for a study of the dependence of physical quantities on this choice for the  $O(1)$  model. From now on, we only discuss renormalised quantities, and drop the hats for the sake of readability.

Finally, we have to specify the regularisation. For this, the action is amended by

$$\Delta S = \int d^3x \left( \frac{1}{2} \chi \mathfrak{R}_\chi \left( \frac{p^2}{k^2} \right) \chi + \bar{\psi} \mathfrak{R}_\psi \left( \frac{p^2}{k^2} \right) \frac{\mathbb{1}_{N_f} \otimes \not{p}}{p} \psi \right). \tag{5.15}$$

Momentum arguments are to be understood as the momenta after Wick rotation. As a further quality check of the truncation, we will study several regulator kernels. We will



study the dependence of the results on the one-parameter family of regulators

$$\begin{aligned}\mathfrak{R}_\chi(x) &= \frac{k^2}{2e^{x^a} - 1}, \\ \mathfrak{R}_\psi(x) &= \frac{k}{2e^{x^a} - 1}.\end{aligned}\tag{5.16}$$

In all cases, for the numerical integration of the threshold functions, an adaptive Gauß-Kronrod 7-15 rule was employed [359]. It is enough to consider a finite momentum range due to the regulator insertion in the flow equation. For the class of exponential regulators we use, the integration range was chosen as

$$q \in \left[ 0, \sqrt{\frac{6}{5} (-\log(10^{-b}))^{1/a} k} \right].\tag{5.17}$$

Here,  $b$  is the number of significant digits of the numeric type used, *e.g.* 16 for *double* precision. This range is chosen in a way that  $\partial_t \mathfrak{R}$  at the upper limit is always smaller than  $10^{-b}$  by several orders of magnitude. Aspects of optimisation of the regulator in the present context are discussed *e.g.* in [165, 218, 219, 226, 307, 360–365].

## 5.2.2. Results

Now, we will discuss the results for the flavour numbers  $N_f = 1, 2$ , the latter governing the case of graphene. Since the bosonic anomalous dimension in this system is quite large, one might expect that the derivative expansion converges slowly. Thus when including more operators in a low order of the derivative expansion, it is possible that critical quantities fluctuate rather strongly. This is only partially the case, as will be seen below.

Before we specialise the fermion flavour number, a general remark is in order. It turns out that the flow equations of  $J_\psi$  and  $X_2$  vanish identically if both  $J_\psi$  and  $X_2$  vanish themselves, *i.e.* they have a Gaußian fixed point. The technical reason for this is subtle, and can be understood easiest in the conventions that we chose. Notice that the terms with  $J_\psi$  and  $X_2$  in (5.10) are the only ones which have an explicit factor of  $\mathbf{i}$ . Such a factor could only be generated by the Clifford algebra, but in fact conventions can be chosen such that no explicit factors appear there, see the appendix. The flow equation itself doesn't provide factors of  $\mathbf{i}$  (except the overall prefactor in its Minkowskian form, which is exactly cancelled by the Wick rotation), as is immanent when one stays in position space, rather than momentum space. Hence it is indeed expected that these two functions have a Gaußian fixed point. In systems where one expects a unique fixed point (besides the trivial fully Gaußian and the Wilson-Fisher fixed point), as in our system, such terms can thus be neglected from the outset. From the perspective of a flow, that is away from criticality, we start with the microscopic action (5.2) (with  $\phi^a = 0$ ) in the UV. Since no factor of  $\mathbf{i}$  appears there, quantum

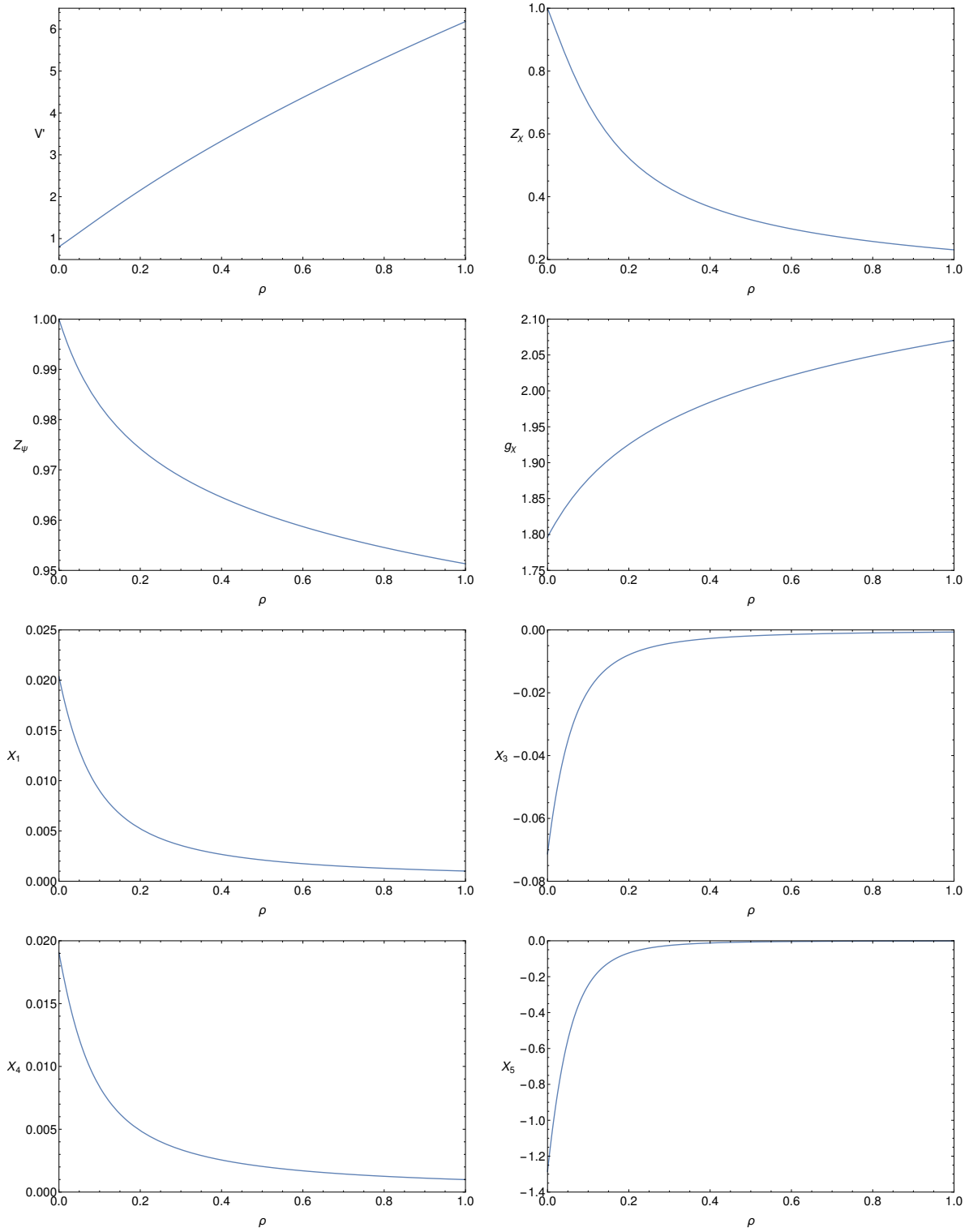


Fig. 5.2.: Fixed point solution to the Gross-Neveu model in three dimensions, for two fermion flavours. The regulator parameter is  $a = 2$ . Importantly, the function  $X_1$  is positive, as it contributes to the denominator of propagator functions, and can be seen as the second order derivative analogue of the usual Yukawa coupling  $g_\chi$ .

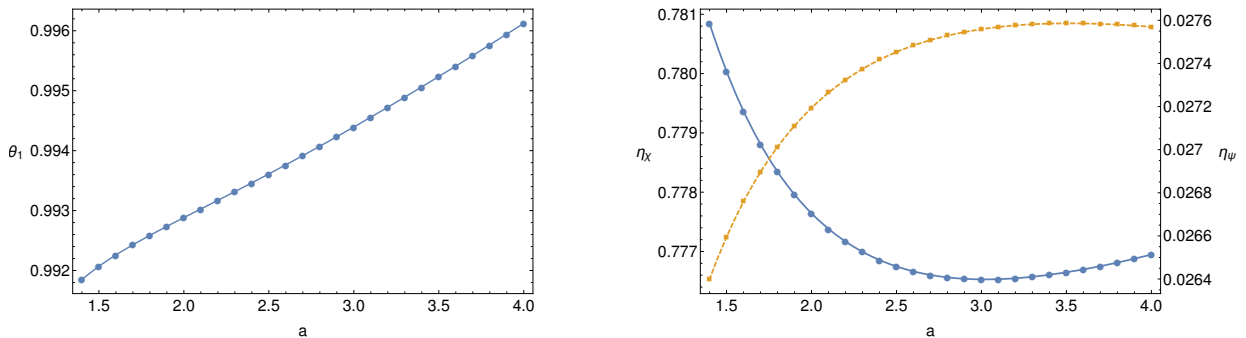


Fig. 5.3.: Regulator dependence of physical quantities of the Gross-Neveu model for  $N_f = 2$ . On the left panel, the first critical exponent is shown. It doesn't display an extremum, and the principle of minimum sensitivity cannot be applied here. On the right panel, the bosonic (blue dots) and fermionic (orange boxes) anomalous dimensions are plotted. Interpolations help to guide the eye.

fluctuations will not generate operators including such a factor. This applies iteratively to all operators that are generated, we thus conclude that no operators with explicit  $\mathbf{i}$  can be induced, independent of the approximation. Physically, this indicates that there could be a hidden symmetry.

We will first discuss the case  $N_f = 2$ . The nonvanishing fixed point functions are shown in Figure 5.2, for the regulator parameter  $a = 2$ . As expected, the derivative of the potential is strictly positive, indicating that we are in the symmetric regime. The operators  $X_1$ ,  $X_3$  and  $X_4$  are parametrically suppressed, as expected from their mass dimension. By contrast,  $X_5$  is quite large, but the corresponding operator comes with  $\sim \chi^3$ , which suppresses it for small field values.

We study the regulator dependence of the first critical exponent and the anomalous dimensions to optimise the choice of  $a$ . This dependence is plotted in Figure 5.3. The optimised values are

$$\begin{aligned} \eta_x^{\text{opt}} &= 0.7765, & a^{\text{opt}} &= 3.02, \\ \eta_\psi^{\text{opt}} &= 0.0276, & a^{\text{opt}} &= 3.52. \end{aligned} \quad (5.18)$$

The first critical exponent doesn't show an extremum, and cannot be optimised by the principle of minimum sensitivity (PMS). In the parameter region that was considered, it ranges between 0.992 and 0.996, thus we estimate

$$\theta_1 = 0.994(2). \quad (5.19)$$

In Table 5.1, we compare to results from the literature. The general agreement of all methods is satisfactory, except for the results coming from unresummed  $\epsilon$ -expansions. This deviation is not surprising since for the case discussed here,  $\epsilon = 1$ . Notably, the result for the fermionic anomalous dimension obtained by the two-sided Padé approximation [366] is much closer to our result, in contrast to results that only take into account either the expansion around

	$\theta_1$	$\eta_\chi$	$\eta_\psi$
FRG (this work)	0.994(2)	0.7765	0.0276
FRG [358]	0.996	0.789	0.031
Monte Carlo [372]	1.00(4)	0.754(8)	—
large- $N_f$ [92, 373]	0.962	0.776	0.044
$(2 + \epsilon)$ 3rd order [367–369]	0.764	0.602	0.081
$(2 + \epsilon)$ 4th order resummed [370]	0.931	0.745	0.082
$(4 - \epsilon)$ 2nd order [354]	1.055	0.695	0.065
2-sided Padé of $\epsilon$ -expansions [366]	0.948	0.739	0.041
conformal bootstrap [374]	0.88	0.742	0.044

Tab. 5.1.: Comparison of the first critical exponent and the anomalous dimensions of the Gross-Neveu model with the literature, for two fermion flavours,  $N_f = 2$ . Apart from the unresummed  $\epsilon$ -expansions, all methods are in good agreement.

the upper or the lower critical dimension [354, 367–370]. In comparison to the former FRG results [358], the critical exponent only changes on the per mille level, depending on the choice of regulator. The bosonic anomalous dimension changes by 2%, the fermionic anomalous dimension by roughly 10%. Let us also mention that recent work [371] suggested that the compatibility with the cubic-lattice Monte Carlo results [372] might be a coincidence, as there a sign problem was ignored, and it is even not clear if the symmetries in the continuum are the same.

Let us now discuss the case of a single fermion flavour,  $N_f = 1$ . The optimisation with respect to the regulator is shown in Figure 5.4, and the optimised values are

$$\begin{aligned} \eta_\chi^{\text{opt}} &= 0.5506, & a^{\text{opt}} &= 2.96, \\ \eta_\psi^{\text{opt}} &= 0.0645, & a^{\text{opt}} &= 3.23. \end{aligned} \tag{5.20}$$

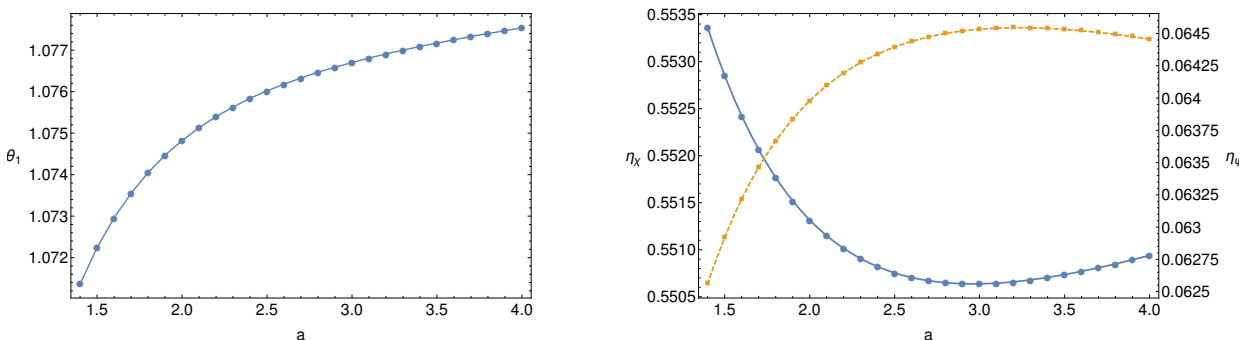


Fig. 5.4.: Regulator dependence of physical quantities of the Gross-Neveu model for  $N_f = 1$ . On the left panel, the first critical exponent is shown. Similar to the case of two fermion flavours, it shows no extremum, and the principle of minimum sensitivity cannot be applied here. On the right panel, the bosonic (blue dots) and fermionic (orange boxes) anomalous dimensions are plotted. Interpolations help to guide the eye.

	$\theta_1$	$\eta_\chi$	$\eta_\psi$
FRG (this work)	1.075(4)	0.5506	0.0645
FRG [358]	1.077	0.602	0.069
Monte Carlo [375]	1.25(3)	0.302(7)	—
large- $N_f$ [92, 373, 376]	1.361	0.635	0.105
$(4 - \epsilon)$ 2nd order [354]	1.160	0.502	0.110
2-sided Padé of $\epsilon$ -expansions [366]	0.852	0.506	0.096
conformal bootstrap [374]	0.76	0.544	0.084

Tab. 5.2.: Comparison of the first critical exponent and the anomalous dimensions of the Gross-Neveu model with the literature, for one fermion flavour,  $N_f = 1$ . The Monte Carlo results conflict with the results obtained by the other methods, and the critical exponent from the conformal bootstrap also deviates from other estimates.

As for the case  $N_f = 2$ , also here the critical exponent doesn't show an extremum, and from the dependence on the parameter  $a$  we estimate

$$\theta_1 = 1.075(4). \quad (5.21)$$

We again compare to different methods in Table 5.2. In contrast to the case of two fermion flavours, the situation here is less settled, and different methods don't agree as well. In particular, the results obtained by Monte Carlo methods [375] deviate significantly from other results. Future work will have to show which results are more trustworthy. When compared to earlier FRG results, the situation is similar to  $N_f = 2$ : the critical exponent already converged, and only changes by per mille, depending on the regulator. Both anomalous dimensions change by almost 10%.

Let us at the end note that the long anticipated results from the conformal bootstrap [374] didn't resolve the tension between different estimates of the critical exponent. This is to be contrasted with the situation for  $O(N)$  models, where the conformal bootstrap method obtains the best results.

### 5.3. $\mathcal{N} = 1$ Wess-Zumino model

As a final model, let us study the case  $N_f = 1/4$ , which corresponds to the supersymmetric version of the Gross-Neveu-Yukawa model, also known as  $\mathcal{N} = 1$  Wess-Zumino model. For this, we formulate everything in a language which explicitly maintains supersymmetry. This was first introduced in [377–379]. The results that will be presented are published in [156], further results from that work which don't fit into the main line of the present text are deferred to appendix I. Related results on supersymmetry and the FRG can be found in [380–384].

### 5.3.1. Supersymmetric flows

Here we shall give a short overview on how to formulate the flow of a supersymmetric theory, and will assume that the reader is familiar with the basic notions of supersymmetry, see *e.g.* [385] for a review. Details on the derivation of the flow equation can also be found in [156, 379].

To formulate the flow equation, we first introduce a real superfield  $\Phi$  which combines the scalar field  $\chi$ , an auxiliary bosonic field  $F$  and the fermion field  $\psi$ ,

$$\Phi = \chi + \bar{\theta}\psi + \frac{1}{2}\bar{\theta}\theta F. \quad (5.22)$$

Here,  $\theta$  and  $\bar{\theta}$  are Grassmann variables with mass dimension  $-1/2$ . Supersymmetry transformations are generated by the fermionic supercharges  $Q$  and  $\bar{Q}$ ,

$$\begin{aligned} Q &= -\mathbf{i}\partial_{\bar{\theta}} - \not{\theta}, \\ \bar{Q} &= -\mathbf{i}\partial_{\theta} - \bar{\theta}\not{\theta}. \end{aligned} \quad (5.23)$$

In three-dimensional Euclidean space, there are no Majorana fermions, thus the derivation of the flow equation has to be done in Minkowski space, and only when performing the integration over the loop momentum, we can Wick-rotate to Euclidean signature.

The next step is the introduction of the superpotential, which can be expanded in powers of the Grassmann variables,

$$W(\Phi) = W(\chi) + \frac{1}{2}W'(\chi)F\bar{\theta}\theta - \frac{1}{4}W''(\chi)\bar{\psi}\psi\bar{\theta}\theta. \quad (5.24)$$

Supersymmetry puts severe constraints on allowed derivative interactions. The only supersymmetric kinetic operator is

$$\mathcal{K} = \frac{1}{2}(\bar{\mathcal{D}}\mathcal{D} - \mathcal{D}\bar{\mathcal{D}}), \quad (5.25)$$

where  $\mathcal{D}$  and  $\bar{\mathcal{D}}$  are the supercovariant derivatives

$$\begin{aligned} \mathcal{D} &= \partial_{\bar{\theta}} + \mathbf{i}\not{\theta}, \\ \bar{\mathcal{D}} &= -\partial_{\theta} - \mathbf{i}\bar{\theta}\not{\theta}. \end{aligned} \quad (5.26)$$

With this, the most general action with up to four derivatives, that is next-to-next-to-leading order (NNLO) in the derivative expansion, reads

$$\Gamma^{\text{WZ}} = \int d^3x d\theta d\bar{\theta} \left[ 2W(\Phi) - \frac{1}{2}Z(\Phi)\mathcal{K}Z(\Phi) - \frac{1}{8}Y_1(\Phi)\mathcal{K}^2\Phi - \frac{1}{8}Y_2(\Phi)(\mathcal{K}\Phi)(\mathcal{K}\Phi) \right]. \quad (5.27)$$

Notice that the conventions slightly differ from the ones used in the nonsupersymmetric case in what concerns the wave function renormalisation. As it turns out, it is useful to introduce new functions  $Y = Y'_2$  and  $X = Y'_1 + Y_2$ , and we will only discuss these in the following.

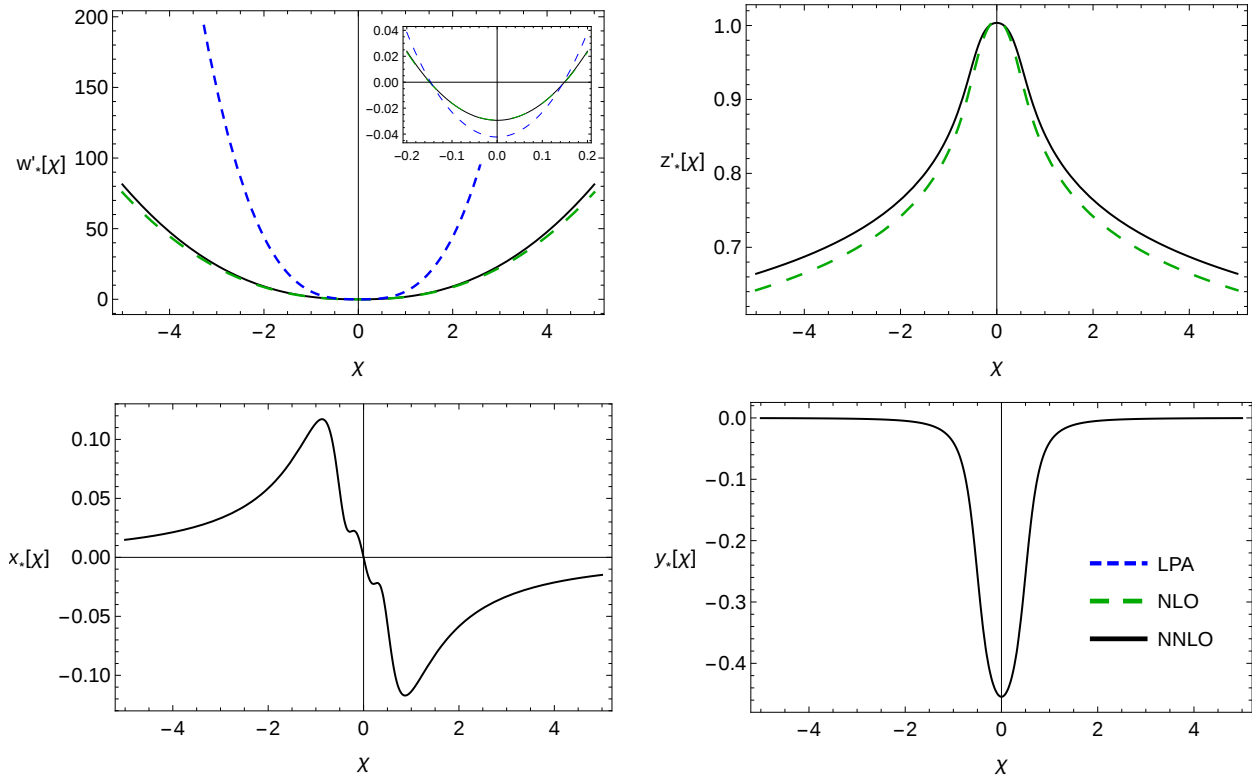


Fig. 5.5.: Fixed point solution of the Wess-Zumino model in three dimensions, at various levels of approximation: LPA (only  $W$ ), NLO ( $W$  and  $Z$ ), NNLO (all four functions).

Finally, the most general supersymmetric regulator reads

$$\Delta S^{\text{WZ}} = \frac{1}{2} \int d^3x d\theta d\bar{\theta} \Phi \left[ 2r_1(-\partial^2) - Z'(\bar{\Phi})^2 r_2(-\partial^2) \mathcal{K} \right] \Phi. \quad (5.28)$$

In this,  $\bar{\Phi}$  is a background field where we normalise the wave function renormalisation. It will be taken as the minimum of the potential. Having specified all ingredients, the derivation of the flow equations follows the standard procedure.

For the results that we present below, we set  $r_1$  to zero, and  $r_2$  to be

$$r_2(q^2) = \left( \frac{k^2}{q^2} - 1 \right) \Theta \left( \frac{k^2}{q^2} - 1 \right), \quad (5.29)$$

where  $q$  is the Euclidean momentum. Further, the anomalous dimension in the supersymmetric conventions reads

$$\eta = -\partial_t \ln(Z'(\bar{\Phi})^2). \quad (5.30)$$

### 5.3.2. Results

As a first result, we prove the so-called superscaling relation

$$\theta_1 = \frac{1}{2}(d - \eta), \quad d \geq 2, \quad (5.31)$$

	$\eta$	$\theta_1$	$\theta_2$	$\theta_3$	$\theta_4$
LPA	0	3/2	-0.702	-3.800	-7.747
NLO	0.186	1.407	-0.771	-1.642	-3.268
NNLO	0.180	1.410	-0.715	-1.490	-2.423
resummed ( $4 - \epsilon$ ) [386]	0.162	1.419			
conformal bootstrap [387]	0.164				

Tab. 5.3.: Comparison of the anomalous dimension and leading critical exponents of the Wess-Zumino model in three dimensions obtained from various levels of approximation of our work, and from perturbation theory and the conformal bootstrap approach.

which was first found in [379], and relates the anomalous dimension and the relevant critical exponent. To prove it, we note that the only flow equation which depends on the first derivative of the superpotential is the flow equation of the superpotential itself. By linearising it around a putative fixed point, we obtain

$$\partial_t \delta W' = \left( \frac{\eta - d}{2} + \mathcal{F}(\chi) \partial_\chi + \mathcal{G}(\chi) \partial_\chi^2 \right) \delta W', \quad (5.32)$$

where  $\delta W$  is the perturbation around the fixed point, and  $\mathcal{F}, \mathcal{G}$  are functions which depend on the field and the fixed point functions. Clearly, a constant  $\delta W'$  is an eigenfunction to the operator on the right-hand side, with eigenvalue  $(\eta - d)/2$ . If the variations of all other functions are set to zero, we clearly get a solution to the full linearised system. Thus, indeed we arrive at (5.31), which is valid nonperturbatively, and exact, as we did not make any assumptions on the specific truncation in its derivation. Note that in this proof, we neglected the variation of the anomalous dimension. For a recent discussion of this issue, also in the context of scaling relations, see [224]. The tentative conclusion there was that to obtain scaling relations within the FRG, the variation of the anomalous dimension has to be neglected, as we did here. On the other hand, from the perspective of a flow near the fixed point, the anomalous dimension changes, which seems to be in conflict with this.

Let us eventually discuss the numerical solution to the fixed point equations. The fixed point functions are shown in Figure 5.5, at different levels of approximation: local potential approximation (LPA), only including the superpotential  $W$ ; NLO, which includes  $W$  and  $Z$ ; NNLO, including all four operators. In Table 5.3, we present the anomalous dimension as well as the leading critical exponents at the same levels of approximation, and compare to literature values obtained by resummed perturbation theory around four dimensions, and the conformal bootstrap. The agreement across the different methods is very satisfying, the methods disagree only by a few percent.



## 6. Conclusion

In this thesis, we investigated scale dependence and, in particular, scale independent points of theories in a variety of physical contexts. Functional renormalisation group methods were employed to carry out these investigations. Since the a priori exact flow equation typically cannot be solved exactly, useful approximations have to be introduced. To obtain quantitatively reliable results, we developed powerful analytical and numerical tools to deal with extended approximations of the flow equation. In particular, on the analytical side, we used the Mathematica package *xAct* [191–196] not only in the gravitational context, but for arbitrary field content. With this, flow equations can be calculated very efficiently and reliably. Numerically, pseudo-spectral methods have been systematically developed in the present context. This includes both the analysis of fixed points as well as the resolution of flows. These methods are heavily used in other contexts, as numerical general relativity [388–391] or the AdS/CFT correspondence [392–394], where high precision and speed are pivotal.

As a test case, we investigated the critical behaviour of the well-known  $O(N)$  model in three dimensions for  $N = 1$  and  $N = 3$ , at NLO in the derivative expansion. The results for the leading critical exponent and the anomalous dimension come out rather well for this simple approximation, and are in qualitative agreement with in this case more accurate methods, as lattice Monte Carlo methods or the conformal bootstrap approach. The discussion of the flow of the  $O(N)$  model, and quantum mechanical potentials, were deferred to the first appendix. There, we showed that also the flow is quantitatively well controlled by pseudo-spectral methods. Most impressively, in  $d = 2.4$  we showed a flow near the separatrix of a multicritical fixed point and the lower dimensional equivalent of the Wilson-Fisher fixed point. In the large  $N$  limit, we could show that the error in the integration of the flow is due to the error in the initial condition, as here we could compare to the analytically known flow. We conclude that the flow is efficiently described by pseudo-spectral methods in large regions of theory space. We also studied bounded potentials in quantum mechanics, which serve as a toy model for Higgs inflation [395]. Here, again a comparison with (numerically) exact results for the ground state and first excited state energy was possible, and the results of the flow yield good estimates of these quantities.

After testing our technical groundwork, we started to investigate several aspects of the Asymptotic Safety Scenario for gravity. One of the main criticisms towards this scenario was the expectation that, as soon as a “proper counterterm”, namely the so-called Goroff-

Sagnotti term, was included in the approximation, the fixed point will fail to exist. In perturbation theory the corresponding divergence arises at the two-loop order and hallmarks the perturbative nonrenormalisability of gravity. Contrasting this expectation, we showed by easy analytical arguments that this counterterm cannot harm the UV fixed point found in the Einstein-Hilbert approximation. The central ingredients for the proof were the choice of a suitable basis and a curvature expansion, which is either way necessary to be able to project uniquely onto the counterterm. Due to the special choice of a tracefree basis, the counterterm doesn't feed back into the Einstein-Hilbert sector, leaving the earlier found UV fixed point intact. From the generic form of the flow equation, it straightforwardly follows that the  $\beta$  function of the coupling corresponding to the counterterm is cubic in itself, and thus has at least one real fixed point. A simple calculation shows that further, there is at least one fixed point where the coupling is irrelevant, in contrast to the situation in perturbation theory. The explicit calculation of the  $\beta$  function for the new coupling then suggested that the counterterm is even strongly irrelevant. This calculation thus refutes this long-standing criticism, and strongly nourishes the possibility that quantum gravity could be asymptotically safe.

We continued by an investigation of gauge and parameterisation dependencies in gravitational RG flows. Contrasting parametrically ordered expansions of observables, off-shell quantities generically show a dependence on choices of gauge fixing and parameterisation. We analysed such dependencies pragmatically, studying the sensitivity and stability of the UV fixed point with respect to variations of generalised parameterisations in an Einstein-Hilbert approximation. Remarkably, the general qualitative dependence on parameterisations is rather weak. For a huge range of possible choices, we found a suitable UV fixed point. However, there is a subtle interplay between gauge choice and parameterisations. The results indicate that exceptional stability w.r.t. variations can be obtained in the exponential split in the limit of the gauge parameter  $\beta \rightarrow -\infty$ , where the trace fluctuation is pure gauge. In this limit, the flow equations in our approximation are independent on the gauge parameter  $\alpha$ , and the phase diagram can be calculated analytically. Moreover, in this special choice the crossover to the IR regime is intact, thus we can make direct contact with general relativity in this limit.

After these single metric results, we turned our attention to genuinely bimetric calculations. This step is crucial in order to solve the Nielsen identities arising due to the use of the background field method. For the first time, we calculated a dynamical Newton's coupling by resolving the three-graviton vertex. We further resolved the momentum dependence of parts of the propagator, and the constant part of the three-point function. The resulting system shows again a viable UV fixed point suitable for AS. Remarkably, the dimension of the critical hypersurface is one below the number of couplings. A new notion of locality was introduced, which is related to a well-defined Wilsonian block spinning, and it was shown that both the two- and three-graviton vertex fulfill this notion nontrivially. Perturbatively

---

renormalisable theories automatically display this kind of locality. We thus conjecture that the nontrivial property of locality is related to the diffeomorphism invariance of our setup.

Subsequently, we studied gauge dependence of correlation functions in a curved background as a combination of the two previous calculations. We have shown that, for suitably chosen regulators, the Landau limit  $\alpha \rightarrow 0$  is a fixed point of the RG flow. Furthermore, in this limit, any choice for the gauge parameter  $\beta$  is a fixed point. Both parameters correspond to marginal operators. We further resolved both gap parameters of the graviton propagator. The enhanced system shows a stronger dependence on gauge choices than the single metric system. This might indicate that either more momentum dependence is needed, or higher order correlation functions need to be resolved. A first step into the latter direction was recently done in [188]. For the first time, we calculated  $\beta$  functions of fluctuation curvature couplings. We restricted the analysis to the five couplings that arise in the graviton propagator to linear order in the background curvature. In a typical gauge choice, we showed that only some of these couplings correspond to relevant operators, again giving a hint to the finite dimension of the critical hypersurface of the underlying fixed point.

In the final section on quantum gravity, we developed the techniques to go beyond the limitations of the vertex expansion employed in all studies so far. In this quest, the Cayley-Hamilton theorem plays a central role. We derived formulas for the inverse and the determinant of the most general parameterisation of the metric not including derivative terms. Some of the explicit formulas for the general case were deferred to the appendix, in particular the explicit exact expression for the exponential split. As the first application of these ideas, we proposed a truncation which resolves the constant part of correlation functions of arbitrarily high order, similarly to a local potential approximation in scalar field theories. The methods that were introduced also can be applied in other contexts. One particular example of functional truncations in a  $U(1)$  gauge theory was presented in the appendix. Truncations of this kind will play a role in future investigations of asymptotically safe quantum gravity coupled to matter - it was for example recently suggested that quantum gravity might solve the triviality problem [332].

There are many future directions to investigate AS in quantum gravity further, and some naturally evolve from the results of this thesis. For once, one should include all curvature invariants up to the third order in the curvature to fully resolve the issue with the Goroff-Sagnotti counterterm. Nontrivial interplay between the counterterm, second order invariants, and thus induced Einstein-Hilbert couplings might still spoil the existence of the fixed point. A potential way to get rid of gauge and parameterisation dependence is the usage of a geometrically inspired quantisation procedure, for first exploratory studies see [40, 178, 181, 304, 331]. In bimetric calculations, we opened up new paths to approximate the effective action, and hopefully we can soon make a big step towards qualitative and quantitative resolution of the Nielsen identities. Last but not least, the best theory of quantum gravity is worthless for the description of our Universe if it cannot account for matter. The inclusion

of matter in AS calculations is currently a hot topic [39, 153, 236, 275, 278, 329, 332, 396–417], and potentially the most important issue at the moment to lend further support to the Asymptotic Safety Scenario.

Not only quantum gravity is potentially described by an interacting fixed point - these scale invariant points also play a crucial role in the description of second order phase transitions in condensed matter systems. In the last chapter, we studied a particular model for the CDW-semimetal phase transition of Dirac materials, of which graphene is a well-known representative. In a bosonised language, we studied a very extended approximation to calculate the leading critical exponent and the anomalous dimensions of the fermions and the fermion condensate. For two fermion flavours, which corresponds to the graphene case, agreeing results are found by various methods, including our work, Monte Carlo methods, large  $N_f$  and  $\epsilon$  expansions. By contrast, for a single flavour, different methods disagree on the value of the critical quantities, and further investigations have to be carried out. Even recent results from the conformal bootstrap approach don't resolve this tension. Still, the surprising robustness of the presented FRG results compared to calculations with presumably much worse truncations makes a strong point for its quantitative reliability in these systems. We finally studied the supersymmetric case of this model, known as Wess-Zumino model, in a manifestly supersymmetric formulation of the flow equation. The high degree of symmetry allowed to include all operators with up to four derivatives. Again, the results are very robust upon inclusion of further operators, emphasising the reliability of the results. Some further results on supersymmetric flows in quantum mechanics were deferred to the appendix. There, we were particularly interested in supersymmetry breaking.

The next steps on the condensed matter side of this thesis are rather obvious. Most naturally, one should study the SDW-semimetal phase transition in a truncation similar to the one studied in the CDW-semimetal transition. Due to the appearance of Pauli matrices, the number of allowed operators increases dramatically, and an analysis will only be possible with the methods that were developed here. If also in this case one finds that much simpler truncations are quantitatively reliable, the final step towards the description of Dirac materials is the combination of the two order parameters. In this setup, fully interacting fixed points are conceivable [114], and they might play a crucial role in the description of the structure of the phase diagram where SDW, CDW and semimetal phase meet. One exciting possibility is the occurrence of a new mixed phase, which might show very interesting material properties, and could be verified experimentally.

# Appendix A.

## Code for the derivation of the flow equations for the $O(N)$ model

On the following pages, we reproduce the Mathematica notebook to derive the flow equations of the  $O(N)$  model in NLO.

This notebook gives a minimal working example on how to calculate flow equations for non-gauge theories with xAct. Specifically, the flow equations for the  $O(N)$ -model in NLO are derived. For convenience, the Wick rotation is already done.

Created with *Mathematica* 10.0.2.0

The distribution of this notebook is without any warranty, neither explicit nor implied.  
 Author: Benjamin Knorr  
 Date: 13.09.2016

---

## Reading Packages

```
<<xAct`xTensor`;  
<<xAct`xTras`;
```

---

## Definitions

First, we define the number of scalars and the dimension of spacetime as constant symbols.

```
DefConstantSymbol [NumScalar , PrintAs->"N"];  
DefConstantSymbol [dimspacetime , PrintAs->"d"];
```

Now, define the spacetime and a flat Euclidean metric.

```
DefManifold[spacetime , dimspacetime , {α, β, γ, δ, ε, ζ, θ, λ, μ, ν, ξ, τ}];  
DefMetric[1, spacetimetric [-α, -β], CD, PrintAs->"η", FlatMetric->True];
```

Here, the field space and a corresponding flat metric are defined.

```
DefManifold[fieldspace, NumScalar , IndexRange[a, z]];  
DefMetric[1, fieldmetric [-a, -b], CDφ, PrintAs->"ηφ", FlatMetric->True];
```

Ordinary derivatives of the field space metric, and field space derivative of spacetime metric vanish.

```
fieldmetric /: CD[_]@fieldmetric [__] = 0;  
spacetimetric /: CDφ[_]@spacetimetric [__] = 0;
```

Define the actual field as a vector in field space, and define the invariant plus replacement rules. constantfields projects onto constant fields.

```
DefTensor[φ[a], fieldspace];  
DefConstantSymbol [ρφ];  
torho = IndexRule[φ[a_] φ[-a_], 2 ρφ];  
constantfields = {CD[_]@φ[_] -> 0};
```

Define momentum vectors and some constant symbols representing lengths of momentum vectors.

```

DefTensor[mom [μ], spacetime];
DefTensor[mom1 [μ], spacetime];
DefTensor[mom2 [μ], spacetime];
DefTensor[mom3 [μ], spacetime];
DefTensor[mom4 [μ], spacetime];
DefTensor[dummymom [μ], spacetime];
DefConstantSymbol[momp, PrintAs->"p"];
DefConstantSymbol[momq, PrintAs->"q"];
DefConstantSymbol[momx, PrintAs->"x"];
DefConstantSymbol[momdummy, PrintAs->"f"];

```

Define scalar functions of the truncation, propagator and regulator functions.

```

DefScalarFunction[V];
DefScalarFunction[Z];
DefScalarFunction[Y];
DefScalarFunction[GφT];
DefScalarFunction[GφL];
DefScalarFunction[Regφ, PrintAs->"Rφ"];
DefScalarFunction[Regφdot, PrintAs->"Rφdot"];

```

Variational derivative in flat space. Product rule etc. Works also on lists, with scalar functions, and to arbitrary order. Arguments are a list of fields that are varied (here  $\phi$ ), then two lists with the scalar momenta of the fields, and their indices, and finally the expression that is varied.

```

VD[scalarlist_?ListQ][momlist_?ListQ, alist_?ListQ][exprlist_?ListQ] :=
  Module[{counting}, Table[VD[scalarlist][momlist, alist][
    exprlist[[counting]], {counting, 1, Length@exprlist}]];
VD[scalarlist_?ListQ][momlist_?ListQ, alist_?ListQ][expr_] :=
  If[Length@momlist == 1, VD[scalarlist[[1]]][momlist[[1]], alist[[1]]][
    expr], VD[Drop[scalarlist, 1]][Drop[momlist, 1], Drop[alist, 1]][
    CollectTensors@
      VD[scalarlist[[1]]][momlist[[1]], alist[[1]][expr]]];
VD[scalar_?xTensorQ][mom_?xTensorQ, a_][CD[μ_@X_] :=
  imom[μ] VD[scalar][mom, a][X];
VD[scalar_?xTensorQ][mom_?xTensorQ, a_][expr_ /; Head[expr] === Plus] :=
  Plus@@Table[VD[scalar][mom, a][expr[[Q]], {Q, 1, Length@expr}]];
VD[scalar_?xTensorQ][mom_?xTensorQ, a_][expr_ /; Head[expr] === Times] :=
  Plus@@Table[VD[scalar][mom, a][expr[[Q]] Drop[expr, {Q}],
    {Q, 1, Length@expr}]];
VD[scalar_?xTensorQ][mom_?xTensorQ, a_][expr_?ConstantQ] = 0;
VD[scalar_?xTensorQ][mom_?xTensorQ, a_][delta[_ , _]] = 0;
VD[scalar_?xTensorQ][mom_?xTensorQ, a_][spacetimetric[_]] = 0;
VD[scalar_?xTensorQ][mom_?xTensorQ, a_][fieldmetric[_]] = 0;
VD[scalar_?xTensorQ][mom_?xTensorQ, a_][
  ten_?xTensorQ[μ_ /; VBundleOfIndex[μ] === Tangentspacetime]] = 0;
VD[scalar_?xTensorQ][mom_?xTensorQ, a_][
  expr_ /; ScalarFunctionQ[Head[expr]] == True] :=
  Plus@@Table[Derivative[UnitVector[Length@expr, counter] /. List[X_] -> X][
    Head[expr]][Table[expr[[counter2]],
      {counter2, 1, Length@expr} /. List[X_] -> X]
    VD[scalar][mom, a][expr[[counter]], {counter, 1, Length@expr}]];
VD[scalar_?xTensorQ][mom_?xTensorQ, a_][expr_Scalar] :=
  VD[scalar][mom, a][NoScalar[expr]];
VD[φ][mom_?xTensorQ, a_][φ[b_]] := fieldmetric[-a, b];

```

## Truncation

Define the truncation: NLO  $O(N)$ -model.

```

Γk := ReplaceDummies [1/2 Z [φ[-z] φ[z]] CD[-μ] @ φ[-b] CD[μ] @ φ[b] +
1/2 Y [φ[-z] φ[z]] CD[-μ] @ (φ[b] φ[-b] / 2) CD[μ] @ (φ[c] φ[-c] / 2) + V [φ[-z] φ[z]]];
ΔSk := ReplaceDummies [1/2 CD[-μ] @ φ[-b] CD[μ] @ φ[b] Regφ[momdummy^2] / momdummy^2];

```

## Calculation of Propagator, Rdot and Vertices

Calculate the second variation.

```

Gamma2PlusR [momp_ , a_ , b_] :=
VD[{φ, φ}] [{mom1 , dummymom } , {-a, -b}] [Γk+ΔSk] /. constantfields/.
dummymom [μ_] => -mom1 [μ] /. momdummy => momp // .
IndexRule[mom1 [μ_] mom1 [-μ_] , momp^2] // .
torho // CollectTensors;

```

General ansatz for the Propagator.

```

Propagator [momp_ , a_ , b_] :=
GφT [momp^2 , ρφ] (fieldmetric [a, b] - φ[a] φ[b] / (2 ρφ)) + GφL [momp^2 , ρφ] φ[a] φ[b] / (2 ρφ);

```

Calculate the propagator functions.

```

PropagatorRules = {GφT → Function[{x, ρφ}, Evaluate@#[[1]]],
GφL → Function[{x, ρφ}, Evaluate@#[[2]]]} & @Module[{tempvar , sol},
tempvar = (Propagator[momp , a, -c] Gamma2PlusR [momp , c, b] //
CollectTensors) // . torho // CollectTensors;
sol = ({GφT [momp^2 , ρφ], GφL [momp^2 , ρφ]} /. SolveConstants [
tempvar == fieldmetric [a, b], {GφT [momp^2 , ρφ],
GφL [momp^2 , ρφ]}] [[1]] // Simplify) /. momp → √x
];

```

Calculate the regulator insertion.

```

RegulatorDot [momp_ , a_ , b_] :=
VD[{φ, φ}] [{mom1 , dummymom } , {-a, -b}] [ΔSk] /. Regφ → Regφdot /.
constantfields/. dummymom [μ_] => -mom1 [μ] /.
momdummy => momp // . IndexRule[mom1 [μ_] mom1 [-μ_] ,
momp^2] // . torho // CollectTensors;

```

Calculate the vertices that are needed.



```

Vertex3[mom1_ , mom2_ , mom3_ , a_ , b_ , c_ ] :=
  VD[{phi, phi, phi}][{mom1_ , mom2_ , mom3_ }, {-a, -b, -c}][rk] /. constantfields //.
  torho // CollectTensors;
Vertex4[mom1_ , mom2_ , mom3_ , mom4_ , a_ , b_ , c_ , d_ ] :=
  VD[{phi, phi, phi, phi}][{mom1_ , mom2_ , mom3_ , mom4_ }, {-a, -b, -c, -d}][rk] /.
  constantfields //. torho // CollectTensors;

```

## Calculation of Flow

Now, we can derive the actual flow equations. All flows are to be understood as integrands, the integration over the loop momentum momq (with integration measure  $\frac{d^d q}{(2\pi)^d}$ ) is still to be done. Also, the fields and operators are bare, and thus at this stage, no anomalous dimensions occur.

### Flow of V

The flow equation for the potential is just the Wetterich equation evaluated at constant fields.

```

flowV =
  (CollectTensors[1/2 Propagator[momq , a, b] RegulatorDot[momq , -a, -b] ] // .
    torho // CollectTensors) /. PropagatorRules

```

### Flow of Z and Y

For the flow of Z and Y, the second derivative of the flow equation, again for constant fields, is considered. One can easily see that 2 diagrams contribute to the flow, a tadpole and a self-energy diagram.

### Tadpole diagram

```

TadpoleMomentumConservationRules =
  {mom2_ [mu_] -> -mom1_ [mu], mom4_ [mu_] -> -mom3_ [mu],
    mom1_ [-mu_] mom1_ [mu_] -> momp^2, mom3_ [-mu_] mom3_ [mu_] -> momq^2};

```

```

-1/2 Vertex4[mom1_ , mom2_ , mom3_ , mom4_ , a, b, c, d]
  Propagator[momq , -c, -e] // CollectTensors;
%RegulatorDot[momq , e, f] // CollectTensors;
%Propagator[momq , -f, -d] // CollectTensors;
% //. torho // TadpoleMomentumConservationRules // CollectTensors;
TadpoleMomdeppart = CollectTensors[
  (Coefficient[% , momp , 2] // CollectTensors) /. PropagatorRules,
  SimplifyMethod -> (Collect[#,
    {Rphi[q^2], (-1+N), 1/(Rphi[q^2] + 2 q^2 rho phi Y[rho phi] + q^2 Z[rho phi] + V[rho phi] + 2 rho phi V''[rho phi]),
    1/(Rphi[q^2] + q^2 Z[rho phi] + V[rho phi]), 1/dimspacetime}, FullSimplify] &)]

```

### Self-energy diagram

For this diagram,  $\text{momx}$  denotes the cos of the angle between the external momentum  $\text{momp}$  (vector  $\text{mom1}$ ) and the loop momentum  $\text{momq}$  (vector  $\text{mom2}$ ). Further,  $\text{mom3}=\text{mom1}+\text{mom2}$ . One can show that  $\text{momx}$  can be replaced by  $\sqrt{1/\text{dimspacetime}}$  here (thanks to Stefan Rechenberger for pointing this out to me).

```
SEMomentumConservationRules =
  Join[{mom1 [-μ_] mom1 [μ_] => momp ^2, mom2 [-μ_] mom2 [μ_] => momq ^2,
    mom3 [-μ_] mom3 [μ_] => momp ^2 + 2 momp momq momx + momq ^2},
    MakeRule[{mom1 [μ] mom2 [-μ], momp momq momx }],
    MakeRule[{mom1 [μ] mom3 [-μ], momp (momp + momq momx )}],
    MakeRule[{mom2 [μ] mom3 [-μ], momq (momq + momp momx )}]];

Vertex3[mom1 , mom2 , mom4 , a, e, f] /. mom4 [μ_] => -mom3 [μ];
%Propagator[√(momp ^2 + 2 momp momq momx + momq ^2), -f, -g] //
  CollectTensors;
%(Vertex3[mom1 , mom3 , mom4 , b, g, h] /. mom1 [μ_] => -mom1 [μ] /.
  mom4 [μ_] => -mom2 [μ]) // CollectTensors;
%Propagator[momq , -h, -i] // CollectTensors;
%RegulatorDot[momq , i, j] // CollectTensors;
%Propagator[momq , -j, -e] // CollectTensors;
%/. torho //. SEMomentumConservationRules // CollectTensors;
SEMomdeppart = CollectTensors[
  (Coefficient[Series[%, {momp , 0, 2}], momp , 2] // CollectTensors) /.
  momx → √(1/dimspacetime) /. PropagatorRules,
  SimplifyMethod → (Collect[#, {R_φ[q^2], (-1+N),
    1/(R_φ[q^2] + 2 q^2 ρ φ Y[ρ φ] + q^2 Z[ρ φ] + V[ρ φ] + 2 ρ φ V''[ρ φ]),
    1/(R_φ[q^2] + q^2 Z[ρ φ] + V[ρ φ]), 1/dimspacetime}], FullSimplify] &)]
```

### Flow equations

Adding both diagrams, we can read off the flow of  $Z$  ( $Y$ ) by taking the prefactor of  $\eta\phi^{ab}$  ( $\phi^a\phi^b$ ).

```
flowZ = Collect[
  (TadpoleMomdeppart + SEMomdeppart) /. φ[a_] → 0 /. fieldmetric[a_, b_] → 1,
  {R_φ[q^2], (-1+N), 1/(R_φ[q^2] + 2 q^2 ρ φ Y[ρ φ] + q^2 Z[ρ φ] + V[ρ φ] + 2 ρ φ V''[ρ φ]),
  1/(R_φ[q^2] + q^2 Z[ρ φ] + V[ρ φ]), 1/dimspacetime}, FullSimplify]
flowY = Collect[
  (TadpoleMomdeppart + SEMomdeppart) /. φ[a_] → 1 /.
  fieldmetric[a_, b_] → 0,
  {R_φ[q^2], (-1+N), 1/(R_φ[q^2] + 2 q^2 ρ φ Y[ρ φ] + q^2 Z[ρ φ] + V[ρ φ] + 2 ρ φ V''[ρ φ]),
  1/(R_φ[q^2] + q^2 Z[ρ φ] + V[ρ φ]), 1/dimspacetime}, FullSimplify]
```

# Appendix B.

## Solving flows with pseudo-spectral methods

In this appendix, we show some results on solutions to flows based on pseudo-spectral numerics, which are also published in [154]. Here, we change conventions slightly, and we refer to the dimensionful potential by  $U$ , to the dimensionless potential by  $u$ , and  $\rho_0$  ( $\tilde{\rho}_0$ ) denotes the dimensionful (dimensionless) vacuum expectation value.

### B.1. Flows of the $O(N)$ model

We first study flows of  $O(N)$  models for various  $N$ . For that, we choose a truncation similar to (3.19), with some simplifications. We shall not consider the radial kinetic term, and only study the scale dependence of the wave function renormalisation, *i.e.* effectively the anomalous dimension, not the field dependence. This approximation is commonly called local potential approximation prime (LPA'). For regularisation, we choose the linear optimised cutoff [226, 360].

#### B.1.1. Flows for $d = 3$ and at large $N$ : A comparison

In order to demonstrate the power of pseudo-spectral methods on a specific example, we compare the analytical flow for large  $N$  with the numerically computed one. For that purpose, we choose trajectories in the symmetry broken phase close to criticality to show stability of the numerical method for 6 orders of magnitude ( $t \in [0, -12.4]$ ). We employ the limit  $N \rightarrow \infty$  [418] (where one only retains the scaling part and the fluctuation part proportional to  $N$ ) and switch to dimensional quantities as soon as the vacuum expectation value starts scaling exponentially in  $t$ . We expand the first derivative of the potential on  $[0, 0.2]$  for the dimensionless and on  $[0, 0.2k_S]$  for the dimensional flow, where  $k_S$  is the scale of switching between both regimes. With this choice, the maximal field value is 10 – 20 times larger than the vacuum expectation value. In general, the field range must not be too small in order to avoid boundary effects.

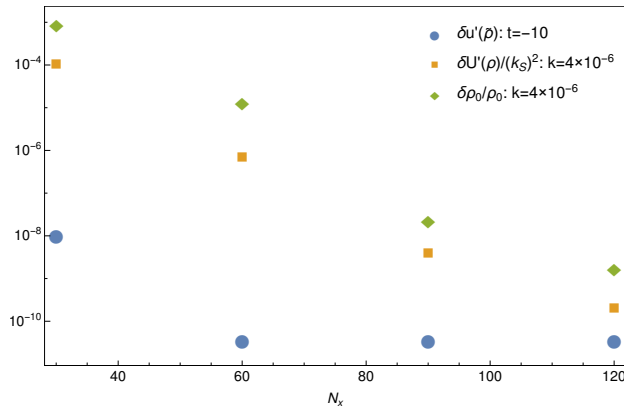


Fig. B.1.: Absolute and relative error ( $\delta u'(\tilde{\rho})$ ,  $\delta U'(\rho)$  and  $\delta \rho_0/\rho_0$ ) of the first derivative of the potential and the vacuum expectation value, respectively, as a function of the number of coefficients  $N_x$  in field direction. The errors  $\delta U'(\rho)$  and  $\delta \rho_0/\rho_0$  decreases exponentially. For the error of  $u'(\tilde{\rho})$  at  $t = -10$ , one can see a plateau which is due to the condition of the differential equation. This indicates that the solution is accurate to almost machine precision.

The initial condition reads

$$U'_\Lambda(\rho) = -0.008443603515625 + 0.5\rho \quad (\text{B.1})$$

at  $t = 0$  or  $k = \Lambda$ , where  $\Lambda$  is the UV cutoff. All dimensional quantities are to be understood in units of  $\Lambda$ , which we set to 1. For switching to the dimensional version, we choose  $t_s = \ln(k_S/\Lambda) = -10.1$ . The pseudo-spectral discretisation in temporal direction is chosen in such a way to achieve exponential convergence to machine precision. In order to compare the analytical potential [418] with the numerically computed one, we employ the maximum norm of their difference as error criterion.

In Figure B.1 the absolute deviation of the numerical flow from the analytical one in dependence of the number of the coefficients  $N_x$  in field direction can be seen. The flow was compared at two scales:  $t = -10$  ( $k = 4.5 \cdot 10^{-5}$ ), before switching to dimensional quantities, and  $k = 4 \cdot 10^{-6}$  ( $t = -12.4$ ), after switching to dimensional quantities, where we have stopped the integration. We also depict the relative error of the vacuum expectation value at this scale. The more coefficients are taken into account, the higher the accuracy, which can be seen by the exponential convergence of  $\delta U'(\rho)$  and  $\delta \rho_0/\rho_0$  in particular. For the error  $\delta u'(\tilde{\rho})$  at  $t = -10$  we see a plateau for  $N_x \gtrsim 60$ . This can be explained by the condition of the differential equation. To illustrate this, we compare two analytically computed solutions, one with the initial condition (B.1), and the other with a small deviation from it. To obtain an error of about  $\sim 10^{-11}$  at  $t = -10$ , one can allow for a deviation of  $10^{-18}$  for the constant term, and  $10^{-16}$  for the linear term, which is about the order of magnitude that we can resolve with *long double*. This example indicates how carefully time integration has to be done for staying close to the original trajectory. On the other hand, it shows that we have integrated

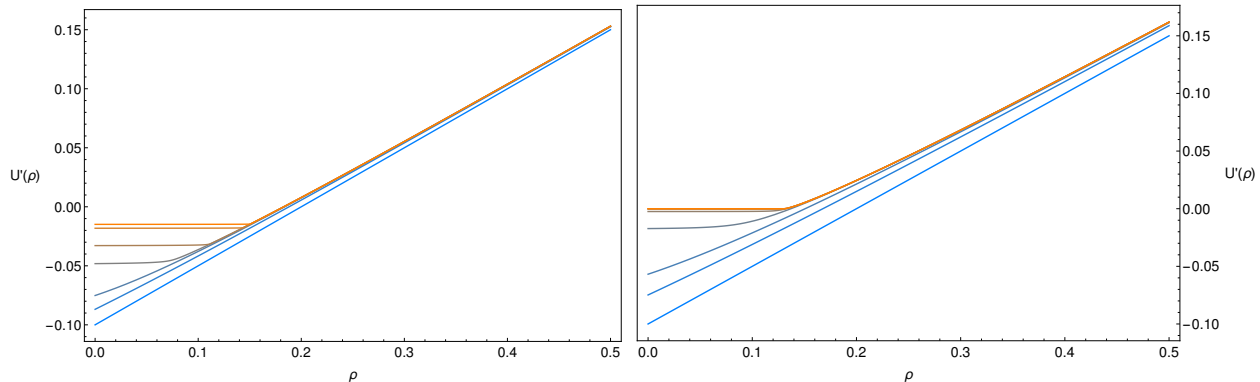


Fig. B.2.: Evolution of  $U'(\rho)$  from blue (bottom) to orange (top) for  $N = 1$  (left panel;  $t = 0, -0.5, -1, -1.5, -1.7, -2, -2.1$ ) and  $N = 4$  (right panel;  $t = 0, -0.5, -1, -2, -3, -4, -5, -13$ ). Convexity is seen in the flattening of  $U'(\rho)$  for small fields  $\rho < \rho_0$ . Whereas  $U''(\rho)$  is still continuous for  $N = 4$ , in the single scalar case a jump occurs.

out the flow close to machine precision over many orders of magnitude for  $N_x \gtrsim 60$ . This fact is supported by the exponential convergence till  $\sim 10^{-18}$  of the coefficients.

For the IR flow, the decrease of the error is slower, but still tends to the lower bound  $\sim 10^{-11}$  for a large number of coefficients. The error is now dominated by the truncation error of the expansion of the potential in field direction since convexity starts to set in. From the asymptotic decrease of the last coefficients for  $N_x \gtrsim 60$ , we obtain a measure for the truncation error which agrees very well with the errors depicted in Figure B.1. It is based on an estimate for the sum over the neglected coefficients. In order to achieve machine precision, more coefficients are needed.

We conclude that in a large part of theory space, the pseudo-spectral flow is highly efficient, and we generically observe exponential convergence for an increasing number of Chebyshev coefficients. Therefore, we concentrate in the following on the most challenging part of theory space involving the build-up of nonanalyticities, the first adumbration of which we just started to discuss.

### B.1.2. Flows for $d = 3$ and $N = 1, 4$

In the spontaneously symmetry broken phase, the effective potential is nonconvex for all intermediate scales  $k > 0$ . On the other hand, it is known that the effective potential has to be convex at  $k = 0$  even in LPA [217, 419]. While the outer region already is convex, the inner region becomes flat during the IR flow. Since the radial mass does not vanish for  $N = 1$ , the curvature jumps at the vacuum expectation value at  $k = 0$ . By contrast for  $N > 1$ , the influence of Goldstone bosons partly suppresses this nonanalyticity. The propagators  $\propto (1 + u'(\tilde{\rho}))^{-1}$  and  $\propto (1 + u'(\tilde{\rho}) + 2\tilde{\rho}u''(\tilde{\rho}))^{-1}$  flow towards the singularity for small  $\tilde{\rho}$ , pushing the convexity mechanism forward.

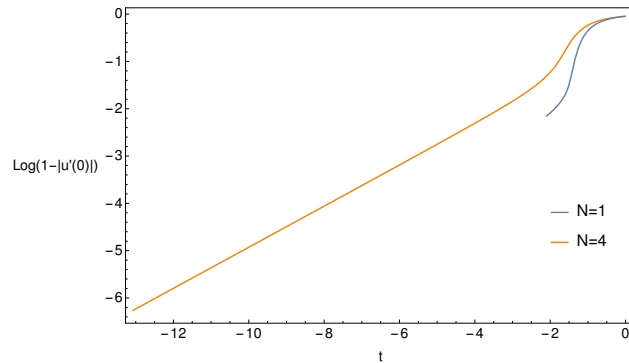


Fig. B.3.:  $u'(0)$  approaches the singularity  $-1$  for  $t \rightarrow -\infty$ . Due to the stronger nonanalyticity in the single scalar case, the numerically computed flow ceases to exist earlier.

We picked out two particular values for  $N$ , namely  $N = 1$  and  $N = 4$ . The following calculations are done with the dimensional version of the flow equation since we chose the initial condition to be far from criticality,  $U'_\Lambda(\rho) = -0.1 + 0.5\rho$ , at  $k = \Lambda$ . It is convenient to use the logarithmic time scale  $t$  instead of  $k$ . After a few orders of magnitude dimensional scaling can be observed.

Figure B.2 depicts the evolution of  $U'(\rho)$  for  $N = 1$  and  $N = 4$ , from large to small scales. The approach to convexity is clearly visible. The build-up of the corresponding nonanalyticity can be monitored over a range of scales, especially for  $N = 4$ . As  $U'(\rho)$  for  $N = 1$  has an edge at  $\rho_0$  at  $k = 0$  where  $U''(\rho_0)$  jumps, the flow is numerically much harder to track and finally breaks down earlier. The reason is as follows: Exponential convergence of the coefficients is only guaranteed if the function is analytic. For  $k = \Lambda$ , the convergence of the coefficients in field direction is very fast. Plateaus that build up for higher order coefficients are on the level of the machine precision. However, for low scales  $k$ , the requirement for exponential convergence is not fulfilled anymore. Thus, we observe a slower convergence of the coefficients till it breaks down. Although this problem cannot be avoided completely, there are two possibilities for improvement: On the one hand, one can simply take more coefficients. This will not cure the problem completely since the convergence becomes too slow and finally, an unacceptably large number of coefficients is needed. On the other hand, one can choose the domains in such a way that the nonanalyticity lies close to the boundary of two neighbouring domains. For that reason, we have used 24 or 16 domains for  $N = 1$  or  $N = 4$ , respectively. The high accuracy of pseudo-spectral methods prevents the flow to jump over the singularity of the propagator for a long time. Figure B.3 shows how the flow approaches the singular point. Due to the reasons given above, for  $N = 4$  we get closer to  $u'(0) = -1$  in comparison to  $N = 1$ .

We have shown that pseudo-spectral methods can also be applied to numerically challenging problems, such as convexity. Let us emphasise that the convergence of the expansion coefficients is strongly connected to the properties of the solution. Therefore, it is not

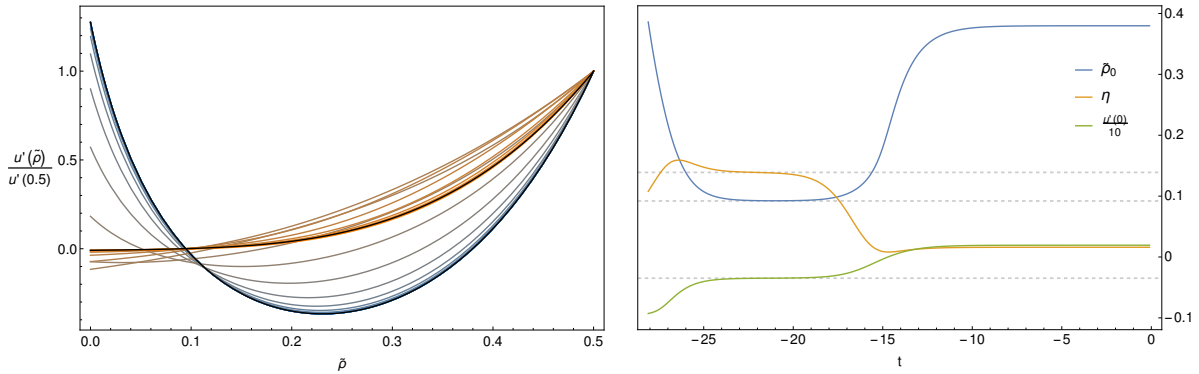


Fig. B.4.: Flow between two criticalities. Left panel: Flow from the tricritical fixed point potential (blue) to the Wilson-Fisher potential (orange),  $t \in [0, -25]$ . The fixed point potential computed from the fixed point equation are depicted as well (black). Right panel: Flow of the anomalous dimension  $\eta$ , the vacuum expectation value and  $u'(0)$ . The grey dashed lines denote the values of the Wilson-Fisher fixed point solution obtained from solving the fixed point equation.

surprising that the numerical effort increases the closer the singularity is approached. In contrast to other approaches adjusted to tackle convexity issues [420, 421], we again point out that pseudo-spectral methods have a striking advantage: The error is controllable by the convergence pattern of the expansion coefficients, which was especially demonstrated in the previous subsection. Furthermore, if only IR quantities are of interest, *e.g.* the vacuum expectation value, they can be inferred from the flow before convexity becomes challenging. We obtain  $\rho_0 = 0.183$  for  $N = 1$  and  $\rho_0 = 0.130$  for  $N = 4$  and the radial mass  $m_{\text{R}}^2 = 2\rho_0 U''(\rho_0) = 0.168$  for  $N = 1$ . It is worth mentioning that the vacuum expectation value for  $N = 4$  deviates by 2% from the vacuum expectation value derived from the analytical large  $N$  solution. That indicates that the large  $N$  limit already is a proper approximation for the  $N = 4$  case.

Let us make a comment on first order phase transitions. In contrast to continuous phase transitions, the order parameter, *i.e.* the vacuum expectation value, jumps. For all quantities, whose flow depend on the order parameter, for example the anomalous dimension, one should adapt the domain decomposition in time direction such that the jump is exactly on the boundary between two domains, as was done in [212].

### B.1.3. Flow between two criticalities for $N = 1$

In the previous section, we have investigated flows far from criticality. However, for  $d < 4$  nontrivial fixed points occur. The first one is the well-known Wilson-Fisher fixed point. Lowering the dimension further, multicritical fixed points emerge at certain critical dimensions  $d_{c,i} = 2i/(i - 1)$  for  $i \geq 3$ . This is discussed in detail in [422–424]. In [153] global solutions of the first four fixed point potentials for  $d = 2.4$  are given. Now, we take a closer

look to the first two fixed points, the Wilson-Fisher fixed point among them, in  $d = 2.4$ . We are interested in a trajectory connecting both (separatrix). Therefore, we start at the tricritical fixed point with a small deviation constructed from a linear combination of its relevant eigenperturbations. As initial conditions we use the results of [153].

For approaching the Wilson-Fisher fixed point during the flow, we have to fine-tune the linear combination of both relevant directions of the tricritical fixed point. The perturbation is mainly along the second relevant (subleading) direction. The flow strongly depends on the numerical parameters. This is not surprising since small perturbations in the relevant direction may lead to large deviations during the flow as already seen for the large  $N$  case. Figure B.4 shows the deformation of the potential  $u'(\tilde{\rho})$  from the tricritical fixed point to the Wilson-Fisher fixed point during the flow. The inner minimum of the tricritical fixed point potential disappears. In the right panel the anomalous dimension, the vacuum expectation value and  $u'(0)$  are plotted over the logarithmic scale. Whereas all quantities and the potential itself stay at the tricritical fixed point for many orders of magnitude, they finally approach the Wilson-Fisher fixed point. This can be seen from the plateaus at  $-17 \gtrsim t \gtrsim -25$ . The relevant direction becomes irrelevant at the Wilson-Fisher fixed point. Finally, the flow carries the critical behaviour of the Wilson-Fisher fixed point although we have started at the tricritical fixed point. We emphasise that for such flows a very stable numerical method is indispensable for which pseudo-spectral methods are well suited.

## B.2. Quantum mechanics with a bounded potential

In this section we present results on the energies of the ground and first excited states of a selection of three quantum-mechanical potentials obtained by solving the flow equation for the derivative of the effective potential. This is specifically suited to test our methods, as a direct comparison with other methods and the exact answer is possible, and in the FRG framework, an extension to quantum field theory is straightforward.

In particular, we will focus on potentials that are bounded both from below and above. Physically, such potentials are interesting, *e.g.*, in the context of Higgs inflation [395]. Technically, the flows of such potentials necessitate a global resolution - if the flow of only a finite region in  $x$  is considered, one encounters boundary effects that destabilise the flow. To put the results in perspective, we will compare them with the (numerically) exact values, as well as values obtained from various analytic approximations.

### B.2.1. Models

We will consider three different potentials. As a first example, we will treat

$$U(x) = \frac{2}{\pi} \arctan(x^2) . \quad (\text{B.2})$$



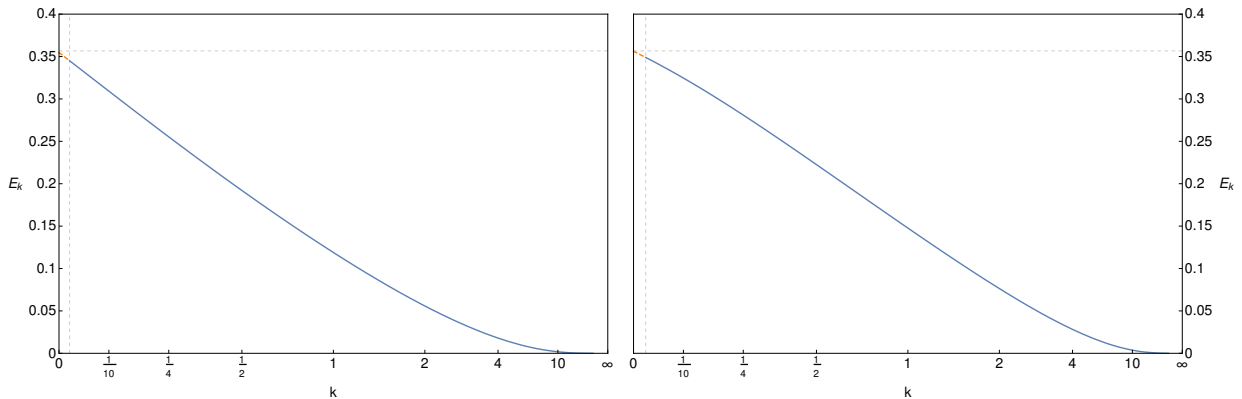


Fig. B.5.: Flow of the effective potential at vanishing position, which gives the effective ground state energy at scale  $k$ ,  $E_k$ , for both Callan-Symanzik (left panel) and optimised (right panel) regulator. The horizontal dashed line indicates the exact value of the ground state energy, whereas the vertical line indicates the value up to which the numerical integration could be done. The orange dashed line is the extrapolation of our numerical values, given in blue. In both cases, the ground state energy is obtained to surprisingly high accuracy.

This potential carries no additional special properties besides the boundedness. We include it, because one can solve the flow in a large  $N$  approximation exactly and explicitly for this potential. As a second potential, we choose a modified version of the well-known Pöschl-Teller potential,

$$U(x) = \frac{\lambda(1+\lambda)}{2} \left( 1 - \frac{1}{\cosh^2(\lambda x)} \right). \quad (\text{B.3})$$

For this potential, the Schrödinger equation can be solved exactly, and all bound states and their corresponding energies are known [425]. In this work, we will specify to the case  $\lambda = 1$ . The Pöschl-Teller potential is also interesting from another point of view: it is reflectionless for  $\lambda \in \mathbb{N}$ , so waves are transmitted completely through the well. Lastly, we shall investigate the influence of nonanalyticities by studying the potential

$$U(x) = e^{-1/x^2}. \quad (\text{B.4})$$

All potentials are normalised such that they go to 1 when the argument goes to infinity, and vanish at their minimum  $x = 0$ .

### B.2.2. Exact results

Here we present the (partly numerically) exact solutions for the ground state and the first excited state (if it exists) for all potentials by solving the Schrödinger equation (in natural units),

$$-\frac{1}{2}\Psi''(x) + U(x)\Psi(x) = E\Psi(x). \quad (\text{B.5})$$

For the Pöschl-Teller potential with  $\lambda = 1$ , there is only one bound state,

$$\Psi_0(x) = \frac{1}{\cosh(x)}, \quad E_0 = 1/2. \quad (\text{B.6})$$

For the other potentials, we apply pseudo-spectral methods along the lines of [153] to obtain the first two bound states. For the potential (B.2), the ground state energy,  $E_0$ , and the energy gap,  $\Delta E = E_1 - E_0$ , are

$$E_0 = 0.448004, \quad \Delta E = 0.509453. \quad (\text{B.7})$$

On the other hand, for the nonanalytic potential (B.4), we get

$$E_0 = 0.356644, \quad \Delta E = 0.542040. \quad (\text{B.8})$$

All energies and their corresponding wave functions were determined with an accuracy of at least  $10^{-20}$ , however there is no need to display more figures in order to discuss all subsequent results.

### B.2.3. WKB approximation

In order to assess the following results, we compare them with the WKB approximation. The formula for the approximated energy levels reads

$$\int_{-x_0}^{x_0} \sqrt{2(E_n - U(x))} = \left(n + \frac{1}{2}\right) \pi, \quad (\text{B.9})$$

where  $x_0$  is the classical turning point,  $U(x_0) = U(-x_0) = E_n$ . The index  $n$  counts the energy level. Evaluating (B.9) for each model, we obtain for the first potential, (B.2),

$$E_0 \approx 0.520, \quad E_1 \approx 0.955, \quad \Delta E \approx 0.435. \quad (\text{B.10})$$

For the Pöschl-Teller potential, (B.3), the ground state energy is

$$E_0 \approx 0.582. \quad (\text{B.11})$$

Finally for the last potential, (B.4), we have

$$E_0 \approx 0.405, \quad E_1 \approx 0.905, \quad \Delta E \approx 0.500. \quad (\text{B.12})$$

It is remarkable that  $E_1$  deviates less than 1% from the exact value, whereas  $E_0$  is off by 13% – 16%. This is to be expected, since the WKB approximation works well in the semiclassical limit  $\lambda \ll 2x_0$ , where  $\lambda/2$  is the distance between two knots of the wave

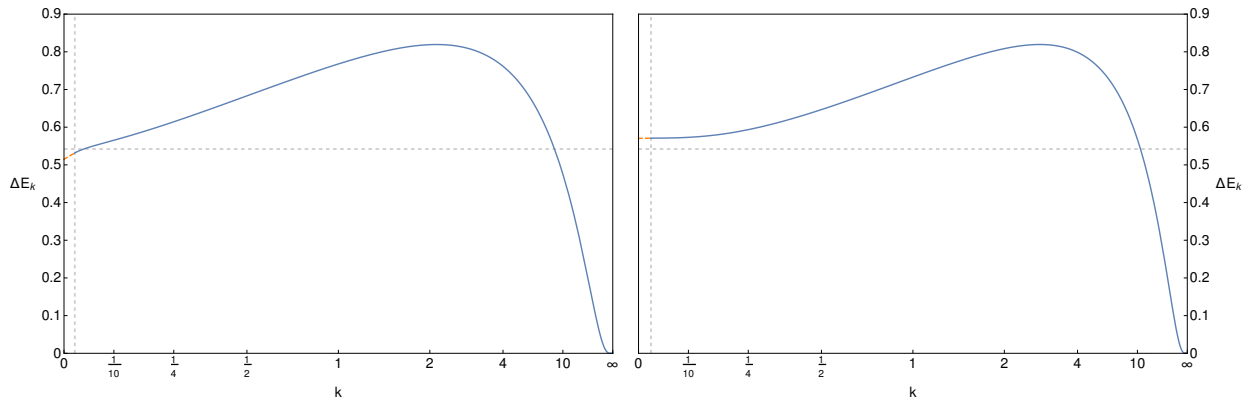


Fig. B.6.: Flow of the derivative of the effective potential at vanishing position, which gives the effective energy gap at scale  $k$ ,  $\Delta E_k$ , for both Callan-Symanzik (left panel) and optimised (right panel) regulator. The horizontal dashed line indicates the exact value of the energy gap, whereas the vertical line indicates the value up to which the numerical integration could be done. The orange dashed line is the extrapolation of our numerical values, given in blue. The energy gap comes out quite well in both cases.

function. This translates into the condition  $n \gg 1$ .

#### B.2.4. One-loop approximation

As a further step to put subsequent results in perspective, we perform a one-loop calculation. The one-loop effective potential reads

$$U_{1l}(x) = U_{cl}(x) + \frac{1}{2} \sqrt{U''_{cl}(x)}, \quad (\text{B.13})$$

which can for example be obtained directly from the flow equation by setting the potential on the right-hand side equal to the classical potential  $U_{cl}$ . The ground state energy is given by the value of the effective potential at its minimum (here in all cases  $x = 0$ ), whereas the energy gap is the square root of the curvature of it, also evaluated at the minimum. One thus obtains for the first potential, (B.2),

$$E_0 = \frac{1}{\sqrt{\pi}} \approx 0.564, \quad \Delta E = \frac{2}{\sqrt{\pi}} \approx 1.128. \quad (\text{B.14})$$

The ground state energy comes out more or less well for such a simple calculation, but the one-loop result predicts that there are no further bound states, as the energy gap is too large.

For the Pöschl-Teller potential, the one-loop result is

$$E_0 = \frac{1}{\sqrt{2}} \approx 0.707, \quad \Delta E = \sqrt{2(1 - \sqrt{2})} \approx 0.910i. \quad (\text{B.15})$$

$U(x) = 2/\pi \arctan(x^2)$			
	exact	CS	opt
$E_0$	0.448004	0.445	0.447
$\Delta E$	0.509453	0.477	0.558
$U(x) = 1 - 1/\cosh^2(x)$			
	exact	CS	opt
$E_0$	1/2	0.496	0.499
$\Delta E$	-	0.464	0.585
$U(x) = \exp(-1/x^2)$			
	exact	CS	opt
$E_0$	0.356644	0.355	0.356
$\Delta E$	0.542040	0.515	0.570

Tab. B.1.: Overview of exact results from solving the Schrödinger equation and results obtained from the flow of the potential for all three potentials. CS and opt indicate that the Callan-Symanzik and the optimised regulator were employed, respectively.

The convexity of the effective potential is not caught by a one-loop calculation, and accordingly, the energy gap is imaginary. This phenomenon is well-known to be an artifact of the loop expansion, and extensively discussed in *e.g.* [426, 427]. The ground state energy is off by about 40%.

Finally, for the nonanalytic potential (B.4), no meaningful one-loop analysis can be done. In fact, any order in perturbation theory fails to produce anything nonzero for the energy levels because of the nonanalyticity.

### B.2.5. Flow of the effective potential

This section is devoted to the numerical study of the actual flow equation for the effective potential. All investigations are done within LPA where  $Z \equiv 1$ . Note, that in quantum mechanics no renormalisation is needed. Therefore, the initial condition can be put at  $k = \Lambda \rightarrow \infty$ . To cover the whole interval  $k \in [0, \infty)$  the time direction is compactified. As in the previous section, for reasons of numerical stability, we actually use the flow equation for the derivative of the effective potential  $U'(\rho) = \partial_\rho U(\rho)$ , and obtain the ground state energy by an additional integration. The flow equation reads

$$\partial_k U'(\rho) = -Ak^B \frac{3U''(\rho) + 2\rho U'''(\rho)}{(k^2 + U'(\rho) + 2\rho U''(\rho))^C}, \quad (\text{B.16})$$

where  $A = 1/\pi$ ,  $B = C = 2$  for the linear optimised regulator ( $\mathfrak{R}(p^2) = (k^2 - p^2)\theta(k^2 - p^2)$ ) and  $A = 1/4$ ,  $B = 1$  and  $C = 3/2$  for the Callan-Symanzik cutoff ( $\mathfrak{R}(p^2) = k^2$ ).

We will first point out some expectations on the outcome of the flow, followed by the discussion of the actual results of the flow. An overview of all results can be found in Table B.1.

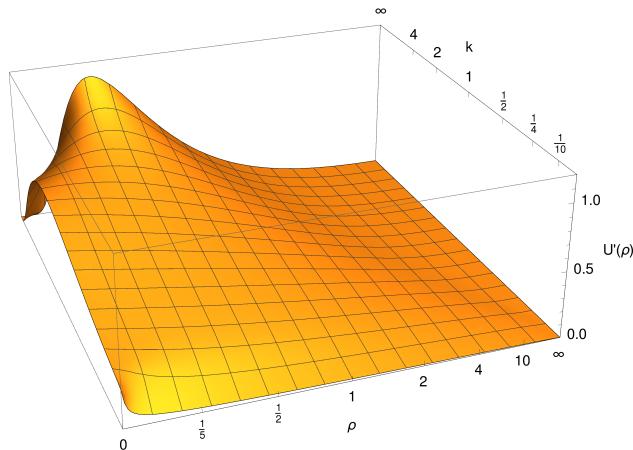


Fig. B.7.: Flow of the derivative of the effective potential for the Callan-Symanzik regulator. One can see that the nonanalyticity of the classical potential quickly smooths out. Convexity problems for small scales arise for large values of the position, in contrast to conventional unbounded potentials.

*Expectations* - The effective potential needs to be convex at  $k = 0$  (except in particular cases, see the discussion in the next subsection). It is immediately clear that any bounded function that is not constant cannot be convex. It follows that if we could integrate the flow equations down to  $k = 0$ , we would end up with a constant potential, and the constant is exactly the ground state energy. One can prove this by considering an alternative definition of the effective potential [428],

$$U(\bar{x}) = \inf_{\Psi: \langle x \rangle = \bar{x}} \langle H \rangle, \quad (\text{B.17})$$

that is, the effective potential at a point  $\bar{x}$  is given by the infimum of the Hamiltonian over all states with position expectation value  $\bar{x}$ . Exhaustive discussions of the effective potential in quantum field theory can be found in *e.g.* [428–431]. Our naïve expectation on the flow is therefore that we can hope to find the ground state energy, but probably not the energy of the first excited state. Surprisingly, it turns out that one can extract some estimate of the excited state energy from the flow.

*Numerical results* - As exemplary case, we display the numerical results from solving the flow equation for the nonanalytical potential (B.4). The other two potentials pose no further challenge and show the same qualitative behaviour.

In Figure B.5, the effective potential at  $x = 0$  as a function of the scale  $k$  is depicted, for both the Callan-Symanzik and the optimised regulator. It corresponds to the effective ground state energy at scale  $k$ . The horizontal dashed line indicates the exact value obtained from the Schrödinger equation. For technical reasons, we cannot integrate down to  $k = 0$ , but only to a finite value, indicated by the vertical dashed line. From thereon, we extrapolate linearly to get an estimate of the true ground state energy. For both regulators, we get very

precise estimates for the ground state energy. Generically, the optimised regulator gives slightly superior results for  $E_0$ .

Next, we shall discuss the results on the energy gap. As argued above, in principle we should not expect to get any meaningful estimate from the effective potential. There is however a loophole in the above argument: it is based on the effective potential at scale  $k = 0$ , when all fluctuations are integrated out. When we consider the flow of the effective potential, we can extract further information, as the scale  $k$  is roughly the (inverse) scale of a finite box that the system lives in, giving an effective cutoff to physics. In this sense, we can indeed extract information on the energy gap, roughly when the scale is large enough to resolve the wave function of the first excited state, but small enough not to be too much influenced by the next-higher states. Bearing this in mind, we shall discuss the first derivative of the flowing potential, again at vanishing position, which gives the effective energy gap at scale  $k$  [432],

$$\Delta E = \sqrt{U'(\rho)}|_{\rho=0}, \quad (\text{B.18})$$

It is shown in Figure B.6, again for both regulators. Remarkably, in both cases again, we get a quite good estimate of the true energy gap, however the finer details are more complicated. For the Callan-Symanzik regulator, we can already see the influence of convexity, as the derivative of the effective potential bends towards zero. This is not the case for the optimised regulator yet. Correspondingly, the optimised regulator overestimates the energy gap, whereas the estimate from the Callan-Symanzik regulator is below the true value. This behaviour is also observed for the other potentials, and influences the prediction of the number of bound states. In this respect, the optimised regulator erroneously predicts only one bound state for the potential (B.2). On the other hand, the Callan-Symanzik regulator predicts a second bound state for the Pöschl-Teller potential (B.3). Either way, any prediction for the energy gap from the flow should be taken with a grain of salt, as convexity has to set in at some point, and also the extrapolation introduces further errors. Presumably one should read off the energy gap at some finite value of the scale, at which the first excited state is completely resolved, however we found no a priori argument on how to set this scale.

In Figure B.7, we depict the actual flow of the derivative of the effective potential, obtained with the Callan-Symanzik regulator. One can see that the nonanalyticity of the classical potential is smoothed out quickly. For small scales  $k$ , one can also see the tendency of the derivative of the effective potential to flow to zero, as it must due to convexity. In contrast to unbounded potentials, where convexity is numerically challenging near the origin, the numerical problems here arise for large values of the position, which makes it increasingly difficult to resolve the flow.

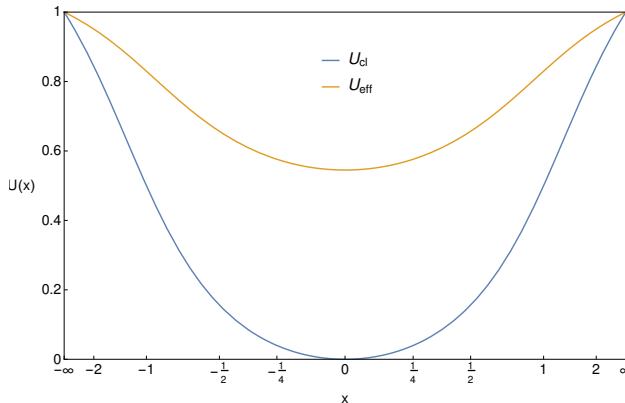


Fig. B.8.: Comparison of the classical potential (B.2) and the corresponding effective potential (B.19) in the large  $N$  limit. In contrast to finite  $N$ , we do not observe convexity of the effective potential, but only that the  $\rho$ -derivative is nonnegative.

### B.2.6. Large $N$ approximation

As a final point, we shall study the potential (B.2) in the limit of infinitely many dimensions, similar to a large  $N$  approximation in the  $O(N)$  model. In this case, the flow equation can be solved implicitly by the method of characteristics [418]. In the case of the potential (B.2), the implicit relation  $x = x(U)$  can be inverted, delivering the full effective potential. It is given by

$$\begin{aligned}
 U(x) = & \frac{-\pi x^2 + \sqrt{16\pi(1+x^4) - \pi^2}}{8\pi(1+x^4)} \\
 & + \frac{2}{\pi} \left( \arctan(x^2) + \arctan \left( \sqrt{\frac{\pi}{16(1+x^4) - \pi}} \right) \right).
 \end{aligned}
 \tag{B.19}$$

Notably, the large  $N$  effective potential is *not* convex. This seeming paradox has the following reason. Convexity is tied to the condition that the propagator avoids a singularity for negative  $U''(x)$  which appears in the equivalent of the radial mode propagator. In the large  $N$  approximation, however, only the equivalent of the Goldstone mode propagator survives, and for it to be finite, it is enough that  $U'(\rho) \equiv U'(x)/x$  is nonnegative. This is indeed the case for the solution given above. A plot of both the classical and the effective potential is given in Figure B.8.

## Appendix C.

# Gauge and parameterisation dependent flow equations

In this appendix, we display the gauge and parameterisation dependent flow equations of section 4.2.1 for general regulators  $\mathfrak{R}(\Delta)$  and in dimension  $d = 4$ . For simplicity, we denote  $\partial_t$ -derivatives by an overdot, and introduce the anomalous dimension  $\eta = (\dot{g} - 2g)/g$ , and refer to terms linear in  $\eta$  as “ $\eta$ -terms”. Let us start with the contribution from the TT-mode:

$$\begin{aligned} \mathcal{S}^{\text{TT}} = & \frac{5}{2}Q_2 \left[ \frac{\dot{\mathfrak{R}} - \eta\mathfrak{R}}{\Delta + \mathfrak{R} - 2\lambda(1 - \tau)} \right] \\ & - \frac{5}{12}R \left( Q_1 \left[ \frac{\dot{\mathfrak{R}} - \eta\mathfrak{R}}{\Delta + \mathfrak{R} - 2\lambda(1 - \tau)} \right] + (4 - 3\tau)Q_2 \left[ \frac{\dot{\mathfrak{R}} - \eta\mathfrak{R}}{(\Delta + \mathfrak{R} - 2\lambda(1 - \tau))^2} \right] \right), \end{aligned} \quad (\text{C.1})$$

where the  $Q$  functionals are defined in terms of Mellin transforms [35]. For the transverse vector, and without field redefinition, let us define

$$\begin{aligned} \mathcal{G}_n^{\text{T}} = & \left[ -(\dot{\mathfrak{R}} - \eta\mathfrak{R}) \left( 2\lambda(1 - \tau) - \frac{1}{\alpha}(\mathfrak{R} + 2\Delta) \right) - 2(\dot{\lambda} + 2\lambda)(1 - \tau)\mathfrak{R} \right] \times \\ & \left( (\Delta + \mathfrak{R}) \left( \frac{\Delta + \mathfrak{R}}{\alpha} + 2\lambda(1 - \tau) \right) \right)^{-n}. \end{aligned} \quad (\text{C.2})$$

With that, we have

$$\mathcal{S}^{\text{T}} = \frac{3}{2}Q_2 [\mathcal{G}_1^{\text{T}}] + R \left( \frac{1}{4}Q_1 [\mathcal{G}_1^{\text{T}}] + \frac{3}{2}(1 - \alpha(1 - \tau))Q_3 [\mathcal{G}_2^{\text{T}}] - \frac{3}{4}\lambda(1 - \tau)Q_2 [\mathcal{G}_2^{\text{T}}] \right). \quad (\text{C.3})$$

On the other hand, the contribution with field redefinition reads,

$$\begin{aligned} \mathcal{S}_{\text{fr}}^{\text{T}} = & \frac{3}{2}Q_2 \left[ \frac{\dot{\mathfrak{R}} - \eta\mathfrak{R}}{\Delta + \mathfrak{R} - 2\alpha\lambda(1 - \tau)} \right] \\ & + R \left( \frac{1}{8}Q_1 \left[ \frac{\dot{\mathfrak{R}} - \eta\mathfrak{R}}{\Delta + \mathfrak{R} - 2\alpha\lambda(1 - \tau)} \right] + \frac{3}{8}(1 - 2\alpha(1 - \tau))Q_2 \left[ \frac{\dot{\mathfrak{R}} - \eta\mathfrak{R}}{(\Delta + \mathfrak{R} - 2\alpha\lambda(1 - \tau))^2} \right] \right). \end{aligned} \quad (\text{C.4})$$



For the scalar contribution, we first define

$$\pi^\sigma = -\frac{3}{4\alpha} \left( 4\alpha\lambda(1-\tau)(\Delta + \mathfrak{R})^2 + (\alpha-3)(\Delta + \mathfrak{R})^3 \right), \quad (\text{C.5})$$

$$\pi^h = -\frac{1}{16\alpha} \left( -4\alpha\lambda(1+\tau) + (3\alpha - \beta^2)(\Delta + \mathfrak{R}) \right), \quad (\text{C.6})$$

$$\pi^x = -\frac{3}{8\alpha}(\alpha - \beta)(\Delta + \mathfrak{R})^2, \quad (\text{C.7})$$

$$\begin{aligned} \rho^\sigma = & -\frac{3}{4\alpha} \left( 4\alpha(\dot{\lambda} + (2-\eta)\lambda)(1-\tau)(2\Delta + \mathfrak{R})\mathfrak{R} \right. \\ & + 8\alpha\lambda(1-\tau)(\Delta + \mathfrak{R})\dot{\mathfrak{R}} \\ & + 3(\alpha-3)(\Delta + \mathfrak{R})^2\dot{\mathfrak{R}} \\ & \left. - (\alpha-3)(3\Delta^2 + 3\Delta\mathfrak{R} + \mathfrak{R}^2)\eta\mathfrak{R} \right), \end{aligned} \quad (\text{C.8})$$

$$\rho^h = -\frac{1}{16\alpha}(3\alpha - \beta^2)(\dot{\mathfrak{R}} - \eta\mathfrak{R}), \quad (\text{C.9})$$

$$\rho^x = -\frac{3}{8\alpha}(\alpha - \beta)(2\dot{\mathfrak{R}}(\Delta + \mathfrak{R}) - \eta\mathfrak{R}(2\Delta + \mathfrak{R})). \quad (\text{C.10})$$

The contribution is

$$\begin{aligned} S^{\sigma h} = & \frac{1}{2}Q_2 \left[ \frac{\pi^\sigma \rho^h + \pi^h \rho^\sigma - 2\pi^x \rho^x}{\pi^\sigma \pi^h - (\pi^x)^2} \right] + R \left\{ \frac{1}{12}Q_1 \left[ \frac{\pi^\sigma \rho^h + \pi^h \rho^\sigma - 2\pi^x \rho^x}{\pi^\sigma \pi^h - (\pi^x)^2} \right] \right. \\ & - \frac{3}{4\alpha}(6 - \alpha(4 - 3\tau))Q_4 \left[ \frac{\rho^h}{\pi^\sigma \pi^h - (\pi^x)^2} \right] + \lambda(1-\tau)Q_3 \left[ \frac{\rho^h}{\pi^\sigma \pi^h - (\pi^x)^2} \right] \\ & - \frac{\alpha - \beta}{4\alpha}Q_3 \left[ \frac{\rho^x}{\pi^\sigma \pi^h - (\pi^x)^2} \right] + \frac{3}{4\alpha}(6 - \alpha(4 - 3\tau))Q_4 \left[ \frac{\pi^h (\pi^\sigma \rho^h + \pi^h \rho^\sigma - 2\pi^x \rho^x)}{(\pi^\sigma \pi^h - (\pi^x)^2)^2} \right] \\ & + \lambda(1-\tau)Q_3 \left[ \frac{\pi^h (\pi^\sigma \rho^h + \pi^h \rho^\sigma - 2\pi^x \rho^x)}{(\pi^\sigma \pi^h - (\pi^x)^2)^2} \right] + \frac{\tau}{32}Q_2 \left[ \frac{\pi^\sigma (\pi^\sigma \rho^h + \pi^h \rho^\sigma - 2\pi^x \rho^x)}{(\pi^\sigma \pi^h - (\pi^x)^2)^2} \right] \\ & \left. + \frac{\alpha - \beta}{16\alpha}Q_2 \left[ \frac{\pi^x (\pi^\sigma \rho^h + \pi^h \rho^\sigma - 2\pi^x \rho^x)}{(\pi^\sigma \pi^h - (\pi^x)^2)^2} \right] - \frac{\tau}{32}Q_2 \left[ \frac{\rho^\sigma}{\pi^\sigma \pi^h - (\pi^x)^2} \right] \right\}. \end{aligned} \quad (\text{C.11})$$

With field redefinition, define

$$\pi_{\text{fr}}^\sigma = -\frac{3}{4\alpha} (4\alpha\lambda(1-\tau) + (\alpha-3)(\Delta + \mathfrak{R})), \quad (\text{C.12})$$

$$\pi_{\text{fr}}^h = -\frac{1}{16\alpha} \left( -4\alpha\lambda(1+\tau) + (3\alpha - \beta^2)(\Delta + \mathfrak{R}) \right), \quad (\text{C.13})$$

$$\pi_{\text{fr}}^x = -\frac{3}{8\alpha}(\alpha - \beta)(\Delta + \mathfrak{R}), \quad (\text{C.14})$$

$$\rho_{\text{fr}}^\sigma = \frac{3}{4\alpha}(3 - \alpha)(\dot{\mathfrak{R}} - \eta\mathfrak{R}), \quad (\text{C.15})$$

$$\rho_{\text{fr}}^h = -\frac{1}{16\alpha}(3\alpha - \beta^2)(\dot{\mathfrak{R}} - \eta\mathfrak{R}), \quad (\text{C.16})$$

$$\rho_{\text{fr}}^{\text{x}} = -\frac{3}{8\alpha}(\alpha - \beta)(\mathfrak{R} - \eta\mathfrak{R}). \quad (\text{C.17})$$

Then, the scalar contribution is

$$\begin{aligned} S_{\text{fr}}^{\sigma\text{h}} = & \frac{1}{2}Q_2 \left[ \frac{\pi_{\text{fr}}^{\sigma}\rho_{\text{fr}}^{\text{h}} + \pi_{\text{fr}}^{\text{h}}\rho_{\text{fr}}^{\sigma} - 2\pi_{\text{fr}}^{\text{x}}\rho_{\text{fr}}^{\text{x}}}{\pi_{\text{fr}}^{\sigma}\pi_{\text{fr}}^{\text{h}} - (\pi_{\text{fr}}^{\text{x}})^2} \right] + R \left\{ \frac{1}{12}Q_1 \left[ \frac{\pi_{\text{fr}}^{\sigma}\rho_{\text{fr}}^{\text{h}} + \pi_{\text{fr}}^{\text{h}}\rho_{\text{fr}}^{\sigma} - 2\pi_{\text{fr}}^{\text{x}}\rho_{\text{fr}}^{\text{x}}}{\pi_{\text{fr}}^{\sigma}\pi_{\text{fr}}^{\text{h}} - (\pi_{\text{fr}}^{\text{x}})^2} \right] \right. \\ & + \frac{\tau}{32}Q_2 \left[ \frac{\pi_{\text{fr}}^{\sigma}(\pi_{\text{fr}}^{\sigma}\rho_{\text{fr}}^{\text{h}} + \pi_{\text{fr}}^{\text{h}}\rho_{\text{fr}}^{\sigma} - 2\pi_{\text{fr}}^{\text{x}}\rho_{\text{fr}}^{\text{x}})}{(\pi_{\text{fr}}^{\sigma}\pi_{\text{fr}}^{\text{h}} - (\pi_{\text{fr}}^{\text{x}})^2)^2} \right] - \frac{\tau}{32}Q_2 \left[ \frac{\rho_{\text{fr}}^{\sigma}}{\pi_{\text{fr}}^{\sigma}\pi_{\text{fr}}^{\text{h}} - (\pi_{\text{fr}}^{\text{x}})^2} \right] \\ & + \frac{3}{8\alpha}(1 - \alpha(1 - \tau)) \left( Q_2 \left[ \frac{\pi_{\text{fr}}^{\text{h}}(\pi_{\text{fr}}^{\sigma}\rho_{\text{fr}}^{\text{h}} + \pi_{\text{fr}}^{\text{h}}\rho_{\text{fr}}^{\sigma} - 2\pi_{\text{fr}}^{\text{x}}\rho_{\text{fr}}^{\text{x}})}{(\pi_{\text{fr}}^{\sigma}\pi_{\text{fr}}^{\text{h}} - (\pi_{\text{fr}}^{\text{x}})^2)^2} \right] - Q_2 \left[ \frac{\rho_{\text{fr}}^{\text{h}}}{\pi_{\text{fr}}^{\sigma}\pi_{\text{fr}}^{\text{h}} - (\pi_{\text{fr}}^{\text{x}})^2} \right] \right) \\ & \left. + \frac{\alpha - \beta}{16\alpha} \left( Q_2 \left[ \frac{\pi_{\text{fr}}^{\text{x}}(\pi_{\text{fr}}^{\sigma}\rho_{\text{fr}}^{\text{h}} + \pi_{\text{fr}}^{\text{h}}\rho_{\text{fr}}^{\sigma} - 2\pi_{\text{fr}}^{\text{x}}\rho_{\text{fr}}^{\text{x}})}{(\pi_{\text{fr}}^{\sigma}\pi_{\text{fr}}^{\text{h}} - (\pi_{\text{fr}}^{\text{x}})^2)^2} \right] - Q_2 \left[ \frac{\rho_{\text{fr}}^{\text{x}}}{\pi_{\text{fr}}^{\sigma}\pi_{\text{fr}}^{\text{h}} - (\pi_{\text{fr}}^{\text{x}})^2} \right] \right) \right\}. \quad (\text{C.18}) \end{aligned}$$

Further, the ghost contribution reads without field redefinition,

$$S^{\text{gh}} = -5Q_2 \left[ \frac{\mathfrak{R}}{\Delta + \mathfrak{R}} \right] - R \left( \frac{7}{12}Q_1 \left[ \frac{\mathfrak{R}}{\Delta + \mathfrak{R}} \right] + \frac{3}{4}Q_2 \left[ \frac{\mathfrak{R}}{(\Delta + \mathfrak{R})^2} \right] + \frac{4}{3 - \beta}Q_3 \left[ \frac{\mathfrak{R}}{(\Delta + \mathfrak{R})^3} \right] \right). \quad (\text{C.19})$$

With field redefinition, it is

$$S_{\text{fr}}^{\text{gh}} = -4Q_2 \left[ \frac{\mathfrak{R}}{\Delta + \mathfrak{R}} \right] - R \left( \frac{5}{12}Q_1 \left[ \frac{\mathfrak{R}}{\Delta + \mathfrak{R}} \right] + \left( \frac{3}{4} + \frac{1}{3 - \beta} \right) Q_2 \left[ \frac{\mathfrak{R}}{(\Delta + \mathfrak{R})^2} \right] \right). \quad (\text{C.20})$$

Finally, the contribution of the Jacobian for the case without field redefinition is

$$\mathcal{S}^{\text{Jac}} = \frac{1}{2}S^{\text{gh}}|_{\beta=0} + Q_2 \left[ \frac{\mathfrak{R}}{\Delta + \mathfrak{R}} \right] + \frac{1}{6}RQ_1 \left[ \frac{\mathfrak{R}}{(\Delta + \mathfrak{R})^2} \right]. \quad (\text{C.21})$$

With field redefinition, all Jacobians cancel, at least to linear order in background curvature that we consider here [37].

# Appendix D.

## Basis for correlation functions

Here, we specify a basis for all fluctuation correlation functions with up to three fluctuation fields, including up to two background derivatives or one background curvature. The one-point correlator has 3 independent monomials,

$$\Gamma^{(1)} \sim a_1 h + a_2 h \bar{R} + a_3 h_{\mu\nu} \bar{S}^{\mu\nu}. \quad (\text{D.1})$$

For the two-point function, there are 2 invariants with neither derivatives nor curvature,

$$\Gamma_\lambda^{(2)} \sim b_1 h^2 + b_2 h_{\mu\nu} h^{\mu\nu}, \quad (\text{D.2})$$

4 invariants with 2 derivatives,

$$\Gamma_D^{(2)} \sim b_3 h \bar{\Delta} h + b_4 h_{\mu\nu} \bar{\Delta} h^{\mu\nu} + b_5 h \bar{D}^\mu \bar{D}^\nu h_{\mu\nu} + b_6 \bar{D}^\mu h_{\mu\rho} \bar{D}^\nu h_\nu{}^\rho, \quad (\text{D.3})$$

and 5 invariants with a single background curvature,

$$\Gamma_R^{(2)} \sim b_7 h_{\mu\nu} \bar{C}^{\mu\rho\nu\sigma} h_{\rho\sigma} + b_8 h_{\mu\nu} \bar{S}^{\mu\rho} h_\rho{}^\nu + b_9 h_{\mu\nu} S^{\mu\nu} h + b_{10} h_{\mu\nu} \bar{R} h^{\mu\nu} + b_{11} h \bar{R} h. \quad (\text{D.4})$$

The three-point correlator can be spanned by 3 terms without any derivatives or curvature,

$$\Gamma_\lambda^{(3)} \sim c_1 h^3 + c_2 h_{\mu\nu} h^{\mu\nu} h + c_3 h_\mu{}^\nu h_\nu{}^\rho h_\rho{}^\mu, \quad (\text{D.5})$$

14 terms with 2 derivatives,

$$\begin{aligned} \Gamma_D^{(3)} \sim & c_4 h^2 \bar{\Delta} h + c_5 h^2 \bar{D}_\mu \bar{D}_\nu h^{\mu\nu} + c_6 h h^{\mu\nu} \bar{D}_\mu \bar{D}_\nu h + c_7 h_\mu{}^\rho h^{\mu\sigma} \bar{D}_{(\rho} \bar{D}_{\sigma)} h \\ & + c_8 h \left( \bar{D}_\rho h_\mu{}^\rho \right) \bar{D}_\sigma h^{\mu\sigma} + c_9 h h_\mu{}^\rho \bar{D}_{(\rho} \bar{D}_{\sigma)} h^{\mu\sigma} + c_{10} h h_{\mu\nu} \bar{\Delta} h^{\mu\nu} \\ & + c_{11} h_{\mu\nu} h^{\mu\nu} \bar{\Delta} h + c_{12} h_\mu{}^\rho h_\rho{}^\nu \bar{\Delta} h_\nu{}^\mu + c_{13} h_{\mu\nu} h_{\rho\sigma} \bar{D}^\mu \bar{D}^\nu h^{\rho\sigma} + c_{14} h_{\mu\nu} h^{\mu\nu} \bar{D}_\rho \bar{D}_\sigma h^{\rho\sigma} \\ & + c_{15} h^{\rho\nu} h_{\sigma\nu} \bar{D}_{(\mu} \bar{D}_{\rho)} h^{\mu\sigma} + c_{16} h_{\nu\sigma} \left( \bar{D}_\mu h^{\mu\nu} \right) \bar{D}_\rho h^{\rho\sigma} + c_{17} h^{\mu\nu} h^{\rho\sigma} \bar{D}_{(\mu} \bar{D}_{\rho)} h_{\nu\sigma}, \end{aligned} \quad (\text{D.6})$$

and 9 invariants with a background curvature,

$$\begin{aligned} \Gamma_{\text{R}}^{(3)} \sim & c_{18} \bar{C}^{\mu\nu\rho\sigma} h_{\nu\sigma} h_{\mu\tau} h_{\rho}{}^{\tau} + c_{19} \bar{C}^{\mu\nu\rho\sigma} h h_{\mu\rho} h_{\nu\sigma} + c_{20} \bar{S}^{\mu\nu} h_{\nu}{}^{\rho} h_{\rho}{}^{\sigma} h_{\sigma\mu} + c_{21} \bar{S}^{\mu\nu} h_{\mu\nu} h^{\rho\sigma} h_{\rho\sigma} \\ & + c_{22} \bar{S}^{\mu\nu} h_{\nu}{}^{\rho} h_{\rho}{}^{\mu} h + c_{23} \bar{S}^{\mu\nu} h_{\mu\nu} h^2 + c_{24} \bar{R} h_{\mu}{}^{\nu} h_{\nu}{}^{\rho} h_{\rho}{}^{\mu} + c_{25} \bar{R} h_{\mu\nu} h^{\mu\nu} h + c_{26} \bar{R} h^3. \end{aligned} \quad (\text{D.7})$$

## Appendix E.

# General inverse and determinant of the metric

In this appendix we present the full formulas for the general inverse and determinant of the full metric, for the most general parameterisation which doesn't include derivatives. The starting point is (4.108), with inverse (4.109). The coefficients of the inverse read

$$\begin{aligned} \mathcal{B}_0 = \frac{1}{216\Delta} & \left[ 216\mathcal{A}_0^2 (\mathcal{A}_2\mathfrak{h}_2 + \mathcal{A}_3\mathfrak{h}_3) + 9\mathcal{A}_0 \left( -12\mathcal{A}_1^2\mathfrak{h}_2 - 12\mathcal{A}_1 \left( 2\mathcal{A}_2\mathfrak{h}_3 + \mathcal{A}_3 \left( \mathfrak{h}_2^2 - 4\mathfrak{h}_4 \right) \right) \right) \right. \\ & + 4\mathcal{A}_2\mathcal{A}_3\mathfrak{h}_2\mathfrak{h}_3 + 6\mathcal{A}_2^2 \left( \mathfrak{h}_2^2 + 4\mathfrak{h}_4 \right) + \mathcal{A}_3^2 \left( -3\mathfrak{h}_2^3 + 24\mathfrak{h}_4\mathfrak{h}_2 + 8\mathfrak{h}_3^2 \right) \\ & + 216\mathcal{A}_2\mathcal{A}_3^2\mathfrak{h}_4^2 + 2\mathfrak{h}_3 \left( 4\mathcal{A}_3^3\mathfrak{h}_3^2 + 9\mathcal{A}_1 \left( (\mathcal{A}_3\mathfrak{h}_2 + 2\mathcal{A}_1)^2 - 2\mathcal{A}_2^2\mathfrak{h}_2 \right) \right. \\ & - 6\mathcal{A}_2\mathfrak{h}_3 \left( \mathcal{A}_3 \left( \mathcal{A}_3\mathfrak{h}_2 + 6\mathcal{A}_1 \right) - 2\mathcal{A}_2^2 \right) \left. \right) - 18\mathfrak{h}_4 \left( 3\mathcal{A}_2 \left( (\mathcal{A}_3\mathfrak{h}_2 + 2\mathcal{A}_1)^2 - 2\mathcal{A}_2^2\mathfrak{h}_2 \right) \right. \\ & \left. \left. + 4\mathcal{A}_3\mathfrak{h}_3 \left( \mathcal{A}_2^2 - \mathcal{A}_3 \left( \mathcal{A}_3\mathfrak{h}_2 + 2\mathcal{A}_1 \right) \right) \right) + 216\mathcal{A}_0^3 \right], \end{aligned} \quad (\text{E.1})$$

$$\begin{aligned} \mathcal{B}_1 = \frac{1}{72\Delta} & \left[ -72\mathcal{A}_3^3\mathfrak{h}_4^2 + \mathfrak{h}_2 \left( 4\mathcal{A}_3^3\mathfrak{h}_3^2 + 9\mathcal{A}_1 \left( (\mathcal{A}_3\mathfrak{h}_2 + 2\mathcal{A}_1)^2 - 2\mathcal{A}_2^2\mathfrak{h}_2 \right) \right) \right. \\ & - 6\mathcal{A}_2\mathfrak{h}_3 \left( \mathcal{A}_3 \left( \mathcal{A}_3\mathfrak{h}_2 + 6\mathcal{A}_1 \right) - 2\mathcal{A}_2^2 \right) \left. \right) - 18\mathfrak{h}_4 \left( 2\mathcal{A}_1 - \mathcal{A}_3\mathfrak{h}_2 \right) \times \\ & \left( \mathcal{A}_3 \left( \mathcal{A}_3\mathfrak{h}_2 + 2\mathcal{A}_1 \right) - 2\mathcal{A}_2^2 \right) - 12\mathcal{A}_0 \left( -\mathfrak{h}_3 \left( \mathcal{A}_3^2\mathfrak{h}_2 + 2\mathcal{A}_2^2 \right) \right. \\ & \left. + 2\mathcal{A}_1 \left( 3\mathcal{A}_2\mathfrak{h}_2 + \mathcal{A}_3\mathfrak{h}_3 \right) + 12\mathcal{A}_2\mathcal{A}_3\mathfrak{h}_4 \right) - 72\mathcal{A}_0^2\mathcal{A}_1 \right], \end{aligned} \quad (\text{E.2})$$

$$\begin{aligned} \mathcal{B}_2 = \frac{1}{216\Delta} & \left[ -18\mathcal{A}_0 \left( -3 \left( \mathcal{A}_3\mathfrak{h}_2 + 2\mathcal{A}_1 \right)^2 + 6\mathcal{A}_2 \left( \mathcal{A}_2\mathfrak{h}_2 + 2\mathcal{A}_0 \right) + 4\mathcal{A}_2\mathcal{A}_3\mathfrak{h}_3 \right) \right. \\ & \left. - 36\mathfrak{h}_4 \left( -3\mathcal{A}_3\mathcal{A}_2 \left( \mathcal{A}_3\mathfrak{h}_2 + 4\mathcal{A}_1 \right) + 2\mathcal{A}_3^2 \left( \mathcal{A}_3\mathfrak{h}_3 + 3\mathcal{A}_0 \right) + 6\mathcal{A}_2^3 \right) \right], \end{aligned} \quad (\text{E.3})$$

$$\begin{aligned} \mathcal{B}_3 = \frac{1}{36\Delta} & \left[ -4\mathcal{A}_3^3\mathfrak{h}_3^2 - 18\mathcal{A}_3\mathfrak{h}_4 \left( \mathcal{A}_3 \left( \mathcal{A}_3\mathfrak{h}_2 + 2\mathcal{A}_1 \right) - 2\mathcal{A}_2^2 \right) \right. \\ & - 9 \left( 4\mathcal{A}_3\mathcal{A}_1^2\mathfrak{h}_2 + \mathcal{A}_1 \left( \mathfrak{h}_2 \left( \mathcal{A}_3^2\mathfrak{h}_2 - 2\mathcal{A}_2^2 \right) - 8\mathcal{A}_0\mathcal{A}_2 \right) + 4\mathcal{A}_1^3 + 4\mathcal{A}_0^2\mathcal{A}_3 \right) \\ & \left. + 6\mathfrak{h}_3 \left( \mathcal{A}_3\mathcal{A}_2 \left( \mathcal{A}_3\mathfrak{h}_2 + 6\mathcal{A}_1 \right) - 2\mathcal{A}_2^3 - 4\mathcal{A}_0\mathcal{A}_3^2 \right) \right], \end{aligned} \quad (\text{E.4})$$

where we already used the ratio of determinants

$$\begin{aligned}
 \Delta \equiv \frac{\det g}{\det \bar{g}} &= \mathcal{A}_0^3 (\mathcal{A}_2 \mathfrak{h}_2 + \mathcal{A}_3 \mathfrak{h}_3) + \frac{1}{24} \mathcal{A}_0^2 \left( -12 \mathcal{A}_1^2 \mathfrak{h}_2 - 12 \mathcal{A}_1 (2 \mathcal{A}_2 \mathfrak{h}_3 + \mathcal{A}_3 (\mathfrak{h}_2^2 - 8 \mathfrak{h}_4)) \right. \\
 &\quad + 4 \mathcal{A}_2 \mathcal{A}_3 \mathfrak{h}_2 \mathfrak{h}_3 + 6 \mathcal{A}_2^2 (\mathfrak{h}_2^2 + 8 \mathfrak{h}_4) + \mathcal{A}_3^2 (-3 \mathfrak{h}_2^3 + 36 \mathfrak{h}_4 \mathfrak{h}_2 + 8 \mathfrak{h}_3^2) \\
 &\quad + \frac{1}{108} \mathcal{A}_0 (432 \mathcal{A}_2 \mathcal{A}_3^2 \mathfrak{h}_4^2 - 18 \mathfrak{h}_4 (3 \mathcal{A}_2 (\mathcal{A}_3^2 \mathfrak{h}_2^2 - 2 (\mathcal{A}_2^2 - 2 \mathcal{A}_1 \mathcal{A}_3) \mathfrak{h}_2 + 8 \mathcal{A}_1^2) \\
 &\quad + \mathcal{A}_3 \mathfrak{h}_3 (2 \mathcal{A}_2^2 - \mathcal{A}_3 (3 \mathcal{A}_3 \mathfrak{h}_2 + 10 \mathcal{A}_1))) \\
 &\quad + \mathfrak{h}_3 (4 \mathcal{A}_3^3 \mathfrak{h}_3^2 + 9 \mathcal{A}_1 ((\mathcal{A}_3 \mathfrak{h}_2 + 2 \mathcal{A}_1)^2 - 2 \mathcal{A}_2^2 \mathfrak{h}_2) \\
 &\quad - 6 \mathcal{A}_2 \mathfrak{h}_3 (\mathcal{A}_3 (\mathcal{A}_3 \mathfrak{h}_2 + 6 \mathcal{A}_1) - 2 \mathcal{A}_2^2)) \\
 &\quad + \frac{1}{36} \mathfrak{h}_4 (36 \mathcal{A}_3^4 \mathfrak{h}_4^2 + \mathcal{A}_1 (4 \mathcal{A}_3^3 \mathfrak{h}_3^2 + 9 \mathcal{A}_1 ((\mathcal{A}_3 \mathfrak{h}_2 + 2 \mathcal{A}_1)^2 - 2 \mathcal{A}_2^2 \mathfrak{h}_2) \\
 &\quad - 6 \mathcal{A}_2 \mathfrak{h}_3 (\mathcal{A}_3 (\mathcal{A}_3 \mathfrak{h}_2 + 6 \mathcal{A}_1) - 2 \mathcal{A}_2^2)) + 6 \mathfrak{h}_4 (-3 \mathcal{A}_3 \mathcal{A}_2^2 (\mathcal{A}_3 \mathfrak{h}_2 + 8 \mathcal{A}_1) \\
 &\quad \left. + 2 \mathcal{A}_3^3 \mathcal{A}_2 \mathfrak{h}_3 + 6 \mathcal{A}_1 \mathcal{A}_3^2 (\mathcal{A}_3 \mathfrak{h}_2 + 2 \mathcal{A}_1) + 6 \mathcal{A}_4^4) \right) + \mathcal{A}_0^4.
 \end{aligned} \tag{E.5}$$

Let us also show how to calculate the  $n$ -th power of  $\mathfrak{h}^{\text{TL}}$  for  $n \geq 4$ . For this, we make the ansatz

$$[\mathfrak{h}^{\text{TL}}]^n = a_n \mathbb{1}_4 + b_n \mathfrak{h}^{\text{TL}} + c_n [\mathfrak{h}^{\text{TL}}]^2 + d_n [\mathfrak{h}^{\text{TL}}]^3. \tag{E.6}$$

From the CHT, we get the initial conditions

$$a_4 = -\mathfrak{h}_4, \quad b_4 = \frac{1}{3} \mathfrak{h}_3, \quad c_4 = \frac{1}{2} \mathfrak{h}_2, \quad d_4 = 0. \tag{E.7}$$

Multiplying (E.6) by  $\mathfrak{h}^{\text{TL}}$  and using the CHT, we get the recursion relations

$$\begin{aligned}
 a_{n+1} &= -\mathfrak{h}_4 d_n, \\
 b_{n+1} &= a_n + \frac{1}{3} \mathfrak{h}_3 d_n, \\
 c_{n+1} &= b_n + \frac{1}{2} \mathfrak{h}_2 d_n, \\
 d_{n+1} &= c_n.
 \end{aligned} \tag{E.8}$$

This recursion relation can be solved by Mathematica, but the result contains *RootSum* expressions and is not very enlightning, thus we shall not present it here. For the special case of an exponential parameterisation, one can transform this set of recursion relations into a set of differential equations in a fiducial variable  $x$  by introducing the functions

$$A(x) = \sum_{n=4}^{\infty} \frac{a_n}{n!} x^n, \quad B(x) = \sum_{n=4}^{\infty} \frac{b_n}{n!} x^n, \quad C(x) = \sum_{n=4}^{\infty} \frac{c_n}{n!} x^n, \quad D(x) = \sum_{n=4}^{\infty} \frac{d_n}{n!} x^n. \tag{E.9}$$

The metric in exponential parameterisation then reads

$$g^{\text{exp}} = \bar{g} e^{\mathfrak{h}_1/4} \left( \mathbb{1}_4(1 + A(1)) + \mathfrak{h}^{\text{TL}} (1 + B(1)) + [\mathfrak{h}^{\text{TL}}]^2 \left( \frac{1}{2} + C(1) \right) + [\mathfrak{h}^{\text{TL}}]^3 \left( \frac{1}{6} + D(1) \right) \right). \quad (\text{E.10})$$

This emphasises again the usefulness of our choice of invariants, since the trace factors out. To obtain the functions  $A, B, C, D$ , (E.8) is multiplied with  $\frac{x^n}{n!}$  and summed over  $n$  from 4 to  $\infty$ , and the resulting set of differential equations reads

$$\begin{aligned} A'(x) &= \mathfrak{h}_4 \left( \frac{x^3}{6} - D(x) \right), \\ B'(x) &= A(x) + \frac{1}{3} \mathfrak{h}_3 \left( \frac{x^3}{6} + D(x) \right), \\ C'(x) &= B(x) + \frac{1}{2} \mathfrak{h}_2 \left( \frac{x^3}{6} + D(x) \right), \\ D'(x) &= C(x). \end{aligned} \quad (\text{E.11})$$

The initial conditions at  $x = 0$  follow from the initial conditions of the recursion and the definition of the functions. Again, this system can be solved explicitly with Mathematica. For this, we introduce the polynomial

$$p(x) = 6\mathfrak{h}_4 - 2\mathfrak{h}_3x - 3\mathfrak{h}_2x^2 + 6x^4, \quad (\text{E.12})$$

which is related to the CHT, *i.e.* the characteristic polynomial of  $\mathfrak{h}$ . The operator  $\mathcal{RS}$  (for *RootSum*) then maps a function to the sum of the values of the function at the roots of the polynomial  $p$ ,

$$\mathcal{RS}[f(x)] = \sum_{x_i: p(x_i)=0} f(x_i). \quad (\text{E.13})$$

With the abbreviation

$$\rho_n = \mathcal{RS} \left[ \frac{e^x x^n}{-\mathfrak{h}_3 - 3\mathfrak{h}_2x + 12x^3} \right], \quad (\text{E.14})$$

the solution to the differential equations at the relevant point is

$$\begin{aligned} A(1) &= \mathcal{RS} \left[ \frac{1}{12x^4 (-\mathfrak{h}_3 + 12x^3 - 3\mathfrak{h}_2x)} \left( \mathfrak{h}_4 e^{-x} (x(x(x+3) + 6) - 6e^x + 6) \times \right. \right. \\ &\quad \left. \left( 2 \left( 2\mathfrak{h}_3^2 \rho_0 - 9\rho_3 x^3 + 9\mathfrak{h}_4 (\rho_2 + x(\rho_1 + \rho_0 x)) + 3\mathfrak{h}_3 (2\rho_3 + x(\rho_2 + \rho_1 x)) \right) \right. \right. \\ &\quad \left. \left. - 9\mathfrak{h}_2^2 \rho_1 x + 3\mathfrak{h}_2 (-6\mathfrak{h}_4 \rho_0 + 2\mathfrak{h}_3 (\rho_0 x - \rho_1) + 3x(2\rho_3 + x(\rho_2 + 2\rho_1 x))) \right) \right) \right], \end{aligned} \quad (\text{E.15})$$

$$\begin{aligned} B(1) &= \mathcal{RS} \left[ \frac{1}{12x^4 (-\mathfrak{h}_3 + 12x^3 - 3\mathfrak{h}_2x)} \left( e^{-x} (x(x(x+3) + 6) - 6e^x + 6) \times \right. \right. \\ &\quad \left. \left( 3\mathfrak{h}_2 \left( \mathfrak{h}_4 (\rho_0 (6x^3 - 2\mathfrak{h}_3) + 6(\rho_3 + x(\rho_2 + \rho_1 x))) - \mathfrak{h}_3 \rho_2 x^2 \right) \right) \right) \right] \end{aligned}$$

$$\begin{aligned}
 & + 2 \left( 9\mathfrak{h}_4 \left( \mathfrak{h}_4 (\rho_1 + \rho_0 x) - x^2 (\rho_3 + \rho_2 x) \right) + 3\mathfrak{h}_3 \left( \mathfrak{h}_4 (\rho_2 + \rho_0 x^2) - \rho_3 x^3 \right) \right. \\
 & \left. - \mathfrak{h}_3^2 x (\rho_2 + \rho_1 x) \right) - 9\mathfrak{h}_4 \mathfrak{h}_2^2 (\rho_1 + \rho_0 x) \Big) , \tag{E.16}
 \end{aligned}$$

$$\begin{aligned}
 C(1) = \mathcal{RS} \left[ -\frac{1}{24x^4 (-\mathfrak{h}_3 + 12x^3 - 3\mathfrak{h}_2 x)} \left( e^{-x} (x(x(x+3) + 6) - 6e^x + 6) \times \right. \right. \\
 \left. \left( 9\mathfrak{h}_2^2 \rho_2 x^2 + 4 \left( 3\mathfrak{h}_3 \left( x^2 (\rho_3 + \rho_2 x) - \mathfrak{h}_4 (\rho_1 + \rho_0 x) \right) + \mathfrak{h}_3^2 \rho_1 x \right. \right. \right. \\
 \left. \left. + 9\mathfrak{h}_4 (x (\rho_3 + x (\rho_2 + \rho_1 x)) - \mathfrak{h}_4 \rho_0) \right) \right. \\
 \left. \left. + 6\mathfrak{h}_2 \left( 3\rho_3 x^3 - 3\mathfrak{h}_4 (\rho_2 + \rho_0 x^2 + 2\rho_1 x) + \mathfrak{h}_3 x (\rho_2 + \rho_1 x) \right) \right) \right] , \tag{E.17}
 \end{aligned}$$

$$\begin{aligned}
 D(1) = \mathcal{RS} \left[ -\frac{1}{4x^4 (-\mathfrak{h}_3 + 12x^3 - 3\mathfrak{h}_2 x)} \left( e^{-x} (x(x(x+3) + 6) - 6e^x + 6) \times \right. \right. \\
 \left. \left( \mathfrak{h}_4 \left( \rho_0 (-4\mathfrak{h}_3 + 6x^3 - 6\mathfrak{h}_2 x) + 6 \left( \rho_3 + \rho_1 (x^2 - \mathfrak{h}_2) + \rho_2 x \right) \right) \right. \right. \\
 \left. \left. + x (3\mathfrak{h}_2 x (\rho_3 + \rho_2 x) + 2\mathfrak{h}_3 (\rho_3 + x (\rho_2 + \rho_1 x))) \right) \right] . \tag{E.18}
 \end{aligned}$$

For the special case where we neglect the invariants  $\mathfrak{h}_3$  and  $\mathfrak{h}_4$ , we find  $A = B = \mathcal{O}(\mathfrak{h}_3, \mathfrak{h}_4)$  and

$$C(1) = -\frac{4 + \mathfrak{h}_2 - 4 \cosh \sqrt{\frac{\mathfrak{h}_2}{2}}}{2\mathfrak{h}_2} + \mathcal{O}(\mathfrak{h}_3, \mathfrak{h}_4) , \tag{E.19}$$

$$D(1) = -\frac{1}{6} - \frac{2}{\mathfrak{h}_2} + \frac{2\sqrt{2} \sinh \sqrt{\frac{\mathfrak{h}_2}{2}}}{\mathfrak{h}_2^{3/2}} + \mathcal{O}(\mathfrak{h}_3, \mathfrak{h}_4) . \tag{E.20}$$



# Appendix F.

## Inversion of tensors

A generic task in FRG studies is the calculation of the inverse of the second variational derivative of the effective action. Here, we want to outline an algorithm to construct the inverse for a general Hessian. For this, we use de Witt's condensed notation, where an abstract index  $A$  labels a number of spacetime and internal indices as well as a spacetime point. The ideas presented here are based on unpublished work together with Stefan Lippoldt.

The regularised Hessian is

$$\left(\Gamma^{(2)} + \mathfrak{R}\right)_B^A, \quad (\text{F.1})$$

and we want to solve

$$G^A{}_B \left(\Gamma^{(2)} + \mathfrak{R}\right)_C^B = \delta_C^A, \quad (\text{F.2})$$

where  $\delta$  denotes the generalised identity operator. For example, if  $A = \mu$ , we have the standard Kronecker delta. By contrast, for a symmetric 2-tensor

$$\delta_B^A = \delta_{\rho\sigma}^{\mu\nu} = \frac{1}{2} \left( \delta_\rho^\mu \delta_\sigma^\nu + \delta_\sigma^\mu \delta_\rho^\nu \right). \quad (\text{F.3})$$

Typically, we are interested in solutions to (F.2) only up to truncated operators  $\mathcal{T}$ ,

$$G^A{}_B \left(\Gamma^{(2)} + \mathfrak{R}\right)_C^B = \delta_C^A + \mathcal{O}(\mathcal{T}). \quad (\text{F.4})$$

This can for example be a certain power in background curvature, or a maximal number of derivatives on the field strength. For the algorithm that we will show now to work, we need the set of operators that are included to be finite. Otherwise, clearly the propagator cannot be calculated on a finite computer.

The calculation of the propagator involves two conceptual steps. We first have to find the complete basis of the operators that we want to resolve. With this, we can make an ansatz for the propagator as a linear combination of these operators. Second, we have to calculate the expansion coefficients.

The algorithm implements these two steps: we will first iteratively construct the basis,

and then solve for the coefficients. For the first step, define

$$G_{0B}^A = \delta_B^A. \quad (\text{F.5})$$

We construct the  $n$ -th iteration  $G_n$  by taking a general linear combination of all operators that are produced by the multiplication of  $G_{n-1}$  with  $\Gamma^{(2)} + \mathfrak{R}$ . Clearly, operators that are truncated will not be taken into account. After a finite number of steps, no new operators will be generated if the basis of the resolved operators is finite, and we thus have an ansatz for the propagator,  $G_N$ . It is important that really only different tensor structures in the sense of indexed objects are included, *i.e.*  $\Delta D^\mu D_\nu$  and  $D^\mu D_\nu$  are not different tensor structures.

To calculate the coefficients, we can use the command *SolveCoefficients* of the *xTras* package which is part of the *xAct* suite for Mathematica. For this, we calculate the product of  $G_N$  and the regularised Hessian, span everything in the tensor basis, and then solve the system of equations by demanding (F.4). The latter step is automatically done by *SolveCoefficients*, which combines the reformulation to a system of linear equations with the *Solve* routine of Mathematica.

Let us illustrate this algorithm by the following example. Consider the Hessian

$$\left(\Gamma^{(2)} + \mathfrak{R}\right)_B^A = (\Delta + \mathfrak{R}(\Delta)) \delta_\nu^\mu + a D^\mu D_\nu + b R_\nu^\mu, \quad (\text{F.6})$$

where  $a$  and  $b$  are constants. For convenience, we introduce  $\Delta_{\mathfrak{R}} = \Delta + \mathfrak{R}(\Delta)$ . We want to calculate the inverse of this operator up to linear order in the curvature, neglecting also derivatives on the curvature. The first iteration gives us the linear combination of operators that appear in the Hessian itself, the second iteration adds two further tensor structures, the third adds a final one. No further structures are then generated, thus the propagator can be parameterised as

$$\begin{aligned} G^\mu{}_\nu = & g_0(\Delta) \delta_\nu^\mu + D^\mu g_1(\Delta) D_\nu + g_2(\Delta) R_\nu^\mu + g_3(\Delta) R^{\alpha\beta} D^\mu D_\alpha D_\beta D_\nu \\ & + g_4(\Delta) R_\rho^\mu D^\rho D_\nu + g_5(\Delta) R_\nu^\rho D^\mu D_\rho + \mathcal{O}(R^2, DR). \end{aligned} \quad (\text{F.7})$$

Multiplying this ansatz with the Hessian, and sorting everything in a standard form, we arrive at

$$\begin{aligned} G^\mu{}_\nu \left(\Gamma^{(2)} + \mathfrak{R}\right)_\rho{}^\nu = & [g_0(\Delta) \Delta_{\mathfrak{R}}] \delta_\rho^\mu \\ & + D^\mu [a g_0(\Delta) + g_1(\Delta) \Delta_{a\mathfrak{R}}] D_\rho \\ & + R_\rho^\mu [b g_0(\Delta) + g_2(\Delta) \Delta_{\mathfrak{R}}] \\ & + [a (g_2(\Delta) - g_0'(\Delta)) + g_4(\Delta) \Delta_{a\mathfrak{R}}] R_\nu^\mu D^\nu D_\rho \\ & + [-g_1(\Delta) (\Delta_{\mathfrak{R}}' - b) + g_5(\Delta) \Delta_{\mathfrak{R}}] R_\rho^\nu D^\mu D_\nu \\ & + [g_3(\Delta) \Delta_{a\mathfrak{R}} + a g_5(\Delta)] R^{\alpha\beta} D^\mu D_\alpha D_\beta D_\rho \\ & + \mathcal{O}(R^2, DR). \end{aligned} \quad (\text{F.8})$$

Here,  $\Delta_{a\mathfrak{R}} = \Delta_{\mathfrak{R}} - a\Delta$  and  $\Delta'_{\mathfrak{R}} = 1 + \mathfrak{R}'(\Delta)$ . We hence find

$$\begin{aligned}
g_0(\Delta) &= \frac{1}{\Delta_{\mathfrak{R}}}, \\
g_1(\Delta) &= -\frac{a}{\Delta_{\mathfrak{R}}\Delta_{a\mathfrak{R}}}, \\
g_2(\Delta) &= -\frac{b}{\Delta_{\mathfrak{R}}^2}, \\
g_3(\Delta) &= \frac{a^2}{\Delta_{\mathfrak{R}}^2\Delta_{a\mathfrak{R}}^2} (1 - b + \mathfrak{R}'(\Delta)), \\
g_4(\Delta) = g_5(\Delta) &= -\frac{a}{\Delta_{\mathfrak{R}}^2\Delta_{a\mathfrak{R}}} (1 - b + \mathfrak{R}'(\Delta)).
\end{aligned} \tag{F.9}$$

A similar application interesting in the context of  $f(R)$  gravity is the full inverse with constant curvature, where  $S = C = 0$ , *i.e.* there is only a (covariantly constant) nontrivial Ricci scalar, but zero tracefree Ricci tensor and Weyl tensor. The general Hessian reads

$$\left(\Gamma^{(2)} + \mathfrak{R}\right)^A_B = A(\Delta, R)\delta^A_B + D^\mu B(\Delta, R)D_\mu. \tag{F.10}$$

Here,  $R$  as an argument indicates the Ricci scalar, and we suppress the dependence on the regulator in the discussion. In the absence of curvature tensors with indices, the two tensor structures present in the Hessian form a basis, thus

$$G^\mu_\nu = g_0(\Delta, R)\delta^\mu_\nu + D^\mu g_1(\Delta, R)D_\nu. \tag{F.11}$$

Calculating the product and neglecting derivatives of  $R$  yields

$$\begin{aligned}
G^\mu_\nu \left(\Gamma^{(2)} + \mathfrak{R}\right)^\nu_\rho &= g_0(\Delta, R)A(\Delta, R)\delta^\mu_\rho \\
&+ D^\mu \left[ g_0\left(\Delta - \frac{R}{4}, R\right) B(\Delta, R) + g_1(\Delta, R) \left( A\left(\Delta - \frac{R}{4}, R\right) - \Delta B(\Delta, R) \right) \right] D_\rho \\
&+ \mathcal{O}(S, C, DR).
\end{aligned} \tag{F.12}$$

This gives the coefficients

$$\begin{aligned}
g_0(\Delta, R) &= \frac{1}{A(\Delta, R)}, \\
g_1(\Delta, R) &= -\frac{B(\Delta, R)}{A\left(\Delta - \frac{R}{4}, R\right) \left[ A\left(\Delta - \frac{R}{4}, R\right) - \Delta B(\Delta, R) \right]}.
\end{aligned} \tag{F.13}$$

To calculate the product, we used the standard commutation relations

$$[D_\mu, \Delta]\sigma = R_{\mu\nu}D^\nu\sigma = \frac{R}{4}D_\mu\sigma + \mathcal{O}(S), \tag{F.14}$$

$$[D_\mu, \Delta]\xi^\mu = -R_{\mu\nu}D^\mu\xi^\nu - \frac{1}{2}\xi^\mu D_\mu R = -\frac{R}{4}D_\mu\xi^\mu + \mathcal{O}(S, DR), \tag{F.15}$$

the Baker-Campbell-Hausdorff formula,

$$e^{s\Delta} D_\mu e^{-s\Delta} = \sum_{n=0}^{\infty} \frac{1}{n!} [D_\mu, (-s\Delta)]_n, \quad (\text{F.16})$$

where  $[X, Y]_n = [[X, Y], Y]_{n-1}$  and  $[X, Y]_0 = X$ , and the Laplace transform

$$f(\Delta) = \int_0^\infty ds \tilde{f}(s) e^{-s\Delta}. \quad (\text{F.17})$$

For example, the shift in the first arguments arises from

$$\begin{aligned} g_0(\Delta, R) D^\mu \sigma &= \int_0^\infty ds \tilde{g}_0(s, R) e^{-s\Delta} D_\mu \sigma \\ &= \int_0^\infty ds \tilde{g}_0(s, R) \sum_{n=0}^{\infty} \frac{1}{n!} [D_\mu, s\Delta]_n e^{-s\Delta} \sigma \\ &= \int_0^\infty ds \tilde{g}_0(s, R) \sum_{n=0}^{\infty} \frac{1}{n!} \left(\frac{sR}{4}\right)^n D_\mu e^{-s\Delta} \sigma \\ &= D^\mu \int_0^\infty ds \tilde{g}_0(s, R) e^{-s\left(\Delta - \frac{R}{4}\right)} \sigma \\ &= D^\mu g_0\left(\Delta - \frac{R}{4}, R\right) \sigma. \end{aligned} \quad (\text{F.18})$$

Here, we again neglected terms of order  $S$  and  $DR$ . Incidentally, it is easy to generalise this last calculation to a general manifold with constant curvature,

$$g_0(\Delta, R) D^\mu \sigma = D_\alpha \int_0^\infty ds \tilde{g}_0(s, R) \left[ e^{-s(\Delta \mathbb{1} - \text{Ric})} \right]_\mu^\alpha \sigma. \quad (\text{F.19})$$

To bring this into a useful form, one again has to employ the CHT.

# Appendix G.

## Functional truncations in pure $U(1)$ gauge theory

This appendix treats a functional truncation of a pure  $U(1)$  gauge theory. We will calculate the  $\beta$  function of the most general function  $V$  of the field strength tensor in the limit of constant field strength tensors. With this, we illustrate the broad applicability of the methods of section 4.4.

The truncation we study reads

$$\Gamma = \int d^4x V(\mathcal{F}, \mathcal{G}) \equiv \int d^4x V\left(\frac{1}{4}F_{\mu\nu}F^{\mu\nu}, \frac{1}{4}F_{\mu\nu}\tilde{F}^{\mu\nu}\right). \quad (\text{G.1})$$

Here,  $\tilde{F}$  is the dual field strength tensor,

$$\tilde{F}_{\mu\nu} = \frac{1}{2}\epsilon_{\mu\nu\rho\sigma}F^{\rho\sigma}. \quad (\text{G.2})$$

In the following, we will only consider the contribution of the transverse gauge field  $A_\mu^T$ , with

$$\partial^\mu A_\mu^T = 0. \quad (\text{G.3})$$

The longitudinal and the ghost modes decouple, and together subtract a total contribution of one free scalar mode, which we will suppress in the discussion. In the following, we sketch the full calculation by neglecting the dependence on  $\mathcal{G}$ . The full calculation with both invariants can be done similarly, all necessary intermediate results will be given. The regulator for the transverse part is chosen as

$$\Delta S = \frac{1}{4} \int d^4x F_{\mu\nu} \frac{\mathfrak{R}(p^2)}{p^2} F^{\mu\nu}. \quad (\text{G.4})$$

The second variation of the action (G.1) reads

$$\Gamma_{\mu\nu}^{(2)} = V'(\mathcal{F})\left(\eta_{\mu\nu}p^2 - p_\mu p_\nu\right) + V''(\mathcal{F})F_{\mu\alpha}p^\alpha F_{\nu\beta}p^\beta, \quad (\text{G.5})$$

where  $\eta$  is the Minkowski metric and  $p$  the momentum vector. The propagator  $G$  can now be obtained by

$$G^{\mu\nu} \left( \Gamma^{(2)} + \Delta S^{(2)} \right)_{\nu\rho} = \delta_{\rho}^{\mu} - \frac{p^{\mu} p_{\rho}}{p^2}, \quad (\text{G.6})$$

paying proper attention to the transversality of  $A_{\mu}^{\text{T}}$ . From this, we find the transverse propagator

$$G^{\mu\nu} = \frac{1}{p^2 V'(\mathcal{F}) + \mathfrak{R}(p^2)} \left( \eta^{\mu\nu} p^2 - p^{\mu} p^{\nu} \right) - \frac{V''(\mathcal{F})}{p^2 V'(\mathcal{F}) (p^2 V'(\mathcal{F}) + \mathcal{P} V''(\mathcal{F}) + \mathfrak{R}(p^2))} F^{\mu\alpha} p_{\alpha} F^{\nu\beta} p_{\beta}. \quad (\text{G.7})$$

Here, we introduced the scalar quantity

$$\mathcal{P} = F^{\mu\alpha} F_{\mu\beta} p_{\alpha} p^{\beta}. \quad (\text{G.8})$$

With this, it is very straightforward to calculate the flow. The result reads

$$\frac{1}{2} \text{STr} [G \cdot \partial_t \mathfrak{R}] = \frac{1}{2} \int \frac{d^4 p}{(2\pi)^4} \frac{p^3}{p^2 V'(\mathcal{F}) + \mathfrak{R}(p^2)} \left( 3 - \frac{\mathcal{P} V''(\mathcal{F})}{p^2 V'(\mathcal{F}) + \mathcal{P} V''(\mathcal{F}) + \mathfrak{R}(p^2)} \right) \partial_t \mathfrak{R}(p^2). \quad (\text{G.9})$$

Now, we have to make sense out of this, since  $\mathcal{P}$  also contains the loop momentum  $p$ . For this, we will assume that we can expand the integrand in  $\mathcal{P}$  in a Taylor series, manipulate the resulting expression, and resum it<sup>15</sup>. We thus have to calculate

$$\int d^d p g(p) \mathcal{P}^n \quad (\text{G.10})$$

for a general function  $g(p)$ . Using the definition of  $\mathcal{P}$ , we can boil this down to the task of determining

$$\int d^d p g(p) p_{\mu_1} \cdots p_{\mu_{2n}}. \quad (\text{G.11})$$

By Lorentz invariance, the tensor structure must be proportional to the product of  $n$  fully symmetrised metrics, *i.e.*

$$\int d^d p g(p) p_{\mu_1} \cdots p_{\mu_{2n}} = \alpha_n \eta_{(\mu_1 \mu_2} \cdots \eta_{\mu_{2n-1} \mu_{2n})} \int d^d p g(p) p^{2n}. \quad (\text{G.12})$$

Multiplying this equation with  $n$  fully symmetrised metrics, one can determine the constants  $\alpha_n$ . They come out to be

$$\alpha_n = \frac{(2n-1)!! (d-2)!!}{(d+2(n-1))!!}. \quad (\text{G.13})$$

The next step is the evaluation of the tensor contractions. For this, let  $T^{\mu\nu}$  be an arbitrary

---

<sup>15</sup>Alternatively, if the eigenvalues of the matrix are known, one can also perform the angular integration over the loop momentum.

tensor. Then,

$$T^{\mu_1\mu_2} \dots T^{\mu_{2n-1}\mu_{2n}} \eta_{(\mu_1\mu_2} \dots \eta_{\mu_{2n-1}\mu_{2n})} = \frac{2^n}{(2n-1)!!} B_n \left( \frac{0!}{2} \tau_1, \frac{1!}{2} \tau_2, \dots, \frac{(n-1)!}{2} \tau_n \right). \quad (\text{G.14})$$

Here,  $B_n$  are the complete Bell polynomials, and by  $\tau_n$  we mean the traces of the covariant  $n$ -cycles of  $T$ ,  $\text{tr}((T \cdot^\mu \eta_\mu)^n)$ . Combining these results, we arrive at

$$\int d^d p g(p) (p_\mu p_\nu T^{\mu\nu})^n = \frac{2^n (d-2)!!}{(d+2(n-1))!!} B_n \int d^d p g(p) p^{2n} = \frac{1}{\left(\frac{d}{2}\right)_n} B_n \int d^d p g(p) p^{2n}, \quad (\text{G.15})$$

where we suppress the arguments of  $B_n$  which are the same as above, and  $(x)_n = \Gamma(x+n)/\Gamma(x)$  is the Pochhammer symbol. To evaluate the Bell polynomials, we can use their exponential generating function,

$$\exp \left( \sum_{n=1}^{\infty} \frac{a_n}{n!} x^n \right) = \sum_{n=0}^{\infty} \frac{B_n(a_1, \dots, a_n)}{n!} x^n. \quad (\text{G.16})$$

With the arguments as above, it turns out that the left-hand side evaluates to

$$\exp \left( \sum_{n=1}^{\infty} \frac{a_n}{n!} x^n \right) = \exp \left( \frac{1}{2} \text{tr} \sum_{n=1}^{\infty} \frac{1}{n} (xT)^n \right) = \exp \left( -\frac{1}{2} \text{tr} \ln(\mathbb{1} - xT) \right) = [\det(\mathbb{1} - xT)]^{-1/2}. \quad (\text{G.17})$$

The complete Bell polynomials are thus proportional to the coefficients of the Taylor series of this expression in  $x$  around zero. Without loss of generality, we can assume that  $T$  is traceless<sup>16</sup>. In four dimensions, we have

$$\det(\mathbb{1} - xT) = 1 - \frac{1}{2} \tau_2 x^2 - \frac{1}{3} \tau_3 x^3 + (\det T) x^4. \quad (\text{G.18})$$

If we neglect the dependence on the determinant, the Taylor series can be calculated explicitly. A lengthy calculation gives the result

$$\frac{1}{\sqrt{1 - \frac{\tau_2}{2} x^2 - \frac{\tau_3}{3} x^3}} = \sum_{n=0}^{\infty} \frac{\left(\frac{\tau_2}{2}\right)^{n/2} \mathbf{i}^n}{\left(\frac{n-3\mu}{2}\right)!} \pi \left( \frac{\sqrt{2}\tau_3}{3\mathbf{i}\tau_2^{3/2}} \right)^\mu x^n \times {}_3F_2^{\text{reg}} \left( \frac{2+\mu-n}{6}, \frac{4+\mu-n}{6}, \frac{7\mu-n}{6}; \mu + \frac{1}{2}, \frac{1+\mu-n}{2} \middle| \frac{6\tau_3^2}{\tau_2^3} \right), \quad (\text{G.19})$$

where  $\mu = n \bmod 2$  and  ${}_3F_2^{\text{reg}}$  is the regularised generalised hypergeometric function.

To apply this knowledge to the case of the four-dimensional  $U(1)$  gauge theory, we further

<sup>16</sup>If it is not traceless, decompose it into trace and traceless part. In the scalar  $\mathcal{P}$ , only the traceless part has nontrivial angular dependence.

need the identities [433]

$$F^{\mu\alpha}\tilde{F}^\nu{}_\alpha = \tilde{F}^{\mu\alpha}F^\nu{}_\alpha = \mathcal{G}\eta^{\mu\nu}, \quad (\text{G.20})$$

$$\tilde{F}^{\mu\alpha}\tilde{F}^\nu{}_\alpha = F^{\mu\alpha}F^\nu{}_\alpha - 2\mathcal{F}\eta^{\mu\nu}, \quad (\text{G.21})$$

from which we can derive

$$F^\rho{}_\mu F^\mu{}_\alpha F^{\alpha\nu} = -2\mathcal{F}F^{\rho\nu} - \mathcal{G}\tilde{F}^{\rho\nu}. \quad (\text{G.22})$$

With this, we can calculate the coefficients of the  $n$ -th power of the field strength tensor,

$$(F^n)^{\mu\nu} = a_n\eta^{\mu\nu} + b_n F^{\mu\nu} + c_n \tilde{F}^{\mu\nu} + d_n (F^2)^{\mu\nu}. \quad (\text{G.23})$$

Multiplying by another field strength tensor, we can derive a recursion for the coefficients  $a_n$  to  $d_n$ . At the end, we are interested in the trace of  $F^n$ , *i.e.*

$$\eta_{\mu\nu}(F^n)^{\mu\nu} = 4a_n - 4\mathcal{F}d_n. \quad (\text{G.24})$$

For odd  $n$ , they clearly vanish due to the antisymmetry of  $F$ . For even  $n = 2k$ , we get

$$\eta_{\mu\nu}(F^n)^{\mu\nu} = 2 \left[ \left( -\mathcal{F} - \sqrt{\mathcal{F}^2 + \mathcal{G}^2} \right)^k + \left( -\mathcal{F} + \sqrt{\mathcal{F}^2 + \mathcal{G}^2} \right)^k \right] = 2(-2\mathcal{F})^k + \mathcal{O}(\mathcal{G}). \quad (\text{G.25})$$

In the case of  $T = -F^2$ , we can evaluate (G.17) exactly, giving

$$\exp \left( \sum_{n=1}^{\infty} \frac{a_n}{n!} x^n \right) = \frac{1}{1 - 2\mathcal{F}x - \mathcal{G}^2 x^2} = \sum_{n=0}^{\infty} \frac{(\mathcal{F} + \sqrt{\mathcal{F}^2 + \mathcal{G}^2})^{n+1} - (\mathcal{F} - \sqrt{\mathcal{F}^2 + \mathcal{G}^2})^{n+1}}{2\sqrt{\mathcal{F}^2 + \mathcal{G}^2}} x^n, \quad (\text{G.26})$$

and thus we can read off the complete Bell polynomials.

Now, we are finally in the position to write the flow (G.9) into a form which we can evaluate. Expanding it in  $\mathcal{P}$ , and using all the results just obtained, finally resumming the series yields

$$\frac{1}{2} \text{STr} [G \cdot \partial_t \mathfrak{R}] = \frac{1}{16\pi^2} \int_0^\infty dp \left[ \frac{2p^3}{p^2 V'(\mathcal{F}) + \mathfrak{R}(p^2)} + \frac{p \ln \left( 1 + \frac{2p^2 \mathcal{F} V''(\mathcal{F})}{p^2 V'(\mathcal{F}) + \mathfrak{R}(p^2)} \right)}{2\mathcal{F} V''(\mathcal{F})} \right] \partial_t \mathfrak{R}(p^2). \quad (\text{G.27})$$

Rather miraculously, the whole calculation can be done with both invariants until the very end. The resulting expression is lengthy, and we won't report it here.



# Appendix H.

## Clifford algebra

Here, we will fix our conventions on the Clifford algebra used in the nonsupersymmetric Gross-Neveu-Yukawa model in section 5.2. We stick to the spin-base invariant formulation [434–436]. Dirac conjugation is given by

$$\bar{\psi} = \psi^\dagger h, \quad (\text{H.1})$$

with an antihermitian spin metric  $h$ . In this convention, the product  $\bar{\psi}\psi$  is real. Furthermore, we want the kinetic term of the fermions to be real. This implies

$$\gamma_\mu^\dagger = h\gamma_\mu(h^\dagger)^{-1} \equiv -h\gamma_\mu h^{-1}. \quad (\text{H.2})$$

Finally, the actual Clifford algebra is taken as

$$\{\gamma_\mu, \gamma_\nu\} = 2\eta_{\mu\nu}. \quad (\text{H.3})$$

With this, one can list all possible products of Dirac matrices ( $\bar{\gamma} = \gamma_0\gamma_1\gamma_2, [\gamma_\mu, \gamma_\nu] = 2\Sigma_{\mu\nu}$ ):

$$\begin{aligned} \gamma_\mu\gamma_\nu &= \eta_{\mu\nu}\mathbb{1} + \Sigma_{\mu\nu}, \\ \gamma_\rho\Sigma_{\mu\nu} &= \eta_{\mu\rho}\gamma_\nu - \eta_{\nu\rho}\gamma_\mu + \epsilon_{\rho\mu\nu}\bar{\gamma}, \\ \gamma_\mu\bar{\gamma} &= \frac{1}{2}\epsilon_{\mu\nu\rho}\Sigma^{\nu\rho}, \\ \Sigma_{\mu\nu}\gamma_\rho &= \eta_{\nu\rho}\gamma_\mu - \eta_{\mu\rho}\gamma_\nu + \epsilon_{\mu\nu\rho}\bar{\gamma}, \\ \Sigma_{\mu\nu}\bar{\gamma} &= -\epsilon_{\mu\nu\rho}\gamma^\rho, \\ \Sigma_{\mu\nu}\Sigma_{\alpha\beta} &= \Sigma_{\alpha\mu}\eta_{\beta\nu} + \Sigma_{\beta\nu}\eta_{\alpha\mu} - \Sigma_{\alpha\nu}\eta_{\beta\mu} - \Sigma_{\beta\mu}\eta_{\alpha\nu} - (\eta_{\mu\alpha}\eta_{\nu\beta} - \eta_{\mu\beta}\eta_{\nu\alpha})\mathbb{1}, \\ \bar{\gamma}\Sigma_{\mu\nu} &= -\epsilon_{\mu\nu\rho}\gamma^\rho, \\ \bar{\gamma}\gamma_\mu &= \frac{1}{2}\epsilon_{\mu\nu\rho}\Sigma^{\nu\rho}, \\ \bar{\gamma}\bar{\gamma} &= -\mathbb{1}. \end{aligned} \quad (\text{H.4})$$

Notice that in these conventions, no explicit factors of  $\mathbf{i}$  appear.

# Appendix I.

## Supersymmetric quantum mechanics

In this appendix, we present results on supersymmetric quantum mechanics, in particular spontaneous breaking of supersymmetry. The results are published in [156].

In order to derive the flow equations for supersymmetric quantum mechanics, we employ the superfield formalism [437]. For more details we refer the reader to [380]. The Euclidean superfield, expanded in terms of the anticommuting Grassmann variables  $\theta$  and  $\bar{\theta}$ , reads

$$\Phi = \chi + \bar{\theta}\psi + \bar{\psi}\theta + \bar{\theta}\theta F. \quad (\text{I.1})$$

Both the superfield and the Grassmann variables  $\theta, \bar{\theta}$  have mass dimension  $-1/2$ . Next, we introduce the superpotential and expand it in powers of the Grassmann variables,

$$W(\Phi) = W(\chi) + (\bar{\theta}\psi + \bar{\psi}\theta) W'(\chi) + \bar{\theta}\theta (FW'(\chi) - W''(\chi)\bar{\psi}\psi). \quad (\text{I.2})$$

The one-dimensional equivalent of the super-Poincaré algebra contains only translations of Euclidean time and is generated by one pair of conserved nilpotent fermionic supercharges  $\mathcal{Q} = \mathbf{i}\partial_{\bar{\theta}} + \theta\partial_{\tau}$  and  $\bar{\mathcal{Q}} = \mathbf{i}\partial_{\theta} + \bar{\theta}\partial_{\tau}$ . The anticommutator of them is the super-Hamiltonian  $\mathcal{H}$ ,

$$\{\mathcal{Q}, \bar{\mathcal{Q}}\} = 2\mathcal{H}, \quad [\mathcal{H}, \mathcal{Q}] = [\mathcal{H}, \bar{\mathcal{Q}}] = 0. \quad (\text{I.3})$$

Supersymmetry variations are generated by  $\delta_{\epsilon} = \bar{\epsilon}\mathcal{Q} - \epsilon\bar{\mathcal{Q}}$ . We may easily read off the following transformation rules of the component fields

$$\delta\chi = \mathbf{i}\bar{\epsilon}\psi - \mathbf{i}\bar{\psi}\epsilon, \quad \delta\psi = (\dot{\chi} - \mathbf{i}F)\epsilon, \quad \delta\bar{\psi} = \bar{\epsilon}(\dot{\chi} + \mathbf{i}F), \quad \delta F = -\bar{\epsilon}\dot{\psi} - \dot{\bar{\psi}}\epsilon, \quad (\text{I.4})$$

by acting with the supersymmetry variations on the superfield:

$$\delta_{\epsilon}\Phi = \bar{\epsilon}(\mathbf{i}\psi + \mathbf{i}\theta F + \theta\dot{\chi} - \bar{\theta}\theta\dot{\psi}) - (\mathbf{i}\bar{\psi} + \mathbf{i}\bar{\theta}F - \bar{\theta}\dot{\chi} + \bar{\theta}\theta\dot{\bar{\psi}})\epsilon. \quad (\text{I.5})$$

Here and in the following, a dot denotes differentiation w.r.t.  $\tau$ , the quantum-mechanical time variable. In order to obtain a supersymmetric action, we further need the supercovariant

derivatives  $\mathcal{D} = \mathbf{i}\partial_{\bar{\theta}} - \theta\partial_{\tau}$  and  $\bar{\mathcal{D}} = \mathbf{i}\partial_{\theta} - \bar{\theta}\partial_{\tau}$ .

The anticommutation relations they satisfy are almost identical to those of the supercharges,

$$\{\mathcal{D}, \mathcal{D}\} = \{\bar{\mathcal{D}}, \bar{\mathcal{D}}\} = 0 \quad \text{and} \quad \{\mathcal{D}, \bar{\mathcal{D}}\} = -2H. \quad (\text{I.6})$$

They further anticommute with the supercharges. With these definitions, one can write down the supersymmetric Euclidean off-shell action within the superfield formalism:

$$\begin{aligned} S[\chi, F, \bar{\psi}, \psi] &= \int d\tau d\theta d\bar{\theta} \left[ -\frac{1}{2}\Phi\mathcal{K}\Phi + \mathbf{i}W(\Phi) \right] \\ &= \int d\tau \left[ \frac{1}{2}\dot{\chi}^2 - \mathbf{i}\bar{\psi}\dot{\psi} + \mathbf{i}FW'(\chi) - \mathbf{i}\bar{\psi}W''(\chi)\psi + \frac{1}{2}F^2 \right], \end{aligned} \quad (\text{I.7})$$

where we introduced the kinetic operator

$$\mathcal{K} = \frac{1}{2}(\bar{\mathcal{D}}\mathcal{D} - \mathcal{D}\bar{\mathcal{D}}). \quad (\text{I.8})$$

Eliminating the auxiliary field  $F$  by its equation of motion,  $F = -\mathbf{i}W'$ , we obtain the on-shell action

$$S_{\text{on}}[\chi, \psi, \bar{\psi}] = \int d\tau \left[ \frac{1}{2}\dot{\chi}^2 - \mathbf{i}\bar{\psi}\dot{\psi} + \frac{1}{2}W'^2(\chi) - \mathbf{i}W''(\chi)\bar{\psi}\psi \right]. \quad (\text{I.9})$$

From (I.9) we read off the bosonic potential  $V(\chi) = \frac{1}{2}W'^2(\chi)$  and the Yukawa term  $W''(\chi)\bar{\psi}\psi$ . If supersymmetry is unbroken, the ground state energy vanishes.

Let us assume the superpotential  $W(\chi)$  to be a polynomial in the scalar field. Then, the global properties of the superpotential  $W(\chi) \sim \chi^n$  for large  $\chi$  determine whether spontaneous breaking of supersymmetry occurs or not. If  $n$  is even, supersymmetry will be intact on all scales. This is realised, *e.g.*, for quartic classical superpotentials

$$W(\chi) = e\chi + \frac{m}{2}\chi^2 + \frac{g}{3}\chi^3 + \frac{a}{4}\chi^4, \quad (\text{I.10})$$

which we will consider in section I.2.2.  $W(\chi)$  represents the microscopic superpotential, *i.e.* the initial potential of our quantum system before fluctuations are taken into account. If  $n$  is odd, the effective potential exhibits a ground state with positive energy and supersymmetry is spontaneously broken, even if we may start with a microscopic potential with vanishing ground state energy. This applies, *e.g.*, to cubic classical superpotentials of the form

$$W(\chi) = e\chi + \frac{g}{3}\chi^3, \quad e < 0, g > 0, \quad (\text{I.11})$$

which will be discussed in detail in section I.3.

## I.1. Flow equation in superspace

The flow equation in superspace reads

$$\partial_t \Gamma = \frac{1}{2} \text{STr} (G \partial_t \mathfrak{R}) = \frac{1}{2} \int dz dz' G(z, z') \partial_t \mathfrak{R}(z', z), \quad G = (\Gamma^{(2)} + \mathfrak{R})^{-1}, \quad (\text{I.12})$$

where  $z = (\tau, \theta, \bar{\theta})$  denotes the coordinates in superspace. Therein the second functional derivative with respect to the superfield  $\Gamma^{(2)}$  is given by

$$\Gamma^{(2)}(z, z') = \frac{\overrightarrow{\delta}}{\delta \Phi(z)} \Gamma \frac{\overleftarrow{\delta}}{\delta \Phi(z')}. \quad (\text{I.13})$$

Note that the supertrace as well as the right and left derivatives take care of the minus signs for anticommuting variables.

### I.1.1. Supercovariant derivative expansion in NNLO

We employ the expansion of  $\Gamma$  in powers of the supercovariant derivatives  $\mathcal{D}$  and  $\bar{\mathcal{D}}$  with mass dimension 1/2. Unfortunately, a systematic and consistent expansion scheme of  $\Gamma$  does not guarantee convergence. One goal of the present calculation is to demonstrate the convergence of the supercovariant derivative expansion at NNLO to numerically known values of observables. We will derive the flow equation in the off-shell formulation with a manifestly supersymmetric regulator such that in each order of the supercovariant derivative expansion the flow preserves supersymmetry.

To this order, the most general ansatz for the scale dependent effective action reads

$$\Gamma[\Phi] = \int dz \left[ \mathbf{i} W(\Phi) - \frac{1}{2} Z(\Phi) \mathcal{K} Z(\Phi) + \frac{\mathbf{i}}{4} Y_1(\Phi) \mathcal{K}^2 \Phi + \frac{\mathbf{i}}{4} Y_2(\Phi) (\mathcal{K} \Phi) (\mathcal{K} \Phi) \right], \quad (\text{I.14})$$

with the scale and field dependent functions  $W, Z, Y_1$  and  $Y_2$  and the kinetic operator  $\mathcal{K}$  introduced in (I.8). A contribution to  $\Gamma$  where the derivatives act on three superfields,  $Y_3(\bar{\mathcal{D}}\Phi)(\mathcal{D}\Phi)(\mathcal{K}\Phi)$ , is already included in our truncation, since

$$\int dz A(\Phi) \mathcal{K}^2 \Phi = \int dz \left[ A'(\Phi) (\mathcal{K}\Phi) (\mathcal{K}\Phi) + A''(\Phi) (\bar{\mathcal{D}}\Phi) (\mathcal{D}\Phi) (\mathcal{K}\Phi) \right]. \quad (\text{I.15})$$

Terms with  $\mathcal{D}, \bar{\mathcal{D}}$  acting on four superfields do not exist since  $(\bar{\mathcal{D}}\Phi \mathcal{D}\Phi)^2 = 0$ . In component

fields the action (I.14) takes the form<sup>17</sup>

$$\begin{aligned} \Gamma[\Phi] = \int d\tau & \left[ \frac{1}{2} Z'^2 \dot{\chi}^2 - \mathbf{i} Z'^2 \bar{\psi} \dot{\psi} - \frac{\mathbf{i}}{2} (Y_1' + Y_2) \dot{\psi} \psi - \mathbf{i} \left( W'' + Z' Z'' \dot{\chi} - \frac{1}{2} Y_1'' \ddot{\chi} - \frac{1}{4} Y_1''' \dot{\chi}^2 \right) \bar{\psi} \psi \right. \\ & + \left( \mathbf{i} W' - Z' Z'' \bar{\psi} \psi - \frac{\mathbf{i}}{2} (Y_1' + Y_2) \ddot{\chi} - \frac{\mathbf{i}}{4} Y_1'' \dot{\chi}^2 + \frac{1}{2} Y_2' \left( \bar{\psi} \dot{\psi} - \dot{\bar{\psi}} \psi \right) \right) F \\ & \left. + \left( \frac{1}{2} Z'^2 - \frac{\mathbf{i}}{4} Y_2'' \bar{\psi} \psi \right) F^2 + \frac{\mathbf{i}}{4} Y_2' F^3 \right], \end{aligned} \quad (\text{I.16})$$

where the terms are ordered according to increasing powers of the auxiliary field  $F$ .

### I.1.2. Supersymmetric regulator functional

The flow of  $\Gamma$  is regularised by adding a suitable regulator functional  $\Delta S$  to the action. Given a supersymmetric truncation  $\Gamma$  and a supersymmetric initial condition, we only need a supersymmetric regulator in order to construct a manifestly supersymmetric flow. Following [378–380], the most general off-shell supersymmetric cutoff action quadratic in the superfields can be written as

$$\Delta S = \frac{1}{2} \int dz \Phi \mathfrak{R}(\mathcal{D}, \bar{\mathcal{D}}) \Phi. \quad (\text{I.17})$$

As  $\mathcal{D}$  and  $\bar{\mathcal{D}}$  satisfy the anticommutation relation (I.6), it can be written as

$$\Delta S = \frac{1}{2} \int dz \Phi \left[ \mathbf{i} r_1(-\partial_\tau^2) - Z'^2(\bar{\Phi}) r_2(-\partial_\tau^2) \mathcal{K} \right] \Phi, \quad (\text{I.18})$$

where  $Z'$  is evaluated at the background field  $\bar{\Phi} = \bar{\chi}$ . The flow equations are derived and shown explicitly in [156], and we will not reproduce them here, as not so much can be learned from their explicit form.

The regulator function  $r_1$  with mass dimension 1 acts like an additional momentum dependent mass and ensures a gap  $\sim k$  for the IR modes. Note that we do not spectrally adjust this regulator function by multiplying it with the wave function renormalisation as has been done in [380]. The latter approach would actually slow down the flow of the higher order operators  $Z, Y_1, Y_2$ . The dimensionless regulator function  $r_2$  can be viewed as a deformation of the momentum dependence of the kinetic term. The term  $q^2 r_2(q^2/k^2)$  represents the supersymmetric analogue of the corresponding regulator function  $r(q^2/k^2)$  in scalar field theory [215]. Here, a spectral adjustment via the inclusion of the wave function renormalisation  $Z'(\bar{\Phi})$  is helpful in order to provide a simple form for the flow of  $\Gamma$  [226]. We did check the influence of the spectral adjustment on the flow of  $\Gamma$  carefully.

<sup>17</sup>From now on, we suppress the explicit field dependence.

## I.2. Effective potential and first excited energy

The low lying energies can be extracted from the bosonic on-shell effective potential  $V_{\text{eff}} = V_{k=0}$ . In order to compute  $V$ , we set the fermionic fields to zero in the truncated effective average action (I.16).

### I.2.1. On-shell effective potential

At a given scale, the auxiliary field  $F$  fulfills the equation of motion

$$F = -\frac{2\mathbf{i}}{3Y} \left( \sqrt{Z'^4 + \frac{3}{4}(4W' - 2X\ddot{\chi} - (X' - Y)\dot{\chi}^2)Y - Z'^2} \right), \quad (\text{I.19})$$

and hence becomes dynamical, in contrast to the situation in the NLO approximation. Next, we eliminate the auxiliary field in the bosonic action by its equation of motion. To calculate the effective potential  $V_{\text{eff}}$ , it is sufficient to consider  $\Gamma$  for constant  $\chi$  in which case

$$V(\chi) = \frac{2}{27Y^2} \left( \sqrt{3W'Y + Z'^4} - Z'^2 \right) \left( 6W'Y + Z'^4 - Z'^2 \sqrt{3W'Y + Z'^4} \right). \quad (\text{I.20})$$

We determine the energy of the first excited state  $E_1$  from the propagator  $G$  at vanishing  $k$ , where the regulator  $\mathfrak{R}$  vanishes. Supersymmetry is unbroken if the potential  $V$  in (I.20) vanishes at its minimum  $\chi_{\text{min}}$ , which is the case if  $W'(\chi_{\text{min}}) = 0$ . Actually, in the strong coupling regime there exists a second solution for which  $[4W'(Y + Z'^4)](\chi_{\text{min}}) = 0$ . However, we believe this solution to be unphysical, see subsection I.2.2.

For a constant  $\chi_{\text{min}}$ , the auxiliary field  $F$  in (I.19) vanishes if  $W'(\chi_{\text{min}}) = 0$ . Thus, we determine the excited energies  $E_1$  by considering the propagator for constant fields  $\chi$  and  $W' = F = 0$ . After an integration over the Grassmann variables, we obtain

$$G(q, \theta, \theta')|_{\bar{\theta}\theta\bar{\theta}'\theta'} = \frac{Z'^2 q^2}{Z'^4 q^2 + (W'' + 1/2Xq^2)^2}. \quad (\text{I.21})$$

The square of the excited energy  $E_1^2$  is then given by the pole of the propagator at the minimum of the effective potential:

$$\lim_{k \rightarrow 0} \left( Z'^4 q_0^2 + \left( W'' + \frac{1}{2}Xq_0^2 \right)^2 \right) \Big|_{\chi_{\text{min}}} = 0 \quad \text{with} \quad q_0^2 = (\mathbf{i}E_1)^2. \quad (\text{I.22})$$

This equation possesses the two solutions

$$E_1^2 = \lim_{k \rightarrow 0} \frac{2}{X^2} \left( Z'^4 + XW'' \pm Z'^2 \sqrt{Z'^4 + 2XW''} \right) \Big|_{\chi_{\text{min}}}, \quad (\text{I.23})$$

where the solution with the negative sign is the correct one, since it reduces to the known limiting value  $E_1 = |W''(\chi_{\text{min}})|$  in the LPA approximation with  $Z' = 1$  and  $X = 0$ . The

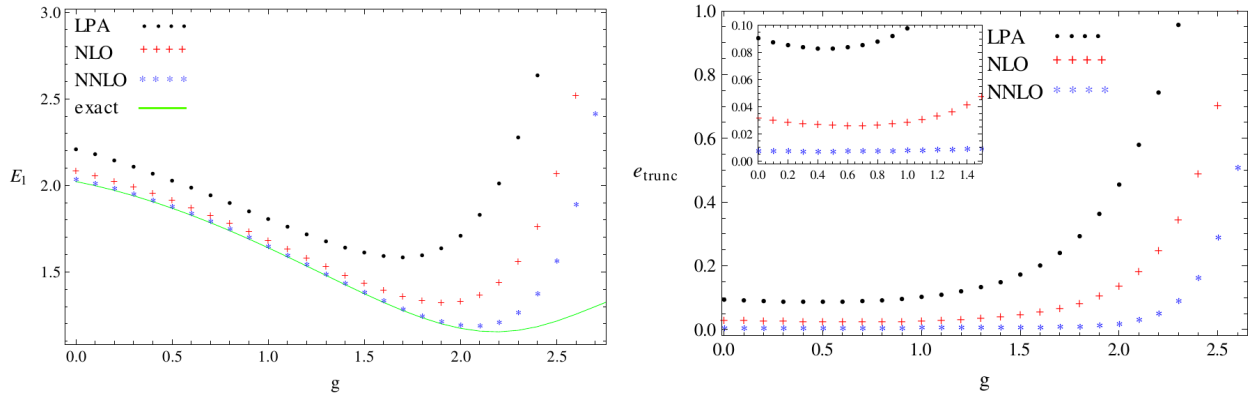


Fig. I.1.: Energy gap  $E_1(g)$  and relative error  $e_{\text{trunc}}$  for classical superpotentials of the form  $W'_\Lambda(\chi) = 1 + \chi + g\chi^2 + \chi^3$  and various  $g$ . For convex initial potentials ( $g < \sqrt{3}$ ) we achieve a nice convergence as well as a relative error of 1% in NNLO. For couplings larger than  $g \approx 2$ , where the classical potential becomes nonconvex, we observe significant deviations from the exact results.

other solution with positive sign diverges in this limit.

Note that if supersymmetry is spontaneously broken,  $W'(\chi_{\min}) \neq 0$  and the corresponding auxiliary field  $F$  does not vanish. Then the first excited energy  $E_1$  is extracted from the pole of the general propagator, *i.e.* of

$$\lim_{k \rightarrow 0} G(q, \theta, \theta')|_{\bar{\theta}\theta \bar{\theta}'\theta'} \quad (\text{I.24})$$

at the (constant) minimum  $\chi_{\min}$  of the potential, where  $F$  has to be replaced by its equation of motion (I.19).

## I.2.2. Numerical results

To obtain numerical results, we specify the regulator functions and choose  $r_2(q^2, k) = 0$  and the Callan-Symanzik regulator  $r_1(q^2, k) = k$ . Then there is no dependence on the background field. We stress that the right hand side of the flow equations only depends via  $W''$  and  $W'''$  on the superpotential. The corresponding microscopic action in the UV is given by (I.9) and we focus on quartic superpotentials of the form (I.10). Thus, the initial conditions for the flow at  $k = \Lambda$  read

$$W'_\Lambda(\chi) = e + m\chi + g\chi^2 + a\chi^3, \quad Z'_\Lambda(\chi) = 1, \quad Y_\Lambda(\chi) = X_\Lambda(\chi) = 0. \quad (\text{I.25})$$

In supersymmetric quantum mechanics the fluctuations in the UV are suppressed and the flow freezes out for  $k \rightarrow \Lambda \rightarrow \infty$ . Hence the initial conditions are stable for large UV cutoffs. Indeed, plugging (I.25) into the flow equations yields

$$\partial_k W'|_\Lambda = O(\Lambda^{-2}), \quad \partial_k Z'|_\Lambda = O(\Lambda^{-4}), \quad \partial_k X|_\Lambda = O(\Lambda^{-5}), \quad \partial_k Y|_\Lambda = O(\Lambda^{-6}). \quad (\text{I.26})$$

$g$	$E_1^{\text{LPA}}$	$E_1^{\text{NLO}}$	$E_1^{\text{NNLO}}$	$E_1^{\text{ex}}$
0.0	2.202	2.086	2.038	2.022
0.2	2.136	2.028	1.986	1.970
0.4	2.061	1.957	1.920	1.905
0.6	1.978	1.876	1.842	1.827
0.8	1.889	1.784	1.752	1.738
1.0	1.797	1.687	1.653	1.639
1.2	1.709	1.584	1.547	1.534
1.4	1.632	1.486	1.440	1.426
1.6	1.583	1.398	1.337	1.323
1.8	1.590	1.339	1.250	1.235
2.0	1.702	1.337	1.199	1.173
2.2	2.005	1.442	1.216	1.153
2.4	2.627	1.764	1.378	1.183
2.6	3.661	2.525	1.895	1.254
2.8	4.988	3.961	3.195	1.343

Tab. I.1.: Energy  $E_1^{\text{NNLO}}$  of the first excited state, calculated according to (I.23) for  $r_1 = k$ ,  $e = m = a = 1$  and various  $g$ . For comparison, also the results  $E_1^{\text{LPA}}$  obtained in LPA,  $E_1^{\text{NLO}}$  derived in NLO as well as the exact values  $E_1^{\text{ex}}$  from numerically diagonalising the Hamiltonian are given. Here,  $E_1^{\text{LPA}}$ ,  $E_1^{\text{NLO}}$  and  $E_1^{\text{NNLO}}$  were derived by solving the respective partial differential equations numerically.

For  $W'_\Lambda$  in (I.25) supersymmetry remains unbroken at all scales. Note that the initial superpotential  $W_\Lambda$  is nonconvex if  $g^2 > 3ma$ . Besides, we may shift the field  $\chi \rightarrow \chi - g/(3a)$  such that the quadratic term of  $W'_\Lambda$  vanishes.

We solved the set of the four coupled partial differential equations for  $W'$ ,  $Z'$ ,  $X$ ,  $Y$  numerically with pseudo-spectral methods. Besides, we repeated the calculations with the implicit Runge-Kutta method of NDSolve of Mathematica 9. In the latter case, we have chosen  $\chi \in (-100, 100)$  and kept the four functions at their classical values at the boundary for all scales, as the flows vanish for  $|\chi| \rightarrow \infty$ . With both methods we obtained the same results to three or four significant digits.

Table I.1 displays the energy gap  $E_1(g)$  for  $e = a = m = 1$  and various values of the coupling  $g$ . We also listed the resulting energies obtained by solving the PDEs in LPA as well as NLO.

Figure I.1 shows the first excited energies  $E_1$  (left figure) and the relative deviation from the exact values  $e_{\text{trunc}} = (E_1 - E_1^{\text{ex}})/E_1^{\text{ex}}$  (right figure) as a function of the coupling  $g$ . Obviously, an inclusion of terms of fourth order in the derivative expansion improves the results for the energy gap considerably. We obtain a relative error of  $< 1\%$  for couplings  $g < \sqrt{3}$ . For couplings  $\sqrt{3} < g < 2.3$  the relative deviations from the exact results lie within a 10% error.

Note that for couplings larger than  $g \approx 2$  the error increases exponentially and the supercovariant derivative approximation breaks down. The breakdown of the NNLO approximation



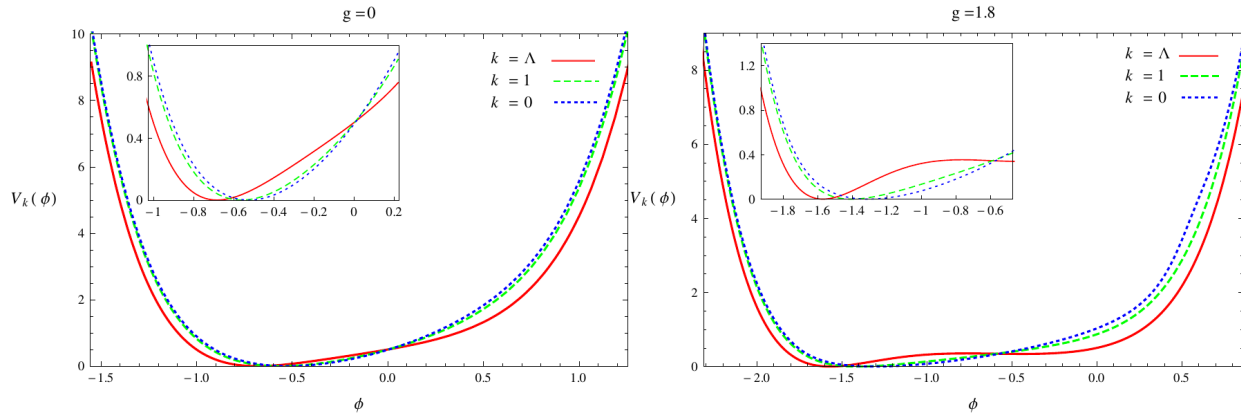


Fig. I.2.: Flow of the effective average potential  $V(\phi)$  as obtained by solving the system of PDEs numerically in NNLO in the derivative expansion with initial conditions (I.25), where  $e = m = a = 1$  and  $g = 0$  (left panel) and  $g = 1.8$  (right panel).

for couplings  $g \gtrsim 2$  is also indicated by the structure of the effective average potential. In this regime,  $V(\chi)$  becomes complex for all scales smaller than a  $k_0 > 0$  for field values close to the local minimum of  $W'_\Lambda$ . This is due to the expression  $\sqrt{3W'Y + Z'^4}$  appearing in (I.20) which becomes complex near the local minimum of  $W'_\Lambda$  for nonconvex initial potentials, owing to an increasingly negative  $Y$ ; see also Figure I.3 and Figure I.4. Another sign of the breakdown is given by the appearance of a further mass at  $g \approx 1.7$ , splitting in two masses for even larger couplings  $g$ . This is due to the formation of one/two further minima of the effective potential, where  $4W'Y + Z'^4|_{\chi_{\min}} = 0$  holds. Here, the fourth order correction  $Y$  is of the same order as the leading and next-to-leading order terms  $W'$  and  $Z'$  indicating the invalidity of the truncation. The corresponding masses become parametrically large. These large masses in the strong coupling regime are probably an artifact of the regularisation and have no physical significance. Similar artifacts have already been encountered in  $O(N)$ -symmetric Wess-Zumino models [383].

We thus observe a very good convergence of the derivative expansion in case of the local barrier of the classical potential being small. However, as the nonconvexity of  $V_\Lambda$  increases, tunneling events are exponentially suppressed and are no longer captured by the flow equations in the derivative expansion. Here, the inclusion of nonlocal operators should lead to a better convergence behaviour in the strong coupling regime.

The flow of the bosonic potential  $V(\chi)$  for  $g = 0$  and  $g = 1.8$  is depicted in Figure I.2. Apparently, nonconvexities appearing in the classical potential diminish as more and more long range quantum fluctuations are taken into account such that the effective potentials in Figure I.2 become convex<sup>18</sup>. Furthermore, Figure I.3 and Figure I.4 show the flow of  $W'$ ,  $Z'$ ,  $X$  and  $Y$  for  $g = 1.8$ . From (I.26) we infer the following deviation of the solutions at

<sup>18</sup>However, note that the structure of the flow equation forces rather the superpotential than the scalar potential to become convex in the IR. Since the scalar potential is a complicated function of  $W'$ ,  $Z'$ ,  $Y$ , *i.e.* of the form (I.20), the flow equation does not immediately imply  $V_{k \rightarrow 0}$  to be convex.

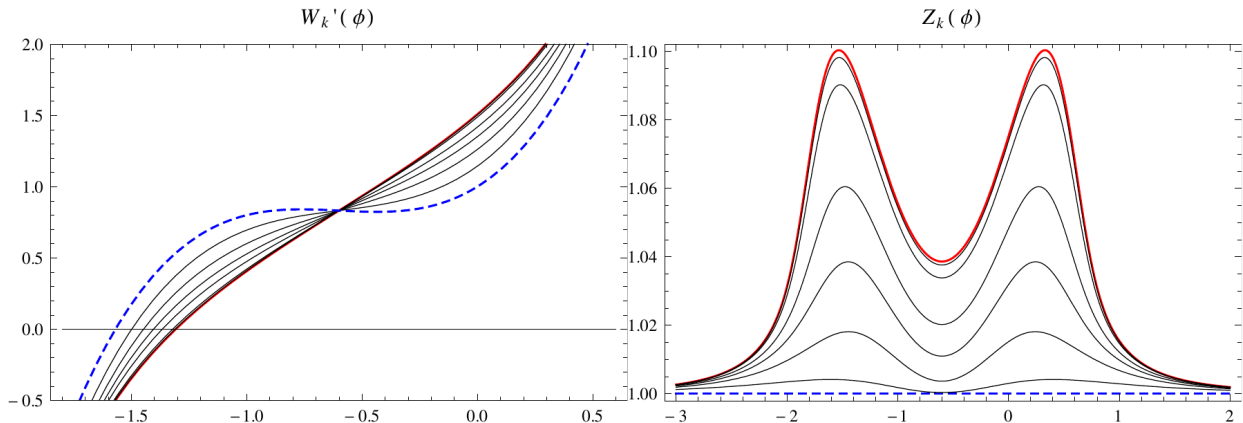


Fig. I.3.: The superpotential  $W'(\phi)$  and the wave function renormalisation  $Z'(\phi)$  for different scales  $k$ . Starting in the UV at  $k = \Lambda = 10^4$  (blue, dashed line) the flow evolves to the IR at  $k = 0$  (red solid line). The intermediate scales are  $k = 5, 2, 1, 0.5, 0.1, 0.02$ .

$k = 0$  from their classical values for large values of  $|\chi|$ :

$$W'_0 - W'_\Lambda \sim \frac{1}{2\chi}, \quad Z'_0 - Z'_\Lambda \sim \frac{1}{12\chi^4}, \quad X_0 - X_\Lambda \sim \frac{1}{18\chi^6}, \quad Y_0 - Y_\Lambda \sim -\frac{1}{9\chi^7}. \quad (\text{I.27})$$

As expected, the higher order operators show a faster decay for large field values, see Figure I.3 and Figure I.4.

### I.3. Supersymmetry breaking

If we choose the classical superpotential to be a polynomial of the form  $W'_\Lambda(\chi) \sim \mathcal{O}(\chi^n)$  with leading power  $n$  even, we expect spontaneous supersymmetry breaking to occur during the flow towards the IR [379, 438, 439]. It is known that spontaneous supersymmetry breaking is an IR effect, where the ground state is lifted to  $E_0 > 0$  [440].

#### I.3.1. Problems with the expansion in powers of $F$

In order to study breaking of supersymmetry within the FRG framework we focus on the  $\mathbb{Z}_2$  symmetric even function

$$W'_\Lambda(\chi) = e + g\chi^2, \quad e < 0, \quad g > 0. \quad (\text{I.28})$$

Then the RG flow preserves the symmetry and  $W'(\chi)$  will remain  $\mathbb{Z}_2$ -symmetric for all scales.

For unbroken supersymmetry we employed an expansion in the auxiliary field around  $F = 0$  to derive the flow equations in terms of the scalar fields  $\chi$ . However, this expansion point is inappropriate when supersymmetry is broken in which case the vacuum expectation value of the average field  $F$  does not vanish. The problem with expanding around  $F = 0$

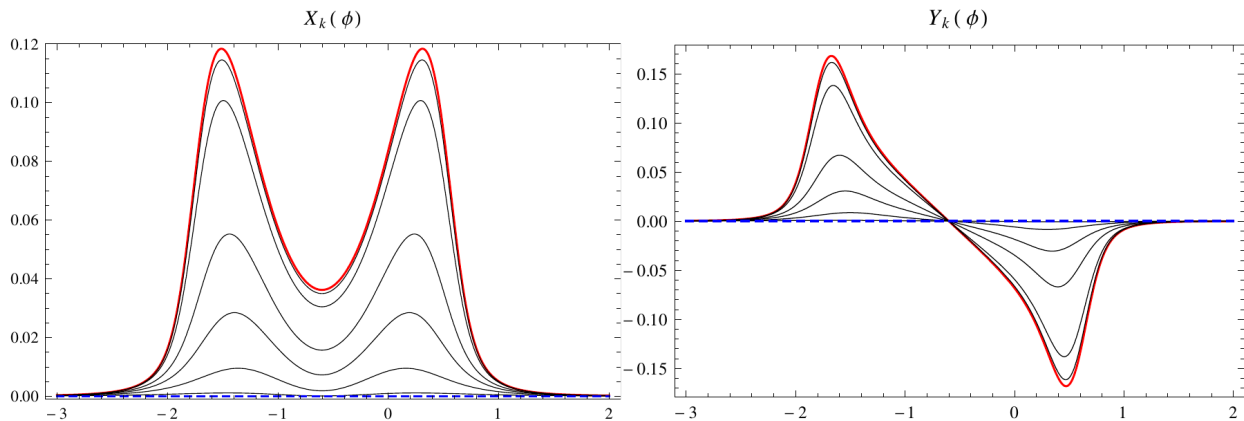


Fig. I.4.: The flow of the fourth order couplings  $X(\phi), Y(\phi)$  for different scales  $k$ . Starting in the UV at  $k = \Lambda = 10^4$  (blue, dashed line) the flow evolves to the IR at  $k = 0$  (red solid line). The intermediate scales are  $k = 5, 2, 1, 0.5, 0.1, 0.02$

can be seen already in the LPA where  $W''(\chi)$  represents a "mass term" in the denominator of the flow equation. Hence, the regulator  $r_1$  does not regularise since  $\mathcal{W}''(\chi) = W''(\chi) + k$  will vanish for some value(s) of  $\chi$ . This means that the RG equation detects the massless fermionic excitation - the Goldstino mode - associated with the spontaneous breaking of supersymmetry. This mode mediates between the two degenerate ground states at  $E_0 > 0$ , one in the bosonic and one in the fermionic sector [438]. Hence, at the minimum of  $V(\chi)$  the denominator in the flow equation simply contains the squared Goldstino mass  $m_G^2 = W''(0)^2 = 0$ . Thus, the flow of the superpotential diverges in the IR limit at the origin. This apparently leads to infinitely large excited energies, since  $E_1 = W'(0)W^{(3)}(0) > 0$  for broken supersymmetry. We find that this divergence occurs independently of the choice of the regulator  $r_2$  and of the order of truncation<sup>19</sup>.

Thus, we are lead to Taylor-expand in powers of  $F - F_0$  with finite  $F_0$ . We shall do this in NLO in the derivative expansion. First we consider the equation of motion for the auxiliary field in NLO, given by

$$F = -iW'(\chi)/Z'(\chi)^2. \quad (\text{I.29})$$

If supersymmetry is spontaneously broken,  $W'(\chi) > 0$  for all  $\chi$ . Again we observe that  $F$  assumes a finite vacuum expectation value implying a breakdown of the flow equation when  $W'$  ceases to have a zero. Now we expand around a nonzero auxiliary field - determined by its equation of motion - and rewrite the left-hand side of the flow equation as

$$\text{Flow} = iF\partial_t W' + \frac{1}{2}(\partial_t Z'^2)F^2 + \mathcal{O}(F^3)$$

<sup>19</sup>Of course, this IR problem represents a low dimensional issue as the divergences diminish with increasing dimension  $d$ , see [378, 379, 441].

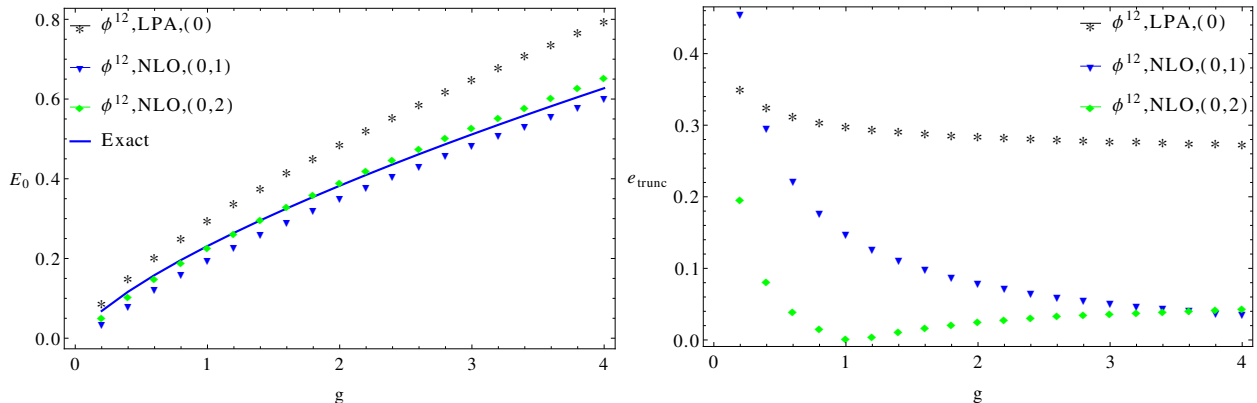


Fig. I.5.: Ground state energy  $E_0$  and its relative error  $e_{\text{trunc}}$  for initial potentials of the form  $W_\Lambda = -0.1 + \frac{g}{3}\phi^3$  as a function of  $g$  obtained via a polynomial expansion of  $W'(\phi)$  up to  $\phi^{12}$ . The brackets encode the projection scheme, *i.e.*  $(i, j)$  corresponds to a projection onto  $(F - F_0)^i$  and  $(F - F_0)^j$ .

$$\begin{aligned}
 &= \frac{W'(Z'\partial_t W' - W'\partial_t Z')}{Z'^3} + \mathbf{i} \left( \partial_t W' - \frac{2W'\partial_t Z'}{Z'} \right) (F - F_0) + Z'\partial_t(Z')(F - F_0)^2 + \dots \\
 &\text{with } F_0(\chi) = -\mathbf{i}W'(\chi)/Z'(\chi)^2.
 \end{aligned} \tag{I.30}$$

Obviously the term  $\mathcal{O}(F^3)$  will contribute to all orders around this new expansion point. Unfortunately, there is no unique projection onto the flows of  $W'$  and  $Z'$ . We may project onto the constant, the linear or the quadratic term in  $(F - F_0)$ . Hence, the system is overdetermined. Note that higher order terms contain no information about the flows of  $W'$  and  $Z'$ . Solving all three equations using an expansion of the right-hand side of the flow equation yields no consistent solution, since higher derivative operators contribute to these lower orders as well. To obtain a maximally self-consistent truncation it is therefore necessary to minimise these contributions. Assuming a nice convergence behaviour of the derivative expansion, it is sensible to project onto the lowest orders in  $(F - F_0)$ .

### I.3.2. Numerical results

In order to solve the flow equations for  $W'$  and  $Z'$  we now limit our discussion to the approximation of a uniform wave function renormalisation by setting  $Z'(\chi) = Z'$ . This corresponds to neglecting the field and momentum dependence of  $Z'$ . To analyse the flow of the effective average potential we proceed in two steps. First we start with a classical potential of the form (I.11) in the UV at  $k = \Lambda$ . Down to some scale  $k_0 > 0$ ,  $W'$  will have a zero. In this regime  $k \in (k_0, \Lambda)$  we employ the flow equations obtained by an expansion around  $F = 0$ . Starting with  $k_0$  down to the IR limit  $k = 0$  the scale dependence of  $W'$ ,  $Z'$  is determined by the flow equations derived via an expansion around  $F_0 \neq 0$ . As regulator functions we choose  $r_1 = 0$  and  $r_2 = (k^2/p^2 - 1)\theta(k^2 - p^2)$ . To calculate the ground state

energies  $E_0$  we expand  $W'$  in a Taylor series around  $\chi = 0$  up to some order and solve the system of coupled ODEs numerically. This is a sensible approach when  $W'$  becomes flat in the IR, because due to supersymmetry the physics happens at vanishing field, in contrast to for example  $O(N)$  models [382, 383], where the situation is exactly opposite: in the unbroken regime, the derivative of the potential is positive, whereas in the broken phase, one has a zero. As in the case of unbroken supersymmetry, we compare our results for  $E_0$  with the ones obtained by numerically diagonalising the Hamiltonian of the system.

Figure I.5 displays the ground state energies as well as the relative error  $e_{\text{trunc}}$  in LPA and NLO as obtained via two different projection methods. Here,  $(i, j)$  corresponds to a projection onto  $(F - F_0)^i$  and  $(F - F_0)^j$ .

Apparently, the results are significantly improved by including a constant wave function renormalisation. In particular, this applies to large couplings  $g$ , where the relative error is approximately 4%. Contrary to unbroken supersymmetry, the relative error increases with decreasing  $g$ . This originates from the fact that for decreasing  $g$  the minima of the potential drift apart and tunneling effects become effective, see [442].

In NLO, a  $(0, 2)$ -projection shows a smaller relative error than the  $(0, 1)$ -projection up to some  $g_{\text{max}} \approx 3.6$ , since the flow of  $Z'$  slows down when including the higher order term  $(F - F_0)^2$  resulting in a higher ground state energy  $E_0 = V(0) = W'(0)/Z'(0)^2$ . However, for large  $g > g_{\text{max}}$  the  $(0, 1)$ -projection leads to superior results. This may be due to a larger truncation error in  $(F - F_0)^2$  compared to  $(F - F_0)^1$  with increasing coupling  $g$ , originating from the missing higher order terms  $X, Y$  which are of importance there.



# Bibliography

- [1] *Scale of the Universe*, <http://scaleofuniverse.com/>, Accessed: 20/03/2017.
- [2] R. Munroe, *What If?: Serious Scientific Answers to Absurd Hypothetical Questions*, John Murray Publishers Ltd, 2015.
- [3] B. Odom, D. Hanneke, B. D’Urso, and G. Gabrielse, *New Measurement of the Electron Magnetic Moment Using a One-Electron Quantum Cyclotron*, Phys. Rev. Lett. **97** (3 July 2006), 030801, DOI: 10.1103/PhysRevLett.97.030801.
- [4] *unification, spacetime foam, quantum vacuum, quantum fluctuations*, <http://abyss.uoregon.edu/~js/ast123/lectures/lec17.html>, Accessed: 22/03/2017.
- [5] C. Rovelli, *Quantum Gravity (Cambridge Monographs on Mathematical Physics)*, Cambridge University Press, 2007.
- [6] T. Jacobson and L. Smolin, *The left-handed spin connection as a variable for canonical gravity*, Physics Letters B **196** (1987), 39–42, DOI: [http://dx.doi.org/10.1016/0370-2693\(87\)91672-8](http://dx.doi.org/10.1016/0370-2693(87)91672-8).
- [7] T Jacobson and L Smolin, *Covariant action for Ashtekar’s form of canonical gravity*, Classical and Quantum Gravity **5** (1988), 583.
- [8] A. Perez, *Introduction to loop quantum gravity and spin foams*, in: 2nd International Conference on Fundamental Interactions (ICFI 2004) Domingos Martins, Espirito Santo, Brazil, June 6-12, 2004, 2004, arXiv: [gr-qc/0409061](https://arxiv.org/abs/gr-qc/0409061) [gr-qc].
- [9] S. Alexandrov and P. Roche, *Critical overview of loops and foams*, Physics Reports **506** (2011), 41–86, DOI: <http://dx.doi.org/10.1016/j.physrep.2011.05.002>.
- [10] A. Ashtekar, “Introduction to Loop Quantum Gravity and Cosmology,” in: *Quantum Gravity and Quantum Cosmology*, ed. by G. Calcagni, L. Papantonopoulos, G. Siopsis, and N. Tsamis, Berlin, Heidelberg: Springer Berlin Heidelberg, 2013, pp. 31–56, DOI: 10.1007/978-3-642-33036-0\_2.
- [11] B. Dittrich, S. Mizera, and S. Steinhaus, *Decorated tensor network renormalization for lattice gauge theories and spin foam models*, New J. Phys. **18** (2016), 053009, DOI: 10.1088/1367-2630/18/5/053009, arXiv: 1409.2407 [gr-qc].
- [12] A. Ashtekar, *Introduction to loop quantum gravity and cosmology*, Lect. Notes Phys. **863** (2013), 31–56, DOI: 10.1007/978-3-642-33036-0\_2, arXiv: 1201.4598 [gr-qc].
- [13] S. Mercuri, *Introduction to Loop Quantum Gravity*, PoS **ISFTG** (2009), 016, arXiv: 1001.1330 [gr-qc].
- [14] T. Thiemann, *Lectures on loop quantum gravity*, Lect. Notes Phys. **631** (2003), [41(2002)], 41–135, DOI: 10.1007/978-3-540-45230-0\_3, arXiv: [gr-qc/0210094](https://arxiv.org/abs/gr-qc/0210094) [gr-qc].
- [15] J. Polchinski, *String Theory, Vol. 1 (Cambridge Monographs on Mathematical Physics)*, Cambridge University Press, 2005.

- [16] J. Polchinski, *String Theory, Vol. 2 (Cambridge Monographs on Mathematical Physics)*, Cambridge University Press, 2005.
- [17] M. B. Green, J. H. Schwarz, and E. Witten, *Superstring Theory: 1 (Cambridge Monographs on Mathematical Physics)*, Cambridge University Press, 2012.
- [18] M. B. Green, J. H. Schwarz, and E. Witten, *Superstring Theory: Volume 2, Loop Amplitudes, Anomalies and Phenomenology (Cambridge Monographs on Mathematical Physics)*, Cambridge University Press, 1987.
- [19] K. Becker, M. Becker, and J. H. Schwarz, *String Theory and M-Theory: A Modern Introduction*, Cambridge University Press, 2006.
- [20] B. Zwiebach, *A First Course in String Theory*, Cambridge University Press, 2009.
- [21] J. Ambjørn and R. Loll, *Non-perturbative Lorentzian quantum gravity, causality and topology change*, Nuclear Physics B **536** (1998), 407–434, DOI: [http://dx.doi.org/10.1016/S0550-3213\(98\)00692-0](http://dx.doi.org/10.1016/S0550-3213(98)00692-0).
- [22] J. Ambjørn, A. Görlich, J. Jurkiewicz, A. Kreienbuehl, and R. Loll, *Renormalization group flow in CDT*, Classical and Quantum Gravity **31** (2014), 165003.
- [23] J. Ambjørn, A. Goerlich, J. Jurkiewicz, and R. Loll, *Nonperturbative Quantum Gravity*, Phys. Rept. **519** (2012), 127–210, DOI: [10.1016/j.physrep.2012.03.007](https://doi.org/10.1016/j.physrep.2012.03.007), arXiv: [1203.3591](https://arxiv.org/abs/1203.3591) [hep-th].
- [24] J. Ambjørn, A. Görlich, J. Jurkiewicz, and R. Loll, *Causal dynamical triangulations and the search for a theory of quantum gravity*, Int. J. Mod. Phys. **D22** (2013), 1330019, DOI: [10.1142/S021827181330019X](https://doi.org/10.1142/S021827181330019X).
- [25] J. Ambjørn, A. Görlich, J. Jurkiewicz, A. Kreienbuehl, and R. Loll, *Renormalization Group Flow in CDT*, Class. Quant. Grav. **31** (2014), 165003, DOI: [10.1088/0264-9381/31/16/165003](https://doi.org/10.1088/0264-9381/31/16/165003), arXiv: [1405.4585](https://arxiv.org/abs/1405.4585) [hep-th].
- [26] J. Ambjørn, D. N. Coumbe, J. Gizbert-Studnicki, and J. Jurkiewicz, *Signature Change of the Metric in CDT Quantum Gravity?* JHEP **08** (2015), [JHEP08,033(2015)], 033, DOI: [10.1007/JHEP08\(2015\)033](https://doi.org/10.1007/JHEP08(2015)033), arXiv: [1503.08580](https://arxiv.org/abs/1503.08580) [hep-th].
- [27] J. Ambjørn, D. Coumbe, J. Gizbert-Studnicki, and J. Jurkiewicz, *Searching for a continuum limit in causal dynamical triangulation quantum gravity*, Phys. Rev. **D93** (2016), 104032, DOI: [10.1103/PhysRevD.93.104032](https://doi.org/10.1103/PhysRevD.93.104032), arXiv: [1603.02076](https://arxiv.org/abs/1603.02076) [hep-th].
- [28] L. Bombelli, J. Lee, D. Meyer, and R. D. Sorkin, *Space-time as a causal set*, Phys. Rev. Lett. **59** (5 Aug. 1987), 521–524, DOI: [10.1103/PhysRevLett.59.521](https://doi.org/10.1103/PhysRevLett.59.521).
- [29] C. Moore, *Comment on “Space-time as a causal set”*, Phys. Rev. Lett. **60** (7 Feb. 1988), 655–655, DOI: [10.1103/PhysRevLett.60.655](https://doi.org/10.1103/PhysRevLett.60.655).
- [30] L. Bombelli, J. Lee, D. Meyer, and R. D. Sorkin, *Bombelli et al. reply*, Phys. Rev. Lett. **60** (7 Feb. 1988), 656–656, DOI: [10.1103/PhysRevLett.60.656](https://doi.org/10.1103/PhysRevLett.60.656).
- [31] F. Dowker, *Causal sets and the deep structure of spacetime*, in: 100 Years Of Relativity: space-time structure: Einstein and beyond, ed. by A. Ashtekar, 2005, pp. 445–464, DOI: [10.1142/9789812700988\\_0016](https://doi.org/10.1142/9789812700988_0016), arXiv: [gr-qc/0508109](https://arxiv.org/abs/gr-qc/0508109) [gr-qc].
- [32] J. Henson, *The Causal set approach to quantum gravity* (2006), arXiv: [gr-qc/0601121](https://arxiv.org/abs/gr-qc/0601121) [gr-qc].
- [33] F. Dowker, *Introduction to causal sets and their phenomenology*, General Relativity and Gravitation **45** (2013), 1651–1667, DOI: [10.1007/s10714-013-1569-y](https://doi.org/10.1007/s10714-013-1569-y).



- 
- [34] A. Eichhorn, S. Mizera, and S. Surya, *Echoes of Asymptotic Silence in Causal Set Quantum Gravity* (2017), arXiv: 1703.08454 [gr-qc].
- [35] M. Reuter, *Nonperturbative evolution equation for quantum gravity*, Phys.Rev. **D57** (1998), 971–985, DOI: 10.1103/PhysRevD.57.971, arXiv: hep-th/9605030 [hep-th].
- [36] W. Souma, *Nontrivial ultraviolet fixed point in quantum gravity*, Prog. Theor. Phys. **102** (1999), 181–195, DOI: 10.1143/PTP.102.181, arXiv: hep-th/9907027 [hep-th].
- [37] O. Lauscher and M. Reuter, *Ultraviolet fixed point and generalized flow equation of quantum gravity*, Phys.Rev. **D65** (2002), 025013, DOI: 10.1103/PhysRevD.65.025013, arXiv: hep-th/0108040 [hep-th].
- [38] O. Lauscher and M. Reuter, *Flow equation of quantum Einstein gravity in a higher derivative truncation*, Phys. Rev. **D66** (2002), 025026, DOI: 10.1103/PhysRevD.66.025026, arXiv: hep-th/0205062 [hep-th].
- [39] E. Manrique, M. Reuter, and F. Saueressig, *Matter Induced Bimetric Actions for Gravity*, Annals Phys. **326** (2011), 440–462, DOI: 10.1016/j.aop.2010.11.003, arXiv: 1003.5129 [hep-th].
- [40] I. Donkin and J. M. Pawłowski, *The phase diagram of quantum gravity from diffeomorphism-invariant RG-flows* (2012), arXiv: 1203.4207 [hep-th].
- [41] N. Christiansen, D. F. Litim, J. M. Pawłowski, and A. Rodigast, *Fixed points and infrared completion of quantum gravity*, Phys.Lett. **B728** (2014), 114–117, DOI: 10.1016/j.physletb.2013.11.025, arXiv: 1209.4038 [hep-th].
- [42] K. Falls, D. Litim, K. Nikolakopoulos, and C. Rahmede, *A bootstrap towards asymptotic safety* (2013), arXiv: 1301.4191 [hep-th].
- [43] N. Christiansen, B. Knorr, J. M. Pawłowski, and A. Rodigast, *Global Flows in Quantum Gravity* (2014), arXiv: 1403.1232 [hep-th].
- [44] D. Becker and M. Reuter, *En route to Background Independence: Broken split-symmetry, and how to restore it with bi-metric average actions*, Annals Phys. **350** (2014), 225–301, DOI: 10.1016/j.aop.2014.07.023, arXiv: 1404.4537 [hep-th].
- [45] N. Christiansen, B. Knorr, J. Meibohm, J. M. Pawłowski, and M. Reichert, *Local Quantum Gravity*, Phys. Rev. **D92** (2015), 121501, DOI: 10.1103/PhysRevD.92.121501, arXiv: 1506.07016 [hep-th].
- [46] A. Nink and M. Reuter, *The unitary conformal field theory behind 2D Asymptotic Safety* (2015), arXiv: 1512.06805 [hep-th].
- [47] H. Gies, B. Knorr, S. Lippoldt, and F. Saueressig, *The Gravitational Two-Loop Counterterm is Asymptotically Safe* (2016), arXiv: 1601.01800 [hep-th].
- [48] D. Oriti, *The Group field theory approach to quantum gravity* (2006), arXiv: gr-qc/0607032 [gr-qc].
- [49] D. Oriti, *The microscopic dynamics of quantum space as a group field theory*, in: Proceedings, Foundations of Space and Time: Reflections on Quantum Gravity: Cape Town, South Africa, 2011, pp. 257–320, arXiv: 1110.5606 [hep-th].
- [50] S. Gielen, D. Oriti, and L. Sindoni, *Cosmology from Group Field Theory Formalism for Quantum Gravity*, Phys. Rev. Lett. **111** (2013), 031301, DOI: 10.1103/PhysRevLett.111.031301, arXiv: 1303.3576 [gr-qc].

- [51] A. Eichhorn and T. Koslowski, *Continuum limit in matrix models for quantum gravity from the Functional Renormalization Group*, Phys. Rev. **D88** (2013), 084016, DOI: 10.1103/PhysRevD.88.084016, arXiv: 1309.1690 [gr-qc].
- [52] D. Oriti, *Group field theory as the 2nd quantization of Loop Quantum Gravity*, Class. Quant. Grav. **33** (2016), 085005, DOI: 10.1088/0264-9381/33/8/085005, arXiv: 1310.7786 [gr-qc].
- [53] S. Gielen, D. Oriti, and L. Sindoni, *Homogeneous cosmologies as group field theory condensates*, JHEP **06** (2014), 013, DOI: 10.1007/JHEP06(2014)013, arXiv: 1311.1238 [gr-qc].
- [54] A. Eichhorn and T. Koslowski, *Towards phase transitions between discrete and continuum quantum spacetime from the Renormalization Group*, Phys. Rev. **D90** (2014), 104039, DOI: 10.1103/PhysRevD.90.104039, arXiv: 1408.4127 [gr-qc].
- [55] J. Ben Geloun, R. Martini, and D. Oriti, *Functional Renormalisation Group analysis of Tensorial Group Field Theories on  $\mathbb{R}^d$* , Phys. Rev. **D94** (2016), 024017, DOI: 10.1103/PhysRevD.94.024017, arXiv: 1601.08211 [hep-th].
- [56] A. Eichhorn and T. Koslowski, *Flowing to the continuum in discrete tensor models for quantum gravity* (2017), arXiv: 1701.03029 [gr-qc].
- [57] A. Ashtekar, M. Reuter, and C. Rovelli, *From General Relativity to Quantum Gravity* (2014), arXiv: 1408.4336 [gr-qc].
- [58] H. Elvang and G. T. Horowitz, *Quantum gravity via supersymmetry and holography* (2013), arXiv: 1311.2489 [gr-qc].
- [59] IOM (Institute of Medicine), *Dietary Reference Intakes for Calcium and Vitamin D*, The National Academies Press, Mar. 2011, DOI: 10.17226/13050.
- [60] J. Zinn-Justin, *Quantum Field Theory and Critical Phenomena (International Series of Monographs on Physics)*, Clarendon Press, 2002.
- [61] D. J. Bishop and J. D. Reppy, *Study of the Superfluid Transition in Two-Dimensional  $^4\text{He}$  Films*, Phys. Rev. Lett. **40** (26 June 1978), 1727–1730, DOI: 10.1103/PhysRevLett.40.1727.
- [62] J. Maps and R. B. Hallock, *Onset of Superfluid Flow in  $^4\text{He}$  Films Adsorbed on Mylar*, Phys. Rev. Lett. **47** (21 Nov. 1981), 1533–1536, DOI: 10.1103/PhysRevLett.47.1533.
- [63] Z. Hadzibabic, P. Krüger, M. Cheneau, B. Battelier, and J. Dalibard, *Berezinskii–Kosterlitz–Thouless crossover in a trapped atomic gas*, Nature **441** (2006), 1118–1121, DOI: 10.1038/nature04851.
- [64] S. Tung, G. Lamporesi, D. Lobser, L. Xia, and E. A. Cornell, *Observation of the Presuperfluid Regime in a Two-Dimensional Bose Gas*, Phys. Rev. Lett. **105** (23 Dec. 2010), 230408, DOI: 10.1103/PhysRevLett.105.230408.
- [65] P. A. Murthy et al., *Observation of the Berezinskii–Kosterlitz–Thouless Phase Transition in an Ultracold Fermi Gas*, Phys. Rev. Lett. **115** (1 June 2015), 010401, DOI: 10.1103/PhysRevLett.115.010401.
- [66] R. Desbuquois et al., *Superfluid behaviour of a two-dimensional Bose gas*, Nature Physics **8** (2012), 645–648, DOI: 10.1038/nphys2378.
- [67] E. Ising, *Beitrag zur Theorie des Ferromagnetismus*, Zeitschrift für Physik **31** (1925), 253–258, DOI: 10.1007/BF02980577.

- [68] J. des Cloizeaux and G. Jannink, *Polymers in Solution: Their Modelling and Structure (Oxford Classic Texts in the Physical Sciences)*, Oxford University Press, 2010.
- [69] N. Asherie et al., *Oligomerization and phase separation in globular protein solutions*, *Biophysical Chemistry* **75** (1998), 213–227, DOI: [http://dx.doi.org/10.1016/S0301-4622\(98\)00208-7](http://dx.doi.org/10.1016/S0301-4622(98)00208-7).
- [70] M. L. Broide, C. R. Berland, J Pande, O. O. Ogun, and G. B. Benedek, *Binary-liquid phase separation of lens protein solutions*. *Proceedings of the National Academy of Sciences* **88** (1991), 5660–5664, DOI: 10.1073/pnas.88.13.5660, eprint: <http://www.pnas.org/content/88/13/5660.full.pdf>.
- [71] R. D. Pisarski and F. Wilczek, *Remarks on the chiral phase transition in chromodynamics*, *Phys. Rev. D* **29** (2 Jan. 1984), 338–341, DOI: 10.1103/PhysRevD.29.338.
- [72] R. V. Gavai, J. Potvin, and S. Sanielevici, *Metastabilities in Three Flavor QCD at Low Quark Masses*, *Phys. Rev. Lett.* **58** (1987), 2519, DOI: 10.1103/PhysRevLett.58.2519.
- [73] S. Gavin, A. Gocksch, and R. D. Pisarski, *QCD and the chiral critical point*, *Phys. Rev. D* **49** (7 Apr. 1994), R3079–R3082, DOI: 10.1103/PhysRevD.49.R3079.
- [74] F. Karsch, E. Laermann, and C. Schmidt, *The Chiral critical point in three-flavor QCD*, *Phys. Lett.* **B520** (2001), 41–49, DOI: 10.1016/S0370-2693(01)01114-5, arXiv: [hep-lat/0107020](https://arxiv.org/abs/hep-lat/0107020) [hep-lat].
- [75] O. Chwolson, *Über eine mögliche Form fiktiver Doppelsterne*, *Astronomische Nachrichten* **221** (1924), 329–330, DOI: 10.1002/asna.19242212003.
- [76] A. Einstein, *LENS-LIKE ACTION OF A STAR BY THE DEVIATION OF LIGHT IN THE GRAVITATIONAL FIELD*, *Science* **84** (1936), 506–507, DOI: 10.1126/science.84.2188.506, eprint: <http://science.sciencemag.org/content/84/2188/506.full.pdf>.
- [77] D. Walsh, R. F. Carswell, and R. J. Weymann, *0957 + 561 A, B: twin quasistellar objects or gravitational lens?* *Nature* **279** (May 1979), 381–384, DOI: 10.1038/279381a0.
- [78] B. P. Abbott et al., *Observation of Gravitational Waves from a Binary Black Hole Merger*, *Phys. Rev. Lett.* **116** (6 Feb. 2016), 061102, DOI: 10.1103/PhysRevLett.116.061102.
- [79] *The 2010 Nobel Prize in Physics - Press Release*, [http://www.nobelprize.org/nobel\\_prizes/physics/laureates/2010/press.html](http://www.nobelprize.org/nobel_prizes/physics/laureates/2010/press.html), Accessed: 20/03/2017.
- [80] T. Wehling, A. Black-Schaffer, and A. Balatsky, *Dirac materials*, *Advances in Physics* **63** (2014), 1–76, DOI: 10.1080/00018732.2014.927109.
- [81] , I. F. Herbut, and G. W. Semenoff, *Coulomb interaction at the metal-insulator critical point in graphene*, *Phys. Rev. B* **80** (8 Aug. 2009), 081405, DOI: 10.1103/PhysRevB.80.081405.
- [82] Y. Araki and G. W. Semenoff, *Spin versus charge-density-wave order in graphenelike systems*, *Phys. Rev. B* **86** (12 Sept. 2012), 121402, DOI: 10.1103/PhysRevB.86.121402.
- [83] E. V. Gorbar, V. P. Gusynin, V. A. Miransky, and I. A. Shovkovy, *Magnetic field driven metal-insulator phase transition in planar systems*, *Phys. Rev. B* **66** (4 July 2002), 045108, DOI: 10.1103/PhysRevB.66.045108.

- [84] A. M. Black-Schaffer and S. Doniach, *Resonating valence bonds and mean-field d-wave superconductivity in graphite*, Phys. Rev. B **75** (13 Apr. 2007), 134512, DOI: 10.1103/PhysRevB.75.134512.
- [85] I. F. Herbut, *Interactions and Phase Transitions on Graphene's Honeycomb Lattice*, Phys. Rev. Lett. **97** (14 Oct. 2006), 146401, DOI: 10.1103/PhysRevLett.97.146401.
- [86] C. Honerkamp, *Density Waves and Cooper Pairing on the Honeycomb Lattice*, Phys. Rev. Lett. **100** (14 Apr. 2008), 146404, DOI: 10.1103/PhysRevLett.100.146404.
- [87] I. F. Herbut, V. Juricic, and O. Vafek, *Relativistic Mott criticality in graphene*, Phys. Rev. **B80** (2009), 075432, DOI: 10.1103/PhysRevB.80.075432, arXiv: 0904.1019 [cond-mat.str-el].
- [88] S. Raghu, X.-L. Qi, C. Honerkamp, and S.-C. Zhang, *Topological Mott Insulators*, Phys. Rev. Lett. **100** (15 Apr. 2008), 156401, DOI: 10.1103/PhysRevLett.100.156401.
- [89] A. G. Grushin et al., *Charge instabilities and topological phases in the extended Hubbard model on the honeycomb lattice with enlarged unit cell*, Phys. Rev. B **87** (8 Feb. 2013), 085136, DOI: 10.1103/PhysRevB.87.085136.
- [90] M. Daghofer and M. Hohenadler, *Phases of correlated spinless fermions on the honeycomb lattice*, Phys. Rev. B **89** (3 Jan. 2014), 035103, DOI: 10.1103/PhysRevB.89.035103.
- [91] I. F. Herbut, and B. Roy, *Theory of interacting electrons on the honeycomb lattice*, Phys. Rev. B **79** (8 Feb. 2009), 085116, DOI: 10.1103/PhysRevB.79.085116.
- [92] L. Janssen and I. F. Herbut, *Antiferromagnetic critical point on graphene's honeycomb lattice: A functional renormalization group approach*, Phys. Rev. **B89** (2014), 205403, DOI: 10.1103/PhysRevB.89.205403, arXiv: 1402.6277 [cond-mat.str-el].
- [93] C.-Y. Hou, C. Chamon, and C. Mudry, *Electron Fractionalization in Two-Dimensional Graphenelike Structures*, Phys. Rev. Lett. **98** (18 May 2007), 186809, DOI: 10.1103/PhysRevLett.98.186809.
- [94] B. Roy and I. F. Herbut, *Unconventional superconductivity on honeycomb lattice: Theory of Kekule order parameter*, Phys. Rev. B **82** (3 July 2010), 035429, DOI: 10.1103/PhysRevB.82.035429.
- [95] M. Kharitonov, *Phase diagram for the  $\nu = 0$  quantum Hall state in monolayer graphene*, Phys. Rev. B **85** (15 Apr. 2012), 155439, DOI: 10.1103/PhysRevB.85.155439.
- [96] L. Classen, M. M. Scherer, and C. Honerkamp, *Instabilities on graphene's honeycomb lattice with electron-phonon interactions*, Phys. Rev. B **90** (3 July 2014), 035122, DOI: 10.1103/PhysRevB.90.035122.
- [97] D. D. Scherer, M. M. Scherer, and C. Honerkamp, *Correlated spinless fermions on the honeycomb lattice revisited*, Phys. Rev. B **92** (15 Oct. 2015), 155137, DOI: 10.1103/PhysRevB.92.155137.
- [98] T. O. Wehling et al., *Strength of Effective Coulomb Interactions in Graphene and Graphite*, Phys. Rev. Lett. **106** (23 June 2011), 236805, DOI: 10.1103/PhysRevLett.106.236805.

- 
- [99] W. Metzner, M. Salmhofer, C. Honerkamp, V. Meden, and K. Schönhammer, *Functional renormalization group approach to correlated fermion systems*, Rev. Mod. Phys. **84** (1 Mar. 2012), 299–352, DOI: 10.1103/RevModPhys.84.299.
- [100] L. Rosa, P. Vitale, and C. Wetterich, *Critical Exponents of the Gross-Neveu Model from the Effective Average Action*, Phys. Rev. Lett. **86** (6 Feb. 2001), 958–961, DOI: 10.1103/PhysRevLett.86.958.
- [101] F. Gehring, H. Gies, and L. Janssen, *Fixed-point structure of low-dimensional relativistic fermion field theories: Universality classes and emergent symmetry*, Phys. Rev. **D92** (2015), 085046, DOI: 10.1103/PhysRevD.92.085046, arXiv: 1506.07570 [hep-th].
- [102] S. Hands and C. Strouthos, *Quantum critical behavior in a graphenelike model*, Phys. Rev. B **78** (16 Oct. 2008), 165423, DOI: 10.1103/PhysRevB.78.165423.
- [103] W. Armour, S. Hands, and C. Strouthos, *Monte Carlo simulation of the semimetal-insulator phase transition in monolayer graphene*, Phys. Rev. B **81** (12 Mar. 2010), 125105, DOI: 10.1103/PhysRevB.81.125105.
- [104] A Cortijo, F Guinea, and M. A. H. Vozmediano, *Geometrical and topological aspects of graphene and related materials*, Journal of Physics A: Mathematical and Theoretical **45** (2012), 383001.
- [105] C. Weeks and M. Franz, *Interaction-driven instabilities of a Dirac semimetal*, Phys. Rev. B **81** (8 Feb. 2010), 085105, DOI: 10.1103/PhysRevB.81.085105.
- [106] B. Roy, and I. F. Herbut, *Quantum superconducting criticality in graphene and topological insulators*, Phys. Rev. B **87** (4 Jan. 2013), 041401, DOI: 10.1103/PhysRevB.87.041401.
- [107] O. Vafek, *Interacting fermions on the honeycomb bilayer: From weak to strong coupling*, Phys. Rev. B **82** (20 Nov. 2010), 205106, DOI: 10.1103/PhysRevB.82.205106.
- [108] A. Jakovác and A. Patkós, *Local potential approximation for the renormalization group flow of fermionic field theories*, Phys. Rev. D **88** (6 Sept. 2013), 065008, DOI: 10.1103/PhysRevD.88.065008.
- [109] Y. Otsuka, S. Yunoki, and S. Sorella, *Universal quantum criticality in the metal-insulator transition of two-dimensional interacting Dirac electrons*, Phys. Rev. **X6** (2016), 011029, DOI: 10.1103/PhysRevX.6.011029, arXiv: 1510.08593 [cond-mat.str-el].
- [110] A. Jakovác, A. Patkós, and P. Pósfay, *Non-Gaussian fixed points in fermionic field theories without auxiliary Bose fields*, The European Physical Journal C **75** (2015), 1–10, DOI: 10.1140/epjc/s10052-014-3228-1.
- [111] M. M. Scherer and I. F. Herbut, *Gauge-field-assisted Kekulé quantum criticality* (2016), arXiv: 1609.03208 [cond-mat.str-el].
- [112] B. Roy, *Multi-critical behavior of  $Z_2 \times O(2)$  Gross-Neveu-Yukawa theory in graphene*, Phys. Rev. **B84** (2011), 113404, DOI: 10.1103/PhysRevB.84.113404, arXiv: 1106.1419 [cond-mat.str-el].
- [113] B. Roy and V. Juricic, *Strain-induced time-reversal odd superconductivity in graphene*, Phys. Rev. **B90** (2014), 041413, DOI: 10.1103/PhysRevB.90.041413, arXiv: 1309.0507 [cond-mat.mes-hall].

- [114] L. Classen, I. F. Herbut, L. Janssen, and M. M. Scherer, *Competition of density waves and quantum multicritical behavior in Dirac materials from functional renormalization*, Phys. Rev. **B93** (2016), 125119, DOI: 10.1103/PhysRevB.93.125119, arXiv: 1510.09003 [cond-mat.str-el].
- [115] K. S. Novoselov et al., *Two-dimensional gas of massless Dirac fermions in graphene*, Nature **438** (Nov. 2005), 197–200, DOI: 10.1038/nature04233.
- [116] A. K. Geim and K. S. Novoselov, *The rise of graphene*, Nature Materials **6** (Mar. 2007), 183–191, DOI: 10.1038/nmat1849.
- [117] A. H. Castro Neto, F. Guinea, N. M. R. Peres, K. S. Novoselov, and A. K. Geim, *The electronic properties of graphene*, Rev. Mod. Phys. **81** (2009), 109–162, DOI: 10.1103/RevModPhys.81.109.
- [118] S. Das Sarma, S. Adam, E. H. Hwang, and E. Rossi, *Electronic transport in two-dimensional graphene*, Rev. Mod. Phys. **83** (2 May 2011), 407–470, DOI: 10.1103/RevModPhys.83.407.
- [119] G. G. Guzmán-Verri and L. C. Lew Yan Voon, *Electronic structure of silicon-based nanostructures*, Phys. Rev. B **76** (7 Aug. 2007), 075131, DOI: 10.1103/PhysRevB.76.075131.
- [120] B. Aufray et al., *Graphene-like silicon nanoribbons on Ag(110): A possible formation of silicene*, Applied Physics Letters **96**, 183102 (2010), DOI: 10.1063/1.3419932.
- [121] P. Vogt et al., *Silicene: Compelling Experimental Evidence for Graphenelike Two-Dimensional Silicon*, Phys. Rev. Lett. **108** (15 Apr. 2012), 155501, DOI: 10.1103/PhysRevLett.108.155501.
- [122] Y. Du et al., *Tuning the Band Gap in Silicene by Oxidation*, ACS Nano **8** (2014), 10019–10025, DOI: 10.1021/nn504451t.
- [123] S. Cahangirov, M. Topsakal, E. Aktürk, and S. Ciraci, *Two- and One-Dimensional Honeycomb Structures of Silicon and Germanium*, Phys. Rev. Lett. **102** (23 June 2009), 236804, DOI: 10.1103/PhysRevLett.102.236804.
- [124] E. Bianco et al., *Stability and Exfoliation of Germanane: A Germanium Graphane Analogue*, ACS Nano **7** (2013), 4414–4421, DOI: 10.1021/nn4009406.
- [125] M. Derivaz et al., *Continuous Germanene Layer on Al(111)*, Nano Letters **15** (2015), 2510–2516, DOI: 10.1021/acs.nanolett.5b00085.
- [126] C.-H. Park, L. Yang, Y.-W. Son, M. L. Cohen, and S. G. Louie, *New Generation of Massless Dirac Fermions in Graphene under External Periodic Potentials*, Phys. Rev. Lett. **101** (12 Sept. 2008), 126804, DOI: 10.1103/PhysRevLett.101.126804.
- [127] F. Guinea and T. Low, *Band structure and gaps of triangular graphene superlattices*, Philosophical Transactions of the Royal Society of London A: Mathematical, Physical and Engineering Sciences **368** (2010), 5391–5402, DOI: 10.1098/rsta.2010.0214.
- [128] C. Ortix, L. Yang, and J. van den Brink, *Graphene on incommensurate substrates: Trigonal warping and emerging Dirac cone replicas with halved group velocity*, Phys. Rev. B **86** (8 Aug. 2012), 081405, DOI: 10.1103/PhysRevB.86.081405.
- [129] M. Yankowitz et al., *Emergence of superlattice Dirac points in graphene on hexagonal boron nitride*, Nat Phys **8** (Mar. 2012), 382–386, DOI: 10.1038/nphys2272.

- [130] L. A. Ponomarenko et al., *Cloning of Dirac fermions in graphene superlattices*, Nature **497** (May 2013), 594–597, DOI: 10.1038/nature12187.
- [131] B. Hunt et al., *Massive Dirac Fermions and Hofstadter Butterfly in a van der Waals Heterostructure*, Science **340** (2013), 1427–1430, DOI: 10.1126/science.1237240.
- [132] P. Soltan-Panahi et al., *Multi-component quantum gases in spin-dependent hexagonal lattices*, Nat Phys **7** (Feb. 2011), 434–440, DOI: 10.1038/nphys1916.
- [133] G. Weick, C. Woollacott, W. L. Barnes, O. Hess, and E. Mariani, *Dirac-like Plasmons in Honeycomb Lattices of Metallic Nanoparticles*, Phys. Rev. Lett. **110** (10 Mar. 2013), 106801, DOI: 10.1103/PhysRevLett.110.106801.
- [134] S. Banerjee, J. Fransson, A. M. Black-Schaffer, H. Ågren, and A. V. Balatsky, *Granular superconductor in a honeycomb lattice as a realization of bosonic Dirac material*, Phys. Rev. B **93** (13 Apr. 2016), 134502, DOI: 10.1103/PhysRevB.93.134502.
- [135] M. Gibertini et al., *Engineering artificial graphene in a two-dimensional electron gas*, Phys. Rev. B **79** (24 June 2009), 241406, DOI: 10.1103/PhysRevB.79.241406.
- [136] L. Tarruell, D. Greif, T. Uehlinger, G. Jotzu, and T. Esslinger, *Creating, moving and merging Dirac points with a Fermi gas in a tunable honeycomb lattice*, Nature **483** (Mar. 2012), 302–305, DOI: 10.1038/nature10871.
- [137] M. Polini, F. Guinea, M. Lewenstein, H. C. Manoharan, and V. Pellegrini, *Artificial honeycomb lattices for electrons, atoms and photons*, Nature Nanotech **8** (Sept. 2013), 625–633, DOI: 10.1038/nnano.2013.161.
- [138] S. M. Young et al., *Dirac Semimetal in Three Dimensions*, Phys. Rev. Lett. **108** (14 Apr. 2012), 140405, DOI: 10.1103/PhysRevLett.108.140405.
- [139] Z. K. Liu et al., *Discovery of a Three-Dimensional Topological Dirac Semimetal,  $Na_3Bi$* , Science **343** (2014), 864–867, DOI: 10.1126/science.1245085.
- [140] M. Neupane et al., *Observation of a three-dimensional topological Dirac semimetal phase in high-mobility  $Cd_3As_2$* , Nature Communications **5** (May 2014), DOI: 10.1038/ncomms4786.
- [141] S. Borisenko et al., *Experimental Realization of a Three-Dimensional Dirac Semimetal*, Phys. Rev. Lett. **113** (2 July 2014), 027603, DOI: 10.1103/PhysRevLett.113.027603.
- [142] L. A. Ponomarenko et al., *Chaotic Dirac Billiard in Graphene Quantum Dots*, Science **320** (2008), 356–358, DOI: 10.1126/science.1154663, eprint: <http://science.sciencemag.org/content/320/5874/356.full.pdf>.
- [143] K. G. Wilson, *Confinement of quarks*, Phys. Rev. D **10** (8 Oct. 1974), 2445–2459, DOI: 10.1103/PhysRevD.10.2445.
- [144] A. Wipf, *Statistical Approach to Quantum Field Theory: An Introduction (Lecture Notes in Physics)*, Springer, 2012.
- [145] A. M. Polyakov, *Nonhamiltonian approach to conformal quantum field theory*, Zh. Eksp. Teor. Fiz. **66** (1974), 23–42.
- [146] R. Rattazzi, V. S. Rychkov, E. Tonni, and A. Vichi, *Bounding scalar operator dimensions in 4 D CFT*, Journal of High Energy Physics **2008** (2008), 031.

- [147] S. El-Showk et al., *Solving the 3D Ising Model with the Conformal Bootstrap*, Phys. Rev. **D86** (2012), 025022, DOI: 10.1103/PhysRevD.86.025022, arXiv: 1203.6064 [hep-th].
- [148] S. El-Showk et al., *Solving the 3d Ising Model with the Conformal Bootstrap II. c-Minimization and Precise Critical Exponents*, Journal of Statistical Physics **157** (2014), 869–914, DOI: 10.1007/s10955-014-1042-7.
- [149] D. Poland and D. Simmons-Duffin, *The conformal bootstrap*, Nature Phys. **12** (2016), 535–539, DOI: 10.1038/nphys3761.
- [150] K. G. Wilson, *The renormalization group: Critical phenomena and the Kondo problem*, Rev. Mod. Phys. **47** (4 Oct. 1975), 773–840, DOI: 10.1103/RevModPhys.47.773.
- [151] C. Wetterich, *Exact evolution equation for the effective potential*, Phys.Lett. **B301** (1993), 90–94, DOI: 10.1016/0370-2693(93)90726-X.
- [152] T. R. Morris, *The Exact renormalization group and approximate solutions*, Int. J. Mod. Phys. **A9** (1994), 2411–2450, DOI: 10.1142/S0217751X94000972, arXiv: hep-ph/9308265 [hep-ph].
- [153] J. Borchardt and B. Knorr, *Global solutions of functional fixed point equations via pseudospectral methods*, Phys. Rev. **D91** (2015), [Erratum: Phys. Rev.D93,no.8,089904(2016)], 105011, DOI: 10.1103/PhysRevD.93.089904, 10.1103/PhysRevD.91.105011, arXiv: 1502.07511 [hep-th].
- [154] J. Borchardt and B. Knorr, *Solving functional flow equations with pseudo-spectral methods*, Phys. Rev. **D94** (2016), 025027, DOI: 10.1103/PhysRevD.94.025027, arXiv: 1603.06726 [hep-th].
- [155] H. Gies, B. Knorr, and S. Lippoldt, *Generalized Parametrization Dependence in Quantum Gravity*, Phys. Rev. **D92** (2015), 084020, DOI: 10.1103/PhysRevD.92.084020, arXiv: 1507.08859 [hep-th].
- [156] M. Heilmann, T. Hellwig, B. Knorr, M. Ansorg, and A. Wipf, *Convergence of Derivative Expansion in Supersymmetric Functional RG Flows*, JHEP **1502** (2015), 109, DOI: 10.1007/JHEP02(2015)109, arXiv: 1409.5650 [hep-th].
- [157] C. Pagani and M. Reuter, *Composite Operators in Asymptotic Safety*, Phys. Rev. **D95** (2017), 066002, DOI: 10.1103/PhysRevD.95.066002, arXiv: 1611.06522 [gr-qc].
- [158] R. Alkofer and L. von Smekal, *The Infrared behavior of QCD Green’s functions: Confinement dynamical symmetry breaking, and hadrons as relativistic bound states*, Phys. Rept. **353** (2001), 281, DOI: 10.1016/S0370-1573(01)00010-2, arXiv: hep-ph/0007355 [hep-ph].
- [159] P. Maris and C. D. Roberts, *Dyson-Schwinger equations: A Tool for hadron physics*, Int. J. Mod. Phys. **E12** (2003), 297–365, DOI: 10.1142/S0218301303001326, arXiv: nucl-th/0301049 [nucl-th].
- [160] C. S. Fischer, *Infrared properties of QCD from Dyson-Schwinger equations*, J. Phys. **G32** (2006), R253–R291, DOI: 10.1088/0954-3899/32/8/R02, arXiv: hep-ph/0605173 [hep-ph].
- [161] S. Pokorski, *Gauge Field Theories (Cambridge Monographs on Mathematical Physics)*, Cambridge University Press, 2000.



- [162] C. Roberts and S. Schmidt, *Dyson-Schwinger equations: Density, temperature and continuum strong QCD*, Progress in Particle and Nuclear Physics **45** (2000), S1 – S103, DOI: [http://dx.doi.org/10.1016/S0146-6410\(00\)90011-5](http://dx.doi.org/10.1016/S0146-6410(00)90011-5).
- [163] E. S. Swanson, *A Primer on Functional Methods and the Schwinger-Dyson Equations*, AIP Conf. Proc. **1296** (2010), 75–121, DOI: 10.1063/1.3523221, arXiv: 1008.4337 [hep-ph].
- [164] M. Reuter and C. Wetterich, *Effective average action for gauge theories and exact evolution equations*, Nucl.Phys. **B417** (1994), 181–214, DOI: 10.1016/0550-3213(94)90543-6.
- [165] J. M. Pawłowski, *Aspects of the functional renormalisation group*, Annals Phys. **322** (2007), 2831–2915, DOI: 10.1016/j.aop.2007.01.007, arXiv: hep-th/0512261 [hep-th].
- [166] H. Gies, *Introduction to the functional RG and applications to gauge theories*, Lect.Notes Phys. **852** (2012), 287–348, DOI: 10.1007/978-3-642-27320-9\_6, arXiv: hep-ph/0611146 [hep-ph].
- [167] B. Delamotte, *An Introduction to the nonperturbative renormalization group*, Lect.Notes Phys. **852** (2012), 49–132, DOI: 10.1007/978-3-642-27320-9\_2, arXiv: cond-mat/0702365 [COND-MAT].
- [168] P. Kopietz, L. Bartosch, and F. Schutz, *Introduction to the functional renormalization group*, Lect.Notes Phys. **798** (2010), 1–380, DOI: 10.1007/978-3-642-05094-7.
- [169] J. Braun, *Fermion Interactions and Universal Behavior in Strongly Interacting Theories*, J.Phys. **G39** (2012), 033001, DOI: 10.1088/0954-3899/39/3/033001, arXiv: 1108.4449 [hep-ph].
- [170] J. Berges and D. Mesterhazy, *Introduction to the nonequilibrium functional renormalization group*, Nucl.Phys.Proc.Suppl. **228** (2012), 37–60, DOI: 10.1016/j.nuclphysbps.2012.06.003, arXiv: 1204.1489 [hep-ph].
- [171] A. Aizenbud and D. Gourevitch, *Schwartz Functions on Nash Manifolds*, International Mathematics Research Notices **2008** (2008), rnm155, DOI: 10.1093/imrn/rnm155.
- [172] J. M. Pawłowski, *Geometrical effective action and Wilsonian flows* (2003), arXiv: hep-th/0310018 [hep-th].
- [173] E. Manrique and M. Reuter, *Bimetric Truncations for Quantum Einstein Gravity and Asymptotic Safety*, Annals Phys. **325** (2010), 785–815, DOI: 10.1016/j.aop.2009.11.009, arXiv: 0907.2617 [gr-qc].
- [174] I. H. Bridle, J. A. Dietz, and T. R. Morris, *The local potential approximation in the background field formalism*, JHEP **1403** (2014), 093, DOI: 10.1007/JHEP03(2014)093, arXiv: 1312.2846 [hep-th].
- [175] J. A. Dietz and T. R. Morris, *Background independent exact renormalization group for conformally reduced gravity*, JHEP **04** (2015), 118, DOI: 10.1007/JHEP04(2015)118, arXiv: 1502.07396 [hep-th].
- [176] M. Safari, *Splitting Ward identity*, Eur. Phys. J. **C76** (2016), 201, DOI: 10.1140/epjc/s10052-016-4036-6, arXiv: 1508.06244 [hep-th].
- [177] P. Labus, T. R. Morris, and Z. H. Slade, *Background independence in a background dependent renormalization group*, Phys. Rev. **D94** (2016), 024007, DOI: 10.1103/PhysRevD.94.024007, arXiv: 1603.04772 [hep-th].

- [178] T. R. Morris and A. W. H. Preston, *Manifestly diffeomorphism invariant classical Exact Renormalization Group*, JHEP **06** (2016), 012, DOI: 10.1007/JHEP06(2016)012, arXiv: 1602.08993 [hep-th].
- [179] M. Safari and G. P. Vacca, *Covariant and single-field effective action with the background-field formalism* (2016), arXiv: 1607.03053 [hep-th].
- [180] M. Safari and G. P. Vacca, *Covariant and background independent functional RG flow for the effective average action*, JHEP **11** (2016), 139, DOI: 10.1007/JHEP11(2016)139, arXiv: 1607.07074 [hep-th].
- [181] C. Wetterich, *Gauge invariant flow equation* (2016), arXiv: 1607.02989 [hep-th].
- [182] T. R. Morris, *Large curvature and background scale independence in single-metric approximations to asymptotic safety*, JHEP **11** (2016), 160, DOI: 10.1007/JHEP11(2016)160, arXiv: 1610.03081 [hep-th].
- [183] R. Percacci and G. P. Vacca, *The background scale Ward identity in quantum gravity*, Eur. Phys. J. **C77** (2017), 52, DOI: 10.1140/epjc/s10052-017-4619-x, arXiv: 1611.07005 [hep-th].
- [184] N. Ohta, *Background Scale Independence in Quantum Gravity* (2017), arXiv: 1701.01506 [hep-th].
- [185] E. Manrique, M. Reuter, and F. Saueressig, *Bimetric Renormalization Group Flows in Quantum Einstein Gravity*, Annals Phys. **326** (2011), 463–485, DOI: 10.1016/j.aop.2010.11.006, arXiv: 1006.0099 [hep-th].
- [186] D. Becker and M. Reuter, *Propagating gravitons vs. 'dark matter' in asymptotically safe quantum gravity*, JHEP **12** (2014), 025, DOI: 10.1007/JHEP12(2014)025, arXiv: 1407.5848 [hep-th].
- [187] A. Codello, G. D'Odorico, and C. Pagani, *Consistent closure of renormalization group flow equations in quantum gravity*, Phys. Rev. **D89** (2014), 081701, DOI: 10.1103/PhysRevD.89.081701, arXiv: 1304.4777 [gr-qc].
- [188] T. Denz, J. M. Pawłowski, and M. Reichert, *Towards apparent convergence in asymptotically safe quantum gravity* (2016), arXiv: 1612.07315 [hep-th].
- [189] N. Christiansen, *Four-Derivative Quantum Gravity Beyond Perturbation Theory* (2016), arXiv: 1612.06223 [hep-th].
- [190] D. F. Litim and J. M. Pawłowski, *Renormalization group flows for gauge theories in axial gauges*, JHEP **09** (2002), 049, DOI: 10.1088/1126-6708/2002/09/049, arXiv: hep-th/0203005 [hep-th].
- [191] *xAct: Efficient tensor computer algebra for Mathematica*, <http://xact.es/index.html>, Accessed: 22/03/2017.
- [192] J. M. Martín-García, R. Portugal, and L. R. U. Manssur, *The Invar tensor package*, Computer Physics Communications **177** (Oct. 2007), 640–648, DOI: 10.1016/j.cpc.2007.05.015, arXiv: 0704.1756 [cs.SC].
- [193] J. M. Martín-García, D. Yllanes, and R. Portugal, *The Invar tensor package: Differential invariants of Riemann*, Computer Physics Communications **179** (Oct. 2008), 586–590, DOI: 10.1016/j.cpc.2008.04.018, arXiv: 0802.1274 [cs.SC].
- [194] J. M. Martín-García, *xPerm: fast index canonicalization for tensor computer algebra*, Computer Physics Communications **179** (Oct. 2008), 597–603, DOI: 10.1016/j.cpc.2008.05.009, arXiv: 0803.0862 [cs.SC].

- 
- [195] D. Brizuela, J. M. Martin-Garcia, and G. A. Mena Marugan, *xPert: Computer algebra for metric perturbation theory*, Gen. Rel. Grav. **41** (2009), 2415–2431, DOI: 10.1007/s10714-009-0773-2, arXiv: 0807.0824 [gr-qc].
- [196] T. Nutma, *xTras: A field-theory inspired xAct package for mathematica*, Computer Physics Communications **185** (June 2014), 1719–1738, DOI: 10.1016/j.cpc.2014.02.006, arXiv: 1308.3493 [cs.SC].
- [197] J. P. Boyd, *Chebyshev and Fourier Spectral Methods*, 2nd ed., Dover Publications, 2000.
- [198] D. Funaro, *Polynomial Approximation of Differential Equations*, Springer, 1992.
- [199] B.-Y. Guo, *Spectral Methods and Their Applications*, World Scientific, 1998.
- [200] J. Mason and D. C. Handscomb, *Chebyshev Polynomials*, Chapman and Hall/CRC, 2002.
- [201] B. Knorr, *Ising and Gross-Neveu model in next-to-leading order* (2016), arXiv: 1609.03824 [cond-mat.str-el].
- [202] H. Wang and S. Xiang, *On the convergence rates of Legendre approximation*, Mathematics of Computation **81** (Oct. 2011), 861–877, DOI: 10.1090/s0025-5718-2011-02549-4.
- [203] J. Boyd and R. Petschek, *The relationships between Chebyshev, Legendre and Jacobi polynomials: The generic superiority of chebyshev polynomials and three important exceptions*, Journal of Scientific Computing **59** (Apr. 2014), 1–27, DOI: 10.1007/s10915-013-9751-7.
- [204] J.-P. Berrut and L. N. Trefethen, *Barycentric Lagrange Interpolation*, SIAM Review **46** (Jan. 2004), 501–517, DOI: 10.1137/s0036144502417715.
- [205] C. W. Clenshaw, *A note on the summation of Chebyshev series*, Mathematics of Computation **9** (Sept. 1955), 118–118, DOI: 10.1090/s0025-5718-1955-0071856-0.
- [206] A. Griewank and A. Walther, *Evaluating Derivatives: Principles and Techniques of Algorithmic Differentiation, Second Edition*, Society for Industrial and Applied Mathematics, 2008.
- [207] R. D. Neidinger, *Introduction to Automatic Differentiation and MATLAB Object-Oriented Programming*, SIAM Review **52** (Jan. 2010), 545–563, DOI: 10.1137/080743627.
- [208] *www.Autodiff.org - Community Portal for Automatic Differentiation*, <http://www.autodiff.org/>, Accessed: 21/03/2017.
- [209] *BOOST C++ Libraries 1.57.0*, <http://www.boost.org>, 2014.
- [210] Guennebaud, G. and Jacob, B. and others, *Eigen v3*, <http://eigen.tuxfamily.org>, 2010.
- [211] *The Blitz++ meta-template library*, <http://blitz.sourceforge.net/>, Accessed: 27/01/2015.
- [212] J. Borchardt, H. Gies, and R. Sondenheimer, *Global flow of the Higgs potential in a Yukawa model*, Eur. Phys. J. **C76** (2016), 472, DOI: 10.1140/epjc/s10052-016-4300-9, arXiv: 1603.05861 [hep-ph].

- [213] J. Borchardt and A. Eichhorn, *Universal behavior of coupled order parameters below three dimensions*, Phys. Rev. **E94** (2016), 042105, DOI: 10.1103/PhysRevE.94.042105, arXiv: 1606.07449 [cond-mat.stat-mech].
- [214] K. G. Wilson and M. E. Fisher, *Critical Exponents in 3.99 Dimensions*, Phys. Rev. Lett. **28** (4 Jan. 1972), 240–243, DOI: 10.1103/PhysRevLett.28.240.
- [215] N. Tetradis and C. Wetterich, *Critical exponents from effective average action*, Nucl.Phys. **B422** (1994), 541–592, DOI: 10.1016/0550-3213(94)90446-4, arXiv: hep-ph/9308214 [hep-ph].
- [216] T. R. Morris and M. D. Turner, *Derivative expansion of the renormalization group in  $O(N)$  scalar field theory*, Nucl.Phys. **B509** (1998), 637–661, DOI: 10.1016/S0550-3213(97)00640-8, arXiv: hep-th/9704202 [hep-th].
- [217] J. Berges, N. Tetradis, and C. Wetterich, *Nonperturbative renormalization flow in quantum field theory and statistical physics*, Phys. Rept. **363** (2002), 223–386, DOI: 10.1016/S0370-1573(01)00098-9, arXiv: hep-ph/0005122 [hep-ph].
- [218] L. Canet, B. Delamotte, D. Mouhanna, and J. Vidal, *Optimization of the derivative expansion in the nonperturbative renormalization group*, Phys. Rev. **D67** (2003), 065004, DOI: 10.1103/PhysRevD.67.065004, arXiv: hep-th/0211055 [hep-th].
- [219] L. Canet, B. Delamotte, D. Mouhanna, and J. Vidal, *Nonperturbative renormalization group approach to the Ising model: A Derivative expansion at order partial\*\*4*, Phys. Rev. **B68** (2003), 064421, DOI: 10.1103/PhysRevB.68.064421, arXiv: hep-th/0302227 [hep-th].
- [220] C. Bervillier, A. Juttner, and D. F. Litim, *High-accuracy scaling exponents in the local potential approximation*, Nucl.Phys. **B783** (2007), 213–226, DOI: 10.1016/j.nuclphysb.2007.03.036, arXiv: hep-th/0701172 [hep-th].
- [221] F. Benitez et al., *Solutions of renormalization group flow equations with full momentum dependence*, Phys.Rev. **E80** (2009), 030103, DOI: 10.1103/PhysRevE.80.030103, arXiv: 0901.0128 [cond-mat.stat-mech].
- [222] D. F. Litim and D. Zappala, *Ising exponents from the functional renormalisation group*, Phys.Rev. **D83** (2011), 085009, DOI: 10.1103/PhysRevD.83.085009, arXiv: 1009.1948 [hep-th].
- [223] P. Mati, *Vanishing beta function curves from the functional renormalization group*, Phys. Rev. **D91** (2015), 125038, DOI: 10.1103/PhysRevD.91.125038, arXiv: 1501.00211 [hep-th].
- [224] I. Boettcher, *Scaling relations and multicritical phenomena from Functional Renormalization*, Phys. Rev. **E91** (2015), 062112, DOI: 10.1103/PhysRevE.91.062112, arXiv: 1503.07817 [cond-mat.stat-mech].
- [225] A. Pelissetto and E. Vicari, *Critical phenomena and renormalization group theory*, Phys.Rept. **368** (2002), 549–727, DOI: 10.1016/S0370-1573(02)00219-3, arXiv: cond-mat/0012164 [cond-mat].
- [226] D. F. Litim, *Optimized renormalization group flows*, Phys.Rev. **D64** (2001), 105007, DOI: 10.1103/PhysRevD.64.105007, arXiv: hep-th/0103195 [hep-th].
- [227] M. Hasenbusch, *Finite size scaling study of lattice models in the three-dimensional Ising universality class*, Phys. Rev. B **82** (17 Nov. 2010), 174433, DOI: 10.1103/PhysRevB.82.174433.

- [228] F. Benitez et al., *Non-perturbative renormalization group preserving full-momentum dependence: implementation and quantitative evaluation*, Phys.Rev. **E85** (2012), 026707, DOI: 10.1103/PhysRevE.85.026707, arXiv: 1110.2665 [cond-mat.stat-mech].
- [229] M. Hasenbusch and E. Vicari, *Anisotropic perturbations in three-dimensional  $O(N)$ -symmetric vector models*, Phys. Rev. B **84** (12 Sept. 2011), 125136, DOI: 10.1103/PhysRevB.84.125136.
- [230] F. Kos, D. Poland, D. Simmons-Duffin, and A. Vichi, *Precision islands in the Ising and  $O(N)$  models*, JHEP **08** (2016), 036, DOI: 10.1007/JHEP08(2016)036, arXiv: 1603.04436 [hep-th].
- [231] R. L. Arnowitt, S. Deser, and C. W. Misner, *Dynamical Structure and Definition of Energy in General Relativity*, Phys. Rev. **116** (1959), 1322–1330, DOI: 10.1103/PhysRev.116.1322.
- [232] R. L. Arnowitt, S. Deser, and C. W. Misner, *The Dynamics of general relativity*, Gen. Rel. Grav. **40** (2008), 1997–2027, DOI: 10.1007/s10714-008-0661-1, arXiv: gr-qc/0405109 [gr-qc].
- [233] E. Manrique, S. Rechenberger, and F. Saueressig, *Asymptotically Safe Lorentzian Gravity*, Phys. Rev. Lett. **106** (2011), 251302, DOI: 10.1103/PhysRevLett.106.251302, arXiv: 1102.5012 [hep-th].
- [234] S. Rechenberger and F. Saueressig, *A functional renormalization group equation for foliated spacetimes*, JHEP **03** (2013), 010, DOI: 10.1007/JHEP03(2013)010, arXiv: 1212.5114 [hep-th].
- [235] J. Biemans, A. Platania, and F. Saueressig, *Quantum gravity on foliated spacetime - asymptotically safe and sound* (2016), arXiv: 1609.04813 [hep-th].
- [236] J. Biemans, A. Platania, and F. Saueressig, *Renormalization group fixed points of foliated gravity-matter systems* (2017), arXiv: 1702.06539 [hep-th].
- [237] W. B. Houthoff, A. Kurov, and F. Saueressig, *Impact of topology in foliated Quantum Einstein Gravity* (2017), arXiv: 1705.01848 [hep-th].
- [238] M. H. Goroff and A. Sagnotti, *QUANTUM GRAVITY AT TWO LOOPS*, Phys. Lett. **B160** (1985), 81–86, DOI: 10.1016/0370-2693(85)91470-4.
- [239] M. H. Goroff and A. Sagnotti, *The Ultraviolet Behavior of Einstein Gravity*, Nucl. Phys. **B266** (1986), 709–736, DOI: 10.1016/0550-3213(86)90193-8.
- [240] A. E. M. van de Ven, *Two loop quantum gravity*, Nucl. Phys. **B378** (1992), 309–366, DOI: 10.1016/0550-3213(92)90011-Y.
- [241] A. Ashtekar, *The Winding road to quantum gravity*, Curr. Sci. **88** (2005), 2064–2074.
- [242] H. W. Hamber, *Quantum gravitation: The Feynman path integral approach*, Berlin: Springer, 2009, DOI: 10.1007/978-3-540-85293-3.
- [243] C. Kiefer, *Quantum gravity*, vol. 155, International series of monographs on physics, Oxford, UK: Oxford Univ. Pr., 2012.
- [244] K. G. Wilson, *Quantum field theory models in less than four-dimensions*, Phys. Rev. **D7** (1973), 2911–2926, DOI: 10.1103/PhysRevD.7.2911.

- [245] S. Weinberg, *Critical Phenomena for Field Theorists*, in: 14th International School of Subnuclear Physics: Understanding the Fundamental Constituents of Matter Erice, Italy, July 23-August 8, 1976, 1976, p. 1.
- [246] S. Weinberg, *ULTRAVIOLET DIVERGENCES IN QUANTUM THEORIES OF GRAVITATION*, in: General Relativity: An Einstein Centenary Survey, 1980, pp. 790–831.
- [247] M. Niedermaier and M. Reuter, *The Asymptotic Safety Scenario in Quantum Gravity*, Living Rev.Rel. **9** (2006), 5–173, DOI: 10.12942/lrr-2006-5.
- [248] A. Codello, R. Percacci, and C. Rahmede, *Investigating the Ultraviolet Properties of Gravity with a Wilsonian Renormalization Group Equation*, Annals Phys. **324** (2009), 414–469, DOI: 10.1016/j.aop.2008.08.008, arXiv: 0805.2909 [hep-th].
- [249] D. F. Litim, *Renormalisation group and the Planck scale*, Phil. Trans. Roy. Soc. Lond. **A369** (2011), 2759–2778, DOI: 10.1098/rsta.2011.0103, arXiv: 1102.4624 [hep-th].
- [250] M. Reuter and F. Saueressig, *Quantum Einstein Gravity*, New J. Phys. **14** (2012), 055022, DOI: 10.1088/1367-2630/14/5/055022, arXiv: 1202.2274 [hep-th].
- [251] O. Lauscher and M. Reuter, *Is quantum Einstein gravity nonperturbatively renormalizable?* Class. Quant. Grav. **19** (2002), 483–492, DOI: 10.1088/0264-9381/19/3/304, arXiv: hep-th/0110021 [hep-th].
- [252] A. Codello and R. Percacci, *Fixed points of higher derivative gravity*, Phys. Rev. Lett. **97** (2006), 221301, DOI: 10.1103/PhysRevLett.97.221301, arXiv: hep-th/0607128 [hep-th].
- [253] A. Codello, R. Percacci, and C. Rahmede, *Ultraviolet properties of  $f(R)$ -gravity*, Int. J. Mod. Phys. **A23** (2008), 143–150, DOI: 10.1142/S0217751X08038135, arXiv: 0705.1769 [hep-th].
- [254] P. F. Machado and F. Saueressig, *On the renormalization group flow of  $f(R)$ -gravity*, Phys. Rev. **D77** (2008), 124045, DOI: 10.1103/PhysRevD.77.124045, arXiv: 0712.0445 [hep-th].
- [255] A. Bonanno, A. Contillo, and R. Percacci, *Inflationary solutions in asymptotically safe  $f(R)$  theories*, Class. Quant. Grav. **28** (2011), 145026, DOI: 10.1088/0264-9381/28/14/145026, arXiv: 1006.0192 [gr-qc].
- [256] D. Benedetti, P. F. Machado, and F. Saueressig, *Asymptotic safety in higher-derivative gravity*, Mod. Phys. Lett. **A24** (2009), 2233–2241, DOI: 10.1142/S0217732309031521, arXiv: 0901.2984 [hep-th].
- [257] D. Benedetti, P. F. Machado, and F. Saueressig, *Taming perturbative divergences in asymptotically safe gravity*, Nucl. Phys. **B824** (2010), 168–191, DOI: 10.1016/j.nuclphysb.2009.08.023, arXiv: 0902.4630 [hep-th].
- [258] S. Rechenberger and F. Saueressig, *The  $R^2$  phase-diagram of QEG and its spectral dimension*, Phys. Rev. **D86** (2012), 024018, DOI: 10.1103/PhysRevD.86.024018, arXiv: 1206.0657 [hep-th].
- [259] M. Demmel, F. Saueressig, and O. Zanusso, *A proper fixed functional for four-dimensional Quantum Einstein Gravity*, JHEP **08** (2015), 113, DOI: 10.1007/JHEP08(2015)113, arXiv: 1504.07656 [hep-th].

- [260] A. Eichhorn, H. Gies, and M. M. Scherer, *Asymptotically free scalar curvature-ghost coupling in Quantum Einstein Gravity*, Phys. Rev. **D80** (2009), 104003, DOI: 10.1103/PhysRevD.80.104003, arXiv: 0907.1828 [hep-th].
- [261] K. Groh and F. Saueressig, *Ghost wave-function renormalization in Asymptotically Safe Quantum Gravity*, J. Phys. **A43** (2010), 365403, DOI: 10.1088/1751-8113/43/36/365403, arXiv: 1001.5032 [hep-th].
- [262] A. Eichhorn and H. Gies, *Ghost anomalous dimension in asymptotically safe quantum gravity*, Phys. Rev. **D81** (2010), 104010, DOI: 10.1103/PhysRevD.81.104010, arXiv: 1001.5033 [hep-th].
- [263] A. Nink and M. Reuter, *On the physical mechanism underlying Asymptotic Safety*, JHEP **01** (2013), 062, DOI: 10.1007/JHEP01(2013)062, arXiv: 1208.0031 [hep-th].
- [264] D. Becker and M. Reuter, *Towards a C-function in 4D quantum gravity*, JHEP **03** (2015), 065, DOI: 10.1007/JHEP03(2015)065, arXiv: 1412.0468 [hep-th].
- [265] G. 't Hooft and M. J. G. Veltman, *One loop divergencies in the theory of gravitation*, Ann. Inst. H. Poincaré Phys. Théor. **A20** (1974), 69–94.
- [266] D. Benedetti, K. Groh, P. F. Machado, and F. Saueressig, *The Universal RG Machine*, JHEP **1106** (2011), 079, DOI: 10.1007/JHEP06(2011)079, arXiv: 1012.3081 [hep-th].
- [267] A. O. Barvinsky and G. A. Vilkovisky, *The Generalized Schwinger-Dewitt Technique in Gauge Theories and Quantum Gravity*, Phys. Rept. **119** (1985), 1–74, DOI: 10.1016/0370-1573(85)90148-6.
- [268] D. V. Vassilevich, *Heat kernel expansion: User's manual*, Phys. Rept. **388** (2003), 279–360, DOI: 10.1016/j.physrep.2003.09.002, arXiv: hep-th/0306138 [hep-th].
- [269] Y. Decanini and A. Folacci, *Off-diagonal coefficients of the Dewitt-Schwinger and Hadamard representations of the Feynman propagator*, Phys. Rev. **D73** (2006), 044027, DOI: 10.1103/PhysRevD.73.044027, arXiv: gr-qc/0511115 [gr-qc].
- [270] D. Anselmi and A. Benini, *Improved Schwinger-DeWitt techniques for higher-derivative corrections to operator determinants*, JHEP **10** (2007), 099, DOI: 10.1088/1126-6708/2007/10/099, arXiv: 0704.2840 [hep-th].
- [271] K. Groh, S. Rechenberger, F. Saueressig, and O. Zanusso, *Higher Derivative Gravity from the Universal Renormalization Group Machine*, PoS **EPS-HEP2011** (2011), 124, arXiv: 1111.1743 [hep-th].
- [272] K. Groh, F. Saueressig, and O. Zanusso, *Off-diagonal heat-kernel expansion and its application to fields with differential constraints* (2011), arXiv: 1112.4856 [math-ph].
- [273] A. Nink, *Field Parametrization Dependence in Asymptotically Safe Quantum Gravity*, Phys. Rev. **D91** (2015), 044030, DOI: 10.1103/PhysRevD.91.044030, arXiv: 1410.7816 [hep-th].
- [274] M. Demmel and A. Nink, *Connections and geodesics in the space of metrics*, Phys. Rev. **D92** (2015), 104013, DOI: 10.1103/PhysRevD.92.104013, arXiv: 1506.03809 [gr-qc].
- [275] R. Percacci and G. P. Vacca, *Search of scaling solutions in scalar-tensor gravity* (2015), arXiv: 1501.00888 [hep-th].

- [276] K. Falls, *Critical scaling in quantum gravity from the renormalisation group* (2015), arXiv: 1503.06233 [hep-th].
- [277] K. Falls, *Renormalization of Newton's constant*, Phys. Rev. **D92** (2015), 124057, DOI: 10.1103/PhysRevD.92.124057, arXiv: 1501.05331 [hep-th].
- [278] P. Labus, R. Percacci, and G. P. Vacca, *Asymptotic safety in  $O(N)$  scalar models coupled to gravity*, Phys. Lett. **B753** (2016), 274–281, DOI: 10.1016/j.physletb.2015.12.022, arXiv: 1505.05393 [hep-th].
- [279] M. Reuter and F. Saueressig, *Renormalization group flow of quantum gravity in the Einstein-Hilbert truncation*, Phys. Rev. **D65** (2002), 065016, DOI: 10.1103/PhysRevD.65.065016, arXiv: hep-th/0110054 [hep-th].
- [280] S. R. Coleman, J. Wess, and B. Zumino, *Structure of phenomenological Lagrangians. 1*, Phys. Rev. **177** (1969), 2239–2247, DOI: 10.1103/PhysRev.177.2239.
- [281] R. E. Kallosh and I. V. Tyutin, *The Equivalence theorem and gauge invariance in renormalizable theories*, Yad. Fiz. **17** (1973), [Sov. J. Nucl. Phys.17,98(1973)], 190–209.
- [282] G. 't Hooft and M. J. G. Veltman, *DIAGRAMMAR*, NATO Sci. Ser. B **4** (1974), 177–322.
- [283] J. Zinn-Justin, *Quantum field theory and critical phenomena*, Int. Ser. Monogr. Phys. **113** (2002), 1–1054.
- [284] R. Jackiw, *Functional evaluation of the effective potential*, Phys. Rev. **D9** (1974), 1686, DOI: 10.1103/PhysRevD.9.1686.
- [285] N. K. Nielsen, *On the Gauge Dependence of Spontaneous Symmetry Breaking in Gauge Theories*, Nucl. Phys. **B101** (1975), 173–188, DOI: 10.1016/0550-3213(75)90301-6.
- [286] P. M. Stevenson, *Optimized Perturbation Theory*, Phys. Rev. **D23** (1981), 2916, DOI: 10.1103/PhysRevD.23.2916.
- [287] R. D. Ball, P. E. Haagensen, I. Latorre Jose, and E. Moreno, *Scheme independence and the exact renormalization group*, Phys. Lett. **B347** (1995), 80–88, DOI: 10.1016/0370-2693(95)00025-G, arXiv: hep-th/9411122 [hep-th].
- [288] B. S. DeWitt, *The global approach to quantum field theory. Vol. 1, 2*, Int. Ser. Monogr. Phys. **114** (2003), 1–1042.
- [289] H. Kawai, Y. Kitazawa, and M. Ninomiya, *Scaling exponents in quantum gravity near two-dimensions*, Nucl. Phys. **B393** (1993), 280–300, DOI: 10.1016/0550-3213(93)90246-L, arXiv: hep-th/9206081 [hep-th].
- [290] H. Kawai, Y. Kitazawa, and M. Ninomiya, *Quantum gravity in  $(2+\epsilon)$ -dimensions*, Prog. Theor. Phys. Suppl. **114** (1993), 149–174, DOI: 10.1143/PTPS.114.149.
- [291] H. Kawai, Y. Kitazawa, and M. Ninomiya, *Ultraviolet stable fixed point and scaling relations in  $(2+\epsilon)$ -dimensional quantum gravity*, Nucl. Phys. **B404** (1993), 684–716, DOI: 10.1016/0550-3213(93)90594-F, arXiv: hep-th/9303123 [hep-th].
- [292] T. Aida, Y. Kitazawa, H. Kawai, and M. Ninomiya, *Conformal invariance and renormalization group in quantum gravity near two-dimensions*, Nucl. Phys. **B427** (1994), 158–180, DOI: 10.1016/0550-3213(94)90273-9, arXiv: hep-th/9404171 [hep-th].



- [293] H. Kawai, Y. Kitazawa, and M. Ninomiya, *Renormalizability of quantum gravity near two-dimensions*, Nucl. Phys. **B467** (1996), 313–331, DOI: 10.1016/0550-3213(96)00119-8, arXiv: hep-th/9511217 [hep-th].
- [294] C. Kiefer, *Quantum gravity*, Int. Ser. Monogr. Phys. **124** (2004), [Int. Ser. Monogr. Phys.155,1(2012)], 1–308.
- [295] J. F. Donoghue, *Leading quantum correction to the Newtonian potential*, Phys. Rev. Lett. **72** (1994), 2996–2999, DOI: 10.1103/PhysRevLett.72.2996, arXiv: gr-qc/9310024 [gr-qc].
- [296] N. E. J Bjerrum-Bohr, J. F. Donoghue, and B. R. Holstein, *Quantum gravitational corrections to the nonrelativistic scattering potential of two masses*, Phys. Rev. **D67** (2003), [Erratum: Phys. Rev.D71,069903(2005)], 084033, DOI: 10.1103/PhysRevD.71.069903, 10.1103/PhysRevD.67.084033, arXiv: hep-th/0211072 [hep-th].
- [297] S. P. Robinson and F. Wilczek, *Gravitational correction to running of gauge couplings*, Phys. Rev. Lett. **96** (2006), 231601, DOI: 10.1103/PhysRevLett.96.231601, arXiv: hep-th/0509050 [hep-th].
- [298] U. Ellwanger, M. Hirsch, and A. Weber, *Flow equations for the relevant part of the pure Yang-Mills action*, Z. Phys. **C69** (1996), 687–698, DOI: 10.1007/s002880050073, arXiv: hep-th/9506019 [hep-th].
- [299] D. F. Litim and J. M. Pawłowski, *Flow equations for Yang-Mills theories in general axial gauges*, Phys.Lett. **B435** (1998), 181–188, DOI: 10.1016/S0370-2693(98)00761-8, arXiv: hep-th/9802064 [hep-th].
- [300] E. S. Fradkin and A. A. Tseytlin, *On the New Definition of Off-shell Effective Action*, Nucl. Phys. **B234** (1984), 509–523, DOI: 10.1016/0550-3213(84)90075-0.
- [301] G. A. Vilkovisky, *The Unique Effective Action in Quantum Field Theory*, Nucl. Phys. **B234** (1984), 125–137, DOI: 10.1016/0550-3213(84)90228-1.
- [302] C. P. Burgess and G. Kunstatter, *On the Physical Interpretation of the Vilkovisky-de Witt Effective Action*, Mod. Phys. Lett. **A2** (1987), [Erratum: Mod. Phys. Lett.A2,1003(1987)], 875, DOI: 10.1142/S0217732387001117.
- [303] G. Kunstatter, *The Path integral for gauge theories: A Geometrical approach*, Class. Quant. Grav. **9** (1992), S157–S168, DOI: 10.1088/0264-9381/9/S/009.
- [304] M. Demmel, F. Saueressig, and O. Zanusso, *RG flows of Quantum Einstein Gravity in the linear-geometric approximation* (2014), arXiv: 1412.7207 [hep-th].
- [305] D. Dou and R. Percacci, *The running gravitational couplings*, Class. Quant. Grav. **15** (1998), 3449–3468, DOI: 10.1088/0264-9381/15/11/011, arXiv: hep-th/9707239 [hep-th].
- [306] S. Gonzalez-Martin, T. R. Morris, and Z. H. Slade, *Asymptotic solutions in asymptotic safety* (2017), arXiv: 1704.08873 [hep-th].
- [307] D. F. Litim, *Critical exponents from optimized renormalization group flows*, Nucl.Phys. **B631** (2002), 128–158, DOI: 10.1016/S0550-3213(02)00186-4, arXiv: hep-th/0203006 [hep-th].
- [308] D. Benedetti, *Asymptotic safety goes on shell*, New J. Phys. **14** (2012), 015005, DOI: 10.1088/1367-2630/14/1/015005, arXiv: 1107.3110 [hep-th].

- [309] H. Gies, J. Jaeckel, and C. Wetterich, *Towards a renormalizable standard model without fundamental Higgs scalar*, Phys. Rev. **D69** (2004), 105008, DOI: 10.1103/PhysRevD.69.105008, arXiv: hep-ph/0312034 [hep-ph].
- [310] H. W. Hamber, *On the gravitational scaling dimensions*, Phys. Rev. **D61** (2000), 124008, DOI: 10.1103/PhysRevD.61.124008, arXiv: hep-th/9912246 [hep-th].
- [311] H. W. Hamber, *Scaling Exponents for Lattice Quantum Gravity in Four Dimensions*, Phys. Rev. **D92** (2015), 064017, DOI: 10.1103/PhysRevD.92.064017, arXiv: 1506.07795 [hep-th].
- [312] A. Eichhorn, *On unimodular quantum gravity*, Class. Quant. Grav. **30** (2013), 115016, DOI: 10.1088/0264-9381/30/11/115016, arXiv: 1301.0879 [gr-qc].
- [313] A. Eichhorn, *The Renormalization Group flow of unimodular  $f(R)$  gravity* (2015), arXiv: 1501.05848 [gr-qc].
- [314] S. Falkenberg and S. D. Odintsov, *Gauge dependence of the effective average action in Einstein gravity*, Int. J. Mod. Phys. **A13** (1998), 607–623, DOI: 10.1142/S0217751X98000263, arXiv: hep-th/9612019 [hep-th].
- [315] A. Bonanno and M. Reuter, *Cosmology of the Planck era from a renormalization group for quantum gravity*, Phys. Rev. **D65** (2002), 043508, DOI: 10.1103/PhysRevD.65.043508, arXiv: hep-th/0106133 [hep-th].
- [316] A. Bonanno and M. Reuter, *Cosmological perturbations in renormalization group derived cosmologies*, Int. J. Mod. Phys. **D13** (2004), 107–122, DOI: 10.1142/S0218271804003809, arXiv: astro-ph/0210472 [astro-ph].
- [317] M. Hindmarsh, D. Litim, and C. Rahmede, *Asymptotically Safe Cosmology*, JCAP **1107** (2011), 019, DOI: 10.1088/1475-7516/2011/07/019, arXiv: 1101.5401 [gr-qc].
- [318] B. Koch and I. Ramirez, *Exact renormalization group with optimal scale and its application to cosmology*, Class. Quant. Grav. **28** (2011), 055008, DOI: 10.1088/0264-9381/28/5/055008, arXiv: 1010.2799 [gr-qc].
- [319] A. Babic, B. Guberina, R. Horvat, and H. Stefancic, *Renormalization-group running cosmologies. A Scale-setting procedure*, Phys. Rev. **D71** (2005), 124041, DOI: 10.1103/PhysRevD.71.124041, arXiv: astro-ph/0407572 [astro-ph].
- [320] M. Reuter and F. Saueressig, *From big bang to asymptotic de Sitter: Complete cosmologies in a quantum gravity framework*, JCAP **0509** (2005), 012, DOI: 10.1088/1475-7516/2005/09/012, arXiv: hep-th/0507167 [hep-th].
- [321] M. Reuter and F. Saueressig, *Asymptotic Safety, Fractals, and Cosmology*, Lect. Notes Phys. **863** (2013), 185–223, DOI: 10.1007/978-3-642-33036-0\_8, arXiv: 1205.5431 [hep-th].
- [322] A. Bonanno and F. Saueressig, *Asymptotically safe cosmology - a status report* (2017), arXiv: 1702.04137 [hep-th].
- [323] D. F. Litim, *Fixed points of quantum gravity*, Phys. Rev. Lett. **92** (2004), 201301, DOI: 10.1103/PhysRevLett.92.201301, arXiv: hep-th/0312114 [hep-th].
- [324] P. Fischer and D. F. Litim, *Fixed points of quantum gravity in extra dimensions*, Phys. Lett. **B638** (2006), 497–502, DOI: 10.1016/j.physletb.2006.05.073, arXiv: hep-th/0602203 [hep-th].

- [325] A. Nink and M. Reuter, *On quantum gravity, Asymptotic Safety, and paramagnetic dominance* (2012), [Int. J. Mod. Phys.D22,1330008(2013)], 138–157, DOI: 10.1142/S0218271813300085, arXiv: 1212.4325 [hep-th].
- [326] C. S. Fischer and J. M. Pawłowski, *Uniqueness of infrared asymptotics in Landau gauge Yang-Mills theory II*, Phys. Rev. **D80** (2009), 025023, DOI: 10.1103/PhysRevD.80.025023, arXiv: 0903.2193 [hep-th].
- [327] D. Benedetti, *On the number of relevant operators in asymptotically safe gravity*, Europhys. Lett. **102** (2013), 20007, DOI: 10.1209/0295-5075/102/20007, arXiv: 1301.4422 [hep-th].
- [328] K. Falls, D. F. Litim, K. Nikolakopoulos, and C. Rahmede, *Further evidence for asymptotic safety of quantum gravity*, Phys. Rev. **D93** (2016), 104022, DOI: 10.1103/PhysRevD.93.104022, arXiv: 1410.4815 [hep-th].
- [329] S. Folkerts, D. F. Litim, and J. M. Pawłowski, *Asymptotic freedom of Yang-Mills theory with gravity*, Phys.Lett. **B709** (2012), 234–241, DOI: 10.1016/j.physletb.2012.02.002, arXiv: 1101.5552 [hep-th].
- [330] K. Falls, *Asymptotic safety and the cosmological constant*, JHEP **01** (2016), 069, DOI: 10.1007/JHEP01(2016)069, arXiv: 1408.0276 [hep-th].
- [331] C. Wetterich, *Gauge symmetry from decoupling*, Nucl. Phys. **B915** (2017), 135–167, DOI: 10.1016/j.nuclphysb.2016.12.008, arXiv: 1608.01515 [hep-th].
- [332] N. Christiansen and A. Eichhorn, *An asymptotically safe solution to the  $U(1)$  triviality problem* (2017), arXiv: 1702.07724 [hep-th].
- [333] D. C. Elias et al., *Dirac cones reshaped by interaction effects in suspended graphene*, Nature Physics **7** (July 2011), 701–704, DOI: 10.1038/nphys2049.
- [334] A. S. Mayorov et al., *How Close Can One Approach the Dirac Point in Graphene Experimentally?* Nano Letters **12** (2012), PMID: 22935053, 4629–4634, DOI: 10.1021/nl301922d, eprint: <http://dx.doi.org/10.1021/nl301922d>.
- [335] M. Rösner, C. Friedrich, S. Blügel, and T. O. Wehling, *Wannier function approach to realistic Coulomb interactions in layered materials and heterostructures*, Phys. Rev. B **92** (8 Aug. 2015), 085102, DOI: 10.1103/PhysRevB.92.085102.
- [336] M. V. Ulybyshev, P. V. Buividovich, M. I. Katsnelson, and M. I. Polikarpov, *Monte Carlo Study of the Semimetal-Insulator Phase Transition in Monolayer Graphene with a Realistic Interelectron Interaction Potential*, Phys. Rev. Lett. **111** (5 July 2013), 056801, DOI: 10.1103/PhysRevLett.111.056801.
- [337] D. Smith and L. von Smekal, *Monte Carlo simulation of the tight-binding model of graphene with partially screened Coulomb interactions*, Phys. Rev. B **89** (19 May 2014), 195429, DOI: 10.1103/PhysRevB.89.195429.
- [338] W. Wu and A.-M. S. Tremblay, *Phase diagram and Fermi liquid properties of the extended Hubbard model on the honeycomb lattice*, Phys. Rev. B **89** (20 May 2014), 205128, DOI: 10.1103/PhysRevB.89.205128.
- [339] J. Braun, H. Gies, and D. D. Scherer, *Asymptotic safety: a simple example*, Phys.Rev. **D83** (2011), 085012, DOI: 10.1103/PhysRevD.83.085012, arXiv: 1011.1456 [hep-th].

- [340] H. Gies, C. Gneiting, and R. Sondenheimer, *Higgs Mass Bounds from Renormalization Flow for a simple Yukawa model*, Phys.Rev. **D89** (2014), 045012, DOI: 10.1103/PhysRevD.89.045012, arXiv: 1308.5075 [hep-ph].
- [341] D. U. Jungnickel and C. Wetterich, *Effective action for the chiral quark-meson model*, Phys. Rev. **D53** (1996), 5142–5175, DOI: 10.1103/PhysRevD.53.5142, arXiv: hep-ph/9505267 [hep-ph].
- [342] B.-J. Schaefer and J. Wambach, *The Phase diagram of the quark meson model*, Nucl. Phys. **A757** (2005), 479–492, DOI: 10.1016/j.nuclphysa.2005.04.012, arXiv: nucl-th/0403039 [nucl-th].
- [343] J. Braun, B. Klein, H. J. Pirner, and A. H. Rezaeian, *Volume and quark mass dependence of the chiral phase transition*, Phys. Rev. **D73** (2006), 074010, DOI: 10.1103/PhysRevD.73.074010, arXiv: hep-ph/0512274 [hep-ph].
- [344] B.-J. Schaefer and J. Wambach, *Renormalization group approach towards the QCD phase diagram*, Phys. Part. Nucl. **39** (2008), 1025–1032, DOI: 10.1134/S1063779608070083, arXiv: hep-ph/0611191 [hep-ph].
- [345] J. Braun, B. Klein, and P. Piasecki, *On the scaling behavior of the chiral phase transition in QCD in finite and infinite volume*, Eur. Phys. J. **C71** (2011), 1576, DOI: 10.1140/epjc/s10052-011-1576-7, arXiv: 1008.2155 [hep-ph].
- [346] J. Braun, B. Klein, and B.-J. Schaefer, *On the Phase Structure of QCD in a Finite Volume*, Phys.Lett. **B713** (2012), 216–223, DOI: 10.1016/j.physletb.2012.05.053, arXiv: 1110.0849 [hep-ph].
- [347] T. K. Herbst, J. M. Pawłowski, and B.-J. Schaefer, *Phase structure and thermodynamics of QCD*, Phys. Rev. **D88** (2013), 014007, DOI: 10.1103/PhysRevD.88.014007, arXiv: 1302.1426 [hep-ph].
- [348] R.-A. Tripolt, J. Braun, B. Klein, and B.-J. Schaefer, *Effect of fluctuations on the QCD critical point in a finite volume*, Phys.Rev. **D90** (2014), 054012, DOI: 10.1103/PhysRevD.90.054012, arXiv: 1308.0164 [hep-ph].
- [349] R.-A. Tripolt, N. Strodthoff, L. von Smekal, and J. Wambach, *Spectral Functions for the Quark-Meson Model Phase Diagram from the Functional Renormalization Group*, Phys. Rev. **D89** (2014), 034010, DOI: 10.1103/PhysRevD.89.034010, arXiv: 1311.0630 [hep-ph].
- [350] J. M. Pawłowski and F. Rennecke, *Higher order quark-mesonic scattering processes and the phase structure of QCD*, Phys. Rev. **D90** (2014), 076002, DOI: 10.1103/PhysRevD.90.076002, arXiv: 1403.1179 [hep-ph].
- [351] I. Boettcher et al., *Sarma phase in relativistic and non-relativistic systems*, Phys. Lett. **B742** (2015), 86–93, DOI: 10.1016/j.physletb.2015.01.014, arXiv: 1409.5232 [cond-mat.quant-gas].
- [352] A. J. Helmboldt, J. M. Pawłowski, and N. Strodthoff, *Towards quantitative precision in the chiral crossover: masses and fluctuation scales*, Phys. Rev. **D91** (2015), 054010, DOI: 10.1103/PhysRevD.91.054010, arXiv: 1409.8414 [hep-ph].
- [353] D. J. Gross and A. Neveu, *Dynamical Symmetry Breaking in Asymptotically Free Field Theories*, Phys. Rev. **D10** (1974), 3235, DOI: 10.1103/PhysRevD.10.3235.
- [354] B. Rosenstein, H.-L. Yu, and A. Kovner, *Critical exponents of new universality classes*, Phys. Lett. **B314** (1993), 381–386, DOI: 10.1016/0370-2693(93)91253-J.

- [355] D. D. Scherer and H. Gies, *Renormalization Group Study of Magnetic Catalysis in the 3d Gross-Neveu Model*, Phys. Rev. **B85** (2012), 195417, DOI: 10.1103/PhysRevB.85.195417, arXiv: 1201.3746 [cond-mat.str-el].
- [356] K. Osterwalder and R. Schrader, *Axioms for Euclidean Green's functions*, Comm. Math. Phys. **31** (1973), 83–112.
- [357] F. Hofling, C. Nowak, and C. Wetterich, *Phase transition and critical behavior of the  $D = 3$  Gross-Neveu model*, Phys. Rev. **B66** (2002), 205111, DOI: 10.1103/PhysRevB.66.205111, arXiv: cond-mat/0203588 [cond-mat].
- [358] G. P. Vacca and L. Zambelli, *Multimeson Yukawa interactions at criticality*, Phys. Rev. **D91** (2015), 125003, DOI: 10.1103/PhysRevD.91.125003, arXiv: 1503.09136 [hep-th].
- [359] D. Kahaner, C. Moler, and S. Nash, *Numerical Methods and Software*, Prentice Hall, 1989.
- [360] D. F. Litim, *Optimization of the exact renormalization group*, Phys. Lett. **B486** (2000), 92–99, DOI: 10.1016/S0370-2693(00)00748-6, arXiv: hep-th/0005245 [hep-th].
- [361] D. F. Litim, *Mind the gap*, Int. J. Mod. Phys. **A16** (2001), 2081–2088, DOI: 10.1142/S0217751X01004748, arXiv: hep-th/0104221 [hep-th].
- [362] L. Canet, *Optimization of field-dependent nonperturbative renormalization group flows*, Phys. Rev. **B71** (2005), 012418, DOI: 10.1103/PhysRevB.71.012418, arXiv: hep-th/0409300 [hep-th].
- [363] D. F. Litim, *Universality and the renormalisation group*, JHEP **07** (2005), 005, DOI: 10.1088/1126-6708/2005/07/005, arXiv: hep-th/0503096 [hep-th].
- [364] C. S. Fischer, A. Maas, and J. M. Pawłowski, *On the infrared behavior of Landau gauge Yang-Mills theory*, Annals Phys. **324** (2009), 2408–2437, DOI: 10.1016/j.aop.2009.07.009, arXiv: 0810.1987 [hep-ph].
- [365] J. M. Pawłowski, M. M. Scherer, R. Schmidt, and S. J. Wetzel, *Physics and the choice of regulators in functional renormalisation group flows* (2015), arXiv: 1512.03598 [hep-th].
- [366] L. Fei, S. Giombi, I. R. Klebanov, and G. Tarnopolsky, *Yukawa CFTs and Emergent Supersymmetry* (2016), arXiv: 1607.05316 [hep-th].
- [367] J. A. Gracey, *Three loop calculations in the  $O(N)$  Gross-Neveu model*, Nucl. Phys. **B341** (1990), 403–418, DOI: 10.1016/0550-3213(90)90186-H.
- [368] J. A. Gracey, *Computation of the three loop Beta function of the  $O(N)$  Gross-Neveu model in minimal subtraction*, Nucl. Phys. **B367** (1991), 657–674, DOI: 10.1016/0550-3213(91)90012-M.
- [369] C. Luperini and P. Rossi, *Three loop Beta function(s) and effective potential in the Gross-Neveu model*, Annals Phys. **212** (1991), 371–401, DOI: 10.1016/0003-4916(91)90120-W.
- [370] J. A. Gracey, T. Luthe, and Y. Schroder, *Four loop renormalization of the Gross-Neveu model* (2016), arXiv: 1609.05071 [hep-th].
- [371] S. Chandrasekharan and A. Li, *Quantum critical behavior in three dimensional lattice Gross-Neveu models*, Phys. Rev. **D88** (2013), 021701, DOI: 10.1103/PhysRevD.88.021701, arXiv: 1304.7761 [hep-lat].

- [372] L. Karkkainen, R. Lacaze, P. Lacock, and B. Petersson, *Critical behavior of the 3-d Gross-Neveu and Higgs-Yukawa models*, Nucl.Phys. **B415** (1994), 781–796, DOI: 10.1016/0550-3213(94)90309-3, arXiv: hep-lat/9310020 [hep-lat].
- [373] J. Gracey, *Computation of critical exponent  $\eta$  at  $O(1/N^{**3})$  in the four Fermi model in arbitrary dimensions*, Int.J.Mod.Phys. **A9** (1994), 727–744, DOI: 10.1142/S0217751X94000340, arXiv: hep-th/9306107 [hep-th].
- [374] L. Iliesiu, F. Kos, D. Poland, S. S. Pufu, and D. Simmons-Duffin, *Bootstrapping 3D Fermions with Global Symmetries* (2017), arXiv: 1705.03484 [hep-th].
- [375] L. Wang, P. Corboz, and M. Troyer, *Fermionic Quantum Critical Point of Spinless Fermions on a Honeycomb Lattice*, New J. Phys. **16** (2014), 103008, DOI: 10.1088/1367-2630/16/10/103008, arXiv: 1407.0029 [cond-mat.str-el].
- [376] J. A. Gracey, *Computation of Beta-prime ( $g(c)$ ) at  $O(1/N^{**2})$  in the  $O(N)$  Gross-Neveu model in arbitrary dimensions*, Int. J. Mod. Phys. **A9** (1994), 567–590, DOI: 10.1142/S0217751X94000285, arXiv: hep-th/9306106 [hep-th].
- [377] H. Gies, F. Synatschke, and A. Wipf, *Supersymmetry breaking as a quantum phase transition*, Phys. Rev. **D80** (2009), 101701, DOI: 10.1103/PhysRevD.80.101701, arXiv: 0906.5492 [hep-th].
- [378] F. Synatschke, H. Gies, and A. Wipf, *Phase Diagram and Fixed-Point Structure of two dimensional  $N=1$  Wess-Zumino Models*, Phys. Rev. **D80** (2009), 085007, DOI: 10.1103/PhysRevD.80.085007, arXiv: 0907.4229 [hep-th].
- [379] F. Synatschke, J. Braun, and A. Wipf,  *$N=1$  Wess Zumino Model in  $d=3$  at zero and finite temperature*, Phys. Rev. **D81** (2010), 125001, DOI: 10.1103/PhysRevD.81.125001, arXiv: 1001.2399 [hep-th].
- [380] F. Synatschke, G. Bergner, H. Gies, and A. Wipf, *Flow Equation for Supersymmetric Quantum Mechanics*, JHEP **03** (2009), 028, DOI: 10.1088/1126-6708/2009/03/028, arXiv: 0809.4396 [hep-th].
- [381] F. Synatschke-Czerwonka, T. Fischbacher, and G. Bergner, *The two dimensional  $N = (2,2)$  Wess-Zumino Model in the Functional Renormalization Group Approach*, Phys. Rev. **D82** (2010), 085003, DOI: 10.1103/PhysRevD.82.085003, arXiv: 1006.1823 [hep-th].
- [382] D. F. Litim, M. C. Mastaler, F. Synatschke-Czerwonka, and A. Wipf, *Critical behavior of supersymmetric  $O(N)$  models in the large- $N$  limit*, Phys. Rev. **D84** (2011), 125009, DOI: 10.1103/PhysRevD.84.125009, arXiv: 1107.3011 [hep-th].
- [383] M. Heilmann, D. F. Litim, F. Synatschke-Czerwonka, and A. Wipf, *Phases of supersymmetric  $O(N)$  theories*, Phys. Rev. **D86** (2012), 105006, DOI: 10.1103/PhysRevD.86.105006, arXiv: 1208.5389 [hep-th].
- [384] T. Hellwig, A. Wipf, and O. Zanusso, *Scaling and superscaling solutions from the functional renormalization group*, Phys. Rev. **D92** (2015), 085027, DOI: 10.1103/PhysRevD.92.085027, arXiv: 1508.02547 [hep-th].
- [385] A. Wipf, *Non-perturbative methods in supersymmetric theories* (2005), arXiv: hep-th/0504180 [hep-th].
- [386] L. N. Mihaila, N. Zerf, B. Ihrig, I. F. Herbut, and M. M. Scherer, *Gross-Neveu-Yukawa model at three loops and Ising critical behavior of Dirac systems* (2017), arXiv: 1703.08801 [cond-mat.str-el].

- [387] L. Iliesiu et al., *Fermion-Scalar Conformal Blocks*, JHEP **04** (2016), 074, DOI: 10.1007/JHEP04(2016)074, arXiv: 1511.01497 [hep-th].
- [388] M. Thierfelder, S. Bernuzzi, and B. Bruegmann, *Numerical relativity simulations of binary neutron stars*, Phys. Rev. **D84** (2011), 044012, DOI: 10.1103/PhysRevD.84.044012, arXiv: 1104.4751 [gr-qc].
- [389] R. P. Macedo and M. Ansorg, *Axisymmetric fully spectral code for hyperbolic equations*, J.Comput.Phys. **276** (2014), 357–379, DOI: 10.1016/j.jcp.2014.07.040, arXiv: 1402.7343 [physics.comp-ph].
- [390] D. Hilditch, A. Weyhausen, and B. Brügmann, *Pseudospectral method for gravitational wave collapse*, Phys. Rev. **D93** (2016), 063006, DOI: 10.1103/PhysRevD.93.063006, arXiv: 1504.04732 [gr-qc].
- [391] M. Kalisch and M. Ansorg, *Pseudo-spectral construction of non-uniform black string solutions in five and six spacetime dimensions*, Class. Quant. Grav. **33** (2016), 215005, DOI: 10.1088/0264-9381/33/21/215005, arXiv: 1607.03099 [gr-qc].
- [392] M. Ammon, S. Griener, A. Jimenez-Alba, R. P. Macedo, and L. Melgar, *Holographic quenches and anomalous transport*, JHEP **09** (2016), 131, DOI: 10.1007/JHEP09(2016)131, arXiv: 1607.06817 [hep-th].
- [393] M. Ammon, M. Heinrich, A. Jiménez-Alba, and S. Moeckel, *Surface States in Holographic Weyl Semimetals* (2016), arXiv: 1612.00836 [hep-th].
- [394] M. Ammon, M. Kaminski, R. Koirala, J. Leiber, and J. Wu, *Quasinormal modes of charged magnetic black branes & chiral magnetic transport* (2017), arXiv: 1701.05565 [hep-th].
- [395] I. D. Saltas, *Higgs inflation and quantum gravity: An exact renormalisation group approach* (2015), arXiv: 1512.06134 [hep-th].
- [396] R. Percacci and D. Perini, *Constraints on matter from asymptotic safety*, Phys. Rev. **D67** (2003), 081503, DOI: 10.1103/PhysRevD.67.081503, arXiv: hep-th/0207033 [hep-th].
- [397] R. Percacci and D. Perini, *Asymptotic safety of gravity coupled to matter*, Phys. Rev. **D68** (2003), 044018, DOI: 10.1103/PhysRevD.68.044018, arXiv: hep-th/0304222 [hep-th].
- [398] O. Zanusso, L. Zambelli, G. P. Vacca, and R. Percacci, *Gravitational corrections to Yukawa systems*, Phys. Lett. **B689** (2010), 90–94, DOI: 10.1016/j.physletb.2010.04.043, arXiv: 0904.0938 [hep-th].
- [399] J.-E. Daum, U. Harst, and M. Reuter, *Running Gauge Coupling in Asymptotically Safe Quantum Gravity*, JHEP **01** (2010), 084, DOI: 10.1007/JHEP01(2010)084, arXiv: 0910.4938 [hep-th].
- [400] G. Narain and R. Percacci, *Renormalization Group Flow in Scalar-Tensor Theories. I*, Class.Quant.Grav. **27** (2010), 075001, DOI: 10.1088/0264-9381/27/7/075001, arXiv: 0911.0386 [hep-th].
- [401] G. P. Vacca and O. Zanusso, *Asymptotic Safety in Einstein Gravity and Scalar-Fermion Matter*, Phys. Rev. Lett. **105** (2010), 231601, DOI: 10.1103/PhysRevLett.105.231601, arXiv: 1009.1735 [hep-th].
- [402] U. Harst and M. Reuter, *QED coupled to QEG*, JHEP **1105** (2011), 119, DOI: 10.1007/JHEP05(2011)119, arXiv: 1101.6007 [hep-th].

- [403] A. Eichhorn and H. Gies, *Light fermions in quantum gravity*, New J.Phys. **13** (2011), 125012, DOI: 10.1088/1367-2630/13/12/125012, arXiv: 1104.5366 [hep-th].
- [404] P. Dona and R. Percacci, *Functional renormalization with fermions and tetrads*, Phys. Rev. **D87** (2013), 045002, DOI: 10.1103/PhysRevD.87.045002, arXiv: 1209.3649 [hep-th].
- [405] B. Dobrich and A. Eichhorn, *Can we see quantum gravity? Photons in the asymptotic-safety scenario*, JHEP **06** (2012), 156, DOI: 10.1007/JHEP06(2012)156, arXiv: 1203.6366 [gr-qc].
- [406] A. Eichhorn, *Quantum-gravity-induced matter self-interactions in the asymptotic-safety scenario*, Phys. Rev. **D86** (2012), 105021, DOI: 10.1103/PhysRevD.86.105021, arXiv: 1204.0965 [gr-qc].
- [407] P. Donà, A. Eichhorn, and R. Percacci, *Matter matters in asymptotically safe quantum gravity*, Phys.Rev. **D89** (2014), 084035, DOI: 10.1103/PhysRevD.89.084035, arXiv: 1311.2898 [hep-th].
- [408] T. Henz, J. M. Pawłowski, A. Rodigast, and C. Wetterich, *Dilaton Quantum Gravity*, Phys.Lett. **B727** (2013), 298–302, DOI: 10.1016/j.physletb.2013.10.015, arXiv: 1304.7743 [hep-th].
- [409] A. Eichhorn and M. M. Scherer, *Planck scale, Higgs mass, and scalar dark matter*, Phys. Rev. **D90** (2014), 025023, DOI: 10.1103/PhysRevD.90.025023, arXiv: 1404.5962 [hep-ph].
- [410] P. Donà, A. Eichhorn, P. Labus, and R. Percacci, *Asymptotic safety in an interacting system of gravity and scalar matter*, Phys. Rev. **D93** (2016), [Erratum: Phys. Rev.D93,no.12,129904(2016)], 044049, DOI: 10.1103/PhysRevD.93.129904, 10.1103/PhysRevD.93.044049, arXiv: 1512.01589 [gr-qc].
- [411] J. Meibohm, J. M. Pawłowski, and M. Reichert, *Asymptotic safety of gravity-matter systems*, Phys. Rev. **D93** (2016), 084035, DOI: 10.1103/PhysRevD.93.084035, arXiv: 1510.07018 [hep-th].
- [412] A. Eichhorn, A. Held, and J. M. Pawłowski, *Quantum-gravity effects on a Higgs-Yukawa model*, Phys. Rev. **D94** (2016), 104027, DOI: 10.1103/PhysRevD.94.104027, arXiv: 1604.02041 [hep-th].
- [413] J. Meibohm and J. M. Pawłowski, *Chiral fermions in asymptotically safe quantum gravity*, Eur. Phys. J. **C76** (2016), 285, DOI: 10.1140/epjc/s10052-016-4132-7, arXiv: 1601.04597 [hep-th].
- [414] A. Eichhorn and S. Lippoldt, *Quantum gravity and Standard-Model-like fermions*, Phys. Lett. **B767** (2017), 142–146, DOI: 10.1016/j.physletb.2017.01.064, arXiv: 1611.05878 [gr-qc].
- [415] T. Henz, J. M. Pawłowski, and C. Wetterich, *Scaling solutions for Dilaton Quantum Gravity* (2016), DOI: 10.1016/j.physletb.2017.01.057, arXiv: 1605.01858 [hep-th].
- [416] A. Eichhorn and A. Held, *Viability of quantum-gravity induced ultraviolet completions for matter* (2017), arXiv: 1705.02342 [gr-qc].
- [417] N. Christiansen, A. Eichhorn, and A. Held, *Is scale-invariance in gauge-Yukawa systems compatible with the graviton?* (2017), arXiv: 1705.01858 [hep-th].



- [418] N. Tetradis and D. F. Litim, *Analytical solutions of exact renormalization group equations*, Nucl. Phys. **B464** (1996), 492–511, DOI: 10.1016/0550-3213(95)00642-7, arXiv: hep-th/9512073 [hep-th].
- [419] D. F. Litim, J. M. Pawłowski, and L. Vergara, *Convexity of the effective action from functional flows* (2006), arXiv: hep-th/0602140 [hep-th].
- [420] M. Peláez and N. Wschebor, *The ordered phase of  $O(N)$  model within the Non-Perturbative Renormalization Group* (2015), arXiv: 1510.05709 [cond-mat.stat-mech].
- [421] A. Bonanno and G. Lacagnina, *Spontaneous symmetry breaking and proper time flow equations*, Nucl. Phys. **B693** (2004), 36–50, DOI: 10.1016/j.nuclphysb.2004.06.003, arXiv: hep-th/0403176 [hep-th].
- [422] A. Codello and G. D’Odorico,  *$O(N)$ -Universality Classes and the Mermin-Wagner Theorem*, Phys.Rev.Lett. **110** (2013), 141601, DOI: 10.1103/PhysRevLett.110.141601, arXiv: 1210.4037 [hep-th].
- [423] A. Codello, *Scaling Solutions in Continuous Dimension*, J.Phys. **A45** (2012), 465006, DOI: 10.1088/1751-8113/45/46/465006, arXiv: 1204.3877 [hep-th].
- [424] A. Codello, N. Defenu, and G. D’Odorico, *Critical exponents of  $O(N)$  models in fractional dimensions*, Phys. Rev. **D91** (2015), 105003, DOI: 10.1103/PhysRevD.91.105003, arXiv: 1410.3308 [hep-th].
- [425] G. Pöschl and E. Teller, *Bemerkungen zur Quantenmechanik des anharmonischen Oszillators*, Zeitschrift für Physik **83** (Mar. 1933), 143–151, DOI: 10.1007/bf01331132.
- [426] Y. Fujimoto, L. O’Raifeartaigh, and G. Parravicini, *Effective Potential for Nonconvex Potentials*, Nucl. Phys. **B212** (1983), 268, DOI: 10.1016/0550-3213(83)90305-X.
- [427] S. R. Coleman and E. J. Weinberg, *Radiative Corrections as the Origin of Spontaneous Symmetry Breaking*, Phys. Rev. **D7** (1973), 1888–1910, DOI: 10.1103/PhysRevD.7.1888.
- [428] T. L. Curtright and C. B. Thorn, *The Effective Potential in Quantum Mechanics*, J. Math. Phys. **25** (1984), 541, DOI: 10.1063/1.526204.
- [429] S. Coleman, *Aspects of Symmetry*, Cambridge Books Online, Cambridge University Press, 1985.
- [430] K. Symanzik, *Renormalizable models with simple symmetry breaking. 1. Symmetry breaking by a source term*, Commun. Math. Phys. **16** (1970), 48–80, DOI: 10.1007/BF01645494.
- [431] P. M. Stevenson, *The Gaussian Effective Potential. 1. Quantum Mechanics*, Phys. Rev. **D30** (1984), 1712, DOI: 10.1103/PhysRevD.30.1712.
- [432] A. S. Kapoyannis and N. Tetradis, *Quantum mechanical tunneling and the renormalization group*, Phys. Lett. **A276** (2000), 225–232, DOI: 10.1016/S0375-9601(00)00671-X, arXiv: hep-th/0010180 [hep-th].
- [433] W. Dittrich and H. Gies, *Probing the quantum vacuum. Perturbative effective action approach in quantum electrodynamics and its application*, Springer Tracts Mod. Phys. **166** (2000), 1–241, DOI: 10.1007/3-540-45585-X.
- [434] H. Gies and S. Lippoldt, *Fermions in gravity with local spin-base invariance*, Phys. Rev. **D89** (2014), 064040, DOI: 10.1103/PhysRevD.89.064040, arXiv: 1310.2509 [hep-th].

- [435] H. Gies and S. Lippoldt, *Global surpluses of spin-base invariant fermions*, Phys. Lett. **B743** (2015), 415–419, DOI: 10.1016/j.physletb.2015.03.014, arXiv: 1502.00918 [hep-th].
- [436] S. Lippoldt, *Spin-base invariance of Fermions in arbitrary dimensions*, Phys. Rev. **D91** (2015), 104006, DOI: 10.1103/PhysRevD.91.104006, arXiv: 1502.05607 [hep-th].
- [437] A. Salam and J. Strathdee, *Supergauge Transformations*, Nucl.Phys. **B76** (1974), 477–482, DOI: 10.1016/0550-3213(74)90537-9.
- [438] C. Wozar and A. Wipf, *Supersymmetry Breaking in Low Dimensional Models*, Annals Phys. **327** (2012), 774–807, DOI: 10.1016/j.aop.2011.11.015, arXiv: 1107.3324 [hep-lat].
- [439] E. Witten, *Dynamical Breaking of Supersymmetry*, Nucl. Phys. **B188** (1981), 513, DOI: 10.1016/0550-3213(81)90006-7.
- [440] M. Dine and J. D. Mason, *Supersymmetry and Its Dynamical Breaking*, Rept. Prog. Phys. **74** (2011), 056201, DOI: 10.1088/0034-4885/74/5/056201, arXiv: 1012.2836 [hep-th].
- [441] F. Synatschke, H. Gies, and A. Wipf, *The Phase Diagram for Wess-Zumino Models*, AIP Conf. Proc. **1200** (2010), 1097–1100, DOI: 10.1063/1.3327547, arXiv: 0909.4189 [hep-th].
- [442] D. Zappala, *Improving the renormalization group approach to the quantum mechanical double well potential*, Phys. Lett. **A290** (2001), 35–40, DOI: 10.1016/S0375-9601(01)00642-9, arXiv: quant-ph/0108019 [quant-ph].

# Lebenslauf

## Kontaktdaten

Name	Benjamin Knorr
Private Adresse	Wenigenjenaer Ufer 2 07749 Jena
Institutsadresse	Theoretisch-Physikalisches Insitut Friedrich-Schiller-Universität Jena Max-Wien-Platz 1 07743 Jena
E-mail	benjamin.knorr@uni-jena.de

## Stammdaten

Geburtsdatum	30. Dezember 1990
Geburtsort	Rodewisch
Staatsangehörigkeit	Deutsch

## Bildung

November 2013	M. Sc. Physik, Ruprecht-Karls-Universität Heidelberg
Juli 2011	B. Sc. Physik IPSP (International Physics Studies Program), Universität Leipzig
Juni 2008	Abitur, Goethe-Gymnasium Auerbach

# Veröffentlichungen

B. Knorr

“Ising and Gross-Neveu model in next-to-leading order”

Phys. Rev. B94, 245102 (2016) [arXiv:1609.03824]

J. Borchardt, B. Knorr

“Solving functional flow equations with pseudo-spectral methods”

Phys. Rev. D94, 025027 (2016) [arXiv:1603.06726]

H. Gies, B. Knorr, S. Lippoldt, F. Saueressig

“Gravitational Two-Loop Counterterm Is Asymptotically Safe”

Phys. Rev. Lett. 116, 211302 (2016) [arXiv:1601.01800]

H. Gies, B. Knorr, S. Lippoldt

“Generalized parametrization dependence in quantum gravity”

Phys. Rev. D92, 084020 (2015) [arXiv:1507.08859]

N. Christiansen, B. Knorr, J. Meibohm, J. M. Pawłowski, M. Reichert

“Local quantum gravity”

Phys. Rev. D92, 121501(R) (2015) [arXiv:1506.07016]

J. Borchardt, B. Knorr

“Global solutions to functional fixed point equations via pseudo-spectral methods”

Phys. Rev. D91, 105011 (2015) [arXiv:1502.07511],

Erratum: Phys. Rev. D93, 089904 (2016)

M. Heilmann, T. Hellwig, B. Knorr, M. Ansorg, A. Wipf

“Convergence of derivative expansion in supersymmetric functional RG flows”

JHEP 02, 109 (2015) [arXiv:1409.5650]

N. Christiansen, B. Knorr, J. M. Pawłowski, A. Rodigast

“Global flows in quantum gravity”

Phys. Rev. D93, 044036 (2016) [arXiv:1403.1232]

## Lehre

Oktober 2010  
bis Juni 2011

Korrektur Übungsaufgaben (Universität Leipzig)

- Theoretical Physics 1
- Physik für Veterinärmediziner
- Theoretical Physics 2

seit April 2013

Tutor in verschiedenen Seminaren der theoretischen Physik:

- Theoretische Physik 2 (Heidelberg)
- Symmetrien der Physik (Jena)
- Eichtheorien (Jena)

## Vorträge

März 2017

“Gross-Neveu-Yukawa models at criticality”

Frühlingstagung der Deutschen Physikalischen Gesellschaft (DPG), Bremen

Februar 2017

“Towards a local potential approximation in bimetric gravity”

Internationaler Workshop: Quantum Spacetime and the RG, Leiden

Dezember 2016

“Gross-Neveu-Yukawa models at criticality”

Monitoring Workshop der Graduiertenkollegs Graz, Wien und Jena, Wien

Juni 2016

“The problem of quantising gravity, and how to possibly overcome it”

Seminar: Fundamental Interactions, Freiburg

Mai 2016

“On the two-loop counterterm in Quantum Gravity”

International Asymptotic Safety Skype Seminar

März 2016

“Correlation Functions in Quantum Gravity”

Frühlingstagung der Deutschen Physikalischen Gesellschaft (DPG), Hamburg

- Februar 2016 “On the fate of perturbative divergences of Quantum Gravity in Asymptotic Safety”  
Treffen der Graduiertenschule, Oppurg
- November 2015 “Parametrisation dependence in non-perturbative approximations of quantum gravity”  
Internationaler Workshop: Strongly-Interacting Field Theories (SIFT 2015), Jena
- September 2015 “Gauge and parametrization dependence in Quantum Gravity”  
Monitoring Workshop der Graduiertenkollegs Graz, Wien und Jena, Jena
- Juli 2015 “Gauge and parametrization dependence in Quantum Gravity”  
Loops '15, Erlangen
- April 2015 “Global solutions of functional fixed point equations via pseudo-spectral methods”  
International Asymptotic Safety Skype Seminar
- Oktober 2014 “Global Flows and Vertex Functions in Quantum Gravity”  
Monitoring Workshop der Graduiertenkollegs Graz und Jena, Graz
- Mai 2014 “Global Flows in Quantum Gravity”  
International Asymptotic Safety Skype Seminar
- Januar 2014 “Global Completeness of Quantum Gravity”  
Seminar: Quantum Theory, Jena
- November 2013 “Global Completeness of Quantum Gravity”  
Seminar: Cold Quantum Coffee, Heidelberg

# Curriculum Vitae

## Contact information

Name	Benjamin Knorr
Private Address	Wenigenjenaer Ufer 2 07749 Jena
Institute Address	Theoretisch-Physikalisches Insitut Friedrich-Schiller-Universität Jena Max-Wien-Platz 1 07743 Jena
E-mail	benjamin.knorr@uni-jena.de

## Personal Information

Date of Birth	December 30, 1990
Place of Birth	Rodewisch
Citizenship	German

## Education

November 2013	M. Sc. Physik, Ruprecht-Karls-Universität Heidelberg
July 2011	B. Sc. Physik IPSP (International Physics Studies Program), Universität Leipzig
June 2008	Abitur, Goethe-Gymnasium Auerbach

# Publications

B. Knorr

“Ising and Gross-Neveu model in next-to-leading order”

Phys. Rev. B94, 245102 (2016) [arXiv:1609.03824]

J. Borchardt, B. Knorr

“Solving functional flow equations with pseudo-spectral methods”

Phys. Rev. D94, 025027 (2016) [arXiv:1603.06726]

H. Gies, B. Knorr, S. Lippoldt, F. Saueressig

“Gravitational Two-Loop Counterterm Is Asymptotically Safe”

Phys. Rev. Lett. 116, 211302 (2016) [arXiv:1601.01800]

H. Gies, B. Knorr, S. Lippoldt

“Generalized parametrization dependence in quantum gravity”

Phys. Rev. D92, 084020 (2015) [arXiv:1507.08859]

N. Christiansen, B. Knorr, J. Meibohm, J. M. Pawłowski, M. Reichert

“Local quantum gravity”

Phys. Rev. D92, 121501(R) (2015) [arXiv:1506.07016]

J. Borchardt, B. Knorr

“Global solutions to functional fixed point equations via pseudo-spectral methods”

Phys. Rev. D91, 105011 (2015) [arXiv:1502.07511],

Erratum: Phys. Rev. D93, 089904 (2016)

M. Heilmann, T. Hellwig, B. Knorr, M. Ansorg, A. Wipf

“Convergence of derivative expansion in supersymmetric functional RG flows”

JHEP 02, 109 (2015) [arXiv:1409.5650]

N. Christiansen, B. Knorr, J. M. Pawłowski, A. Rodigast

“Global flows in quantum gravity”

Phys. Rev. D93, 044036 (2016) [arXiv:1403.1232]



## Teaching

October 2010  
to June 2011

Correction of Exercises (Universität Leipzig)

- Theoretical Physics 1
- Physik für Veterinärmediziner
- Theoretical Physics 2

since April 2013

Tutor for different courses in theoretical physics:

- Theoretische Physik 2 (Heidelberg)
- Symmetrien der Physik (Jena)
- Eichtheorien (Jena)

## Talks

March 2017

“Gross-Neveu-Yukawa models at criticality”

Spring Meeting of the Deutsche Physikalische Gesellschaft (DPG), Bremen

February 2017

“Towards a local potential approximation in bimetric gravity”

International Workshop: Quantum Spacetime and the RG, Leiden

December 2016

“Gross-Neveu-Yukawa models at criticality”

Monitoring Workshop of the Graduate Schools Graz, Wien and Jena, Wien

June 2016

“The problem of quantising gravity, and how to possibly overcome it”

Seminar: Fundamental Interactions, Freiburg

May 2016

“On the two-loop counterterm in Quantum Gravity”

International Asymptotic Safety Skype Seminar

March 2016

“Correlation Functions in Quantum Gravity”

Spring Meeting of the Deutsche Physikalische Gesellschaft (DPG), Hamburg

- February 2016 “On the fate of perturbative divergences of Quantum Gravity in Asymptotic Safety”  
Meeting of the Graduate School, Oppurg
- November 2015 “Parametrisation dependence in non-perturbative approximations of quantum gravity”  
International Workshop: Strongly-Interacting Field Theories (SIFT 2015), Jena
- September 2015 “Gauge and parametrization dependence in Quantum Gravity”  
Monitoring Workshop of the Graduate Schools Graz, Wien and Jena, Jena
- July 2015 “Gauge and parametrization dependence in Quantum Gravity”  
Loops '15, Erlangen
- April 2015 “Global solutions of functional fixed point equations via pseudo-spectral methods”  
International Asymptotic Safety Skype Seminar
- October 2014 “Global Flows and Vertex Functions in Quantum Gravity”  
Monitoring Workshop of the Graduate Schools Graz and Jena, Graz
- May 2014 “Global Flows in Quantum Gravity”  
International Asymptotic Safety Skype Seminar
- January 2014 “Global Completeness of Quantum Gravity”  
Seminar: Quantum Theory, Jena
- November 2013 “Global Completeness of Quantum Gravity”  
Seminar: Cold Quantum Coffee, Heidelberg

# Danksagung

Ich möchte allen danken, die mich während meiner Zeit in Jena wissenschaftlich wie menschlich unterstützt haben.

Ein besonderer Dank gilt natürlich Andreas Wipf für seine Betreuung. Ich durfte sehr frei und unabhängig forschen, und trotzdem habe ich immer ein offenes Ohr bei Problemen vorgefunden. Diesen privilegierten Zustand habe ich sehr genossen.

Auch möchte ich Holger Gies herzlich danken für viele aufschlussreiche Gespräche und seine Unterstützung.

Weiterer Dank gilt meinen (ehemaligen) Kollegen am TPI, insbesondere Julia Borchardt, Marianne Heilmann, Tobias Hellwig, Stefan Lippoldt, René Sondenheimer, Luca Zambelli und Omar Zanusso, für schier unzählige fruchtbare und nicht so fruchtbare Diskussionen rund um die Physik.

Auch meinen Mitstreitern aus Heidelberg und Nijmegen möchte ich an dieser Stelle für die angenehme und erfolgreiche Zusammenarbeit danken: Nicolai Christiansen, Jan Meibohm, Jan Pawlowski, Manuel Reichert, Andreas Rodigast und Frank Saueressig.

Ebenso durfte ich auf einigen Konferenzen zahlreiche interessante Diskussionen führen, insbesondere mit Laura Classen, Astrid Eichhorn, Roberto Percacci, Michael Scherer und Gian Paolo Vacca, aber auch mit vielen anderen.

Zusätzlicher Dank gilt Stefan Lippoldt und Andreas Wipf für das Korrekturlesen der Arbeit.

Zu guter letzt richtet sich mein Dank an meine Familie für ihre Unterstützung und ihr Verständnis, dass ich sie nicht so oft besuchen konnte, wie die örtliche Nähe es zugelassen hätte, sowie an meine engen Freunde Josi, Julia und Sarah, für ihre konstante menschliche Unterstützung.

Die der Arbeit zu Grunde liegende Forschung wurde finanziell gefördert durch die DFG unter den Projektnummern GRK1523/2 sowie Wi777/11. Die Präsentation von Ergebnissen auf den DPG-Tagungen in Hamburg und Bremen wurden durch die Wilhelm und Else Heraeus-Stiftung bezuschusst. Ohne diese großzügigen finanziellen Unterstützungen wäre diese Arbeit nicht möglich gewesen.

# Ehrenwörtliche Erklärung

Ich erkläre hiermit ehrenwörtlich, dass ich die vorliegende Arbeit selbstständig, ohne unzulässige Hilfe Dritter und ohne Benutzung anderer als der angegebenen Hilfsmittel und Literatur angefertigt habe. Die aus anderen Quellen direkt oder indirekt übernommenen Daten und Konzepte sind unter Angabe der Quelle gekennzeichnet.

Ergebnisse, die in Zusammenarbeit mit Mitarbeitern des Theoretisch-Physikalischen Instituts in Jena, der Universität Heidelberg und der Universität Nijmegen entstanden sind, sind in der Arbeit entsprechend benannt.

Weitere Personen waren an der inhaltlich-materiellen Erstellung der vorliegenden Arbeit nicht beteiligt. Insbesondere habe ich hierfür nicht die entgeltliche Hilfe von Vermittlungs- bzw. Beratungsdiensten (Promotionsberater oder andere Personen) in Anspruch genommen. Niemand hat von mir unmittelbar oder mittelbar geldwerte Leistungen für Arbeiten erhalten, die im Zusammenhang mit dem Inhalt der vorgelegten Dissertation stehen.

Die Arbeit wurde bisher weder im In- noch im Ausland in gleicher oder ähnlicher Form einer anderen Prüfungsbehörde vorgelegt.

Die geltende Promotionsordnung der Physikalisch-Astronomischen Fakultät ist mir bekannt. Ich versichere ehrenwörtlich, dass ich nach bestem Wissen die reine Wahrheit gesagt und nichts verschwiegen habe.

Jena,

Benjamin Knorr